



THE UNIVERSITY OF QUEENSLAND
AUSTRALIA

Towards the Total Synthesis of (-)-Phorbol for Novel Anti-Cancer Studies

Tanja Krainz

Diplom Ingenieur

A thesis submitted for the degree of Doctor of Philosophy at

The University of Queensland in 2014

School of Chemistry and Molecular Biosciences

Abstract

Phorbol esters belong to the family of tricyclic diterpenes isolated from *Croton tiglium*, a member of the Euphorbiaceae and Thymelaeaceae plants. Since its isolation in 1935 phorbol has had a rapid rise to fame as a tumor promoter *via* protein kinase C activation and is now a common tool for cancer biologists worldwide. The issue with investigating and evaluating phorbol and its derivatives, in a biological sense, is that these complex molecules are limited only to natural sources (i.e. isolation from plant material). Furthermore, in addition to the supply issue these compounds are only available in one enantiomeric series (i.e. the natural (+)-phorbol), which in combination with that mentioned above places extensive limits on any meaningful biological investigation. The non-natural isomer (-)-phorbol is not known, has never been synthesised and as such never been biologically evaluated. Considering the importance of phorbol to current cancer biologists, investigating the synthesis of the non-natural isomer and its derivatives is of great importance.

This thesis describes fundamental studies towards the total synthesis of (-)-phorbol. The key step in the approach towards the total synthesis is a rhodium catalysed [4+3] cycloaddition reaction between a furan (right hand fragment) and a diazo compound (left hand fragment). The diazo compound was successfully synthesised from commercially available cyclopentenone over four steps *via* a palladium mediated direct diazo coupling protocol. In addition, the assembly of the CD-ring system *en route* to the right hand fragment is presented. Difficulties were encountered in the introduction of the D-ring system *via* cyclopropanation. To circumvent this problem it was discovered that a change of protecting group was essential for the success of this reaction. Moreover, a model study of the proposed [4+3] cycloaddition reaction between the left hand fragment and a number of furans of various substitution patterns is described.

Furthermore, 1,2,3-sulfonyl triazoles are presented as suitable diazo substitutes as they undergo a “ring to chain isomerism” to diazoimines. This equilibrium is being used in a novel approach to substituted cycloheptadiene systems with furans. In a rare case a [3+2] cycloaddition reaction was observed and a discussion of mechanistic insight is presented.

Declaration by author

This thesis is composed of my original work, and contains no material previously published or written by another person except where due reference has been made in the text. I have clearly stated the contribution by others to jointly-authored works that I have included in my thesis.

I have clearly stated the contribution of others to my thesis as a whole, including statistical assistance, survey design, data analysis, significant technical procedures, professional editorial advice, and any other original research work used or reported in my thesis. The content of my thesis is the result of work I have carried out since the commencement of my research higher degree candidature and does not include a substantial part of work that has been submitted to qualify for the award of any other degree or diploma in any university or other tertiary institution. I have clearly stated which parts of my thesis, if any, have been submitted to qualify for another award.

I acknowledge that an electronic copy of my thesis must be lodged with the University Library and, subject to the General Award Rules of The University of Queensland, immediately made available for research and study in accordance with the *Copyright Act 1968*.

I acknowledge that copyright of all material contained in my thesis resides with the copyright holder(s) of that material. Where appropriate I have obtained copyright permission from the copyright holder to reproduce material in this thesis.

Publications during candidature

T. Krainz, C.M. Williams, H.M.L. Davies, *Rhodium Catalysed Formal [4+3] Cycloaddition Reactions of Triazoles with Furans*, 6th Heron Island Conference on Reactive Intermediates and Unusual Molecules: Synthesis and Mechanism, July 2013

Publications included in this thesis

No publications included

Contributions by others to the thesis

A/Prof Craig M. Williams had significant input into the conception and design of the project and to the editing of the thesis.

Dr Sharon Chow performed reduction studies on the Right Hand Fragment; Synthesis and Characterisation of compounds **2.73**, **2.74**, **2.75**, **2.76** and crystallisation of compound **4.11**.

Enantiomeric excesses and chiral HPLC purification were performed by Dr Patricia Y. Hayes and Dr Victoria Challinor.

X-ray crystal raw data collection was performed by Prof Paul V. Bernhardt. Crystal structures were solved by Tanja Krainz.

Statement of parts of the thesis submitted to qualify for the award of another degree

None

Acknowledgements

First and foremost I would like to thank my supervisor A/Prof Craig Williams. Thank you for giving me the opportunity of working in your research group. I am especially thankful for your great support and your guidance over the past few years.

Special thanks to Prof Huw Davies. Thank you for all your support and discussions for this project and for having me at Emory University.

I am greatly indebted to the past and present members of the Williams group who have assisted me in countless ways. Thank you for all your support, laughter and tears and all the memories that we share. You have made my time such an enjoyable one and I am very grateful for all the friendships that I made.

Special thanks to Dr Sharon Chow. I am very grateful for your endless support and encouraging words. Thank you so much for all the time shared in the office and in the lab. I found a teacher, mentor and friend in you and can't thank you enough for sharing your knowledge and love for organic chemistry.

I would also like to thank Dr Paul Malek Mirzayans. Thank you for your endless support, discussions and motivation. You are a brilliant chemist but out of all you are an amazing friend.

To all my friends with whom I had the privilege to share a great four-year journey in Australia. Thank you all for your uniqueness and kindness. I could have not wished for better people sharing this journey.

For financial support I would like to thank the Commonwealth Government for the IPRS and UQCent scholarships as well as the University of Queensland Graduate School and the SCMB Student Support funds for travel grants that enabled me to visit collaborators and to attend and present at conferences.

Finally, I would like to thank my family. Von ganzem Herzen moechte ich meinen Eltern und meinen Geschwistern danken. Danke für eure jahrelange Unterstützung. Ich weiss, dass es nicht immer einfach für euch war. Unter anderem auch, mich ans "andere Ende der Welt" gehen zu lassen. Danke, dass ihr immer für mich da seid und vor allem mich immer wieder ermutigt meinen eigenen Weg zu gehen.

Keywords

total synthesis, phorbol, [4+3] cycloaddition, alkenyldiazoacetate, 1,2,3-sulfonyl triazoles, rhodium catalysis

Australian and New Zealand Standard Research Classifications (ANZSRC)

ANZSRC code: 030503, Organic Chemical Synthesis, 80%

ANZSRC code: 030502, Natural Products Chemistry, 20%

Fields of Research (FoR) Classification

FoR code: 0305, Organic Chemistry, 100%

Table of Contents

List of Schemes	x
List of Figures	xii
List of Tables	xiv
1 Phorbol: Structure and Activity	1
1.1 Introduction	1
1.2 Protein Kinases in Drug Discovery	7
1.2.1 Introduction	7
1.3 Protein Kinase C	8
1.3.1 Protein Kinase Isozymes	9
1.3.2 Protein Kinase C activation	10
1.4 The Euphorbiaceae and Thymelaeaceae Plant Families	12
1.5 Phorbol: A Tigliane Diterpene	14
1.6 Biosynthesis	16
1.7 Previous Synthetic Strategies	17
1.7.1 Wender's Efforts to Phorbol	19
1.7.2 Efforts by Cha	28
1.8 Methods describing effort towards the Tigliane Core	30
1.8.1 Shibasaki's Approach	30
1.8.2 Dauben's Efforts towards the Tigliane Core	35
1.8.3 Evans' Approach	36
1.9 Synthetic Routes to Diterpenes Related to Phorbol	37
1.9.1 Inoue's Strategy towards the Daphnane Diterpene Resiniferatoxin	37
1.9.2 Baran's Total Synthesis of (+)-Ingenol	40
1.10 Project Background and Aim	42
1.11 Retrosynthetic analysis	46

2	Investigations towards the Synthesis of the Right Hand Fragment	50
2.1	Introduction	50
2.2	Approach	51
2.3	Synthesis of the CBS-Oxazaborolidine Catalyst.....	53
2.4	Cyclopropanation Studies.....	56
2.5	The Effect of C-13 Substituent upon Cyclopropanation	62
2.6	Ring C: Reduction Studies	75
3	Synthetic Investigations Towards the Construction of the Left Hand Fragment	80
3.1	Introduction	80
3.2	Diazo Transfer Approach	80
3.3	Diazo Direct Palladium Cross-Coupling Approach	87
3.3.1	First generation Approach.....	87
3.4	Synthesis of Tosyl diazomethane	91
3.4.1	Second Generation Approach	92
4	Studies Towards Seven-Membered Ring Formation	98
4.1	Introduction	98
4.2	Ring-Closing Metathesis	99
4.3	Diels-Alder reaction	100
4.4	[4+3]Cycloaddition reaction	101
4.4.1	Rhodium-catalysed formal [4+3] Cycloaddition reaction	102
4.5	Model Studies with the Left Hand Fragment	103
4.6	Triazole Cycloadditions with Furans	110
4.6.1	Introduction.....	110
5	Conclusion and Future Work	119
5.1	Right Hand Fragment	119

5.2	Left Hand Fragment	121
5.3	Triazoles	123
6	Experimental	125
6.1	General	125
6.1.1	Reactions	125
6.1.2	Purification	125
6.1.3	Characterisation	125
6.2	Experimental Procedures Right Hand Fragment	127
6.3	Experimental Procedures Left Hand Fragment	141
6.3.1	General procedure for rhodium catalysed [4+3] cycloaddition reactions of diazo compound 3.36 with furans	147
6.4	Experimental Procedures for 1,2,3-sulfonyl triazoles	151
6.4.1	General procedure for triflation chemistry	151
6.4.2	General procedure for the CuTC catalysed cycloaddition	152
6.4.3	General procedure for rhodium catalysed [4+3] cycloaddition reactions of 1,2,3-sulfonyl triazoles with furans	154
7	References	158
8	Appendix	163
8.1	Appendix A: Supporting NMR spectra for Chapter 2	165
8.2	Appendix B: Supporting NMR Spectra for Chapter 3	180
8.3	Appendix C: Supporting NMR Spectra for Chapter 5	196
8.4	Appendix D: X-Ray diffraction data	203

List of Schemes

Scheme 1.1 Biosynthetic pathway to tigliane, daphnane and ingenane diterpenes.	17
Scheme 1.2 Proposed precursor for three classes of diterpenes (tiglianes, daphnanes and ingenanes).	18
Scheme 1.3 Wender's first approach to the tigliane core.	20
Scheme 1.4 First half of Wender's first total synthesis of (+)-phorbol. ³⁶	22
Scheme 1.5 Second half of Wender's first total synthesis of (+)-phorbol. ³⁶	24
Scheme 1.6 Retrosynthetic analysis of Wender's second generation approach to (+)-phorbol. ⁴¹	25
Scheme 1.7 Second generation synthesis of (+)-phorbol (1.1). ⁴¹	26
Scheme 1.8 Wender's first asymmetric synthesis of (+)-phorbol. ³⁷	27
Scheme 1.9 Cha's formal asymmetric synthesis of (+)-phorbol 1.1. ³⁸	29
Scheme 1.10 Shibasaki's synthesis to precursor 1.99. ^{42a}	31
Scheme 1.11 Shibasaki's synthesis of phorbol analogue 1.107. ⁴³	32
Scheme 1.12 Dauben's efforts towards the tigliane core 1.122. ⁴⁷	35
Scheme 1.13 Evans' approach towards the tigliane core. ⁴⁸	36
Scheme 1.14 Wender's total synthesis of resiniferatoxin. ⁵¹	38
Scheme 1.15 Inoue's approach to resiniferatoxin. ⁵²	39
Scheme 1.16 Baran's total synthesis of (+)-ingenol. ⁵⁶	41
Scheme 1.17 Natural products containing seven-membered rings.	43
Scheme 1.18 Williams' first generation approach to seven-membered rings.....	43
Scheme 1.19 Davies' approach to (-)-5- <i>epi</i> -vibsanin E.	44
Scheme 1.20 Williams' and Davies' total synthesis of (-)-5- <i>epi</i> -vibsanin E.	45
Scheme 1.21 Retrosynthetic analysis of (-)-phorbol using Davies seven-membered ring formation.	47
Scheme 1.22 Proposed strategy for the synthesis of (-)-phorbol 1.169.	48
Scheme 2.1 Retrosynthetic analysis of the right hand fragment of (-)-phorbol (1.169).	50
Scheme 2.2 Synthesis of methoxy-quinone 2.7.	51
Scheme 2.3 Diels-Alder reaction of 2.7 with cyclopentadiene.	52
Scheme 2.4 Synthetic route to the CBS-oxazaborolidine catalyst.	54
Scheme 2.5 Enantioselective Diels-Alder reaction of 2.7.	55
Scheme 2.6 Synthesis of <i>gem</i> -dimethylcyclopropane.	56
Scheme 2.7 Synthesis of diphenyldiisopropylsulfonium tetrafluoroborate.	56

Scheme 2.8 Formation of the D-ring.	57
Scheme 2.9 Synthesis of triisopropylsulfoxonium tetrafluoroborate.....	59
Scheme 2.10 Possible mechanism for the low yield of D-ring formation.	60
Scheme 2.11 Synthesis of 2.34 <i>via</i> retro Diels-Alder reaction.	61
Scheme 2.12 Access to C-13 substituted Diels-Alder adducts.	63
Scheme 2.13 Cyclopropanation attempts on 2.36, 2.37 and 2.39.	64
Scheme 2.14 Change of C-13 protecting group strategy.	65
Scheme 2.15 Synthetic strategy for quinone 2.40.....	65
Scheme 2.16 Synthetic outcome of selective protection of 3-methylcatechol.	66
Scheme 2.17 Selective protection of 2.47 according to Nicolaou <i>et al.</i>	67
Scheme 2.18 Wurm's approach for the direct β -substitution of methoxy to <i>isopropoxy</i>	68
Scheme 2.19 New approach to <i>isopropoxy</i> quinone 2.49.....	68
Scheme 2.20 Diels-Alder reaction of 2.49 with cyclopentadiene.....	69
Scheme 2.21 Synthetic pathway to advanced intermediate 2.55.	70
Scheme 2.22 Harwood's synthesis of CD-ring system of phorbol.....	74
Scheme 2.23 Proposed route to the right hand fragment 2.68.	75
Scheme 2.24 Hydrogenation studies on 2.55.....	76
Scheme 2.25 Alternate approach for reduction of the C-ring.	77
Scheme 2.26 Reduction studies to 2.55 utilising NaBH ₄	78
Scheme 2.27 Synthetic pathway to ketone 2.76.....	78
Scheme 3.1 Retrosynthetic leading to LHF and RHF.....	80
Scheme 3.2 General diazo transfer transformation.	81
Scheme 3.3 Synthetic plan for diazo transfer to construct the LHF.	81
Scheme 3.4 Forward strategy to diazo transfer precursor 3.6.....	82
Scheme 3.5 Double bond isomerisation of 3.6 under acidic conditions.	84
Scheme 3.6 Diazo transfer reaction using either 1.199 or 3.6.	85
Scheme 3.7 Diazo transfer with Kitamura's salt ADMC.	86
Scheme 3.8 Counter-ion exchange for a more stable Kitamura reagent (ADMF).	87
Scheme 3.9 Wang's direct diazo cross-coupling.....	88
Scheme 3.10 Alternate retrosynthetic analysis of the LHF.	88
Scheme 3.11 Alternate forward strategy to the LHF.	89
Scheme 3.12 Possible pyrazole formation during diazo formation.	90
Scheme 3.13 Synthesis of tosyl diazomethane 3.28.	91

Scheme 3.14 Initial direct diazo coupling of 1.200 to 3.28.	92
Scheme 3.15 Possible introduction of the C-2 methyl group.	92
Scheme 3.16 Second generation approach to the coupling precursor 3.35.....	93
Scheme 3.17 Successful synthetic route to the LHF.....	93
Scheme 3.18 Plausible mechanism for the direct diazo coupling to afford 3.36.	94
Scheme 3.19 Direct diazo coupling between 3.35 and 1.204.	97
Scheme 4.1 Ley's total synthesis of thapsivillosin F 4.5.	100
Scheme 4.2 Total synthesis of caribenol A (4.10).	101
Scheme 4.3 Synthetic strategy to 2-methyl-4,5-dimethyl carboxylate.	107
Scheme 4.4 Proposed cycloaddition mechanism.	109
Scheme 4.5 Fallback strategy to the tigliane core.....	109
Scheme 4.6 Huisgen 1,3-dipolar cycloaddition vs. Sharpless.	110
Scheme 4.7 Isomerisation to diazoimine and resulting carbenoid chemistry.	111
Scheme 4.8 Pyrazole formation of alkenyldiazoacetates.....	112
Scheme 4.9 Fokin's synthesis of 1,2,3-sulfonyl triazole 4.33.	112
Scheme 4.10 Azavinyl carbene formation.	113
Scheme 4.11 Synthetic route to 1,2,3-sulfonyl triazoles.....	115
Scheme 4.12 Plausible mechanistic explanation for the [3+2] cycloaddition reaction of compound 4.43.....	117
Scheme 5.1 Synthetic route to advanced intermediate 2.55.	120
Scheme 5.2 Reduction studies on compound 2.55.....	120
Scheme 5.3 Proposed synthetic route for completion of the RHF.....	121
Scheme 5.4 Synthetic route to LHF.	122
Scheme 5.5 Formal [4+3] cycloaddition reaction between LHF and furans.	122
Scheme 5.6 Cycloaddition approach to compound 5.7.....	123
Scheme 5.7 Formal [4+3] cycloaddition reaction of triazoles and furans.	124

List of Figures

Figure 1.1 Influence of natural products as lead therapeutics between 1981–2006. ³	2
Figure 1.2 Structure of (+)-phorbol and TPA.	3
Figure 1.3 Structure of diacylglycerol (DAG).	4

Figure 1.4 Heteroatom overlay between phorbol and DAG.	5
Figure 1.5 Diacylglycerol analogues.	6
Figure 1.6 Human protein kinase dendrogram.....	8
Figure 1.7 Stick-figure of cPKC and nPKC.....	9
Figure 1.8 Protein kinase C activation process.	10
Figure 1.9 Gleevec®.	11
Figure 1.10 Examples of cyanogenic β -glycosides.....	13
Figure 1.11 Three classes of diterpenes.	14
Figure 1.12 Tiglane diterpenes and their numbering system.	15
Figure 1.13 Prostratin.....	16
Figure 1.14 Photo-affinity ligands for PKC cross-linking experiments. ⁴⁴⁻⁴⁵	34
Figure 1.15 Ingenol mebutate (Picato®).....	40
Figure 1.16 William's total syntheses of vibsantin family members.	42
Figure 2.1 Diels-Alder isomers 2.11 and 2.12.	52
Figure 2.2 Corey's prediction model for enantioselective Diels-Alder reaction.....	53
Figure 2.3 ORTEP (30% ellipsoid probability) structure of the cyclopropanation product 2.25.	61
Figure 2.4 ORTEP (30% ellipsoid probability) structure of the cyclopropanation product 2.37.	63
Figure 2.5 By-product 2.52 observed during prolonged reaction times <i>en route</i> to 2.49.	69
Figure 2.6 ORTEP (30% ellipsoid probability) structure of the Diels-Alder product 2.53.....	70
Figure 2.7 2D Correlation Spectroscopy for compound 2.54.	72
Figure 2.8 500 MHz ^{13}C NMR spectrum for 2.54.	72
Figure 2.9 ORTEP (30% ellipsoid probability) structure of the cyclopropanation product 2.54.	74
Figure 3.1 2D-COSY spectrum of exocyclic compound 3.6.	83
Figure 3.2 Distinction of double bond isomerisation products by ^1H NMR.....	84
Figure 3.3 ^{13}C key resonances of compound 3.36.	95
Figure 3.4 Diazo stretch comparison between 3.36 and ethyldiazo acetate.	96
Figure 3.5 GC/MS fragmentation pattern of compound 3.36.	96
Figure 4.1 General representation of natural products containing seven-membered ring cores.....	98
Figure 4.2 Common catalysts for ring-closing metathesis.....	99
Figure 4.3 General representation of natural products containing seven-membered rings formed <i>via</i> [4+3] cycloaddition reaction.	101
Figure 4.4 Selected rhodium catalysts for the formal [4+3] cycloaddition reaction.....	102
Figure 4.5 ^1H NMR spectrum showing the olefinic protons of cycloaddition product 4.14.	105

Figure 4.6 Previous synthetic work on 1,2,3-sulfonyl triazoles and proposed reaction with furans.	114
Figure 4.7 Synthesised triazoles.....	115
Figure 4.8 ORTEP (30% ellipsoid probability) of compound 4.41.....	116
Figure 4.9 ¹ H NMR Spectra of the conversion of imine 5.15 to aldehyde 5.19.	118

List of Tables

Table 1.1 Antileukemic activity of some phorbol derivatives with Eu=Euphorbiaceae, Th=Thymelaeaceae, P-388=mouse leukaemia cells, L-1210=mouse lymphocytic leukaemia cells...3	
Table 1.2 Effect of phorbol analogues on the inhibition of [³ H]PDBu binding to PKC. ⁴³	33
Table 2.1 Protonation studies of 2.19.	55
Table 2.2 Conditions for the introduction of ring D.	57
Table 2.3 Taylor's cyclopropanation results using triisopropylsulfoxonium tetrafluoroborate.	58
Table 2.4 Conditions for selective protection of 3-methylcatechol.	66
Table 2.5 Condition screening for the synthesis of isopropoxy quinone 2.49.....	68
Table 2.6 ¹ H NMR data for compound 2.54 (500MHz, CDCl ₃).	73
Table 2.7 Condition screening for the reduction of 2.55.	76
Table 3.1 Screening of diazo transfer reagents and conditions.....	86
Table 4.1 Model studies of 3.36 with selected furans.....	104
Table 4.2 ¹ H-NMR data for compound 4.13 (500 MHz, CDCl ₃).	106
Table 4.3 Cycloaddition studies with di- and trisubstituted furans.....	108
Table 4.4 Model studies with cyclohexene triazole.	116

Abbreviations

°C	Degrees Celsius
μl	Microliters
Å	Angstrom
Ac	Acetate
b.p.	Boiling point
Boroxine	2,4,6-trihydroxy-1,3,5,2,4,6-trioxatriborinane
cat.	Catalytic
COSY	2D Correlation spectrum
CuTC	Copper(I)-thiophene-2-carboxylic acid
d	Days
DBU	1,8-Diazabicycloundec-1-ene
DCE	1,2-Dichloroethane
DCM	Dichloromethane
DIBAL-H	Diisobutylaluminium hydride
DIPEA	<i>N,N</i> -Diisopropylethylamine
DMAP	<i>N,N</i> -Dimethylpyridine-4-amine
DMF	<i>N,N'</i> -Dimethylformamide
DMSO	Dimethyl sulfoxide
EI	Electron impact
eq.	Equivalents
ESI	Electrospray ionisation

Et	Ethyl
GC/MS	Gas Chromatography/Mass Spectrometry
h	Hours
HMBC	Heteronuclear Multiple-Bond Correlation
HMPA	Hexamethylphosphoramide
HRMS	High Resolution Mass Spectrometry
HSQC	Heteronuclear Single-Quantum Correlation
IBX	2-Iodoxybenzoic acid
LDA	Lithium diisopropylamide
LiHMDS	Lithium hexamethyldisilazide
LRMS	Low Resolution Mass Spectrometry
m.p.	Melting point
Martin sulfurane	Bis[α,α -bis(trifluoromethyl)benzenemethanolato]diphenylsulfur
Me	Methyl
MeCN	Acetonitrile
MeMgBr	Methylmagnesium bromide
MeOH	Methanol
mg	Milligram
Mg	Magnesium
min	Minutes
mol	Moles
MS	Mass Spectrometry

MsN ₃	Mesyl azide
NaBH ₄	Sodium borohydride
NaH	Sodium hydride
<i>n</i> Bu ₄ NBr	Tetra- <i>n</i> -butylammonium bromide
<i>n</i> -BuLi	<i>n</i> -Butyl lithium
NMO	<i>N</i> -Methylmorpholine <i>N</i> -oxide
NMR	Nuclear Magnetic Resonance
o/n	Overnight
OXONE®	Potassium peroxymonosulfate
PCC	Pyridinium chlorochromate
PMA	Phorbol-12-myristate-13-acetate
ppm	Parts per million
PPTS	Pyridinium <i>p</i> -toluenesulfonate
pyr.	Pyridine
quant.	Quantitative
RSM	Recovered starting material
r.t.	Room temperature
Salcomine	<i>N,N'</i> -Bis(salicylidene)ethylenediaminocobalt(II)
TBS	<i>tert</i> -Butyldimethylsilyl
TEG	Triethyleneglycol
Tf	Trifluoromethanesulfonate
THF	Tetrahydrofuran

TLC	Thin Layer Chromatography
TMEDA	<i>N,N,N',N'</i> -Tetramethylethane-1,2-diamine
TMSCl	Trimethylsilyl chloride
TMSCN	Trimethylsilyl cyanide
V-40	1,1'-Azobis(cyclohexane-1-carbonitrile)

1 Phorbol: Structure and Activity

1.1 Introduction

Nature provides us with an extraordinary variety of biologically active compounds and researchers more often let nature inspire them to find cures for a vast amount of diseases. Not only can we learn from nature to better understand disease mechanisms, but we can gain unparalleled information on how nature designs these complex molecules.

A significant drawback to natural product drug discovery is that extraction and isolation from plant material solely is neither feasible nor economical. This is due to many biologically active compounds being isolated in small quantities as well as plants being restricted to certain geographical areas.

The syntheses of these natural products are often arduous journeys over long period of times, normally over years. As a consequence, the popularity of natural products as lead therapeutics and the synthesis for drug discovery purposes decreased significantly.¹

With the increased popularity of combinatorial chemistry in the early 1980's it was envisaged that with its application massive numbers of novel skeletons could be produced and thus, a large number of lead therapeutics could be accessed rather quickly. As a consequence, the focus of pharmaceutical companies was diverted towards identification of fully synthetic small molecules *via* screening of combinatorial libraries.

It is evident today that the rapid production of large libraries is associated with a “lack of complexity”, such as chiral centres and polycyclic structures etc., in contrast to that found in natural products. As a consequence, issues such as for example selectivity are not adequately addressed.²

Figure 1.1 shows a pie chart³ depicting the percentages of small molecule drugs derived from totally synthetic molecules, molecules having a natural product pharmacophore, molecules derived from natural products and pure natural products over nearly three decades. Clearly, nearly 50% of drugs produced are totally synthetic drugs.

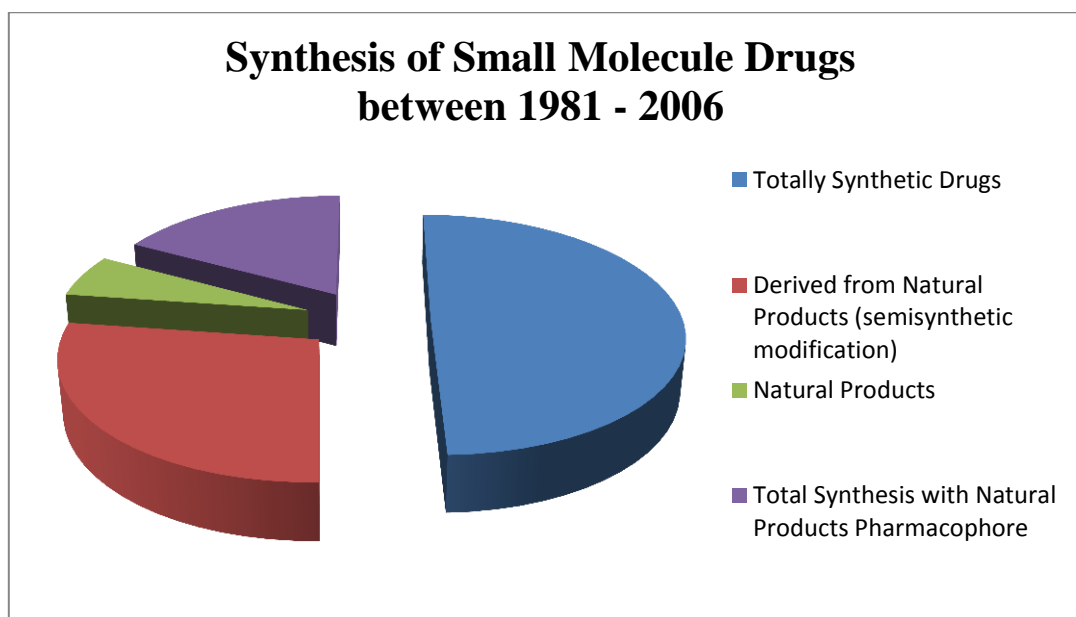


Figure 1.1 Influence of natural products as lead therapeutics between 1981–2006.³

In this view natural product chemistry (isolation and synthesis) in regards to drug discovery is an approach that has proven to be an effective and valuable source of inspiration from nature. One natural product, (+)-phorbol (**1.1**),⁴ isolated in 1935 found significant attention by biologists and chemists alike due to its potent nature as a protein kinase C activator. Boehm successfully isolated phorbol from *Croton tiglium*, a member of the spurge family also called the *Eurphorbiaceae* family. Investigations by Berenblum⁵ showed that the molecules isolated from this species were the first pure tumor promoting compounds in mice skin and as such he introduced the term “co-carcinogenic”. This defines tumor promoters being neither mutagenic nor carcinogenic themselves, but once the initiation process by a carcinogen has occurred, these compounds encourage tumor growth. Tumor growth in contrast to the tumor initiation process is reversible, thus a repeated exposure to this compound is necessary for tumor growth.

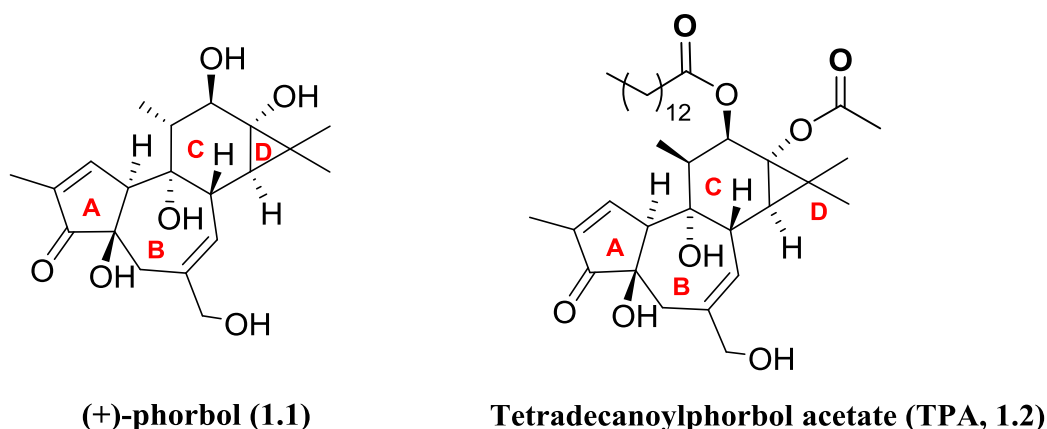


Figure 1.2 Structure of (+)-phorbol and TPA.

A significant feature of phorbol esters is their extraordinary high potency, which both Hecker⁶ and Berenblum⁷ confirmed to be at a nanomolar range. One derivative of the parent polyol phorbol is 12-*O*-Tetradecanoylphorbol-13-acetate (**1.2**) (TPA, figure 1.2), which is the most potent tumor promoter to date.⁸ Phorbol esters were initially studied for their tumor promoting activity, but it was quickly found that they also have profound biological properties such as anti-leukemic,⁹ anti-HIV¹⁰ and anti-cancer.¹¹ Table 1.1 shows four examples of biologically active phorbol derivatives possessing anti-leukemic activity in the P-388 and L-1210 cell lines with phorbol 12-tiglate 13-decanoate showing activity as low as 0.06-0.25mg/kg *in vivo*.

<i>Compound</i>	<i>Botanical Source</i>	<i>Anti-leukemic activity</i>
Phorbol 12-tiglate 13-decanoate	<i>Croton tiglium</i> (Eu)	P-388 <i>in vivo</i> (0.06-0.25mg/kg)
12-Deoxy-5-hydroxyphorbol 13-myristate	<i>B. montanum</i> (Eu)	P-388 <i>in vitro</i>
12- <i>O</i> -Deca-2,4,6-trienoylphorbol 13-acetate	<i>Aquilaria malaccensis</i> (Th)	P-388 <i>in vitro</i> (ED ₅₀ = 0.24 ng/mL)
Mezerein	<i>Daphne mezereum</i> (Th)	P-388 <i>in vivo</i> L-1210 <i>in vivo</i>

Table 1.1 Antileukemic activity of some phorbol derivatives with Eu=Euphorbiaceae, Th=Thymelaeaceae, P-388=mouse leukaemia cells, L-1210=mouse lymphocytic leukaemia cells.

Phorbol esters such as 12-*O*-tetradecanoyl-phorbol-13-acetate (TPA, **1.2**) are PKC activators mimicking diacylglycerol, but unlike DAG, phorbol esters do bind directly to the enzyme.¹² Furthermore, DAG is a short lived species and appears in the membrane cell only transiently, whereas phorbol esters are metabolised at a decreased rate in the cell leading to increased long term activation, thus resulting in unregulated protein phosphorylation. This unregulated phosphorylation leads to proliferation.

It was shown that DAG increases the affinity of the enzyme to Ca^{2+} without increasing the Ca^{2+} concentration. A highly specific “lipid-protein” interaction is necessary for activating the kinase. Active DAG is specific to 1,2-*sn*-conformation, whereas other isomers have not shown to induce a biological response. Once protein kinase C is activated it phosphorylates other cellular proteins such as receptor proteins of some growth factors such as the epidermal growth factor (EGF). Another major feature of the PKC is the down-regulation or “negative feedback control”.

The natural activator for PKC is diacylglycerol **1.3** (DAG, figure 1.3),¹³ a lipophilic second messenger produced in the plasma membrane *via* hydrolysis of inositol phospholipids. Chemically, diacylglycerol is a glyceride with two alcohols being attached to fatty acid chains.

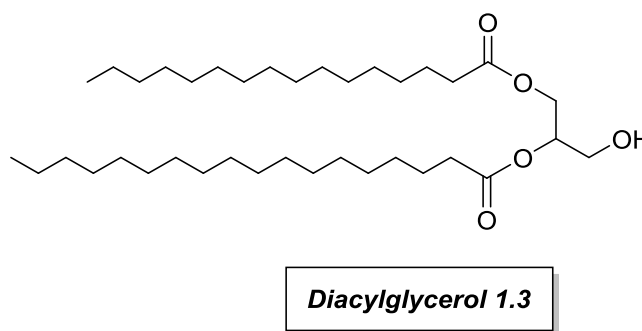


Figure 1.3 Structure of diacylglycerol (DAG).

Figure 1.4 shows the structural analogy of phorbol and its endogenous counterpart DAG. While Nishizuka suggested an analogy of the C-12 and C-13 oxygens to DAG,^{13c,14} Wender found that according to rms deviation calculations a much closer analogy can be drawn to the C-4, C-9 and the C-20 oxygens with the centre of mass of the (*S*)-DAG having a more favourable overlay.¹⁵

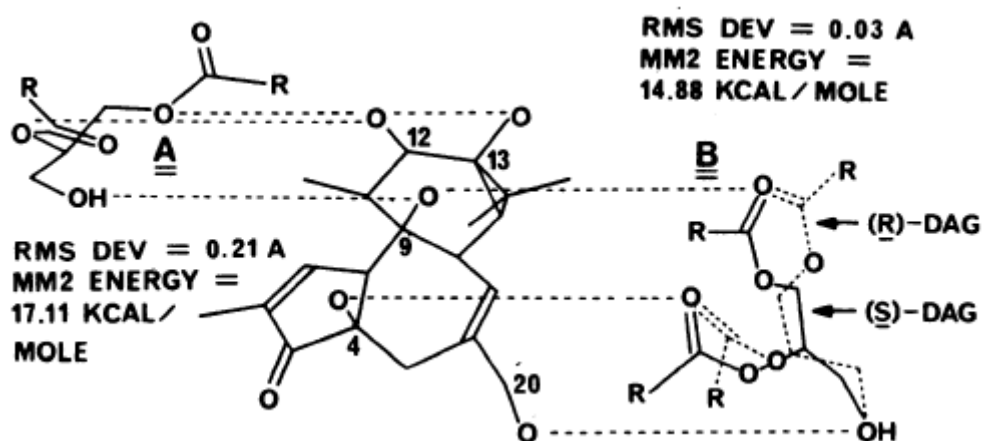
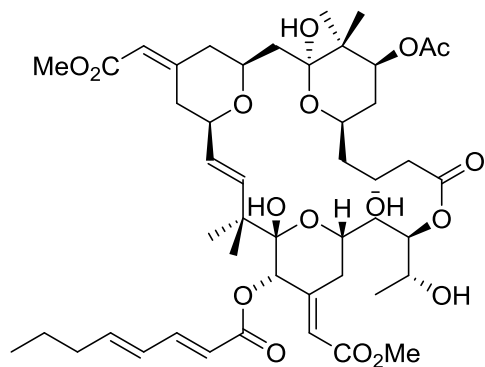


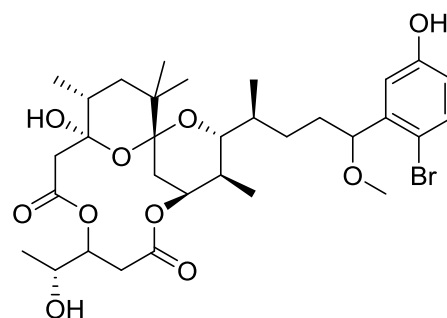
Figure 1.4 Heteroatom overlay between phorbol and DAG.¹

It has been shown that certain ingenane diterpenes isolated from Thymelaceae plants are also able to substitute for DAG. Amongst them ingenol mebutate **1.7** (scheme 1.5) which is an approved drug from the Food and Drug Association (FDA) for the treatment of actinic keratosis. Other promising DAG analogues are bryostatin (**1.4**),¹⁶ teleocidins (**1.6**),¹⁷ and aplyslatoxin (**1.5**)^{17c} as shown in figure 1.5.

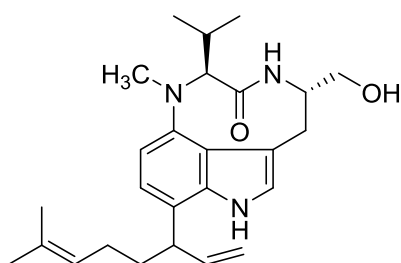
¹ Figure taken from Wender, P.A.; Koehler, K.F.; Sharkey, N.A.; Dell'Aquila, M.L.; Blumberg, P.M. *PNAS*, **1986**, 83, 4214-4218



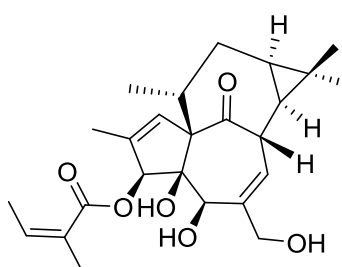
Bryostatin 1.4



Aplysiatoxin 1.5



Teleocidin 1.6



Ingenol mebutate 1.7

Figure 1.5 Diacylglycerol analogues.

In 1982, Nishizuka and co-workers^{13c} reported for the first time that derivatives of phorbol could act as substitutes for the unsaturated diacylglycerol, which is responsible for protein kinase C activation. Some evidence suggested that esters of phorbol directly bind to the cell surface membrane of the serine/threonine dependent protein kinase C (PKC). In order to better understand the influence that phorbol and derivatives have on PKC a brief explanation of the pathway as well as the function of protein kinase C is necessary and will be discussed.

1.2 Protein Kinases in Drug Discovery

1.2.1 Introduction

The search for new chemotherapeutic agents has been greatly aided in recent years by a better understanding of the structure of enzymes and their biological function associated with diseases. One important class of enzymes are protein kinases.¹⁸ These kinases represent a large and diverse family of important biological catalysts transferring the terminal phosphate of adenosine triphosphate (ATP) to a hydroxyl group of target proteins; a mechanism responsible for cellular and enzymatic functions. There are two main classes of protein kinases in eukaryotic organisms, namely, serine/threonine kinases and tyrosine kinases. To date, 538 human protein kinases of the human genome sequence have been identified and encoded, of which 478 can be attributed to one single superfamily (figure 1.6).¹⁹

Seven subgroups are allocated to the superfamily and can be divided into an array of families which only marginally differ in their catalytic sequence. (i) TK – tyrosine kinases (ii) TKL – Tyrosine kinase-like group of kinases (iii) STE – containing homologs of yeast Sterile 7, Sterile 11 and Sterile 20 kinases (iv) CK1 – containing casein kinases 1 (v) AGC containing protein kinase A, G and C (vi) CAMK containing calcium/calmodulin-dependent protein kinases (vii) CMGC containing cyclin-dependent kinase (CDK), mitogen-activated protein kinases (MAPK), glycogen synthase kinases (GSK3) and CDC-like kinases (CLK).

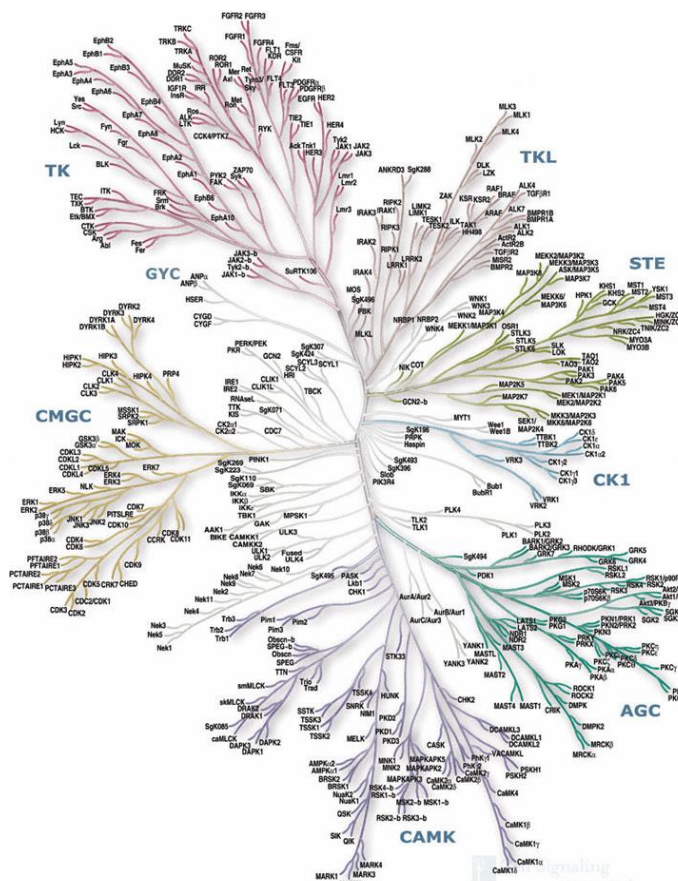


Figure 1.6 Human protein kinase dendrogram.²

Within this superfamily of protein kinases AGC protein kinase family found special interest. This family is comprised of 21 subfamilies and is named after protein kinase A (PKA), protein kinase G (PKG) and protein kinase C (PKC).

1.3 Protein Kinase C

Since its discovery in 1977,²⁰ protein kinase C (PKC) has become the focus of biological investigations. This kinase plays a crucial role in the signalling pathways and in cell growth regulation and proliferation. PKC is crucial for the transfer of extracellular information signals to the cell interior.²¹ It is evenly distributed in tissues and organs and is most abundant in the brain. Protein Kinase C is a calcium ion and phospholipid dependent kinase, in particular phosphatidyl serine is essential for its activation.²²

² Figure taken from <http://www.cellsignal.com/reference/kinase/overview.html>

1.3.1 Protein Kinase Isozymes

Ten mammalian protein Kinase C isozymes are known to date,²¹ which can be categorised into 3 classes; (i) conventional PKCs (cPKC) consist of four isozymes that are Ca^{2+} dependent due to the C2 domain containing a Ca^{2+} binding site. cPKCs contain PKC α , PKC β I, PKC β II (two alternatively spliced variants) and PKC γ . These conventional PKCs can be activated by phorbol esters or DAG and calcium. (ii) Novel protein kinase C (nPKC), which have shown to have structural similarity to cPKCs, but are not Ca^{2+} dependent comprising PKC δ , PKC ϵ , PKC η and PKC θ can be activated by phorbol esters or DAG, but do not respond to calcium. (iii) Atypical protein kinase Cs (aPKC) isozymes, which as the name suggests do not provide strong structural similarities to conventional and novel protein kinases. They consist of PKC ζ and PKC λ and have shown not to respond to either calcium or DAG and thus, not to phorbol esters.¹⁹

Figure 1.7 shows the general structure of conventional and novel protein kinases. All members of the protein kinase C family consist of a cysteine rich *N*-terminal lobe and a *C*-terminal lobe connected *via* a single polypeptide strand, which acts as a “catalytic cleft”.^{18a,23} Typically PKC isozymes contain four conserved regions (C1-C4) with C1 being the diacylglycerol and C2 being the Ca^{2+} sensor. It can be clearly seen that isozymes of PKC only differ in the regulatory domain, but show homology in the catalytic domain.²³⁻²⁴

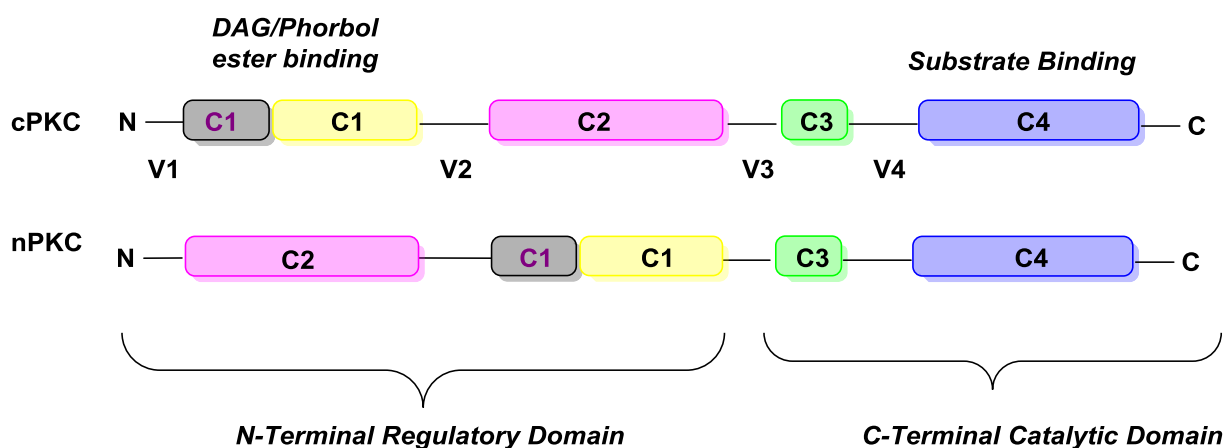


Figure 1.7 Stick-figure of cPKC and nPKC.

1.3.2 Protein Kinase C activation

The lifecycle of a protein kinase C involves three steps: maturation, activation and inactivation.²⁴⁻²⁵ Maturation of protein kinase C is a prerequisite. Work by Newton *et al.*²⁴ has shown that PKCs are only able to become activated once they are “matured”, a process that involves a series of phosphorylation steps. Protein Kinase C in its inactive form shows an “open” conformation, which is pivotal as the unphosphorylated C-terminus is exposed and provides a docking site for PDK-1 (phosphoinositide-dependent kinase 1). Following this, the turn motif and hydrophobic motif are phosphorylated leading to exposure of the C-terminal domain, which, after autophosphorylation stabilizes the enzyme after key conformational rearrangements. Following this maturation process specific substrate binding such as the binding of DAG and calcium can occur to the C1 domain leading to a high affinity interaction between the PKC and the membrane. As a result the pseudo substrate is released, allowing for substrate binding, phosphorylation and the activation of downstream signaling effectors. The interactions with DAG facilitate the dissociation of the pseudo substrate activating the kinase.

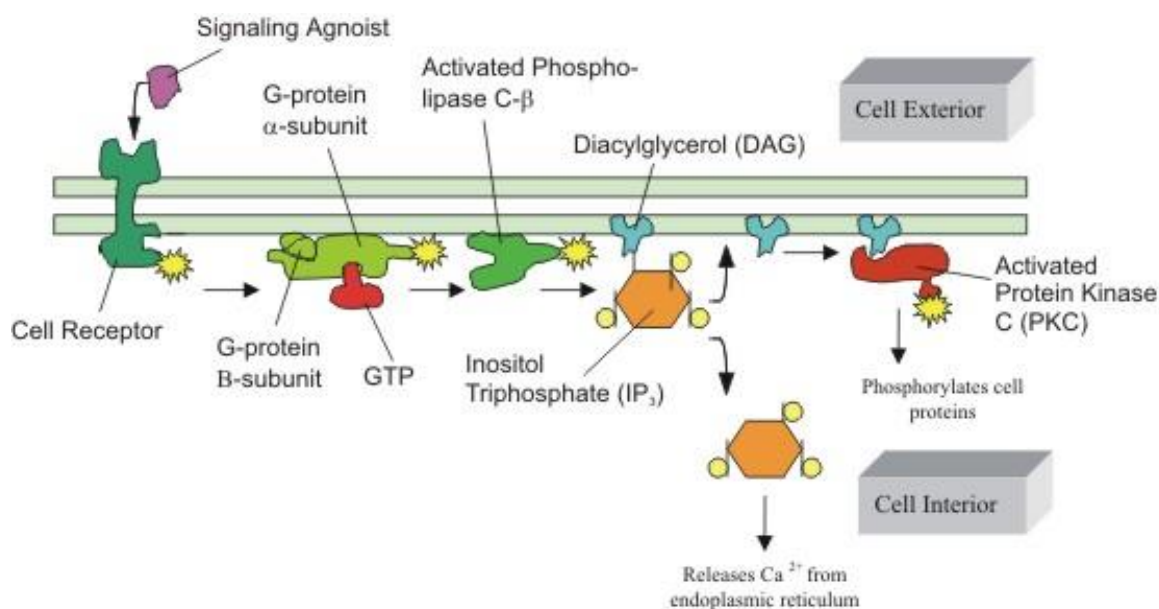


Figure 1.8 Protein kinase C activation process.³

³ Figure taken from http://www.ruf.rice.edu/~rur/issue1_files/barron.html

With phorbol being identified as a DAG substitute for the PKC activation in 1982 by Nishizuka,¹² kinases quickly became desired “targets” for pharmaceutical industries.²⁶ Without full understanding of the structure of enzymes investigations were focused on designing inhibitors targeting the catalytic region, which was believed to be the favoured binding site. Having now a better understanding of the structure of enzymes, we know that the C-terminal domain does not differ significantly between PKCs. As such a lot of selectivity problems have been encountered throughout the years yielding at times health threatening side effects of marketed drugs. A good example is Gleevec® (**1.8**) by Novartis.²⁷ Gleevec® (Imatinib mesylate, figure 1.9) is an anti-cancer drug with a relatively broad activity profile. Even though Gleevec® was a huge therapeutic success in treating chronic myelogenous leukaemia (CML), studies have shown that some patients developed congestive heart failure after being exposed to it.²⁸ In addition, these studies have shown that Imatinib mesylate triggered contractile dysfunction in treated mice.

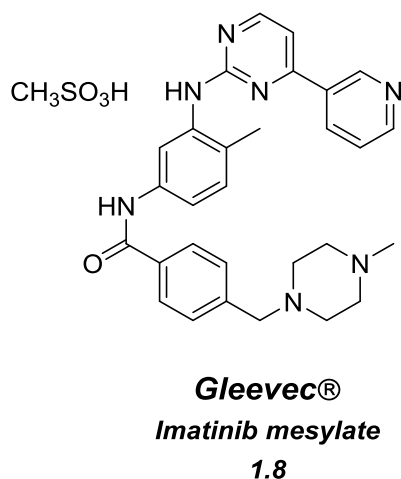


Figure 1.9 Gleevec®.

These side effects could be attributed to the non-specificity of imatinib mesylate – an important reminder of the need for highly selective inhibitors.

1.4 The Euphorbiaceae and Thymelaeaceae Plant Families

The Euphorbiaceae plant family, also called the spurge family contains about 300 genera and more than 8000 species with the largest genera being *Euphorbia*, *Croton*, *Jatropha* and *Sapium*. Compounds isolated from this plant family exhibit a large chemical diversity and are hence of great interest to synthetic organic chemists.²⁹

The Thymelaeaceae family, also known as the daphnane family consists of 90 genera and more than 500 species with *Gridia*, *Pimelea* and *Daphne* the largest amongst them. The Thymelaeaceae family not only consist of tumor promoting members, but also antitumor daphnane derivatives have been isolated and identified.²⁹

Euphorbiaceae and Thymelaeaceae have long been known for their versatile properties and thus have been applied in both, herbal and traditional Chinese medicine, respectively to treat common discomforts such as diarrhoea and migraine. Furthermore, the extracts and plants itself were used as anti-histaminic, anti-asthmatic and anti-leukemic agents among other. Aside from this, these plant families have been used as a major food source. To date cassava or *Manihot esculenta*, a toxic plant isolated from *Euphorbia* still remains one of the top three food sources in developing countries. Extreme care must be taken in the preparation of the cassava root as it contains cyanogenic glycosides (figure 1.10) that, if not properly removed can lead to an increased cyanide concentration in the body. As a consequence, cyanide intoxication and potential partial paralysis could occur.

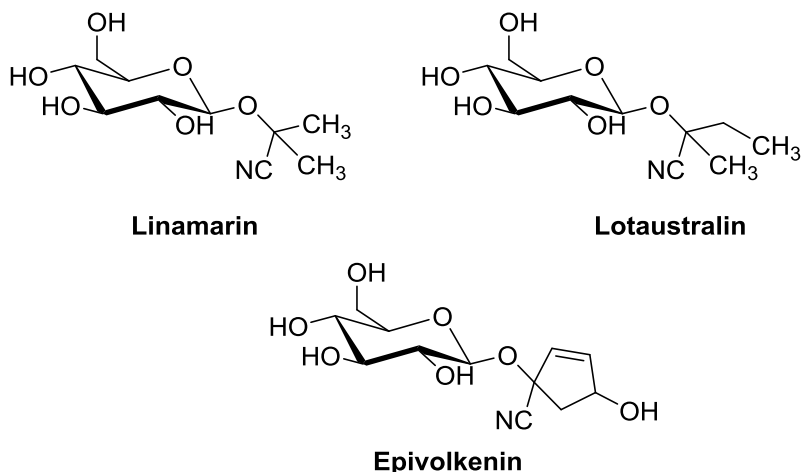


Figure 1.10 Examples of cyanogenic β-glycosides.

The Euphorbiaceae and Thymelaeaceae families have been of great interest for chemists and biologist since the 1940's after the isolation and characterisation of 12-*O*-tetradecanoylphorbol-13-acetate (TPA, **1.2**, scheme 1.2). TPA **1.2** was the first pure tumor promoting compound isolated from natural sources (*Croton tiglium*) and has held this position since its discovery. So far, more than 100 tumor promoting and pro-inflammatory phorbol derivatives have been characterised and are being used to further understand the biological pathway of cancer and pro-inflammatory diseases.

These two plant families comprise a vast amount of toxic diterpenes known as tigliane, daphnane and ingenane diterpenes with their parent polyol being phorbol (**1.1**), resiniferonol (**1.9**) (figure 1.12).

A third family, the ingenane diterpenes have been isolated from the *Euphorbia lathyris* L. species, with (+)-ingenol (**1.10**) as the parent polyol.

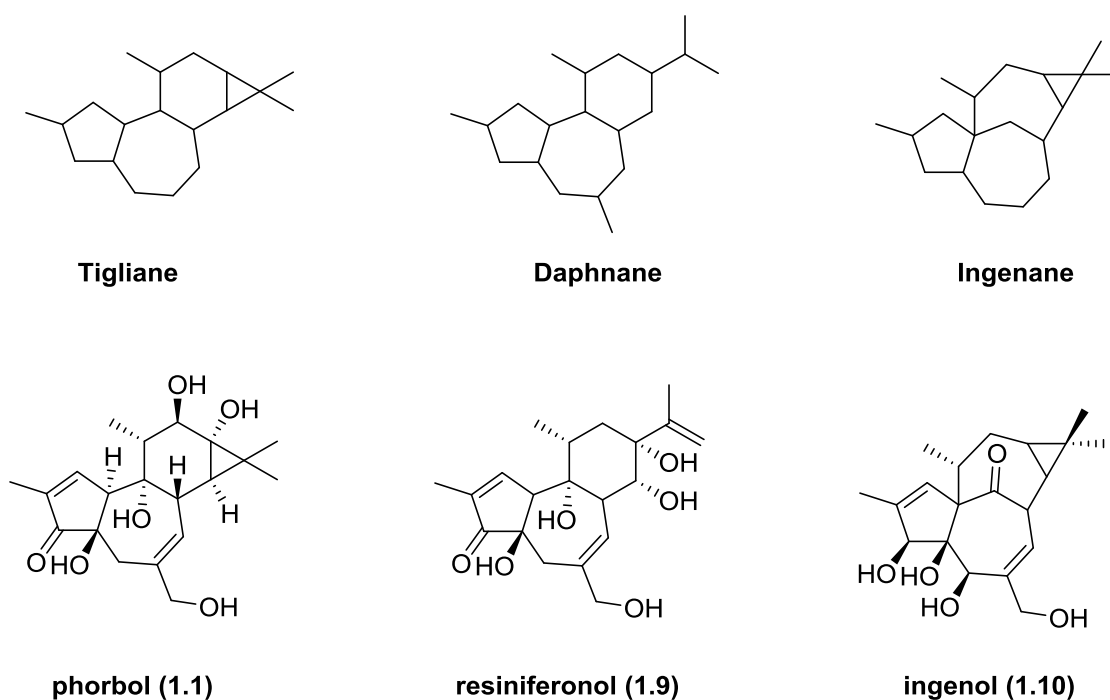


Figure 1.11 Three classes of diterpenes.

1.5 Phorbol: A Tigliane Diterpene

Since its isolation in 1935 phorbol (**1.1**)⁴ has had a meteoric rise to fame as a tumor promoter *via* protein kinase C activation and is now a “house hold” tool for cancer biologists worldwide.^{8a} The issue with investigating and evaluating phorbol (**1.1**) and its derivatives, in a biological sense, is that these complex molecules are limited only to natural sources (i.e. isolation from plant material), of which only some are commercially available. Furthermore, in addition to the supply issue these compounds are only available in one enantiomeric series (i.e. the natural (+)-phorbol), which in combination with that mentioned above places extensive limits on structure-activity relationship studies.

The highly potent biological activity of phorbol derives from their selective ability to activate isoforms of the protein kinase C family as they mimic the behaviour of 1,2-diacylglycerol (DAG), a lipophilic secondary messenger (discussed in detail in section 1.1, page 4), responsible for regulating cellular growth.

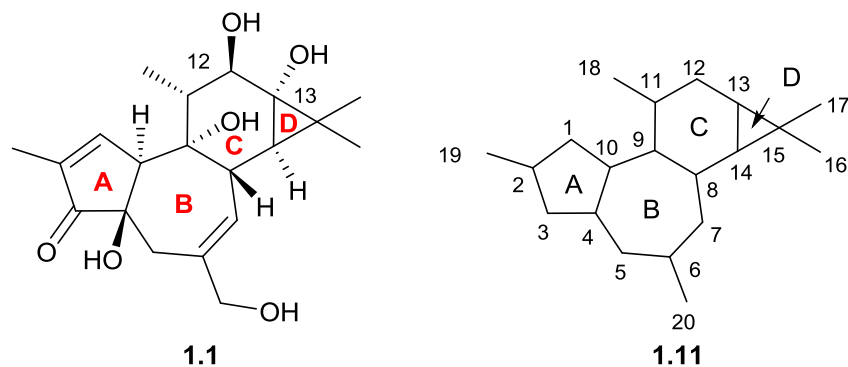


Figure 1.12 Tiglane diterpenes and their numbering system.

The tiglane scaffold of phorbol as shown in figure 1.13 is a fused tetracyclic system with a five-membered A ring, a seven-membered B ring, six-membered C-ring and the cyclopropane moiety designated as ring D. It is a highly oxygenated tetracyclic system with the C-ring system hosting six consecutive stereocentres. *Trans*-annulation between the A and B ring is crucial for phorbol activity as its *cis*- counterpart (4 α) was shown to be entirely biologically inactive. Furthermore, the C-4 hydroxyl group has shown to be pivotal for hydrogen bonding. It has been shown that replacement of the latter for a methyl group leads to a complete loss of activity.³⁰

According to Blumberg *et al.*³¹ the main oxygens that perform hydrogen bonding with the enzyme are located at C-3, C-4 and C-20, with the latter acting as a donor and acceptor respectively. Furthermore, it was suggested that C-9 and C-13 are not hydrogen bonding to the kinase itself but rather form intramolecular hydrogen bonding.

Another representative of the tiglane diterpene family is prostratin **1.12** (figure 1.14).³² Initially used to treat hepatitis by a Samoan healer, prostratin is now in phase 1 human clinical trials for the fight against AIDS. Mostly, these derivatives and analogues are prepared synthetically from the isolated parent polyol phorbol (**1.1**). Of course if a feasible synthesis was available to these systems more drugs could potentially be identified.

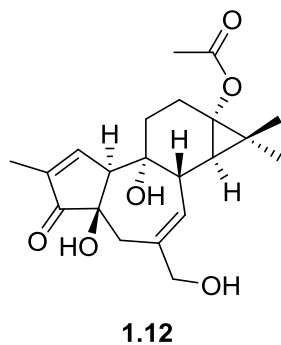
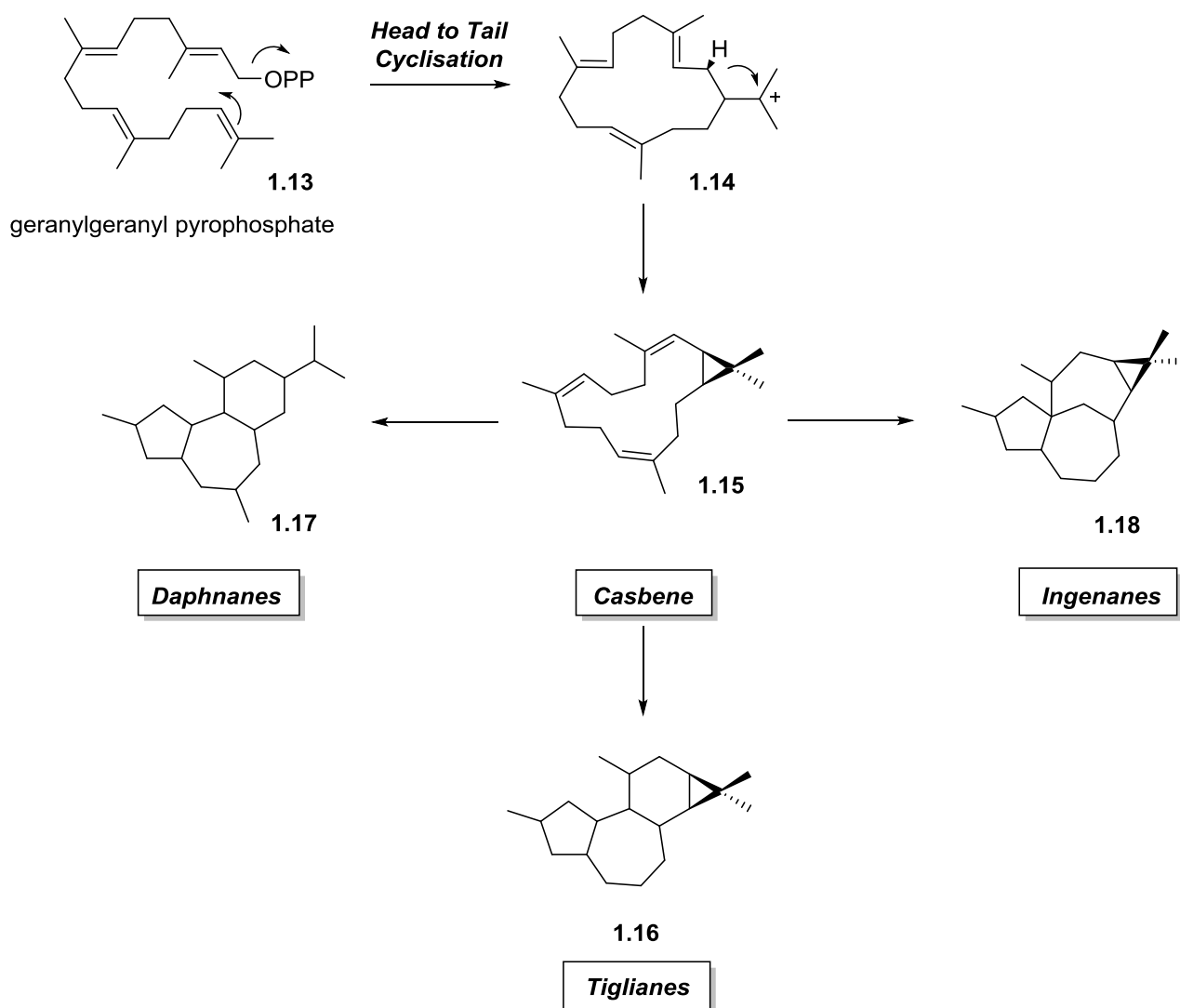


Figure 1.13 Prostratin

1.6 Biosynthesis

The biosynthesis of the tigliane, ingenane and daphnane diterpenes is still reserved.³³ A large number of diterpenes are known from the Euphorbiaceae plant family including mono-, di-, tri- and tetracyclic compounds. While many di- and triterpenoids as well as steroids are biosynthetically derived from a concertina-like cyclisation of geranylgeranyl pyrophosphate (GGPP) as shown by Banthorpe and Charlwood, it was initially believed that tiglianes, daphnanes and ingenanes could be derived *via* a similar route. However, with the existence of the monocyclic compounds such as casbane **1.14** (scheme 1.1), a head to tail cyclisation of GGPP was likely. Although casbane or other monocyclic compounds have not been isolated from the Euphorbiaceae plant family, they are known from other plant sources. Robinson and West isolated casbene **1.15** in 1977 from the castor oil plant *riccinus communis*,³⁴ a species of the spurge family and rationalised its origin to the head-to-tail cyclisation of GGPP initiated by a single enzyme. They suggested that a head to tail cyclisation is preferred as this leads to monocyclic compound **1.14** in only one step compared to a concertina-like cyclisation with the monocycle being accessed in many steps.

Head to tail cyclisation initiated by the enzyme *casbene synthase* provides carbonium intermediate **1.14** followed by the cyclopropane ring closure and stereospecific hydrogen loss at C-1 of GGPP to provide casbene **1.15**. Different enzyme classes then rearrange **1.15** into the various skeletons with elegant atom economy.

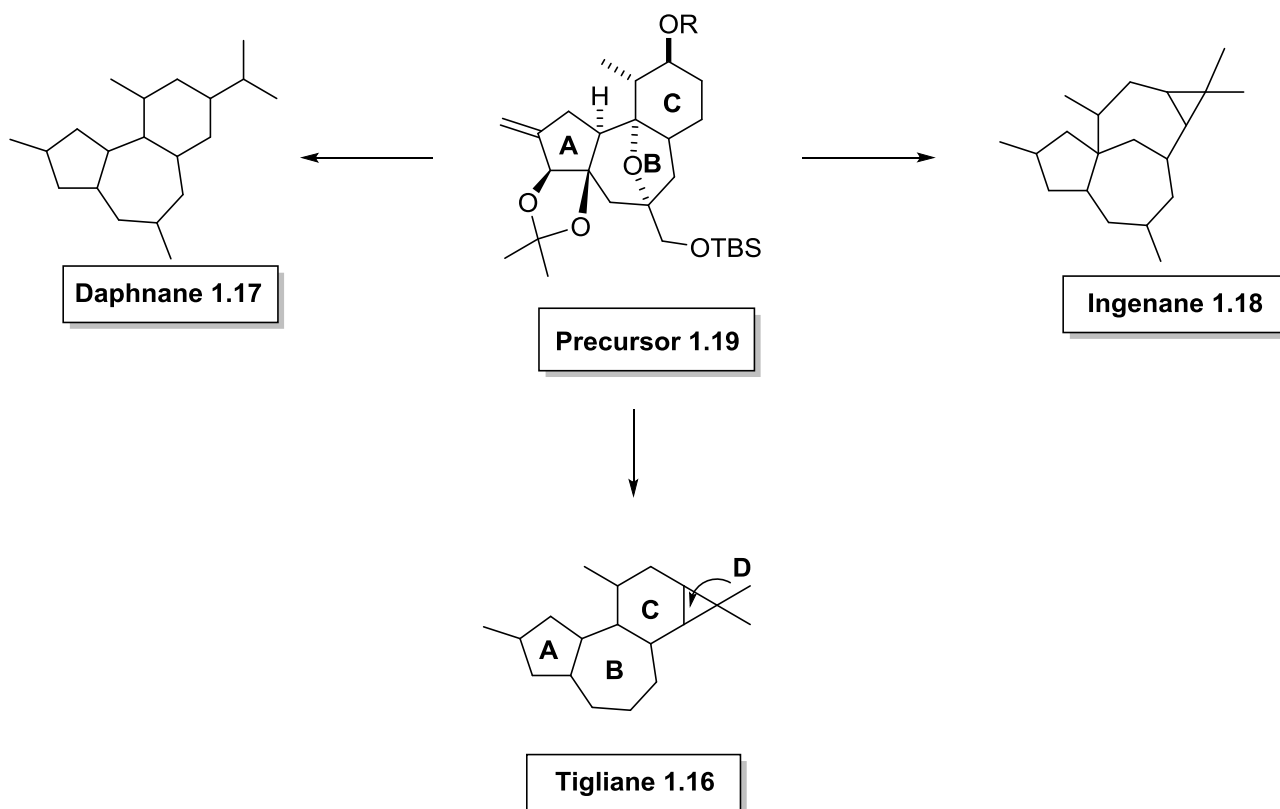


Scheme 1.1 Biosynthetic pathway to tiglane, daphnane and ingenane diterpenes.

1.7 Previous Synthetic Strategies

Considering the attention received by phorbol and related diterpenes, due to their broad range of biological activities and structural complexity, their chemical syntheses still remain a challenge today. To date, 76 years after initial isolation⁴ and 49 years after characterisation,³⁵ a concise and atom economical synthesis of phorbol or derivatives has yet to be achieved. Numerous efforts towards the synthesis of phorbol have been made to date. Amongst these, various ingenious strategies have been employed in the construction of the tiglane core. However, the difficulty in achieving absolute stereocontrol and the introduction of functionalities to further elaborate the natural product have been major challenges. The majority of synthetic approaches have focussed

their attention on the synthesis of the ABC ring system **1.19** (scheme 1.2) in anticipation that this tricycle may serve as an advanced intermediate precursor in the synthesis of phorbol and related family members. The D-ring system is incorporated at a later stage in synthesis. It is worth noting here that this *gem*-dimethylcyclopropane moiety bears its own challenge in both its construction and stability throughout the following synthetic sequences.



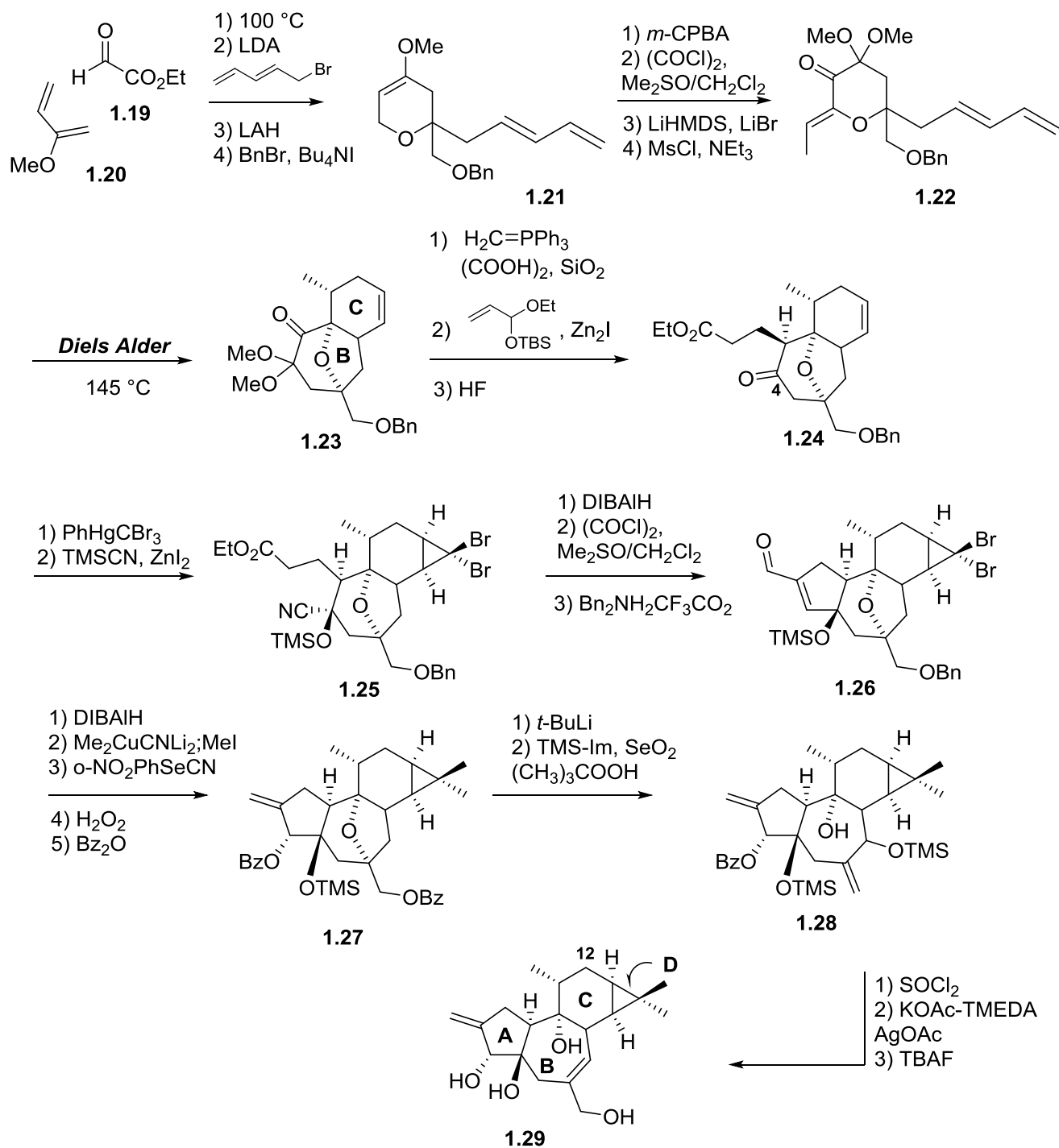
Scheme 1.2 Proposed precursor for three classes of diterpenes (tiglanes, daphnanes and ingenanes).

To date there are only two known total synthesis of phorbol both of which have been achieved by Wender *et al.*³⁶ In addition, a formal asymmetric synthesis has also been reported by Wender³⁷ and Cha,³⁸ respectively. Wender's first total synthesis, a pinnacle achievement in the field of organic synthesis at the time required 52 synthetic steps. His second generation synthesis required 47 steps, and the third, which investigated aspects of asymmetric incorporation, required 34 steps in a total synthesis of phorbol. This was a great achievement in that nearly 20 synthetic steps were removed in the final synthesis, however, 34 steps remains unattractive, especially considering an asymmetric total synthesis has yet to be achieved.

1.7.1 Wender's Efforts to Phorbol

Wender's first generation approach towards the synthesis of phorbol involved the intramolecular Diels-Alder reaction of readily available **1.22** in the construction of the BC ring system **1.23** (scheme 1.3).³⁹ He proposed key intermediate **1.23** could serve as a precursor to the tigliane and daphnane diterpenes respectively. In addition, through chemical rearrangement the third class of diterpenes – the ingenanes – could potentially be accessed.

Wender's studies began with a hetero Diels-Alder reaction of readily available starting materials ethyl glyoxalate **1.19** and 2-methoxybutadiene **1.20** and subsequent instalment of the diene side chain at C-6 was achieved by intermediate **1.21** with LDA and 1-bromo-2,4-pentadiene. Subsequent reduction of the ester at C-6 utilising LiAlH₄ followed by protection of the resulting alcohol as a benzyl ether afforded **1.21**. Selective oxidation with *m*-chloroperbenzoic acid followed by Swern oxidation prepared for the introduction of the ethylidene moiety to afford **1.22**. Upon heating, the latter underwent an intramolecular Diels-Alder reaction to tricyclic core **1.23**. In order to introduce the A-ring moiety it was necessary to install a ester side chain at C-10. This was achieved by an olefination/hydrolysis sequence followed by reaction with acrolein ethyl acetate in presence of zinc iodide to afford **1.24**. The D-ring subunit was then constructed utilising phenyl(tribromo)mercury (Seyfert's reagent)⁴⁰ followed by introduction of the stereocentre at C-4 *via* kinetically controlled addition of cyanide to provide **1.25**. Intramolecular aldol reaction of **1.25** finally installed the A ring. With the tigliane core in place further synthetic manipulations were carried out as outlined in scheme 1.3 to afford **1.29**. This tigliane system incorporated seven of the required eight stereocentres of TPA (**1.2**) and was the first tigliane core system to be synthesised.



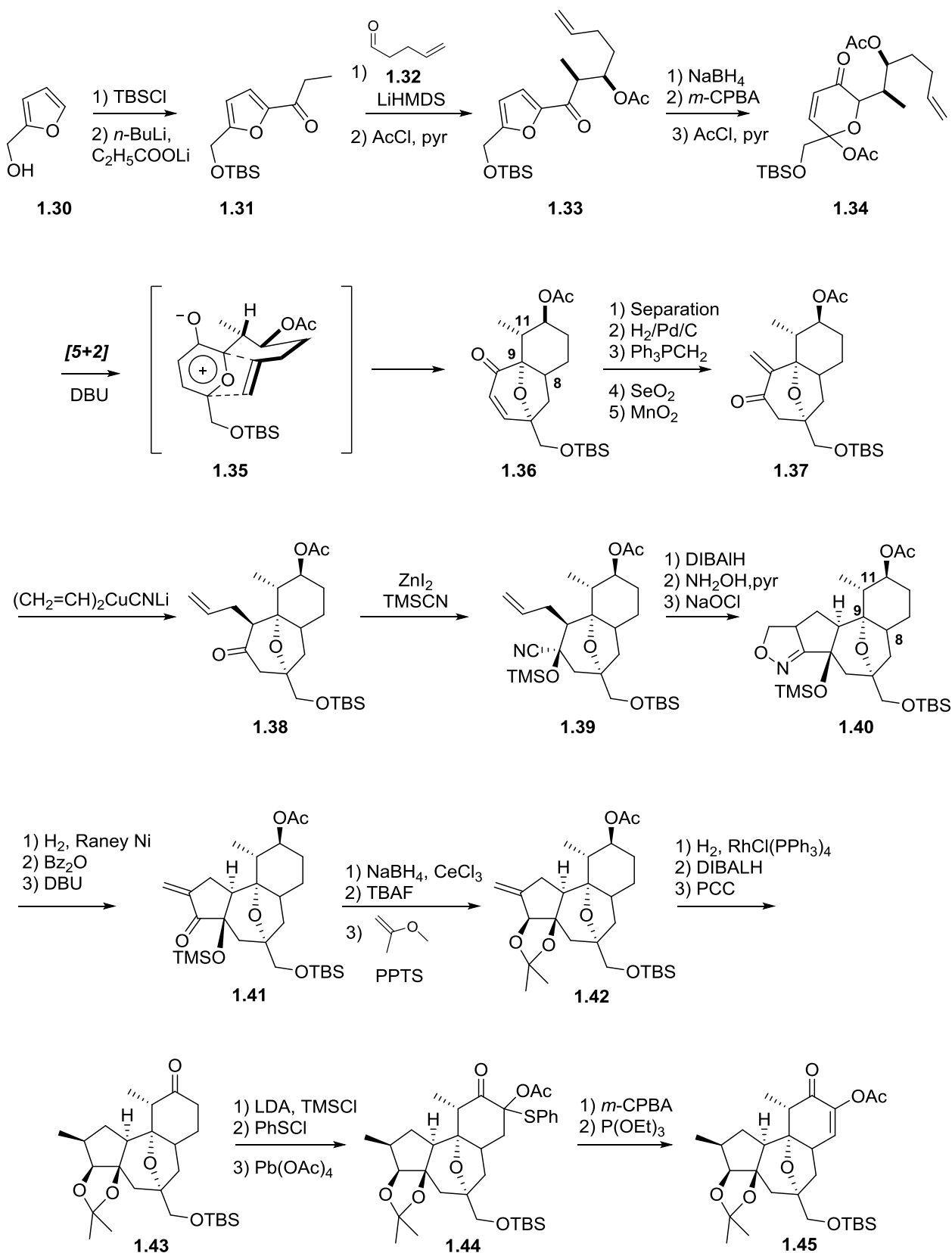
Scheme 1.3 Wender's first approach to the tigiane core.

However, this strategy had its shortcomings in regard to further installing necessary functionalisations at C-12 and C-13 in order to complete the synthesis of phorbol.

Three years later, in 1989, Wender *et al.*³⁶ provided a newly developed synthetic route for the assembly of an altered BC ring system **1.36**, ultimately leading to the first total synthesis of (+)-phorbol **1.1** in 52 steps (scheme 1.4). Synthetic investigations gave direct access to the new BC ring system by means of an intramolecular oxidopyryllium [5+2] cycloaddition reaction.

The starting point of Wender's synthetic studies was the inexpensive, commercially available furfuryl alcohol **1.30**. Protection as a silyl ether followed by acylation at the 5 position using lithium propionate gave rise to compound **1.31**. Subsequent aldol addition of the resulting enol with 4-pentenal afforded **1.33** as a diastereomeric mixture (2:1 erythro: threo). The cycloaddition precursor **1.34** was then accessed by furan oxidation utilising *meta*-chloroperbenzoic acid. Treatment of **1.34** with 1,8-diazabicycloundec-7-ene (DBU) gave access to the BC ring system in one synthetic operation *via* a [5+2] oxidopyryllium cycloaddition. This powerful reaction proceeds in 92% yield with complete selectivity in regard to the stereocentres at C-8, C-9 and C-11. The tether connecting the alkene and pyryllium moiety form a chair-like transition state as shown in **1.35** directing the C-11 methyl moiety into the equatorial position consequently leading to a minimal steric interaction between the methyl and the C-10 oxygen. Thus the chirality installed at the C-11 position conveniently controls the stereochemistry at C-8 and C-9.

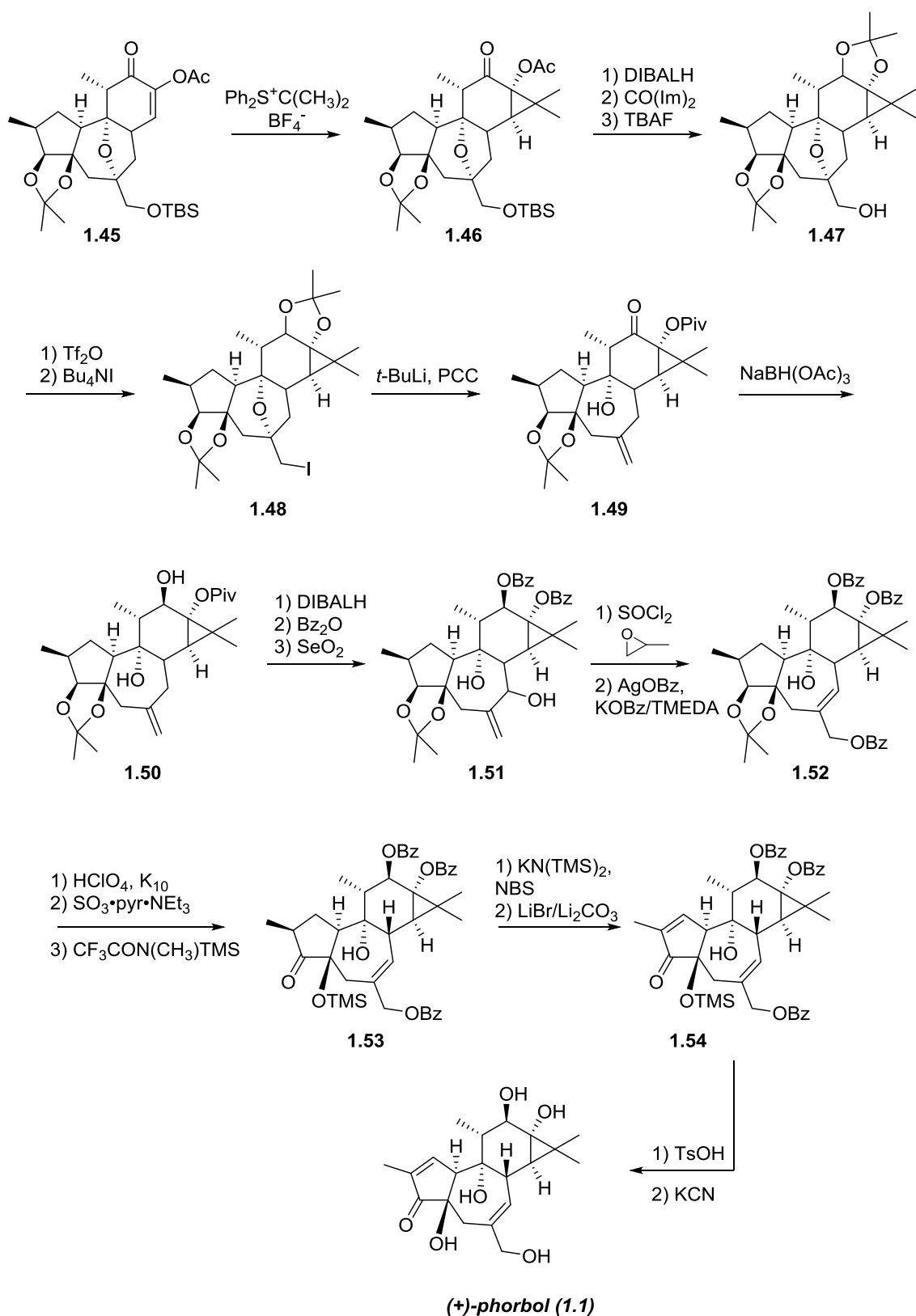
At this stage chiral chromatography afforded the desired enantiomer. Successive hydrogenation and Wittig olefination followed by oxidation installed the ketone at C-4 position (**1.37**). Conjugate addition of vinyl cuprate followed by kinetic addition of cyanide to the less sterically encumbered face of the C-4 carbonyl group gave **1.39**. A nitrile oxide cycloaddition of the latter then provided **1.40**, which after hydrogenation followed by dehydration utilising benzylation and DBU-catalysed elimination gave **1.41**. In order to avoid unwanted side-reactions of the highly reactive A-ring, a sequence of Luche reduction, desilylation and ketal formation utilising 2-methoxypropene and pyridinium *p*-toluenesulfonate (PPTS) was performed to afford **1.42**. With the advanced ABC tricycle (**1.42**) at hand, Wender prepared for the construction of the D-ring. This was accomplished by introducing the double bond *via* a sulfoxide elimination reaction to afford **1.45** followed by the construction of the *gem*-dimethylcyclopropane utilising diphenylisopropyl sulfide (**1.46**, scheme 1.5).



Scheme 1.4 First half of Wender's first total synthesis of (+)-phorbol.³⁶

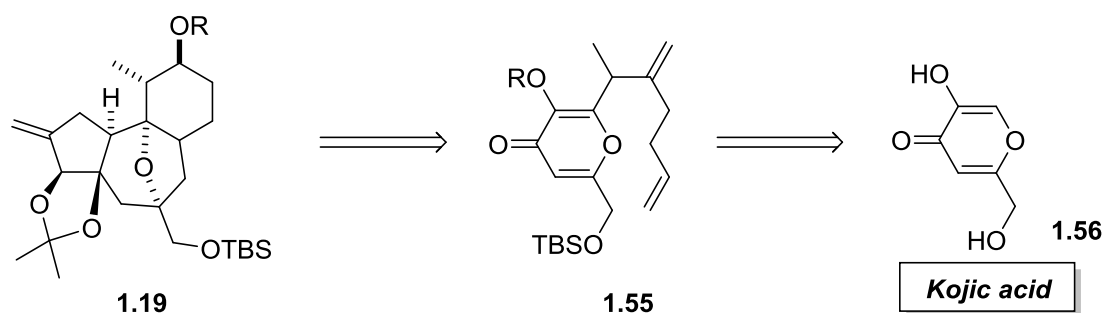
Next, Wender moved on to establish a C-12 ketone reduction stereoselectively. Unfortunately, exposing **1.46** to DIBALH and other common reducing agents did not lead to the desired stereochemistry. In addition, deprotection of the C-13 acetal occurred. Thus, he opted for protection of the C-12, C-13 diol as a carbonate. TBAF deprotection of the C-20 ether followed by treatment of the resulting triflic ester with Bu₄NI provided iodide **1.48**, which after exposure to *t*-BuLi and PCC gave the exocyclic double bond **1.49** and reoxidation of the C-12 alcohol to the ketone. However, NaBH(OAc)₃ was found to be the reducing agent of choice in order to selectively give β-alcohol **1.50** in excellent yield.

B-Ring functionalization was accomplished in 5 steps from **1.50** to afford the benzoyl ether at C-20. The A-ring was revealed *via* hydrolysis of the acetonide followed by re-oxidation of the C-4 alcohol and TMS protection of the C-3 alcohol to afford **1.53**. Introduction of the Δ^{1,2}-double bond was then accomplished *via* α-bromination/elimination sequence. Finally, global deprotection afforded the desired (+)-phorbol (**1.1**) in 86% yield.



Scheme 1.5 Second half of Wender's first total synthesis of (+)-phorbol.³⁶

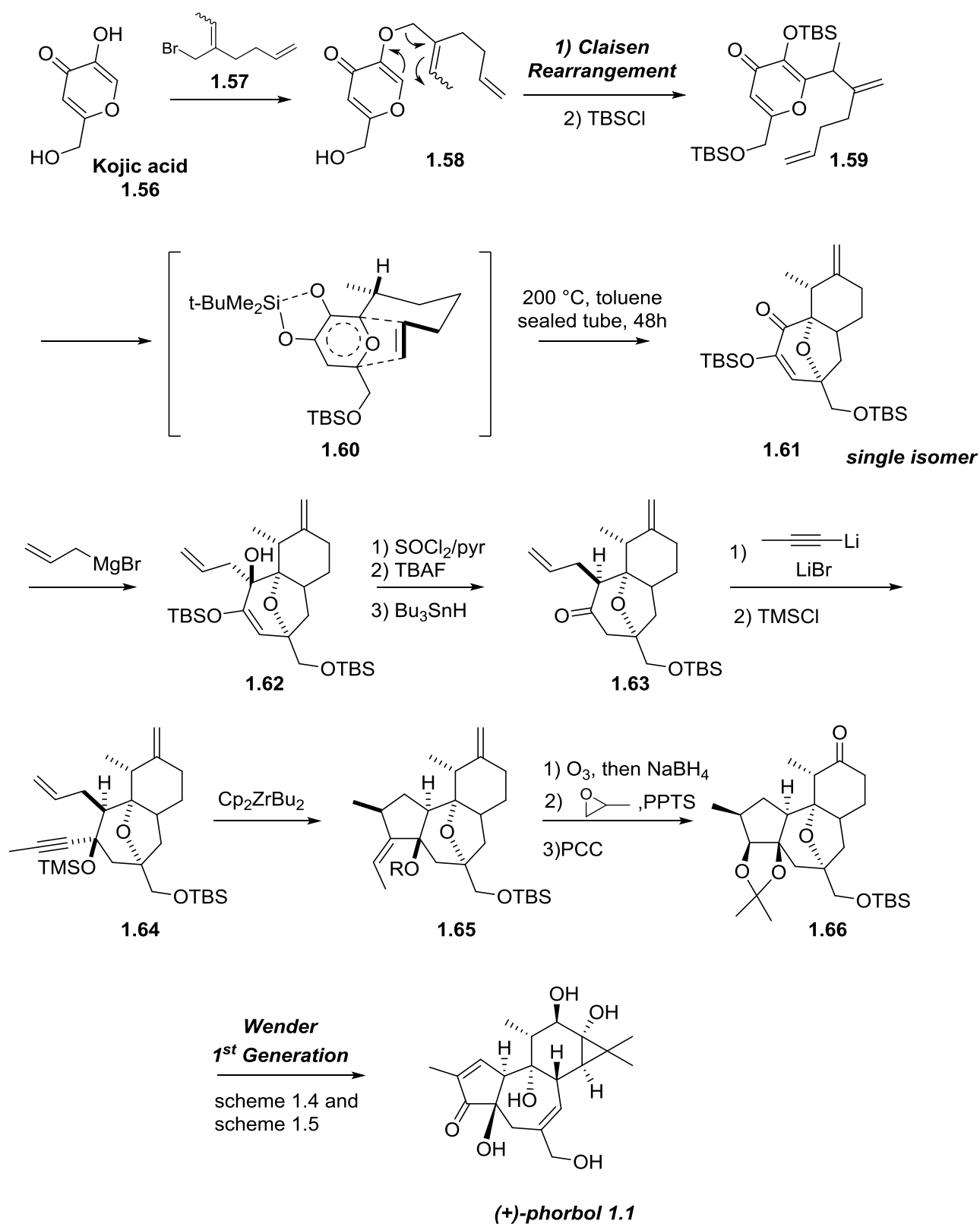
A second generation approach by Wender *et al.*⁴¹ was reported only a year later detailing a more direct route to the tricyclic core **1.19**. This led to the construction of **1.61** with a ketone imbedded at the C-4 position, ultimately simplifying the assembly of the ring A *via* stereocontrolled introduction of the allyl and propynyl groups.



Scheme 1.6 Retrosynthetic analysis of Wender's second generation approach to (+)-phorbol.⁴¹

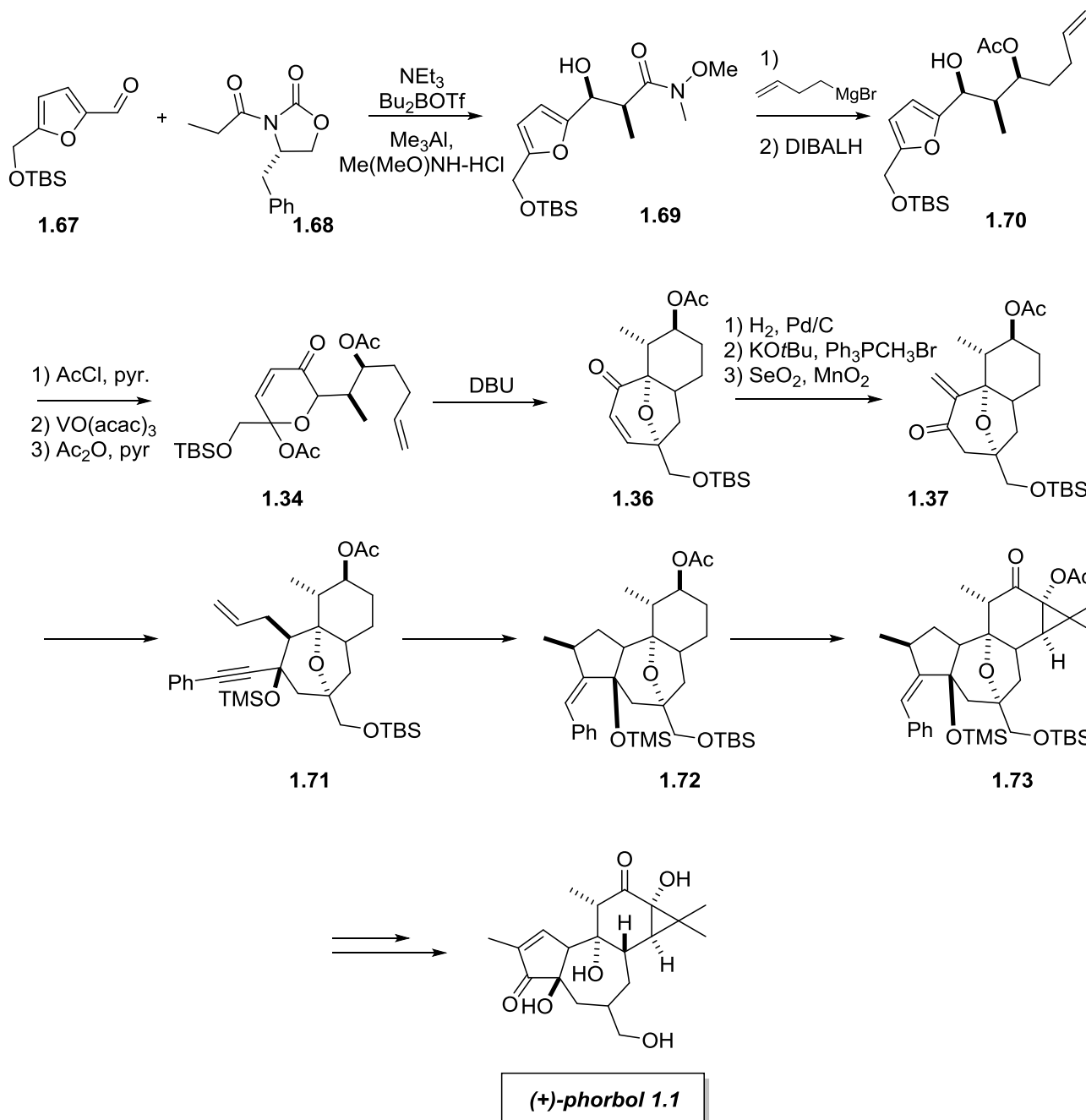
5-Hydroxy-2-(hydroxymethyl)-4H-pyran-4-one **1.56** also known as “kojic acid” was used as the starting material. Reaction with bromide **1.57** afforded **1.58** which then undergoes a Claisen rearrangement to **1.59**. Protection of the alcohols with TBSCl and heating in toluene provided the cyclised product **1.61** as a single isomer. In the same manner as described earlier for the first generation approach the tether forms a chair-like transition state forcing the methyl group into the equatorial position for minimal interaction with the C-10 oxygen thus, leading to the tricyclic core **1.61**. Successive Grignard reaction using allylmagnesium bromide, hydroxyl elimination, TBS deprotection and oxidation ultimately installed the ketone at C-4. This finally called for the stereocontrolled instalment of the propargyl group consequently allowing the concomitant zirconium mediated A-ring closure.

Wender then applied chemistry evolved from his first generation approach to afford the tricyclic **1.65** and used chemistry previously reported in order to install the D-ring system to afford (+)-phorbol **1.1** ultimately in a more direct and slightly shorter sequence.



Scheme 1.7 Second generation synthesis of (+)-phorbol (1.1).⁴¹

Wender's first asymmetric approach in 1997 was accomplished by synthesising the cycloaddition precursor **1.34** using *n*-propionyl oxazolidinone **1.68** as a chiral auxiliary with excellent diastereoselectivity (98% de) and excellent yield (96%).³⁷ In contrast to Wender's second approach to phorbol **1.1** (scheme 1.7), his asymmetric approach addressed many of the difficulties encountered thus leading to a more concise synthesis of (+)-phorbol (**1.1**).



Scheme 1.8 Wender's first asymmetric synthesis of (+)-phorbol.³⁷

1.7.2 Efforts by Cha

In 2001 Cha *et al.* reported a 41 step formal synthesis of (+)-phorbol (**1.1**) (scheme 1.9).³⁸ The key step to produce the oxo-bridged seven-membered ring **1.76** was accomplished by means of a [4+3] cycloaddition reaction of furan **1.74** and oxallyl, readily prepared from trichloropropanone **1.75**. Installation of the allyl and propynyl group at C-4 and C-10 prepared for the assembly of ring A. A BOM deprotection/oxidation sequence followed by Wittig olefination afforded **1.80**. Cha then installed the C-11 methyl group diastereoselectively utilising MeMgBr and CuBr•DMS as reported by Hruby to provide **1.81**. Subsequent intramolecular Heck reaction of the latter allows C ring formation and provides **1.83** as a single isomer. Utilisation of Wender's protocol for the construction of ring A finally affords (+)-phorbol (**1.1**).



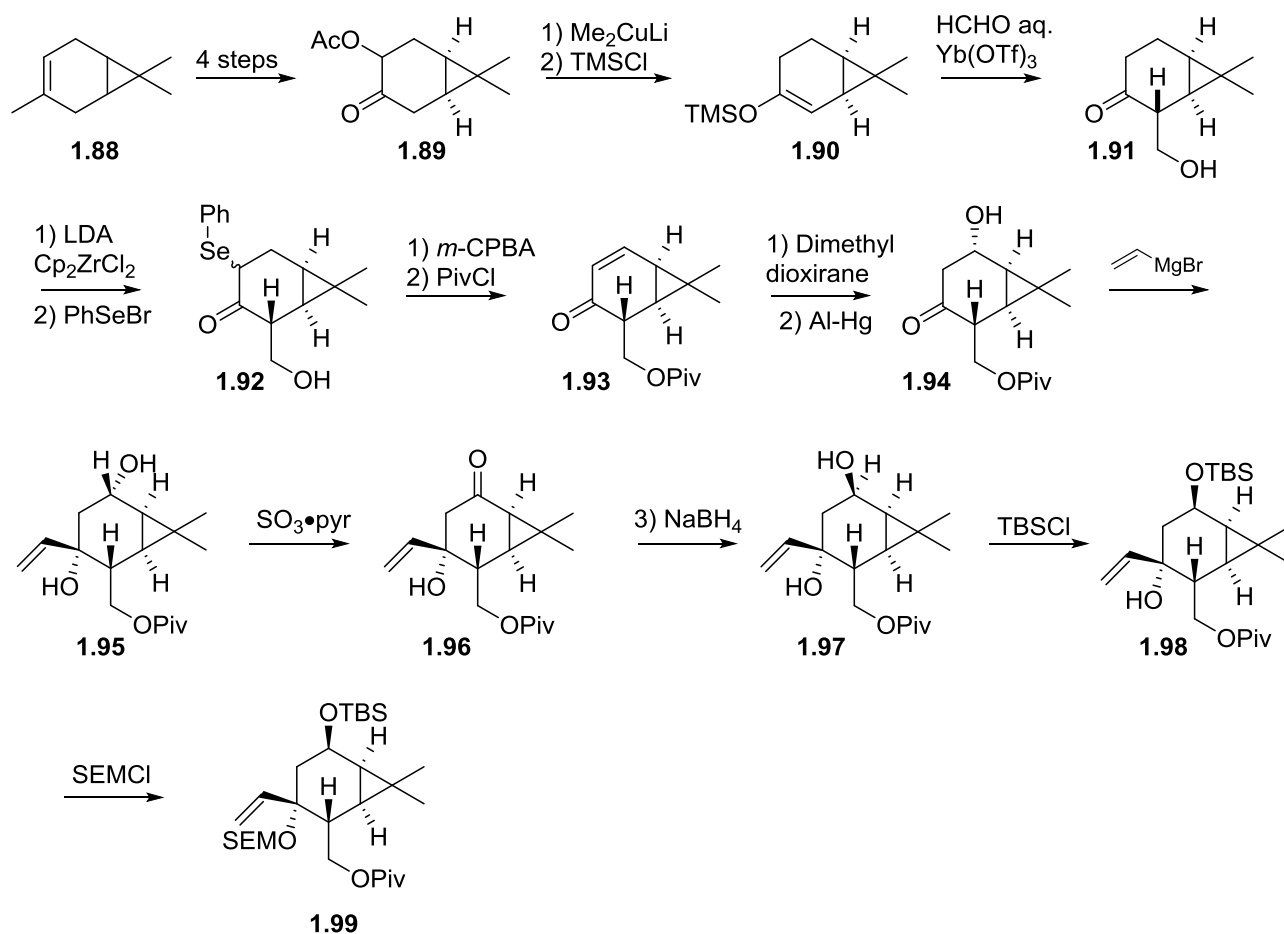
1.8 Methods describing effort towards the Tigliane Core

In addition to the pioneering work of Wender and Cha, a considerable number of investigations towards the tigliane, daphnane, and ingenane classes have been reported. In particular, methods developed by Shibasaki *et al.* by means of an intramolecular nitrile oxide cycloaddition reaction (scheme 1.10) and methods described by Dauben *et al.* whose synthetic approach is based on a stereospecific rhodium(II)acetate catalysed tandem cyclisation-cycloaddition reaction (scheme 1.11).

1.8.1 Shibasaki's Approach

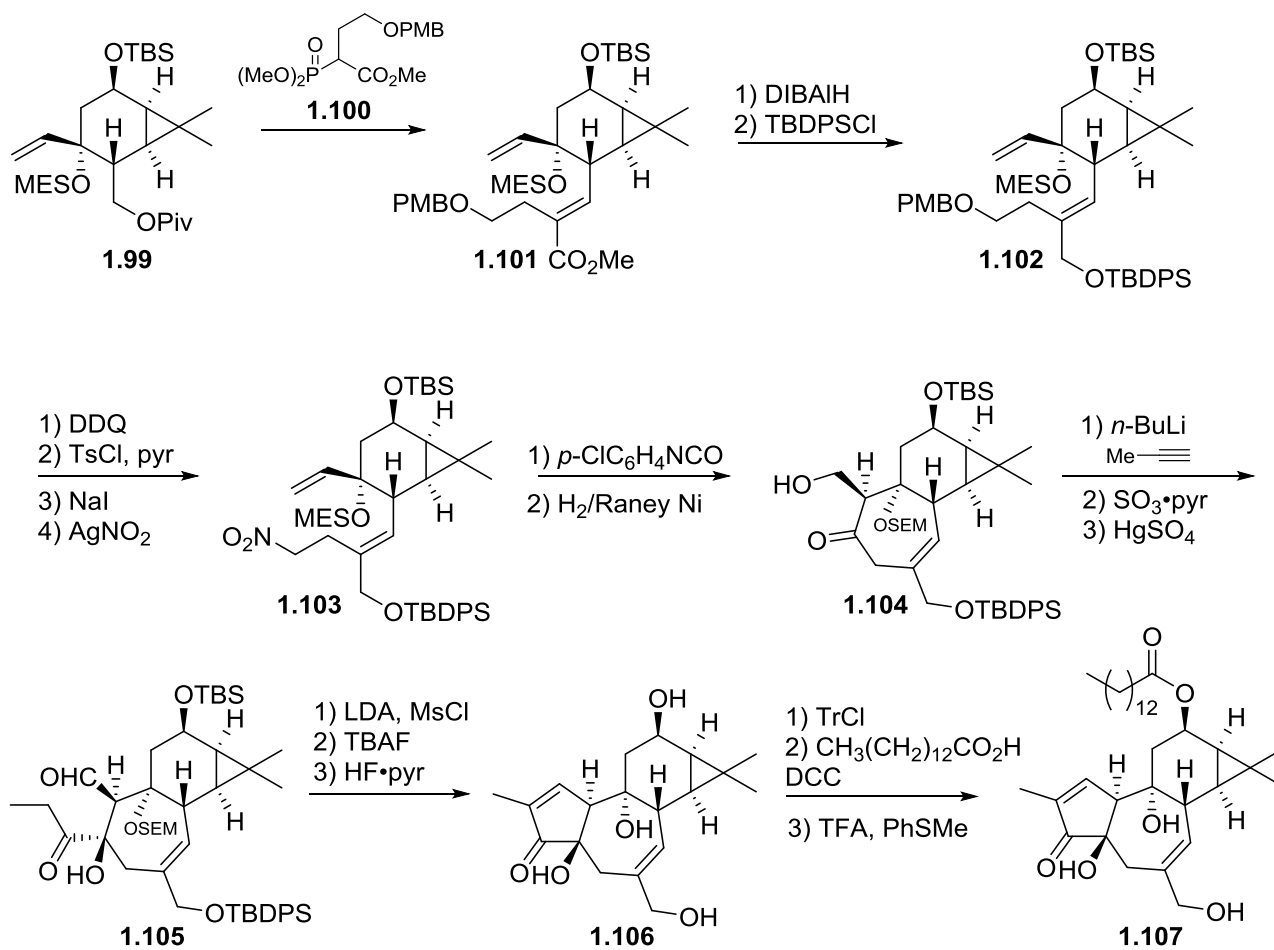
Shibasaki *et al.* had a longstanding interest in phorbol and its derivatives as protein kinase C activators. Over more than 10 years he designed and studied structural features on the parent polyol in order to provide a pharmacophore model for protein kinase C interaction. Early on, Nishizuka suggested that C-12 and C-13 ester chains are necessary for the hydrophobic interaction thus making it possible for phorbol to enter the membrane and as such activate protein kinase C.¹⁴ Wender's calculations (see figure 1.4) showed that in addition to the C-12 and C-13 esters, the C-20, C-3 and C-4 alcohols have significant impact on the interaction.¹⁵

Shibasaki *et al.*⁴² designed a general precursor for the synthesis of a variety of phorbol analogues for biological testing (**1.99**, scheme 1.10). The synthesis for precursor **1.99** started with the commercially available (+)-carene leading to **1.89** in 4 steps. Removal of the acetyl group utilising Me_2CuLi followed by enolisation and TMS protection of the resulting alcohol arrived at **1.90**. Next, instalment of the primary alcohol was accomplished with formaldehyde and $\text{Yb}(\text{OTf})_3$ to afford **1.91**. Compound **1.93** was then prepared *via* the formation of zirconium enolate followed by selenylation, which after oxidation with *m*-chloroperbenzoic acid installed the desired double bond at the $\Delta^{11,12}$ - position. Next, protection of the primary alcohol as a pivaloyl ether was followed by instalment of the C-12 alcohol moiety *via* epoxidation at the $\Delta^{11,12}$ - double bond and treatment with aluminium amalgam for a period of 4 days to afford alcohol **1.94**. The allyl group at C-9 was prepared by treating **1.94** with vinylmagnesium bromide. In order to achieve the desired stereochemistry at the C-12 alcohol, an oxidation/reduction sequence was necessary. The C-12 alcohol was then protected as a TBS ether followed by protection of the C-9 alcohol as a SEM ether giving rise to precursor **1.99**.



Scheme 1.10 Shibasaki's synthesis to precursor **1.99**.^{42a}

With the availability of precursor **1.99** the side chain at C-8 was accomplished *via* a Wittig reaction of phosphonium salt **1.100** and **1.99** to afford **1.101** as the *E*-stereoisomer. Reduction of the ester with DIBALH followed by TBDPS protection of the resulting primary alcohol arrived at **1.102**. Successive PMB deprotection, tosylation and nitration, using NaI as a catalyst, afforded **1.103** which was used for the intramolecular cyclisation to form ring B over two steps. Construction of ring A started with the instalment of an ethyl ketone *via* the corresponding alkyne. Aldol cyclisation and dehydration of the resulting alcohol using MsCl afforded phorbol skeleton **1.106**. Global deprotection followed by instalment of a long chain myristate group at the C-12 moiety finally afforded phorbol analogue **1.107**, which was evaluated biologically and compared to the natural tumor promoter PMA (see table 1.2).⁴³



Scheme 1.11 Shibasaki's synthesis of phorbol analogue 1.107.⁴³

It can be clearly seen that the phorbol analogue **1.107** presented shows inhibition at higher concentrations such as 1 and 10 μM . However, no biological response was observed at a nanomolar range.

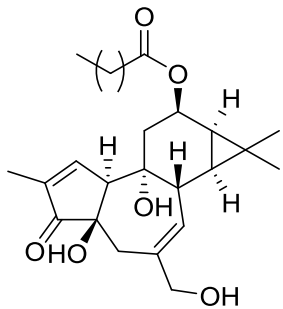
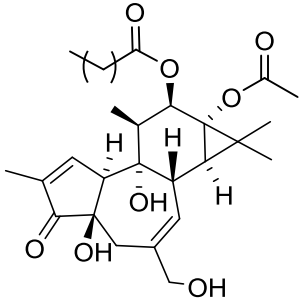
Entry	Compound	Concentration	Inhibition, %
1.107		10 nM	0
		100 nM	0
		1 μ M	30
		10 μ M	70
PMA		10 nM	40
		100 nM	80
		1 μ M	100
		10 μ M	100

Table 1.2 Effect of phorbol analogues on the inhibition of [^3H]PDBu binding to PKC.⁴³

In terms of biological inhibition of PKC the C-11 methyl group does not appear to be of significance in regard to the overall potency of the molecule. Shibasaki showed *via* biological studies of phorbol analogues missing a methyl or acetyl group that the C-13 acetyl moiety is of considerable more importance. In models lacking this moiety a significant decrease in potency is observed. Shibasaki went to great length in order to synthesise a number of phorbol analogues for biological testing. However, only **1.107** was shown to have inhibitory effects.

An important aspect of Shibasaki's work was the binding affinity of phorbol esters to the protein kinase C. The necessity of a highly specific interaction between DAG and PKC for PKC activation is well known. Thus, Shibasaki *et al.* designed a phorbol analogue, phorbol 12(1-pyrenebutyrate) 13 diazoacetate **1.108**,⁴⁴ possessing a photo labile diazoacetyl group at the C-13 position in order to gain a deeper understanding of the interaction between the amino acid residues of PKC isozymes with phorbol. Crosslinking experiments confirmed the importance of the C-13 moiety for a specific PKC-ligand interaction as it is located in close proximity to the PKC.

Moreover, introduction of a trifluorodiazopropionyl moiety as the photo labile group at C-13 (PPTD **1.109**, figure 1.15) would give further evidence for a specific interaction to the amino acid residues.⁴⁵ It is known that the trifluorodiazopropionyl group can react with thiols such as mercaptoethanol and dithiothreitol in a cysteine rich environment. Binding affinities of PPDA and PPTD were comparable to the natural PMA to specific isozymes of PKC.

Further agonist/antagonist studies with modifications of the C-12 side chain (**1.110** and **1.111**, figure 1.15) were undertaken by Shibasaki *et al.*⁴⁶ It was shown that **1.111** exhibits similar biological activity to the natural PMA. However, **1.110** has shown to have a two orders of magnitude lower affinity to the PKC. This is thought to be due to the hydrophilicity of the poly (ethylene glycol) C-12 side chain preventing the translocation of the complex to the membrane, where the protein kinase C activation occurs.

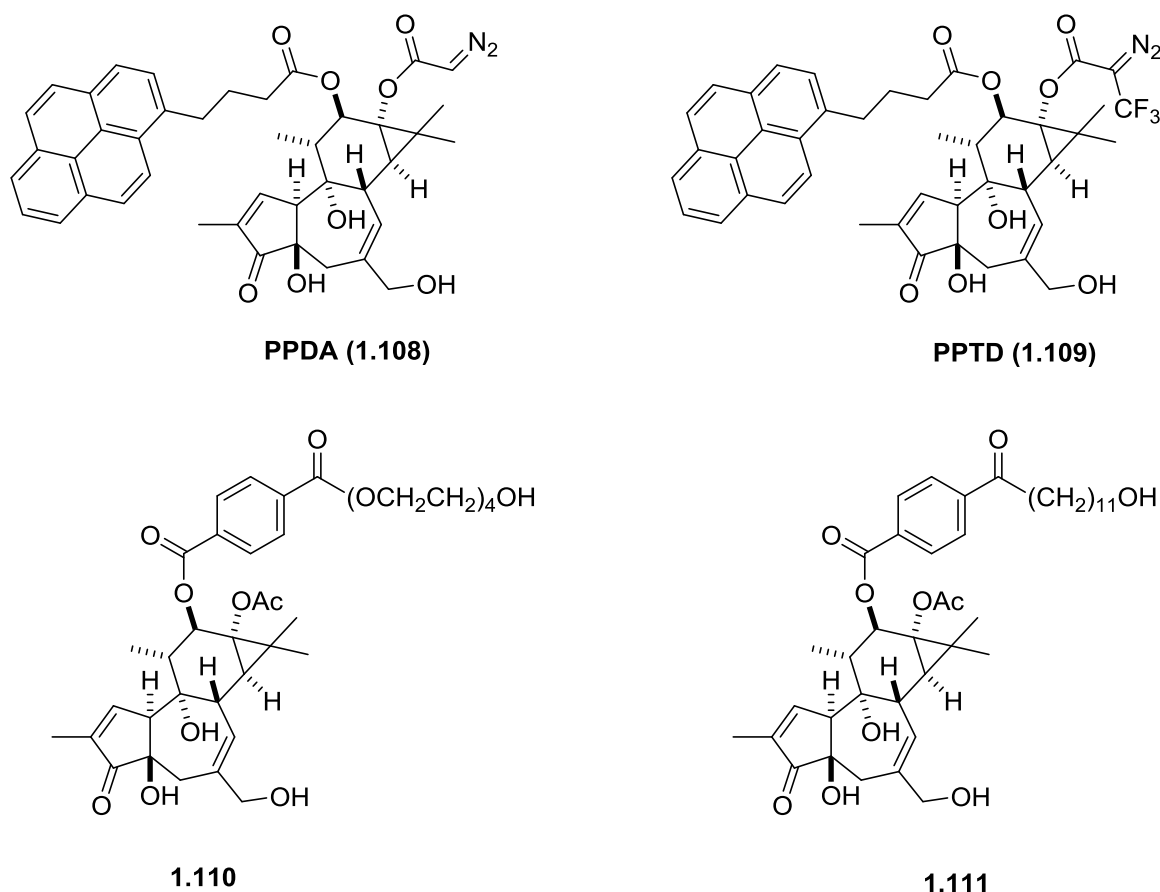
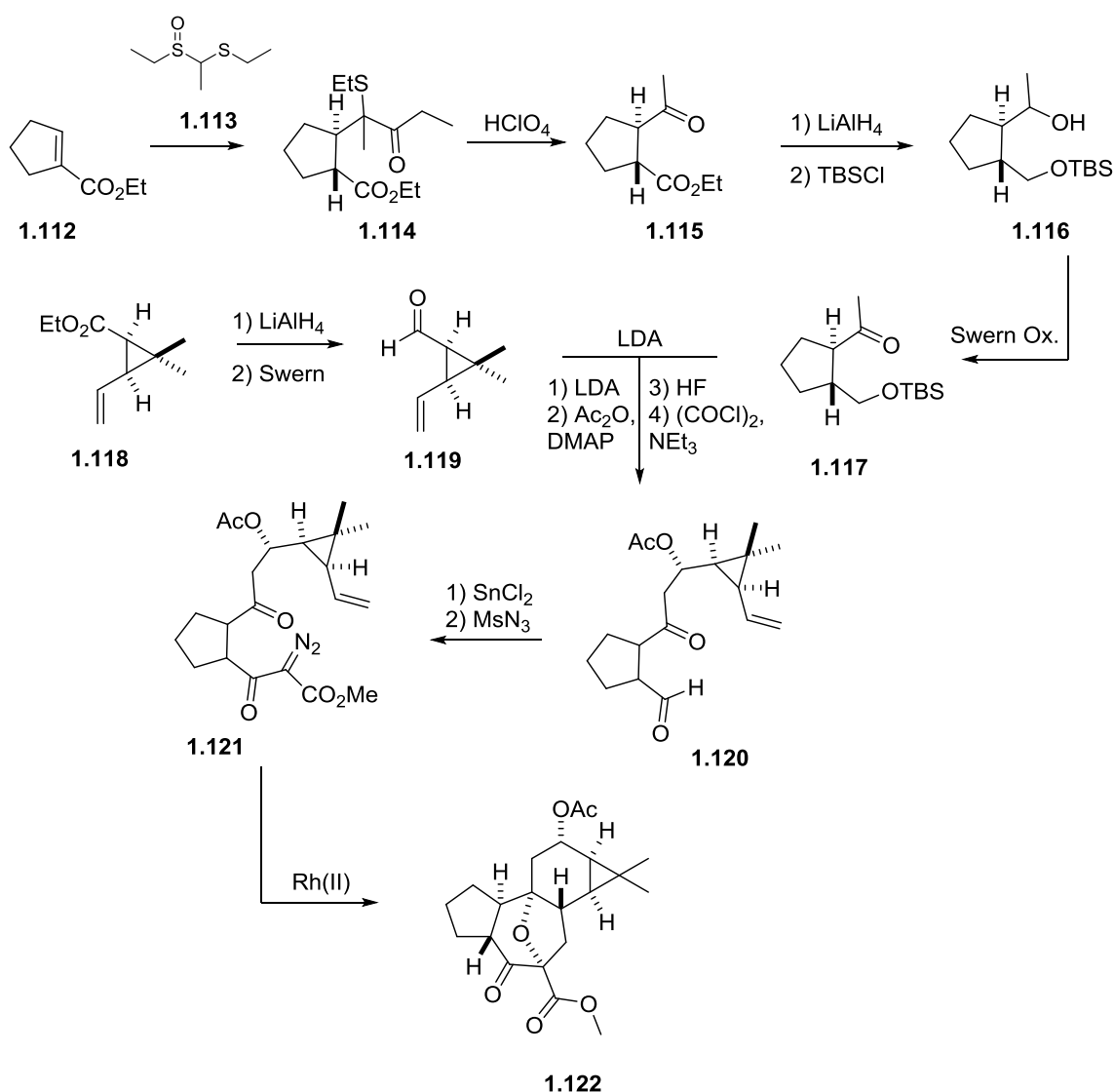


Figure 1.14 Photo-affinity ligands for PKC cross-linking experiments.⁴⁴⁻⁴⁵

1.8.2 Dauben's Efforts towards the Tiglane Core

Dauben *et al.* took a markedly different approach to constructing the tiglane skeleton (scheme 1.12). They envisioned formation of the BC-ring system *via* an intramolecular rhodium catalysed cycloaddition reaction of **1.117** with **1.119** with the A,D-ring in place.⁴⁷ Compound **1.117** could be constructed in five steps from ethyl (cyclopentene)carboxylate **1.112** and 1-(ethylsulfinyl)-1-(ethylthio)-ethane **1.113**. Conjugate addition of the latter two reagents followed by cleavage of the sulfoxide group provided **1.115**.

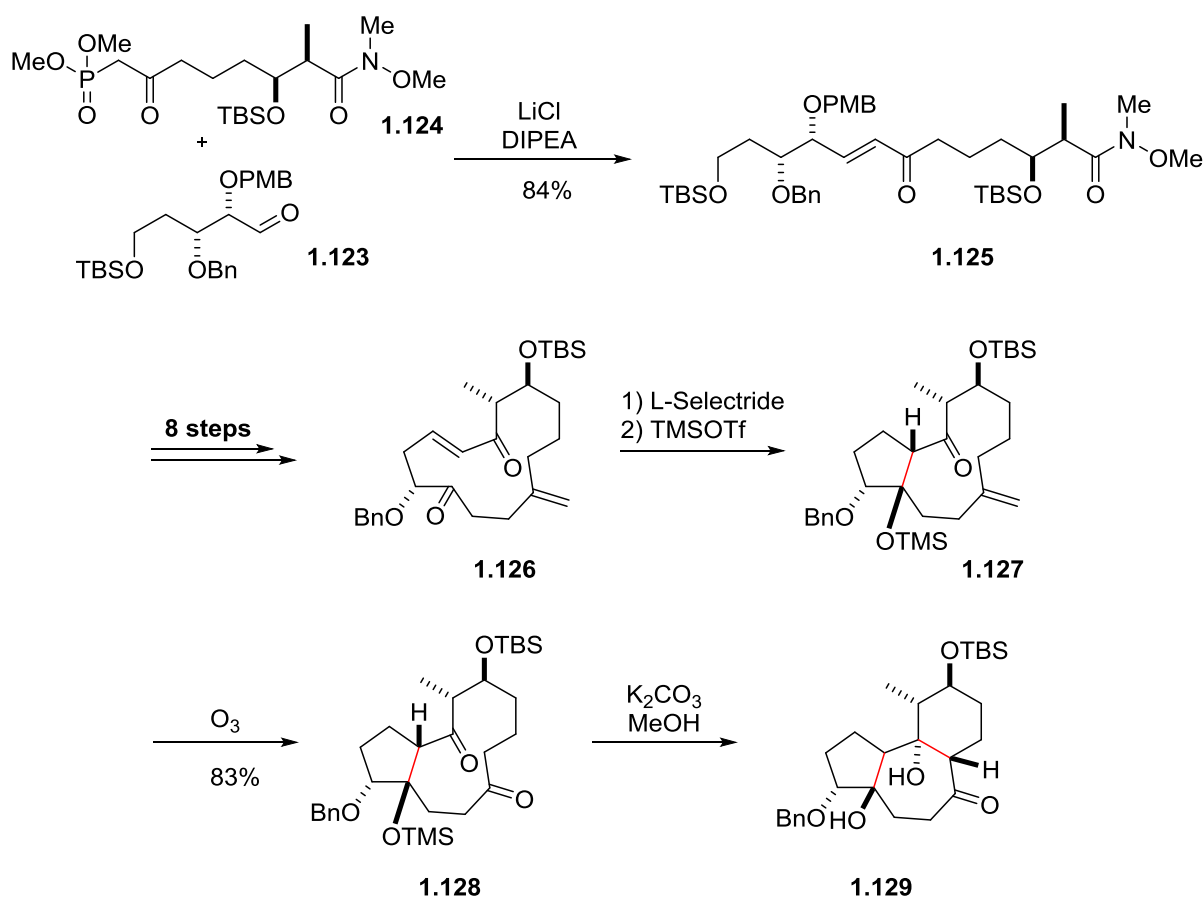


Scheme 1.12 Dauben's efforts towards the tiglane core **1.122**.⁴⁷

The second fragment **1.119** was prepared in a two-step reduction/oxidation sequence from ester **1.118**. Compound **1.120** was then obtained by aldol addition of **1.117** with aldehyde **1.119** followed by introduction of the diazo moiety *via* a diazo transfer approach to afford **1.121**. Intramolecular rhodium catalysed cycloaddition finally gave rise to the tigliane skeleton **1.122**.

1.8.3 Evans' Approach

More recently, the Evans group established a macrocyclic approach towards the tigliane and daphnane tricyclic core by means of a transannular aldol reaction (scheme 1.13).⁴⁸ The dimethylphosphonate **1.124** was accessed in five steps in an overall yield of 67% from benzyl-3-propionyl-2-oxazolidinone.



Scheme 1.13 Evans' approach towards the tigliane core.⁴⁸

Aldehyde **1.123** is obtained in 8 steps from tri-*O*-triacetyl-D-glucal. Subsequent coupling of the prepared starting materials **1.124** and **1.123** via a Horner-Wadsworth-Emmons reaction smoothly afforded *E*-alkene **1.125**. Further synthetic manipulations afforded the monocyclic compound **1.126** which was converted to the tricyclic tigliane core **1.129** via two consecutive transannular aldol reactions.

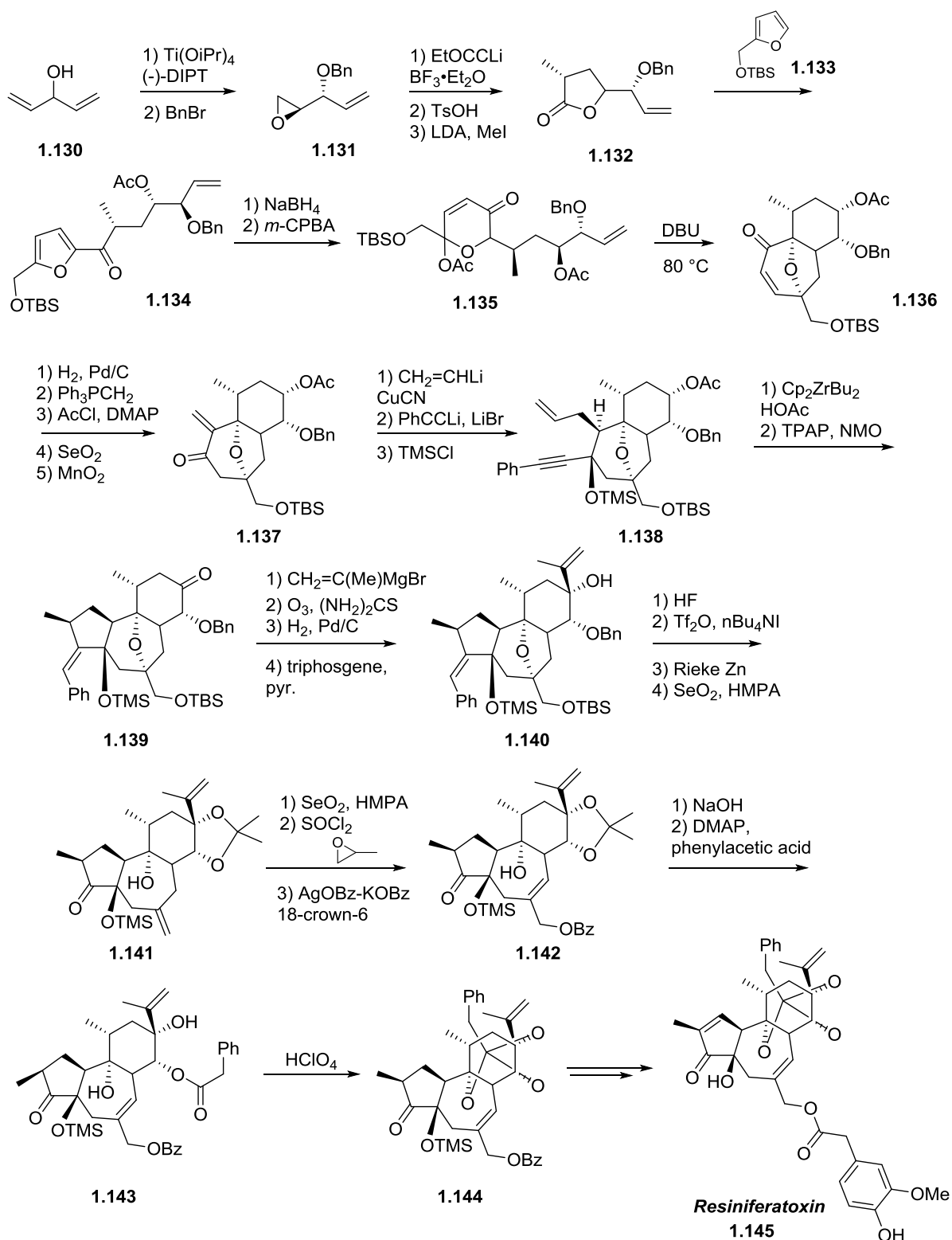
1.9 Synthetic Routes to Diterpenes Related to Phorbol

1.9.1 Inoue's Strategy towards the Daphnane Diterpene Resiniferatoxin

Resiniferatoxin (**1.145**, scheme 1.14) is a member of the daphnane family and was isolated from *Euphorbia resinifera*.⁴⁹ This tetracyclic diterpene bears a unique ortho ester functionality between C-9, C-13 and C-14 and has been widely studied as a potent inhibitor of the vanilloid receptor.⁵⁰ Wender *et al.* reported the first total synthesis of resiniferatoxin in 1997⁵¹ utilising previously developed chemistry for the synthesis of phorbol, i.e. oxidopyryllium cycloaddition reaction. Absolute stereochemistry was controlled in the first step of the synthesis via epoxidation of **1.130** with diisopropyltryptamine to afford **1.131** in 51% yield and 98% ee. Successive epoxide opening and acid catalysed lactone formation followed by introduction of the C-11 methyl moiety afforded intermediate **1.132**. Addition of TBS-protected furfuryl alcohol **1.133** gave rise to **1.134** which after ketone reduction at C-9 and furan oxidation utilising *m*-chloroperbenzoic acid afforded the oxidopyryllium cycloaddition precursor **1.135** in quantitative yield over two steps. The BC-ring was then accessed via the proposed cycloaddition utilising DBU in good yield (84%).

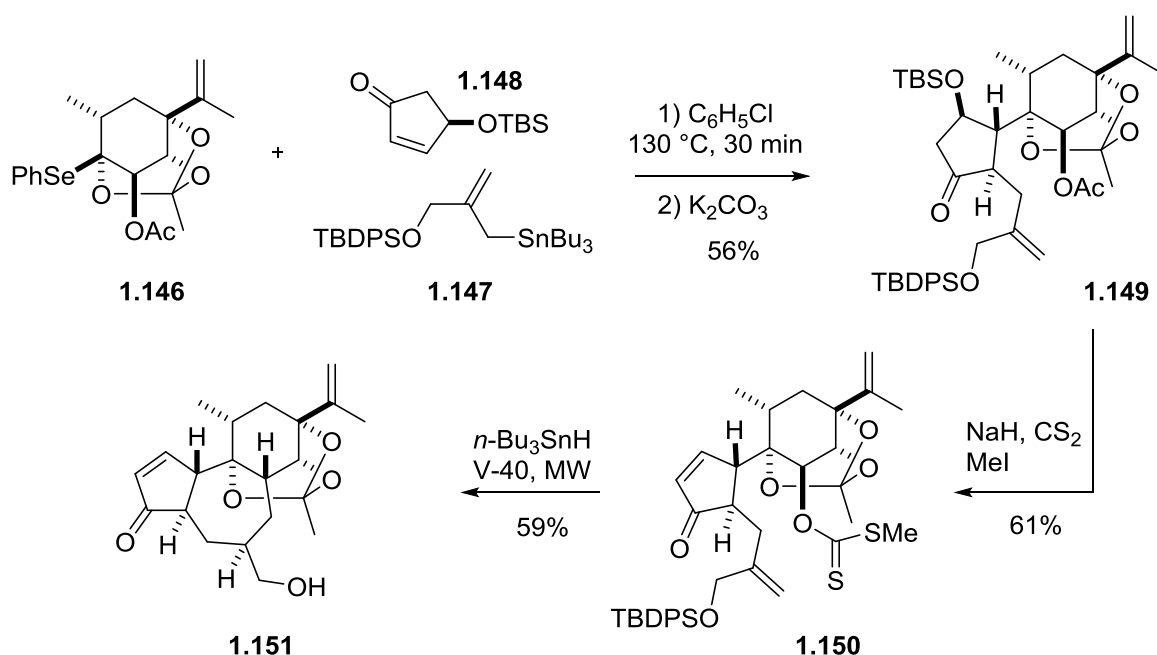
Wender's A-ring construction was then accomplished using zirconium-mediated chemistry reported for the total synthesis of (+)-phorbol (**1.1**) to provide **1.139**. The daphnane skeleton was achieved by introducing the isopropenyl moiety selectively utilising isopropenylmagnesium bromide attacking from the β -face of the C-13 carbonyl. Oxo-bridge opening occurs via the selective C-20 TBS deprotection followed by iodination of the resultant alcohol and iodo ether elimination utilising Rieke zinc to afford **1.141** in 39% yield over four steps. Ring B was then furnished with the desired C-20 alcohol protected as a benzyl ether. Following this, instalment of the phenyl ester at C-14 occurred, which by treatment under mild acidic conditions converted to ortho ester **1.143**. Introduction of the $\Delta^{1,2}$ -double bond via bromination/elimination sequence followed by successive

benzoylation at C-20 and global deprotection finally arrived at the first total synthesis of resiniferatoxin **1.145**.



Scheme 1.14 Wender's total synthesis of resiniferatoxin.⁵¹

Recently, a second approach to the complex core of resiniferatoxin **1.145** appeared in the literature.⁵² Inoue *et al.* accessed the daphnane core **1.151** via a concise radical coupling reaction, which involved three components (scheme 1.15). Firstly, the alkoxy bridgehead **1.146** prefunctionalised with the desired five stereocentres, the synthesis of which required 21 steps from commercially available materials. Secondly, the five-membered ring A **1.148** and thirdly, allyl stannane **1.147**.



Scheme 1.15 Inoue's approach to resiniferatoxin.⁵²

The three components are fused in an intramolecular radical reaction employing 1,1'-azobis(cyclohexane-1-carbonitrile) (V-40) in chlorobenzene to form the desired coupling adduct **1.149** in reasonable yield over two steps (56%). Further modifications prepared for the construction of seven-membered ring B utilising a xanthate function in a second radical reaction to afford **1.151**.

1.9.2 Baran's Total Synthesis of (+)-Ingenol

(+)-Ingenol (**1.10**, figure 1.12) is another important natural product that has attracted widespread efforts towards its synthesis. One derivative of ingenol, ingenol mebutate (**1.7**, Picato®, figure 1.16) is a FDA approved drug and as such its concise synthesis was highly desirable. Due to its very unique *in/out*-[4.4.1]bicyclododecane core, synthesis of ingenol has proven to be very challenging.

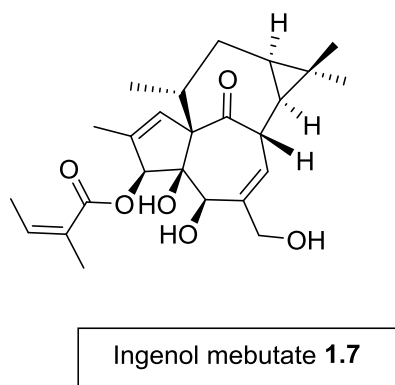


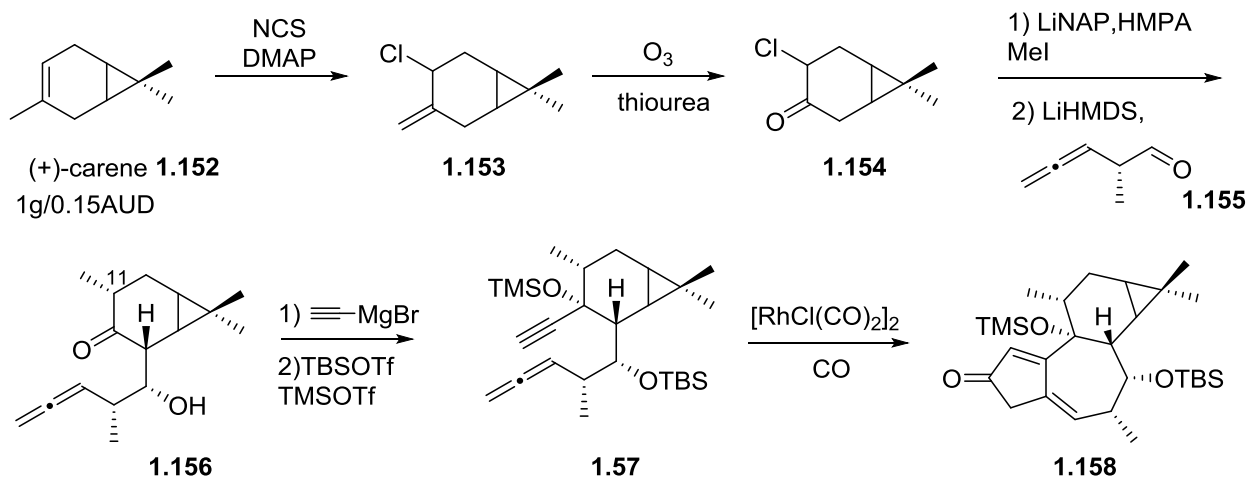
Figure 1.15 Ingenol mebutate (Picato®).

In 2002 Winkler⁵³ presented a racemic total synthesis of ingenol followed by an independent approach by Tanino⁵⁴ a year later. In 2004 Wood *et al.* reported the first asymmetric total synthesis of ingenol requiring 32 steps to complete.⁵⁵

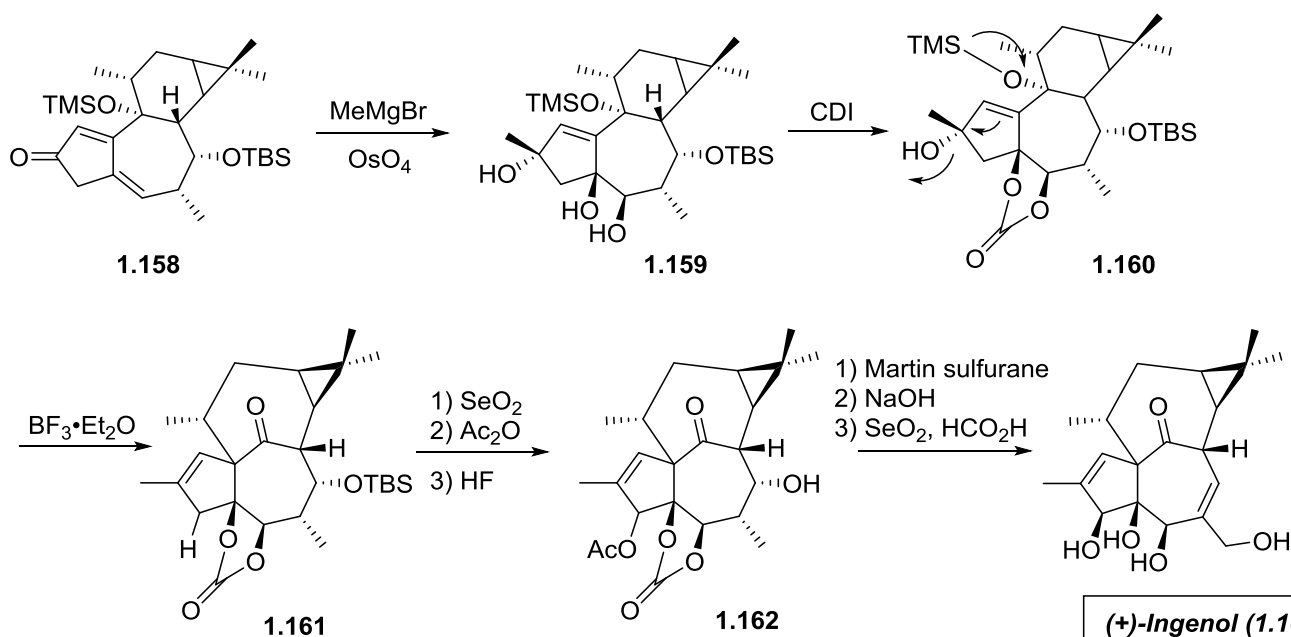
More recently, an elegant total synthesis of (+)-ingenol (**1.10**) requiring only 14 steps from commercially available (+)-carene (**1.152**) was published by Baran *et al.* as a collaborative effort with LEO Pharma (developer of ingenol mebutate, Picato®, scheme 1.16).⁵⁶ The key to this success lies in what is referred to as the cyclase and the oxidation phase, respectively. Drawing inspiration from nature Baran *et al.* constructs the carbon skeleton **1.158** (cyclase phase) followed by the oxidation phase to introduce necessary functionalities leading to (+)-ingenol (**1.10**) in an overall 1.2% yield.

Ortho chlorination of (+)-carene **1.152** followed by ozonolysis affords ketone **1.154**. Allene **1.156** can then be accessed as a single diastereomer in a one pot reaction *via* a halogen-metal exchange /alkylation sequence and subsequent aldol addition at C-8.

Cyclase Phase



Oxidation phase



Scheme 1.16 Baran's total synthesis of (+)-ingenol.⁵⁶

Grignard addition followed by double protection of C-9 and C-7 alcohols provided the precursor for the rhodium catalysed Pauson-Khand reaction which forms ring A and B, respectively and completes the cyclase phase. Next, installation of the C-11 methyl *via* Grignard addition was

accomplished. Within three steps of initiating the oxidase phase the ingenane core **1.161** was obtained. Further oxidative manipulations and deprotections then afforded (+)-ingenol (**1.10**). This was a great achievement for Baran *et al.* and LEO Pharma, however, utilisation of stoichiometric amounts of osmium tetroxide still remains an unattractive feature for the commercialisation and processing on large scale. Furthermore, this collaborative effort led to (+)-ingenol, thus introduction of the C-3 side chain is necessary for the synthesis of ingenol mebutate **1.7**.

1.10 Project Background and Aim

The Williams group has had a longstanding interest in the vibsanan family of natural products successfully synthesising a number of the family members (figure 1.17).⁵⁷

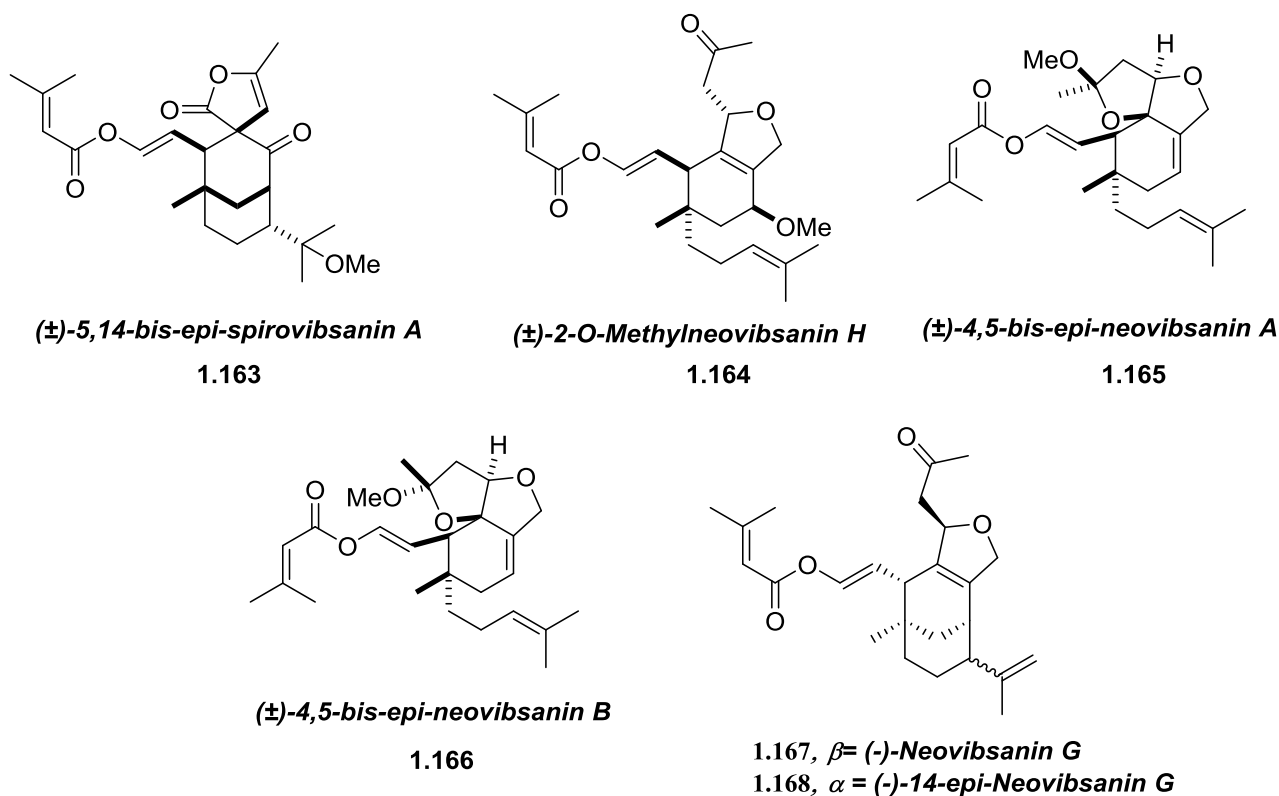
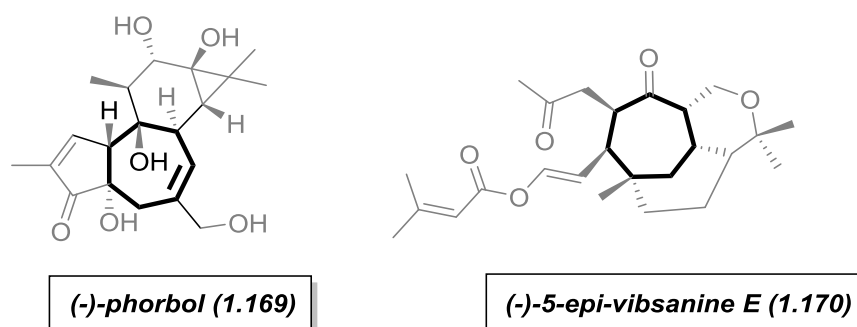


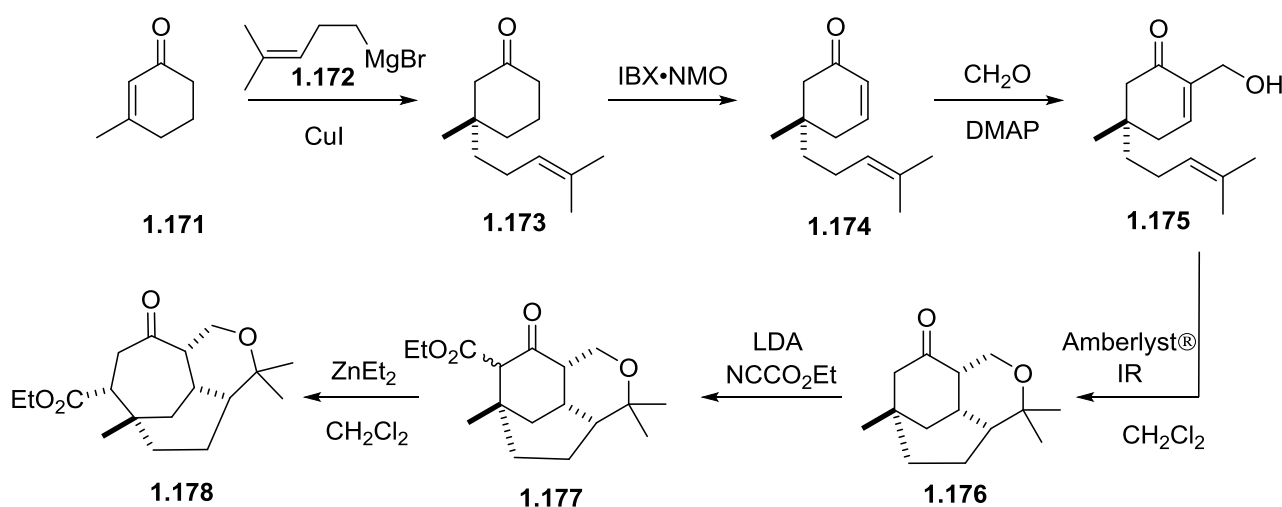
Figure 1.16 Williams' total syntheses of vibsanan family members.

Of particular interest was (-)-5-*epi*-vibsanin E (**1.170**, scheme 1.17) due to the experience gained in the total synthesis.^{57d} When considering (-)-5-*epi*-vibsanin E and (-)-phorbol **1.169** both contain a common seven-membered ring within their core structure (scheme 1.17).



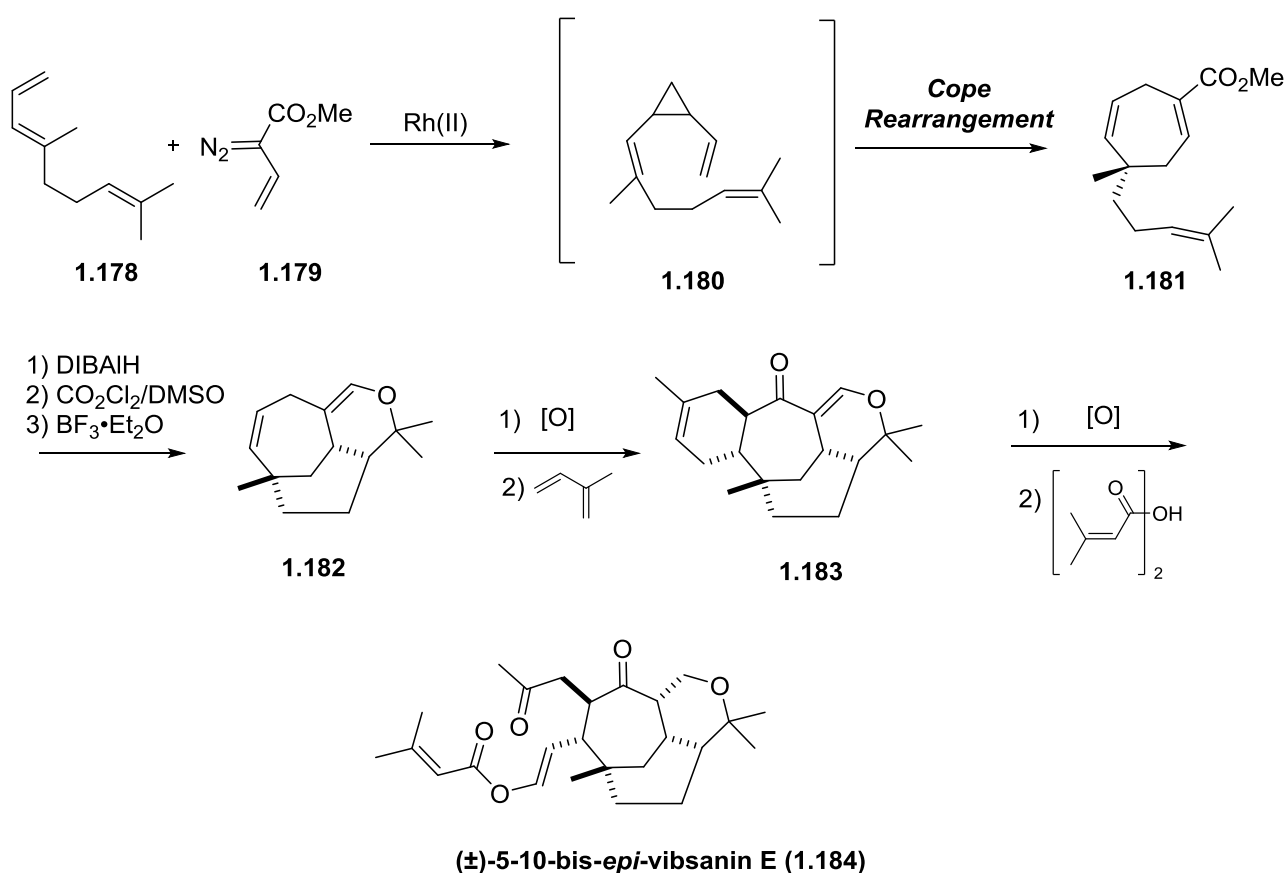
Scheme 1.17 Natural products containing seven-membered rings.

The Williams' group initial approach to the seven-membered ring of (-)-5-*epi*-vibsanin E **1.170** was via the Zercher reaction,⁵⁸ a methodology that has shown to provide γ -keto esters from β -keto esters via ring expansion (scheme 1.18).⁵⁹ As such 3-methylcyclohexenone **1.171** was treated with Grignard **1.172** in a 1,4 addition reaction to afford **1.173**. Dehydrogenation utilising activated IBX followed by Baylis-Hillman reaction afforded allylic alcohol **1.175**. Exposing **1.175** to amberlyst afforded the tricyclic core **1.176** followed by the treatment with ethyl cyanoformate (Mander's reagent)⁶⁰ to yield **1.177**. The latter was treated with diethyl zinc to afford seven-membered ring **1.178**, however, the diastereomeric centre at the C-10 position was epimeric to that of (-)-5-*epi*-vibsanin E **1.170**.⁶¹



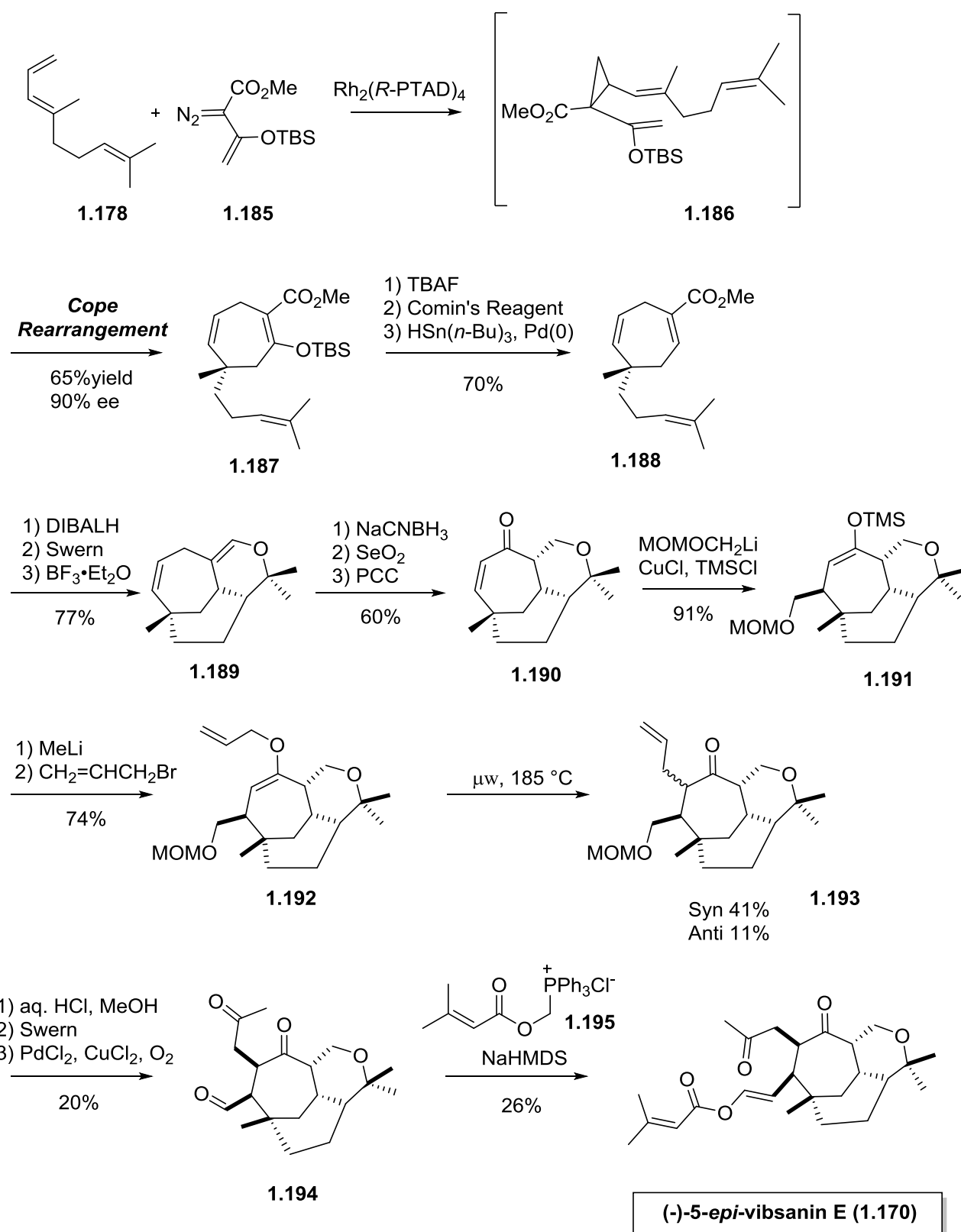
Scheme 1.18 Williams' first generation approach to seven-membered rings.

In an independent approach towards (-)-5-*epi*-vibsanin E **1.170** the Davies group applied a formal [4+3] cycloaddition reaction between diene **1.178** and diazo compound **1.179** to form cycloheptadiene **1.181** through a rhodium catalysed cyclopropanation/Cope rearrangement sequence (scheme 1.19).⁶² Reduction of the methyl ester followed by a hetero Diels-Alder reaction provided tricyclic core **1.182**, which after oxidation and a [4+2] cycloaddition reaction provided **1.183**. However, the product obtained was bis-epimeric at the 5 and 10 positions to the natural (-)-5-*epi*-vibsanin E **1.170**.



Scheme 1.19 Davies' approach to (-)-5-*epi*-vibsanin E.

In 2010 a joint effort between the Williams and the Davies groups, the asymmetric total synthesis of (-)-5-*epi*-vibsanin E **1.170** was achieved (scheme 1.20).^{57d} Their approach successfully constructs the seven-membered ring **1.187** enantioselectively (90% ee) *via* the reaction of diazo compound **1.185** and diene **1.178** utilising a chiral rhodium tetracarboxylate $\text{Rh}_2(R\text{-PTAD})_4$ developed by Davies *et al.* This reaction proceeds *via* an *in situ* generated cyclopropane **1.186** followed by Cope rearrangement of the latter to afford **1.187**.



Scheme 1.20 Williams' and Davies' total synthesis of (-)-5-*epi*-vibsanin E.

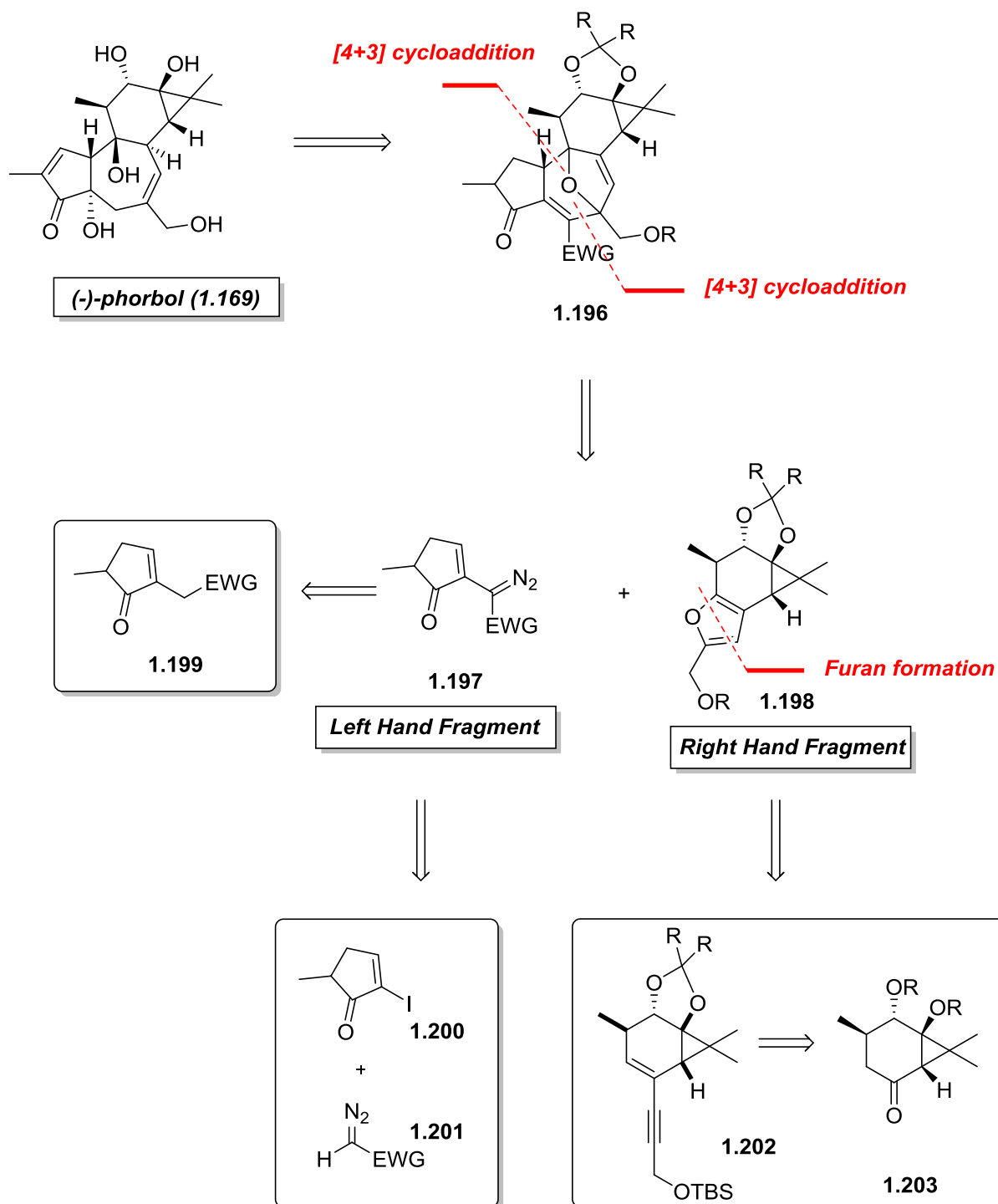
Following this, a number of functional group manipulations arrive at the tricyclic core **1.189**. Conjugate addition and C-alkylation ultimately allowed the elaboration of the C-10 side chain to provide the natural product (-)-5-*epi*-vibsanin E (**1.170**). With a successful proof of concept in the synthesis of (-)-5-*epi*-vibsanin E **1.170** *via* competent seven-membered ring formation attention towards the synthesis of (-)-phorbol **1.169** could be undertaken. Thus, the aim of this project is the first total synthesis of (-)-phorbol **1.169** *via* a concise asymmetric [4+3] cycloaddition reaction.

1.11 Retrosynthetic analysis

As outlined in the general introduction (section 1.5, page 15) it is important to establish a significant biological profile of phorbol as a PKC activator and to better understand the structural features necessary for specific protein binding. Thus, the synthesis of the non-natural isomer (-)-phorbol **1.169** is highly desirable.

In analogy to (-)-5-*epi*-vibsanin E **1.170** the tetracyclic system (**1.196**, scheme 1.21) hosting the seven-membered ring (ring B), was envisaged to be assembled by means of the formal asymmetric [4+3] cycloaddition reaction developed by Davies *et al.*⁶³

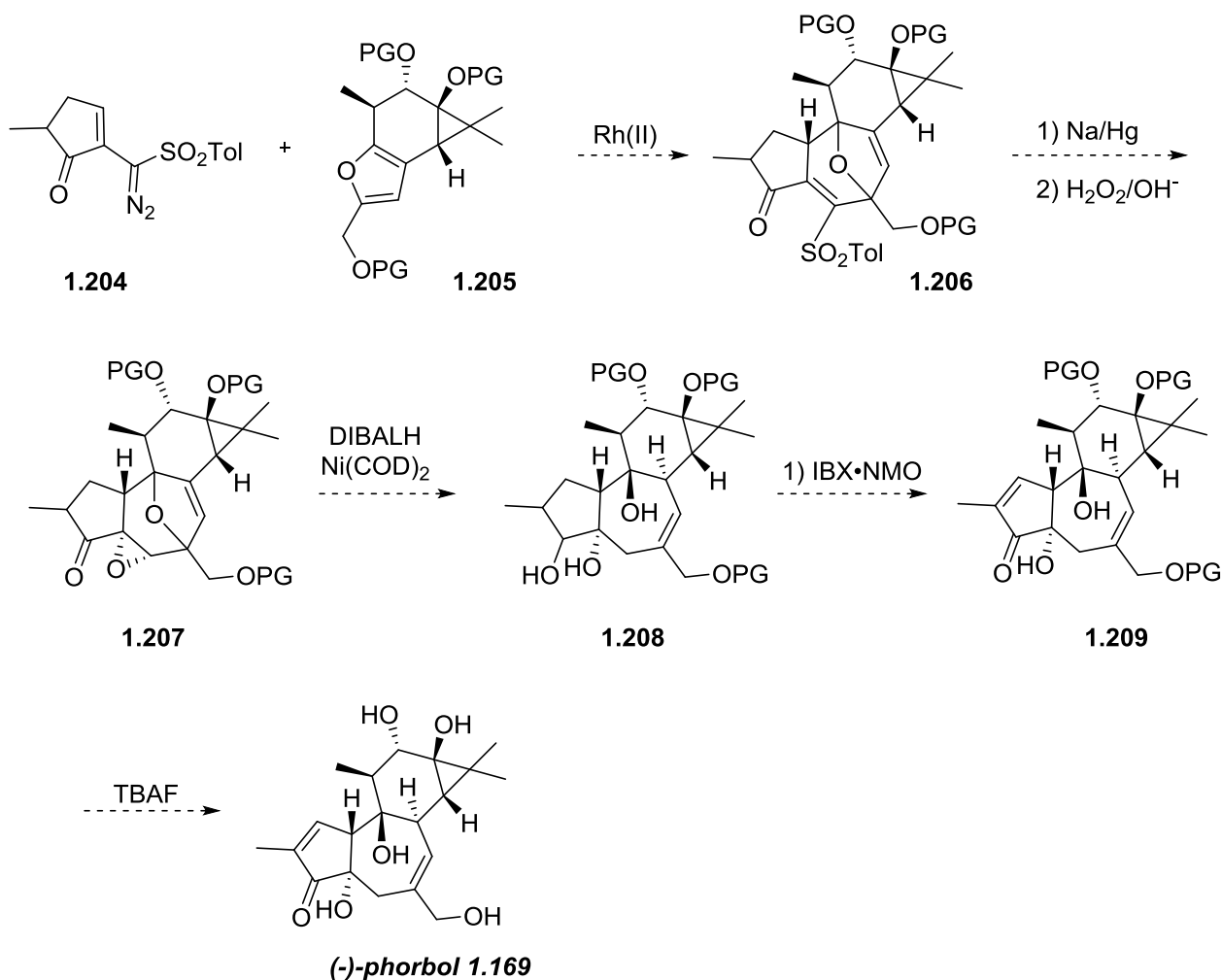
The convergent strategy requires the synthesis of a Left Hand Fragment (LHF) (**1.197**) and a Right Hand Fragment (RHF) (**1.198**), respectively. The left hand fragment can be synthesised either *via* a diazo transfer reaction on an activated methylene group **1.199**, or *via* a direct diazo cross coupling reaction between **1.200** and **1.201**. The right hand fragment can be assembled from key intermediate **1.203** *via* enolisation followed by Sonogashira coupling and metal mediated ring closure to form furan **1.198**.



Scheme 1.21 Retrosynthetic analysis of (-)-phorbol using Davies seven-membered ring formation.

In the synthetic direction treating **1.204** with rhodium in the presence of **1.205** would give advanced intermediate **1.206**. The choice of electron withdrawing group on the diazo compound **1.204** is

important in regard to removal at the later stage of the synthesis. Both an ester function and a sulfone have been shown to successfully undergo cycloaddition reactions. However, the ease of removal of the sulfone function compared to that of an ester dictated choice.



Scheme 1.22 Proposed strategy for the synthesis of (-)-phorbol 1.169.

In the event, removal of the sulfone with sodium-mercury amalgam or samarium diiodide⁶⁴ followed by enone epoxidation⁶⁵ would give rise to **1.207**. Due to the hindered β -face of the molecule the epoxidation is expected to occur from the less hindered α -face affording the desired stereochemistry at C-4. With **1.207** at hand oxo-bridge opening can be affected by treatment with diisobutylaluminium hydride (DIBALH) and nickel cyclooctadiene as reported by Lautens *et al.*⁶⁶ Under these reaction conditions the likely event of ketone reduction is expected to accompany epoxide ring opening. In the absence of such an event further treatment with lithium aluminium

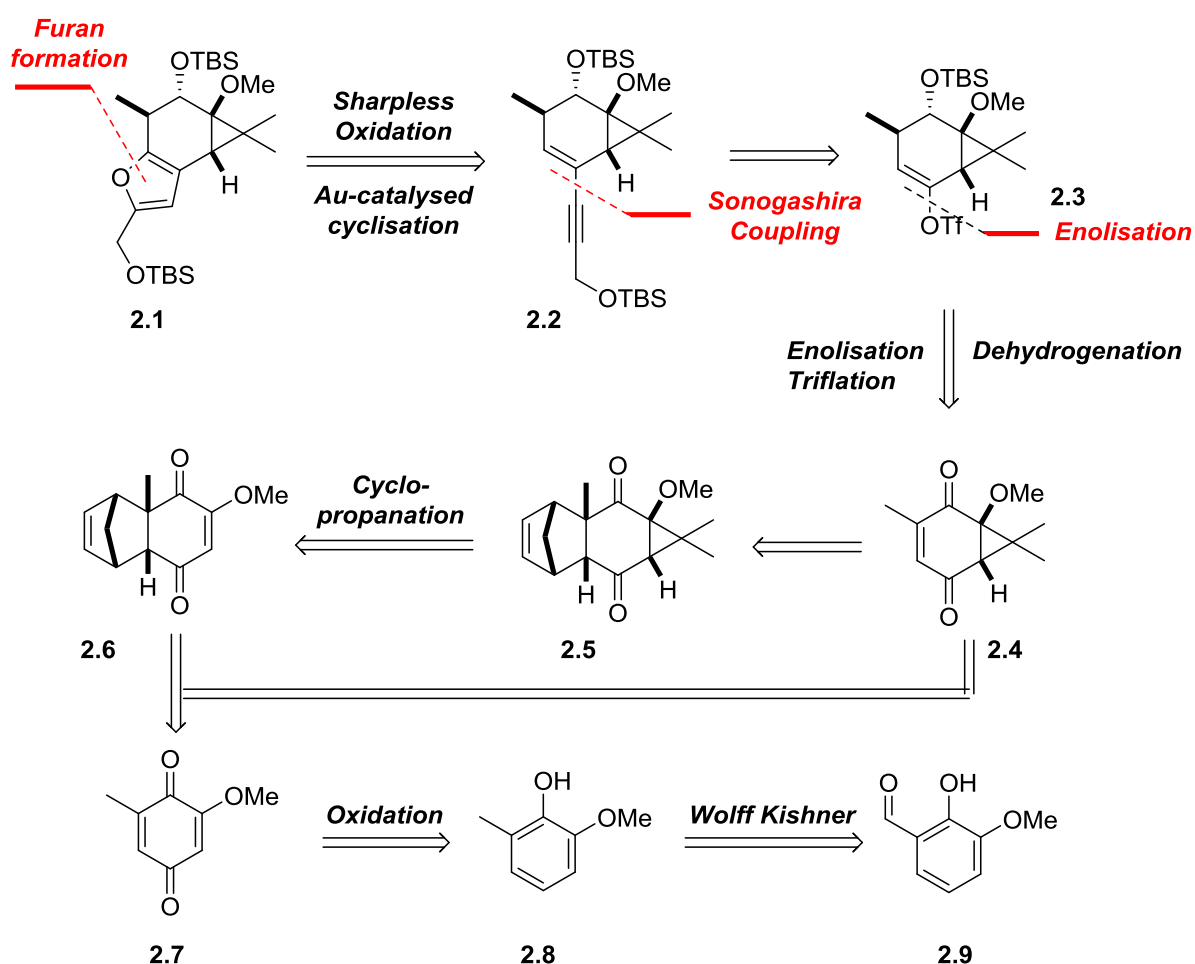
hydride (LiAlH_4) should conveniently afford the reduced ketone **1.208**. Treatment with activated IBX will introduce the desired enone functionality in one step.⁶⁷ Finally, removal of the carefully chosen protecting groups will unmask the target (-)-phorbol **1.169**. The following text will outline the progress towards the total synthesis of (-)-phorbol **1.169**.

2 Investigations towards the Synthesis of the Right Hand Fragment

2.1 Introduction

The construction of the right hand fragment **2.1** is viewed as being achievable both asymmetrically, and *via* a fall back racemic strategy utilising chiral chromatography to resolve the enantiomers. The latter approach would be desirable in regard to the production of novel stereoisomers for biological evaluation.

The first disconnective transformation to the right hand fragment involves the metal catalysed (Au, Pt, Pd) cyclisation reaction of **2.2** to the furan (scheme 2.1).⁶⁸ The precursor for the furan synthesis is a result of epoxidation utilising *meta*-chloroperbenzoic acid of the enolised double bond.



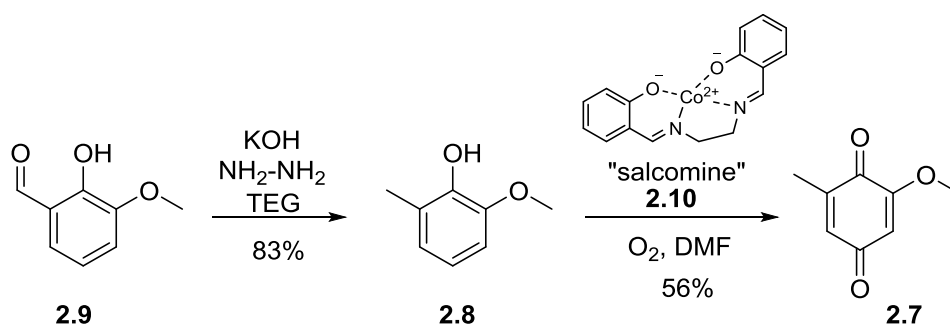
Scheme 2.1 Retrosynthetic analysis of the right hand fragment of (-)-phorbol (1.169).

Compound **2.3** can be accessed *via* enolisation/triflation of the corresponding advanced intermediate **2.4** followed by a Sonogashira coupling⁶⁹ utilising a protected propargyl alcohol. Compound **2.4** could then be derived from either direct cyclopropanation of **2.7** using dimethyldiazomethane or the employment of sulfur ylid chemistry for direct treatment of quinone **2.7**. However, due to the nature of the quinone this could interfere with regiochemistry and selectivity, thus, leading to unwanted side reactions. To bypass this problem “masking” one side of the quinone *via* a Diels-Alder reaction followed by the introduction of the *gem*-dimethylcyclopropane moiety would afford the masked CD ring system **2.5**, which could then be liberated simply by heating.

Lastly, quinone bearing a methoxy group at 2-position is known and could easily be accessed *via* oxidation of 2-methoxy-6-methylphenol **2.8**.⁷⁰

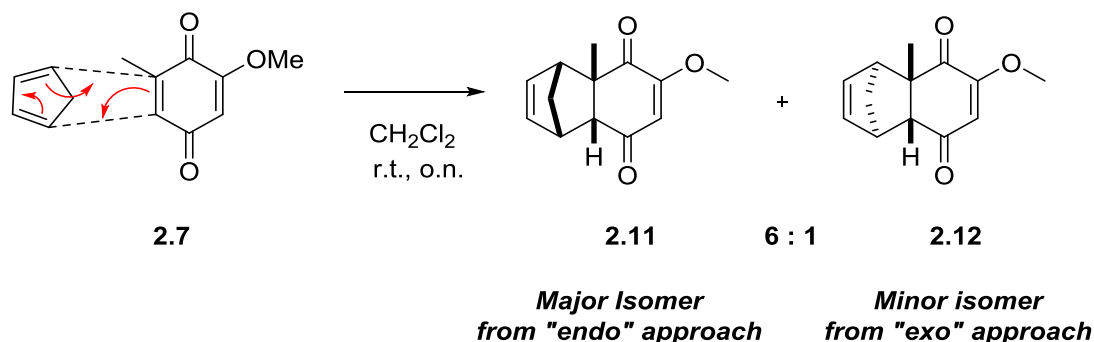
2.2 Approach

Construction of quinone **2.7** started with the commercially available *ortho*-vanillin **2.9** which was converted to **2.8** *via* a classical Wolff-Kishner reduction in 83% yield. Oxidation of the resulting 2-methoxy-6-methylphenol *via* oxygen transfer using the *N,N'*-bis(salicylidene)ethylenediaminocobalt(II)-complex (“salcomine”) **2.10** gave rise to the desired quinone **2.7** in 56 % yield.⁷⁰



Scheme 2.2 Synthesis of methoxy-quinone 2.7.

Diels-Alder reaction of **2.7** with cyclopentadiene was performed in the racemic series to provide **2.11** along with 15% of the *exo*-adduct **2.12** (scheme 2.3).



Scheme 2.3 Diels-Alder reaction of 2.7 with cyclopentadiene.

Figure 2.1 represents a ^1H NMR spectrum of both isomers **2.11** and **2.12** showing the olefinic protons in the cyclopentene portion of the molecule at 6.12 and 6.02 ppm, respectively. The isolated olefinic protons appear as partially resolved singlets at 5.89 ppm.

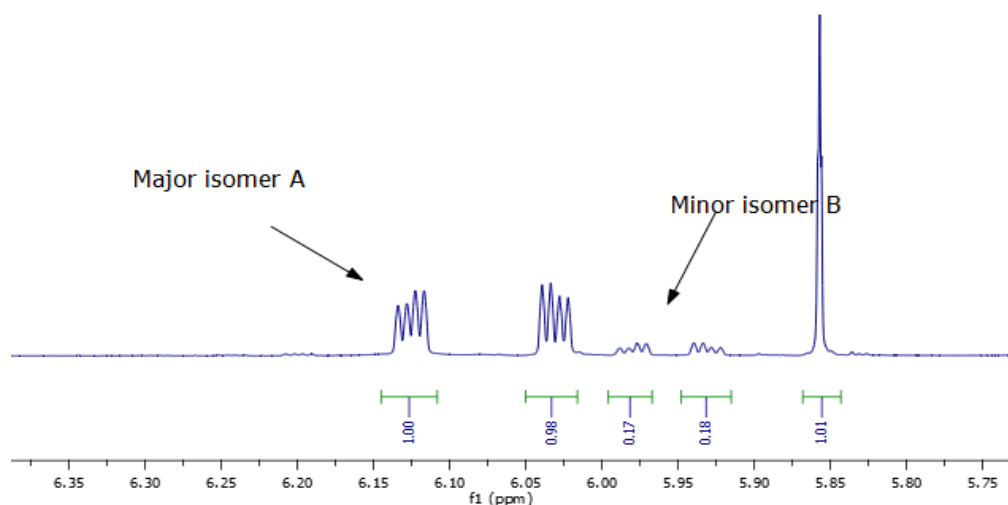


Figure 2.1 Diels-Alder isomers 2.11 and 2.12.

For the synthesis of (-)-phorbol (**1.169**), however, an enantioselective approach was desired. Quinones of type **2.7** are known to undergo regiospecific Diels-Alder reactions with the less electron rich enone.⁷¹ Thus, performing an enantioselective Diels-Alder reaction would block one side of the molecule directing the cyclopropanation to the opposite face hopefully leading to the desired absolute stereochemistry. Enantioselective Diels-Alder reactions have been studied

extensively over the last three decades.⁷² A catalyst that has found widespread use is the oxazaborolidine catalyst known as the Corey-Bakshi-Shibata catalyst (CBS, **2.20**, scheme 2.4).⁷³ In order to investigate the enantioselective Diels-Alder reaction we initiated the synthesis of **2.20**.

2.3 Synthesis of the CBS-Oxazaborolidine Catalyst

The use of CBS oxazaborolidine catalysts have been well established for a wide variety of dienes and dienophiles. Corey *et al.*^{71,74} demonstrated the strength of this catalyst and devised a mechanistic model to predict the stereochemical outcome of this reaction.^{71,74} According to their studies the transition state model in figure 2.2 clearly shows the coordination of the oxazaborolidine catalyst **2.20** to quinone **2.7**, blocking the top face. Hence, cyclopentadiene attack can only occur from the bottom face of the molecule leading to a *cis* annelation.

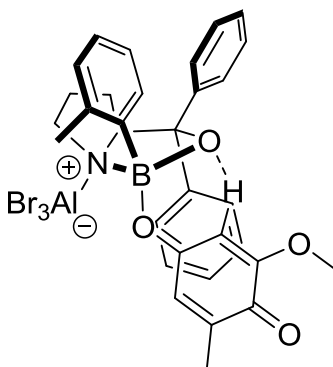
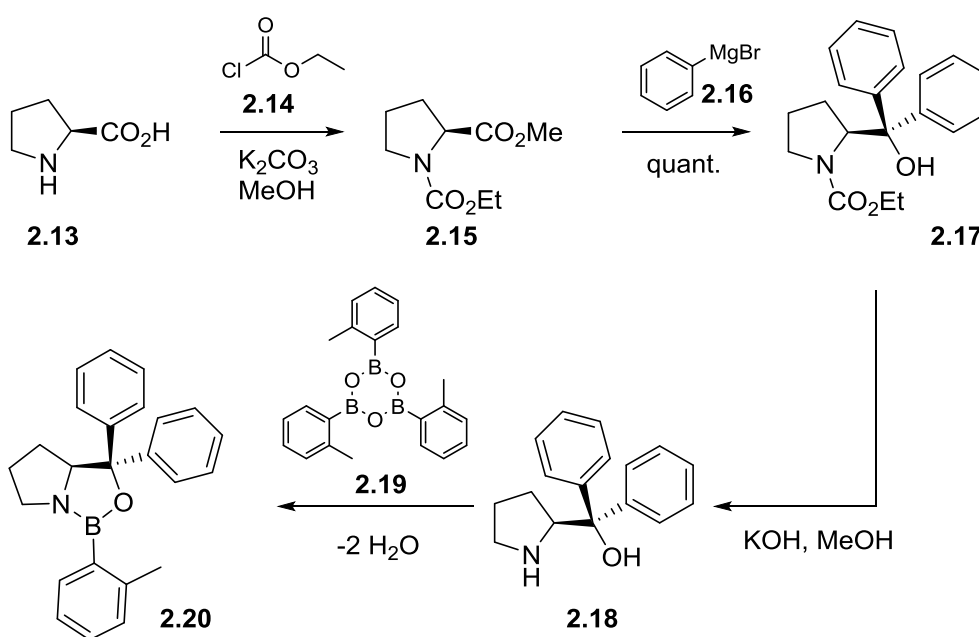


Figure 2.2 Corey's prediction model for enantioselective Diels-Alder reaction.

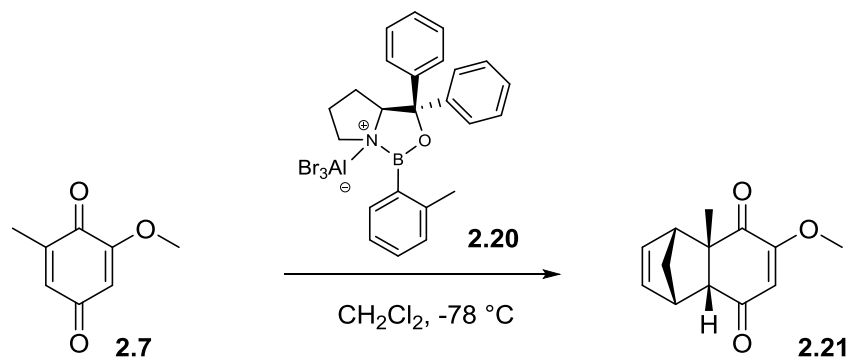
The synthesis of (*S*)-*o*-tolyl-CBS-oxazaborolidine catalyst **2.20** according to the procedure of Corey *et al.*⁷⁵ proved to be very difficult in regard to the last step. The commercially available L-proline **2.13** was treated with ethyl chloroformate **2.14** under basic conditions to give rise to (*S*)-proline-*N*-ethyl-carbamate methyl ester **2.15** (scheme 2.4). Subsequent reaction with phenylmagnesium bromide afforded (*S*)-(-)- α,α -bis(diphenyl)-2-pyrrolidinemethanol **2.17** in quantitative yield. Deprotection of the amine using potassium hydroxide in methanol gave rise to **2.18** in 57% yield. Finally, (*S*)-*o*-tolyl-CBS-oxazaborolidine catalyst **2.20** could then be accessed *via* treatment of (*S*)-(-)- α,α -bis(diphenyl)-2-pyrrolidinemethanol **2.18** with freshly prepared boroxine **2.19** under azeotropic conditions as the reaction produces two equivalents of water.

The method reported by Corey *et al.*⁷⁶ for the preparation of the CBS-oxazaborolidine catalyst involved the reaction of amino alcohol **2.18** with boroxine **2.19** using a Soxhlett extractor. In our hands this method failed to afford the desired product, rather a polymeric mixture was observed. Similar results have been reported by Mathre *et al.*⁷⁷ It is believed to be caused by dimerisation of **2.18** in the presence of small quantities of water. Following the procedure of Mathre *et al.* using a Dean Stark apparatus charged with exactly one equivalent of amino alcohol **2.18** followed by sequential addition of 0.33 equivalents of boroxine ultimately afforded the desired oxazaborolidine catalyst **2.20**.



Scheme 2.4 Synthetic route to the CBS-oxazaborolidine catalyst.

A major hurdle in this synthetic sequence lies in the final condensation of **2.18** and **2.19** to afford **2.20**. Because only small amounts of **2.19** were required to further investigate the proposed synthetic pathway, no further optimisation studies were undertaken. Utilizing **2.20** in a Diels-Alder approach to **2.21** afforded a 3% isolated yield of the desired product. Using the commercially available catalyst (0.5M toluene solution) gave a marked increase in yield (85%, scheme 2.5). This was most probably due to the capricious nature of the catalyst, and subsequent reaction.



Scheme 2.5 Enantioselective Diels-Alder reaction of 2.7.

Regardless of the method of activation (table 2.1), Brønsted or Lewis acids (AlBr_3 and SnCl_4)^{74,78} the desired product **2.21** was obtained in good yields (77-85%) and stereoselectivity (90% ee). Table 2.1 outlines a summary of the reaction conditions trialled.

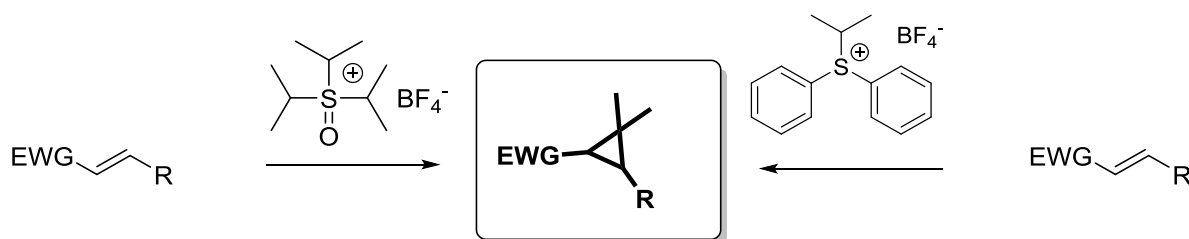
<i>entry</i>	<i>catalyst</i>	<i>protonation</i>	<i>yield, %</i>	<i>ee, %</i>
1	(<i>S</i>)-CBS	AlBr_3	85	87
2	(<i>S</i>)-CBS	SnCl_4	85	90
3	Racemic	-	93	n/a

Table 2.1 Protonation studies of 2.19.

Due to the cost and the difficulty of synthesising the catalyst, all ongoing reactions were performed on a racemic series. From the enantioselective studies undertaken we were confident that the desired stereochemistry could be accessed.

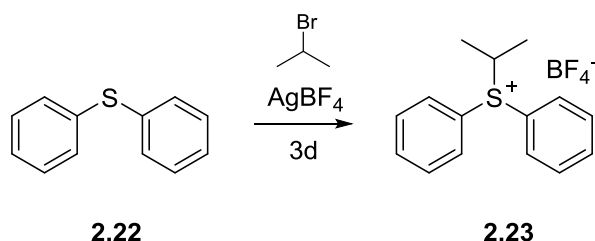
2.4 Cyclopropanation Studies

With **2.21** in hand construction of the D-ring system was envisaged *via* direct cyclopropanation at an early stage of the synthesis. Cyclopropanes are present in a large number of compounds and natural products.⁷⁹ These 3-membered rings can be challenging to synthesise due to their ring strain requiring highly reactive species such as ylids or carbenes for their synthesis.⁸⁰ There are a number of procedures available for the preparation of *gem*-dimethylcyclopropanes from electron rich alkenes.^{36,81} Both Wender with his first formal asymmetric synthesis of phorbol and Corey have successfully demonstrated the use of diphenylisopropylsulfide tetrafluoroborate on a large variety of substrates. A representation of this approach is depicted in scheme 2.6.



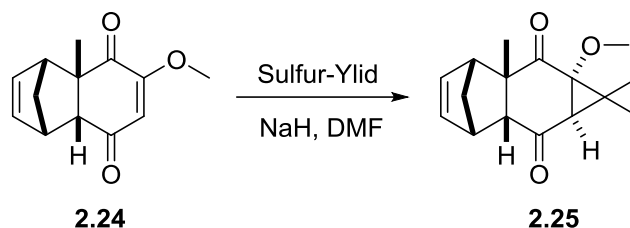
Scheme 2.6 Synthesis of *gem*-dimethylcyclopropane.

With these established methodologies at hand synthetic investigations into the D-ring were commenced utilising the aforementioned diphenylisopropyl tetrafluoroborate **2.23**, which was synthesised in one step as described by Matsuyama *et al.*⁸² by reaction of diphenylsulfide with isopropyl bromide in the presence of silver. (scheme 2.7)



Scheme 2.7 Synthesis of diphenyldiisopropylsulfonium tetrafluoroborate.

Treating **2.24** with LiHMDS (scheme 2.8, table 2.2, entry 1) and a catalytic amount of dichloromethane in DME to allow ylid formation followed by treatment with **2.23** surprisingly afforded recovered starting material.



Scheme 2.8 Formation of the D-ring.

All additional attempts at using diphenylisopropylsulfonium tetrafluoroborate under a variety of conditions summarised in table 2.2 failed to afford **2.25**.

<i>Entry</i>	<i>Solvent</i>	<i>Base</i>	<i>Temperature</i> [°C]	<i>Result</i>
1	DME	LiHMDS	-78	RSM
2	DME	LDA	-78	RSM
3	DMF	NaH	-40	RSM
4	THF	<i>t</i> -BuLi	-78	RSM

Table 2.2 Conditions for the introduction of ring D.

It was Corey and Chaykovsky⁸³ in 1965 that found the more nucleophilic sulfoxonium ylids to be useful for the cyclopropanation of electron-deficient alkenes. As such dimethylsulfoxonium methylide was introduced. Taylor and co-workers were interested in *gem*-dimethylcyclopropanes and directed their focus on sulfoxonium ylid **2.30**.⁸⁴ Table 2.3 outlines a short summary of cyclopropanations undertaken by Taylor *et al.* on a variety of quinone type systems. After only three hours reaction time excellent yields were obtained utilising triisopropylsulfoxonium

tetrafluoroborate. However, unmasked quinones (entry 3) under the same conditions yield a dicyclopropane B as the major compound.

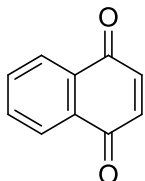
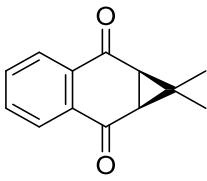
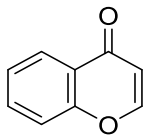
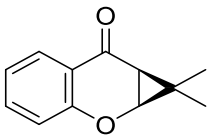
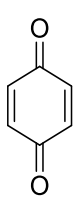
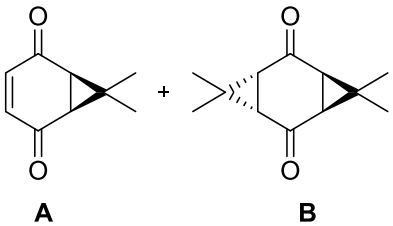
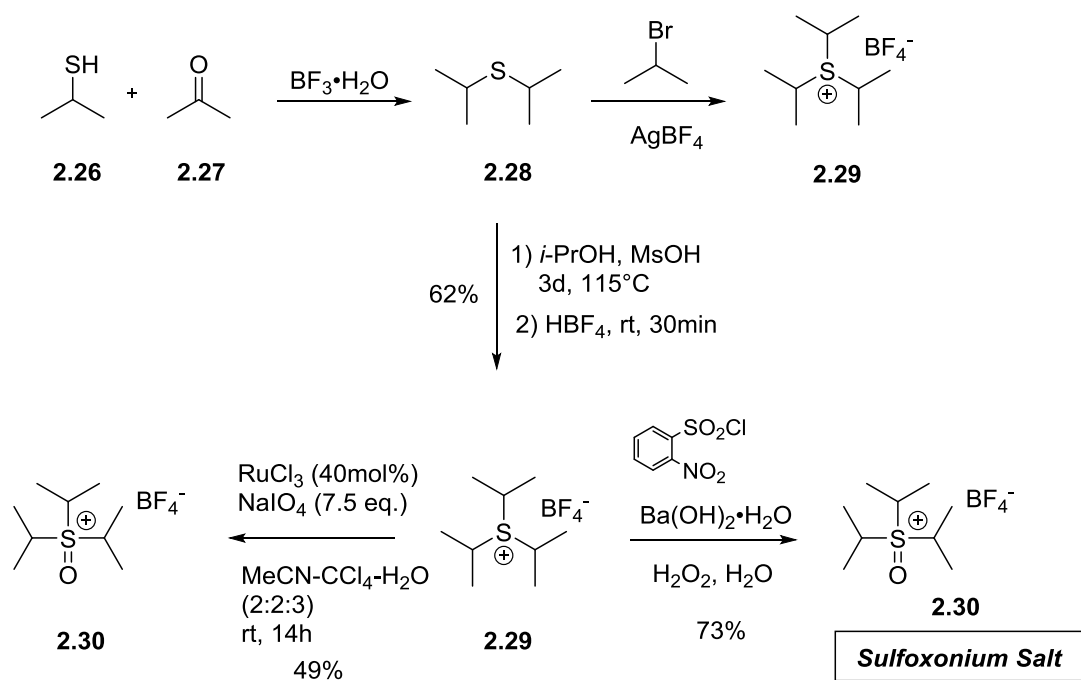
Entry	Substrate	Product	Reaction time, h	yield
1			3	92
2			3	95
3			3	A=7, B=36

Table 2.3 Taylor's cyclopropanation results using triisopropylsulfoxonium tetrafluoroborate.

As such we directed our attention towards the isopropyl transfer reagent triisopropylsulfoxonium tetrafluoroborate **2.30** as described by Taylor *et al.* (scheme 2.9).

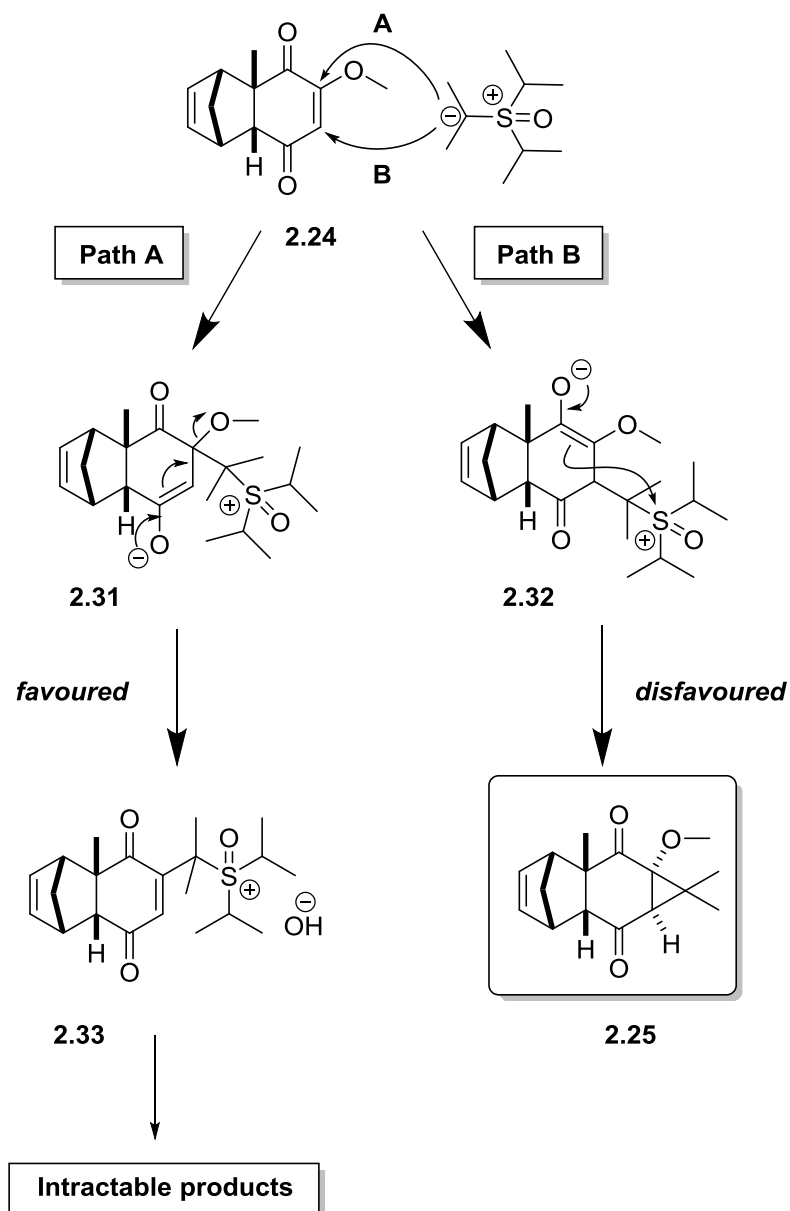
The synthesis of **2.30** begins with the preparation of the diisopropylsulfide **2.28** following the method of Prakash *et al.* Subsequent introduction of the isopropyl group as described by Taylor *et al.* using 2-bromopropane and silver tetrafluoroborate unfortunately gave erratic results and as a consequence, low yields. Having failed *via* this approach, **2.29** was synthesised using an alternate unpublished route kindly provided by Prof Taylor. Subjecting diisopropylsulfide to MsOH using isopropanol as solvent and stirred at 115 °C for a period of three days followed by counter ion exchange using HBF₄ at room temperature afforded **2.29** in 62% yield.



Scheme 2.9 Synthesis of triisopropylsulfoxonium tetrafluoroborate.

Subsequent oxidation of triisopropylsulfonium tetrafluoroborate can then be performed *via* two alternative routes, i.e. utilising Sharpless conditions or barium hydroxide in presence of 2-nitrobenzenesulfonyl chloride. It was found that both approaches gave the desired sulfur salt, with the later procedure performing best (73%).

With the sulfur salt **2.30** at hand, the first attempt at introducing the cyclopropane moiety utilising NaH and DMF at 0°C afforded a 50% conversion to the desired product **2.25** (scheme 2.8). When using an excess of **2.30** and temperatures below 0°C complete conversion to product **2.25** was apparent by TLC. However, only 14% of the desired cyclopropane could be isolated. The observed low yield of the reaction was thought to be a consequence of a 1,4-addition/elimination process (scheme 2.10, path A). For example, a competing elimination of the C-13 methoxide moiety was believed to be favoured over cyclopropanation (path B) leading to water-soluble by-products, presumably *via* **2.33**.



Scheme 2.10 Possible mechanism for the low yield of D-ring formation.

Despite the low yield enough material was obtained for full characterisation. The diastereoisomer readily crystallised from petroleum ether and the X-ray crystal structure was solved (figure 2.3). The structure determination revealed the relative stereochemistry of **2.25**, showing clearly that cyclopropanation is directed by the cyclopentene moiety to the opposite face of the molecule.

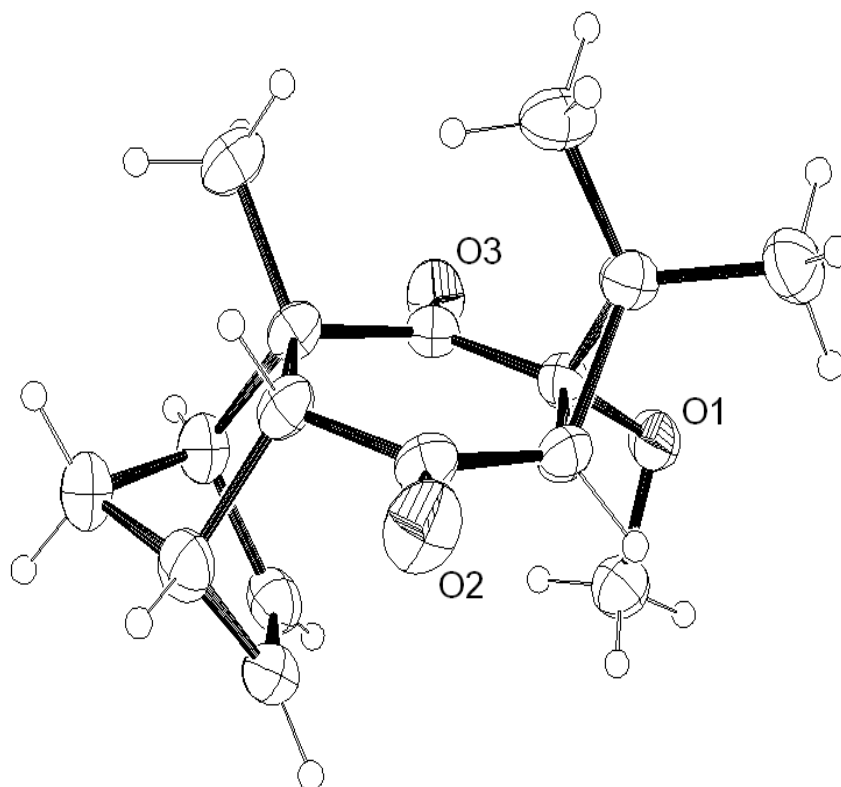
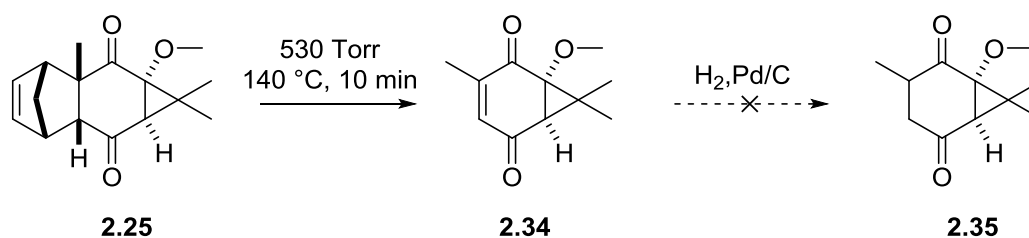


Figure 2.3 ORTEP (30% ellipsoid probability) structure of the cyclopropanation product **2.25**.

With **2.25** at hand the conditions in which the retro Diels-Alder reaction could be performed, were evaluated. This was then successfully accomplished in 93% yield using a Kugelrohr distillation apparatus.



Scheme 2.11 Synthesis of **2.34** *via* retro Diels-Alder reaction.

Despite the retro Diels-Alder reaction working in excellent yield, further investigations and initial reduction studies on **2.34** demonstrated the unsuitability of the methyl group as a protecting group. Furthermore, a 14% yield at such an early stage in synthesis was undesirable, thus, the encountered

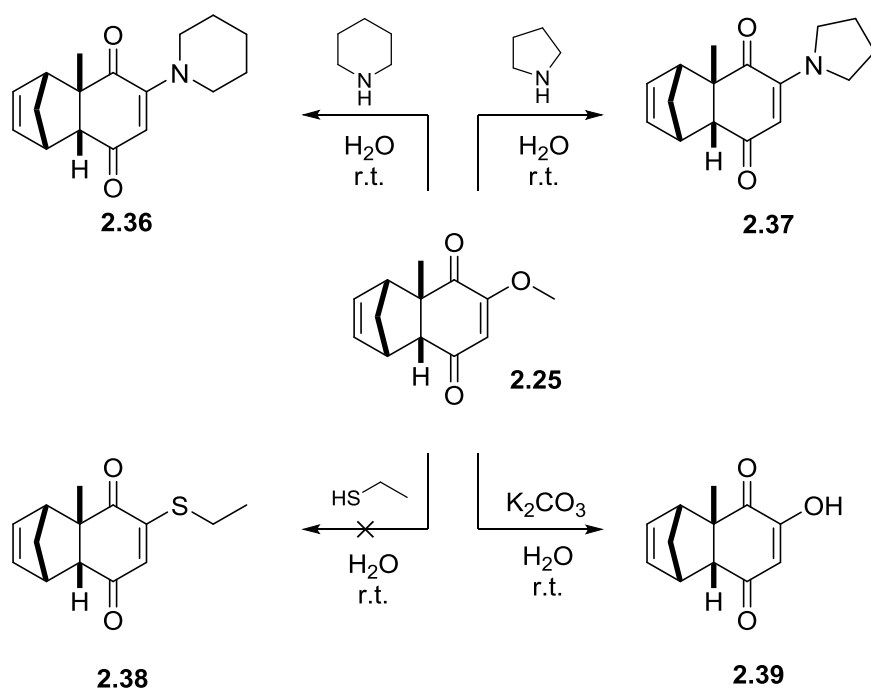
problems needed to be addressed. Based on the proposed mechanism it was considered that a larger (bulkier) protecting group may well block path A.

2.5 The Effect of C-13 Substituent upon Cyclopropanation

To improve the yield of cyclopropanation we sought a deeper understanding of the effect exerted by the C-13 substitution pattern. Outlined below is the reactivity of **2.25** towards NH_2R , NHR_2 , S and OH functionalization at C-13 and the consequences of this upon the following cyclopropanation reaction (scheme 2.12). These efforts demonstrate the capricious nature of this system towards synthetic manipulations as well as the low tolerance of the cyclopropanation towards an increase in electron density at C-13.

Cyclic amines proved to be feasible nucleophiles towards substitution at C-13, whereas acyclic secondary as well as primary amines were unreactive towards this system. This is believed to be a consequence of the well-established higher nucleophilicity of cyclic amines. Treating methoxy quinone **2.25** with an excess of pyrrolidine or piperazine in water afforded **2.36** and **2.37**, respectively in good yield. However, treatment of **2.25** under identical conditions using excess ethylmercaptane did not afford the desired product **2.38**. Surprisingly only recovered starting material was observed.

Moving on to the free hydroxyl at C-13, it was found that the methyl group could be displaced by treatment of **2.25** with an excess of potassium carbonate in water to afford **2.39** in excellent yield.



Scheme 2.12 Access to C-13 substituted Diels-Alder adducts.

An X-ray structure of the crystalline **2.37** was obtained after recrystallization from petroleum ether. Figure 2.4 outlines an ORTEP representation of **2.37** at 30% ellipsoid probability. Compound **2.37** crystallised in the monoclinic P21/c space group with two molecules occupying a single unit cell.

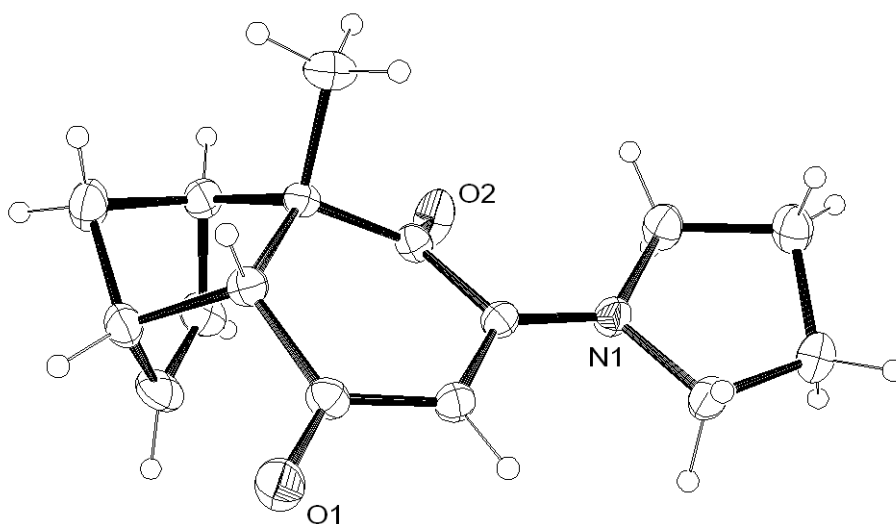
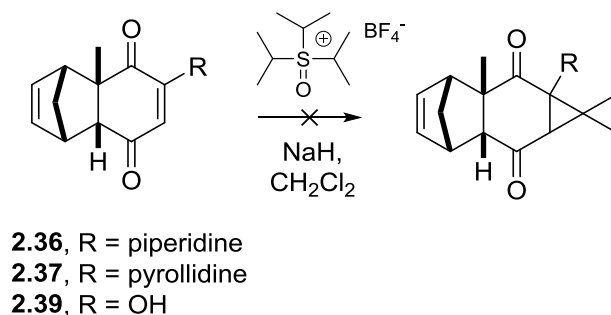


Figure 2.4 ORTEP (30% ellipsoid probability) structure of the cyclopropanation product **2.37.**

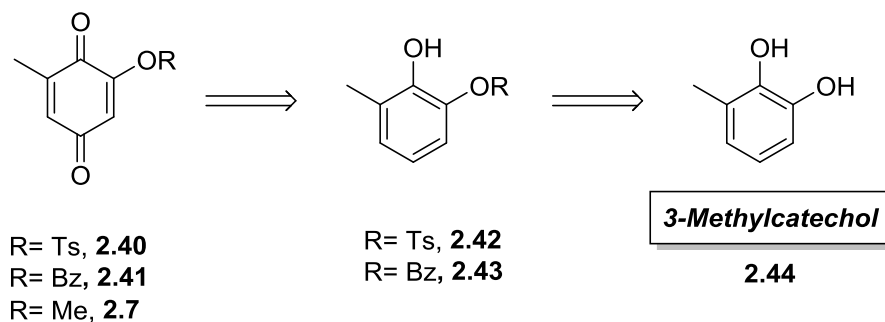
With **2.36**, **2.37** and **2.39** at hand we were in a position to probe their effect upon the instalment of the D-ring system. When exposing all three systems towards the cyclopropanation protocol (scheme 2.13), utilising triisopropylsulfoxonium tetrafluoroborate (**2.30**), the hampering effect of these substituents towards cyclopropanations were evident. In all cases the unaltered starting materials were recovered.



Scheme 2.13 Cyclopropanation attempts on 2.36, 2.37 and 2.39.

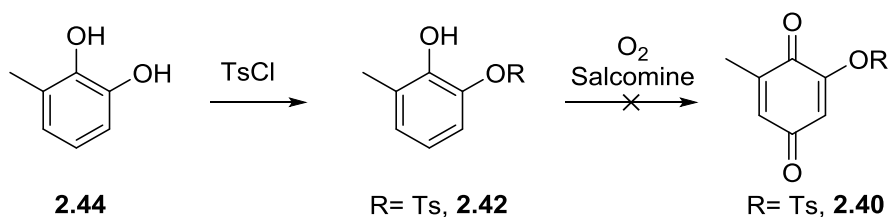
With this insight, and a proven ability to introduce the desired D-ring system when employing a methoxy moiety at C-13, we were convinced that a bulkier alkoxy moiety would be well equipped to resolve the difficulties encountered. In this regard attention was focused on introduction of more hindered alkoxides *via* a number of approaches as outlined below.

Quinones bearing other functional groups than methoxy in 6-position (scheme 2.14) rarely appear in literature. Having successfully synthesised the methoxy equivalent of quinone **2.7**, it was envisaged that selective protection of 3-methylcatechol **2.44** followed by the oxidation of the resulting phenol could lead to the desired products **2.42** and **2.43**. Benzyl as a protecting group was not considered for the synthesis as they are labile under conditions required to hydrogenate the double bond of quinone following the retro Diels-Alder reaction. Thus, attention was focused on the selective protection as a tosyl or the benzoyl ester. However, selective protection proved to be very challenging.



Scheme 2.14 Change of C-13 protecting group strategy.

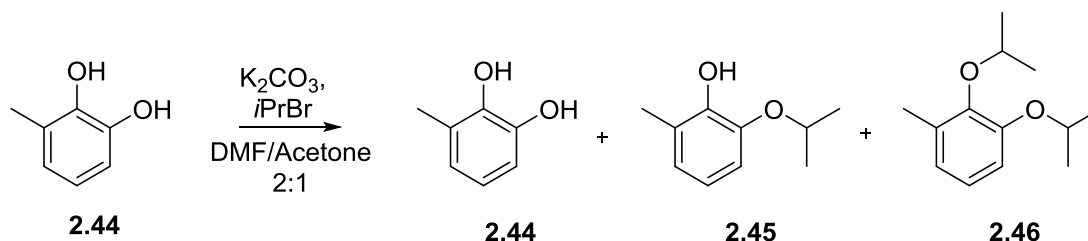
Treating 3-methylcatechol with benzoyl chloride and a variety of different bases did not afford the desired compound **2.43**. Unlike benzoyl chloride, the reaction with tosyl chloride afforded the corresponding protected **2.42**. However, the attempt at the oxidation of **2.42** to the corresponding quinone **2.40** only afforded recovered starting material (scheme 2.15).



Scheme 2.15 Synthetic strategy for quinone 2.40.

The failure to oxidise **2.42** was attributed to both steric and electronic reasons of the tosyl moiety. Thus, a careful interplay between steric bulk and stability towards elimination of the alkoxide was required. As a result the use of an *isopropyl* group as a protecting group was explored. From an extensive study as early as 1962 by Simpson *et al.*⁸⁵ it was evident that the isopropyl moiety was a good candidate due to its stability under a wide variety of conditions and the ease of deprotection under mild conditions employing AlCl_3 as reported by Banwell *et al.*⁸⁶ In addition, some phorbol derivatives such as TPA bear an acyl group at the C-13 position. A promising method to access this moiety from a C-13 isopropoxy has been reported by Williams *et al.*⁸⁷ In their work a transprotection protocol was demonstrated in which a *isopropoxy* moiety could be exchanged for an acyl moiety in a one-pot reaction.

Commercially available 3-methylcatechol was subjected to conditions described by Razafinrabe *et al.*⁸⁸ in which an excess of *isopropyl* bromide under reflux conditions was employed to afford mono protected alcohol **2.45** in 69% yield.



Scheme 2.16 Synthetic outcome of selective protection of 3-methylcatechol.

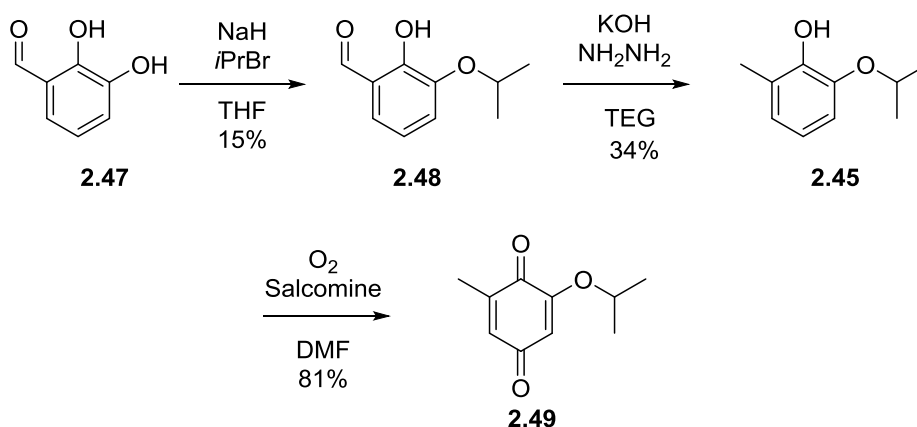
Unfortunately only a 29% yield was obtained of the desired product as a mixture of mono and di-protected alcohols **2.45** and **2.46**. Table 2.4 outlines the results of a variety of conditions attempted.

Entry	Solvent System	Temperature, Duration	Compound 2.44	Compound 2.45	Compound 2.46
1	DMF/Acetone (2:1)	r.t., 40 hours	-	No reaction	-
2	DMF/Acetone (2:1)	Reflux, o.n.	-	29%	43%
3	DMF/Acetone (1:2)	r.t., o.n.	-	No reaction	-
4	DMF/Acetone (1:2)	reflux, o.n.	-	15%	23%
5	Acetone	reflux, o.n.		No reaction	
6	Acetone/DMF cat.	r.t., o.n.	21%	15%	-
7	Acetone/DMF cat.	reflux, o.n.	18%	24%	-

Table 2.4 Conditions for selective protection of 3-methylcatechol.

Unsatisfied with this outcome the literature was consulted for an alternative procedure. Nicolaou *et al.*⁸⁹ has reported the selective protection of 2,3-dihydroxybenzaldehyde using benzyl bromide and sodium hydride as base. With a slight modification of this procedure it was investigated whether the use of *isopropyl* would prove successful under these conditions. Exposing aldehyde **2.47** to

isopropylbromide and sodium hydride (scheme 2.17) only returned a 15% yield of monosubstituted phenol **2.48**.

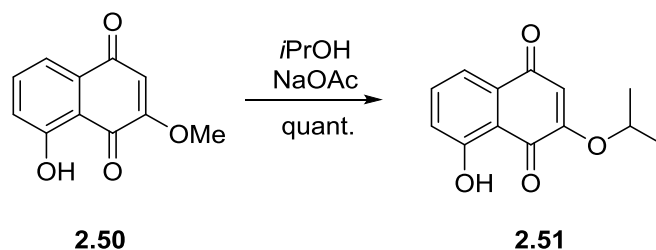


Scheme 2.17 Selective protection of 2.47 according to Nicolaou *et al.*

Subsequent reduction of aldehyde **2.48** afforded the target molecule **2.45** in a discouragely low overall yield of 34%. While offering no improvement over the previous effort the material obtained from both studies could be combined in order to further explore the following synthetic transformations. Gratifyingly, oxidation of **2.45** proceeded smoothly providing **2.49** in 81% yield. A thorough survey of the literature and further optimisation studies unfortunately did not offer any means to convert the initial low yields of 29% and 15% in order to make the synthetic sequence acceptable for a multi-step synthesis.

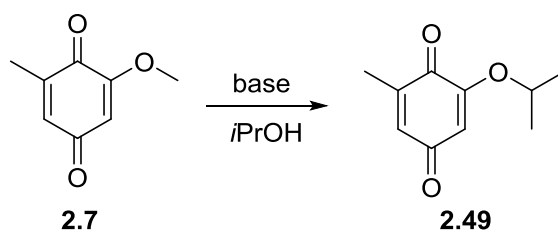
Having outlined the synthesis of **2.7** (see scheme 2.2) in excellent yield and with a large quantity of material at hand attention was directed towards a direct exchange of the methoxy moiety for the *isopropyl*. As an added advantage, in the event this method should prove successful, it would offer an economically viable large scale approach to **2.49** due to the low cost of *o*-vanillin as a starting material.

Wurm *et al.* reported the smooth trans esterification of vinylogous methoxy ester on 1,4-naphthoquinone systems by using primary or secondary alcohols as the solvent and NaOAc as base (scheme 2.18).⁹⁰



Scheme 2.18 Wurm's approach for the direct β -substitution of methoxy to *isopropoxy*.

Applying these conditions to **2.7** (scheme 2.19), afforded **2.49** in 44% yield, now facilitating an efficient synthetic route to the desired quinone **2.49** *via* an addition/elimination mechanism starting from readily available methoxy quinone **2.7**.



Scheme 2.19 New approach to *isopropoxy* quinone **2.49**.

Briefly screening a number of conditions outlined in table 2.5 it was discovered that the change of base from sodium acetate to potassium carbonate further improved the initial yield of 44% to afford **2.49** in an optimised yield of 70%.

<i>entry</i>	<i>base</i>	<i>temperature, °C</i>	<i>time, h</i>	<i>yield, %</i>
1	NaOAc	reflux	5	44
2	NaOAc	r.t.	12	30
3	K ₂ CO ₃	reflux	5	70
4	K ₂ CO ₃	r.t.	12	53

Table 2.5 Condition screening for the synthesis of *isopropoxy* quinone **2.49**.

It is noteworthy that a reaction time of 4.5 hours was crucial in order to avoid the formation of the double addition product **2.52** (figure 2.5). Despite the recovery of starting material along with **2.49**, exceeding this reaction time did not drive the reaction to completion, but rather increased formation of **2.52**.

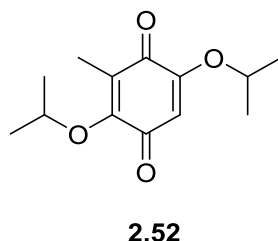
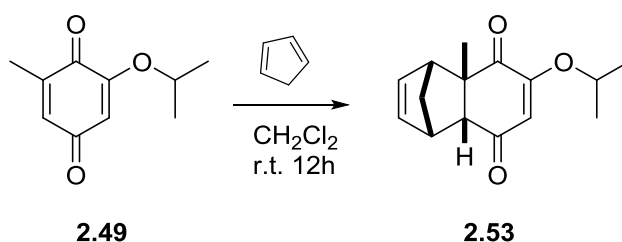


Figure 2.5 By-product **2.52** observed during prolonged reaction times *en route* to **2.49**.

With the *isopropoxy* protected quinone **2.49** at hand a racemic Diels-Alder reaction was performed under standard conditions with freshly cracked cyclopentadiene in dichloromethane to afford the adduct **2.53** in excellent yield (scheme 2.20).



Scheme 2.20 Diels-Alder reaction of **2.49** with cyclopentadiene.

A crystal structure was obtained from adduct **2.53**, which is depicted in figure 2.6 at 30% ellipsoid probability.

yield (93%). This was a very exciting development, following such an arduous journey to result in the formation of the cyclopropane moiety.

Compound **2.54** was confirmed by ^1H NMR using 2D NMR experiments (COSY, HMBC). As can be seen in figure 2.7 and 2.8 the $\Delta^{1,2}$ -olefinic protons both appear as one singlet at 6.53 ppm and correlate to the C-3 (3.48 ppm) and C11 (3.2 ppm) protons, respectively. Assigning the remaining correlations of the former reveals the C-12 bridgehead protons to resonating at 1.25 ppm and 1.01 ppm as a broad doublet and a double of triplets respectively. This can be attributed to a long-range W-correlation seen between the C-12 bridgehead protons and the ring fusion (C-12 to C-3 and C-11).

The remaining C-4 proton is then assigned to a doublet resonating further downfield at 2.58 ppm and, across the six-membered ring, the C-6 proton appears as a singlet at 2.13 ppm. If desired a distinction can be made between the C-5 and C-9 carbonyls respectively. From the HMBC NMR (see appendix 7) of compound **2.53** a two bond correlation can be seen from the C-4 and C-6 protons to the C-5 carbonyl carbon at 206.3 ppm. With the C-5 carbonyl assigned the remaining C-9 carbonyl can be assigned to the signal at 210.3 ppm, which in turn correlates to the C-10 methyl moiety at 1.48 ppm. The isopropyl moiety and the *geminal* methyls at C-7 are then easily distinguished from the remaining signals.

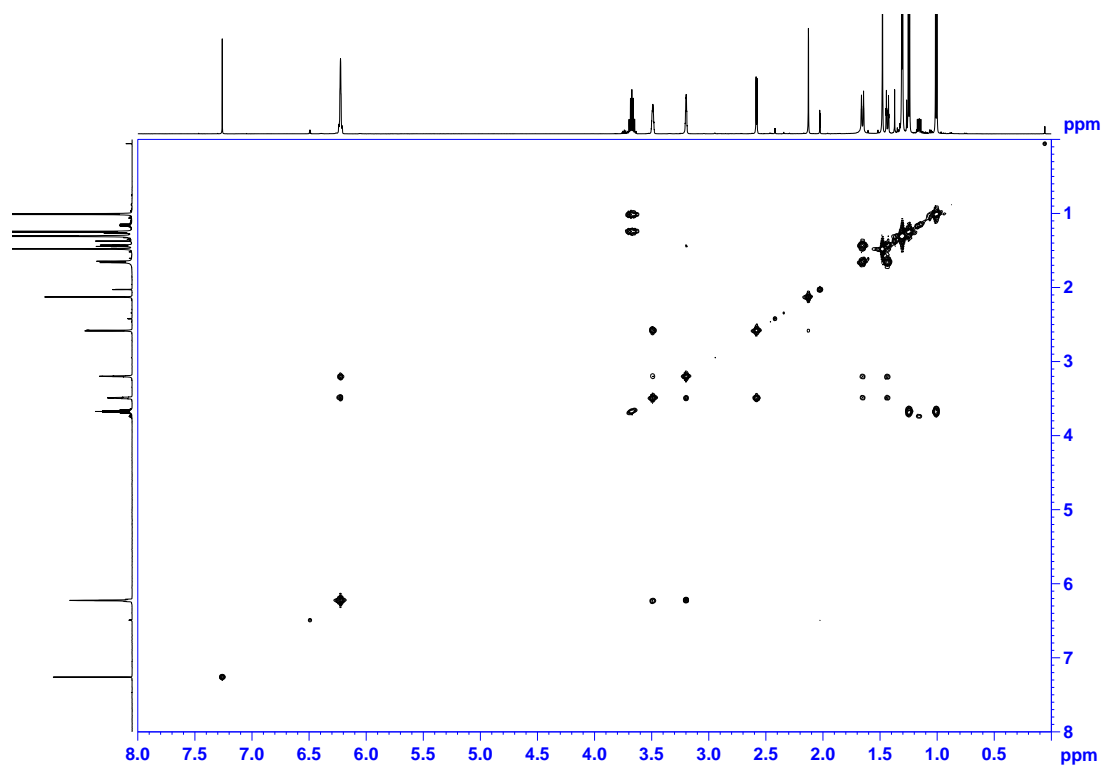


Figure 2.7 2D Correlation Spectroscopy for compound 2.54.

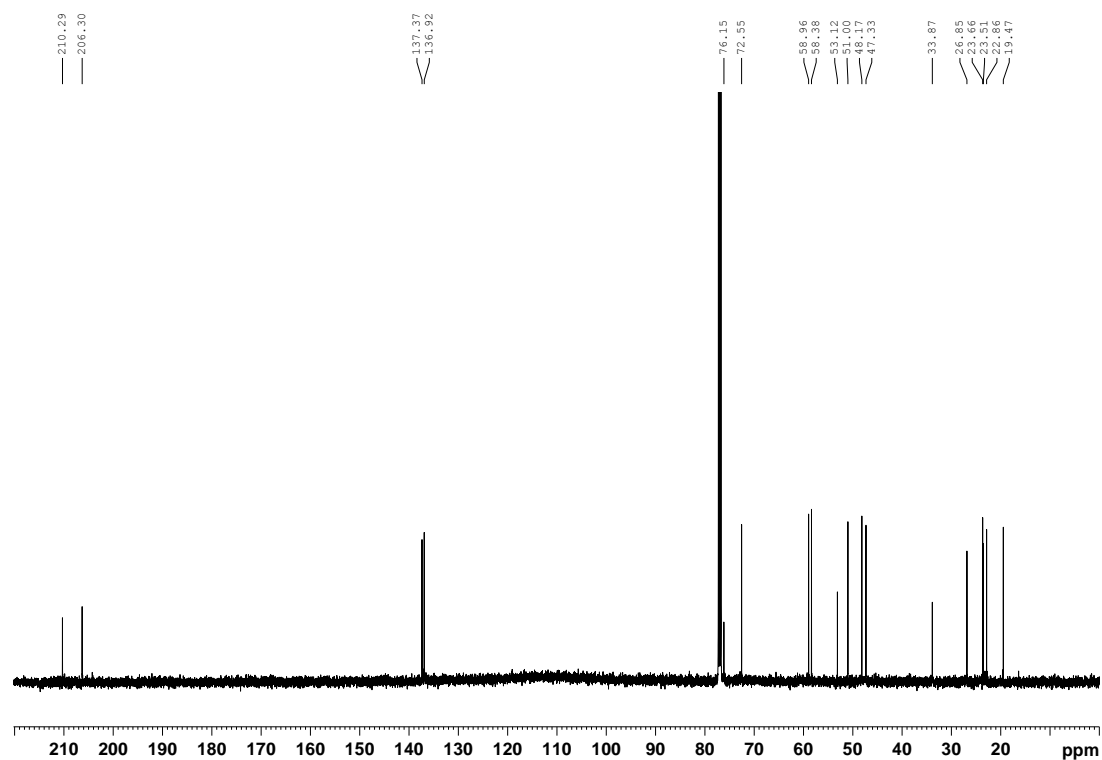
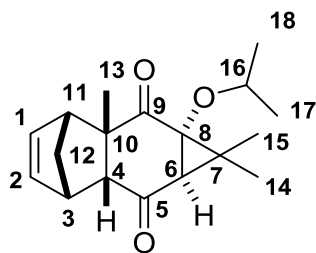


Figure 2.8 500 MHz ^{13}C NMR spectrum for 2.54.



<i>Position</i>	δ_H	<i>Position</i>	δ_H
1,2	6.23 (m, 2H)	13	1.49 (s, 3H)
3	3.50 (m, 1H)	14,15	1.31 (s, 3H)
			1.30 (s, 3H)
4	2.59 (d, $J = 4.2$ Hz, 1H)	16	3.68 (sept, $J = 6.0$ Hz, 1H)
6	2.14 (s, 1H)	17	1.26 (d, $J = 6.0$ Hz, 3H)
11	3.21 (m, 1H)	18	1.02 (d, $J = 6.0$ Hz, 3H)
12	1.68 – 1.65 (m, 1H), 1.44 (dt, $J = 1.7, 9.3$ Hz, 1H),		

Table 2.6 ^1H NMR data for compound **2.54** (500MHz, CDCl_3).

The relative stereochemistry of compound **2.54** was confirmed *via* X-ray crystallography and readily crystallised from petroleum ether. Compound **2.54** crystallised in the monoclinic $P2_1/c$ space group with two molecules occupying a single unit cell.

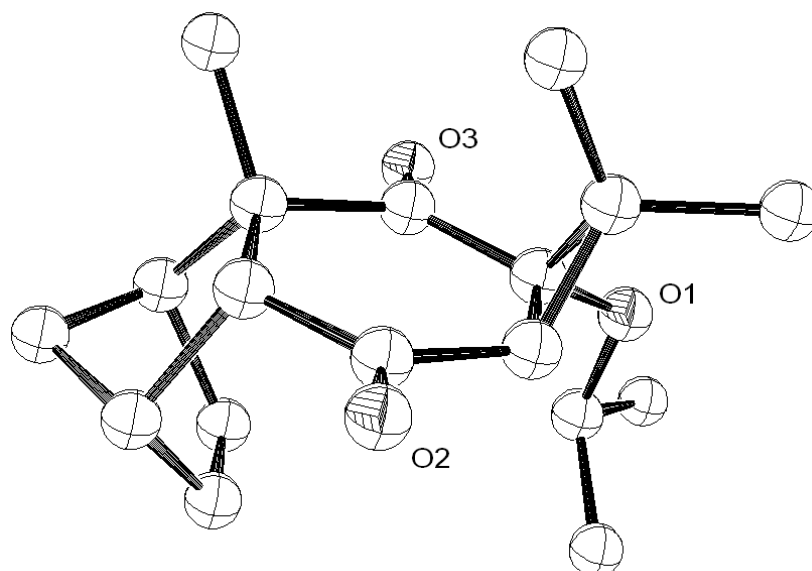
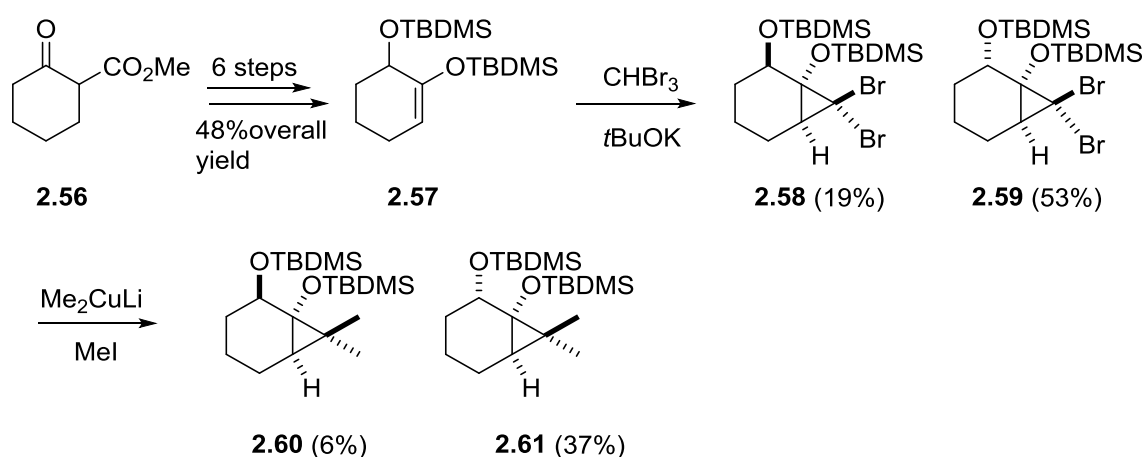


Figure 2.9 ORTEP (30% ellipsoid probability) structure of the cyclopropanation product **2.54**.

To put this exciting cyclopropanation result into perspective Harwood *et al.*⁹¹ showed that bicyclic systems of type **2.61** are difficult to synthesise going to great length to construct **2.59**, requiring a dibromo cyclopropanation followed by transmetallation, which proceeded in poor yield (scheme 2.22). It was shown that these compounds are thermally unstable and in the case of Harwood's approach towards the synthesis of the CD ring system of phorbol that **2.60** and **2.61** degrade at room temperature within 1 week.

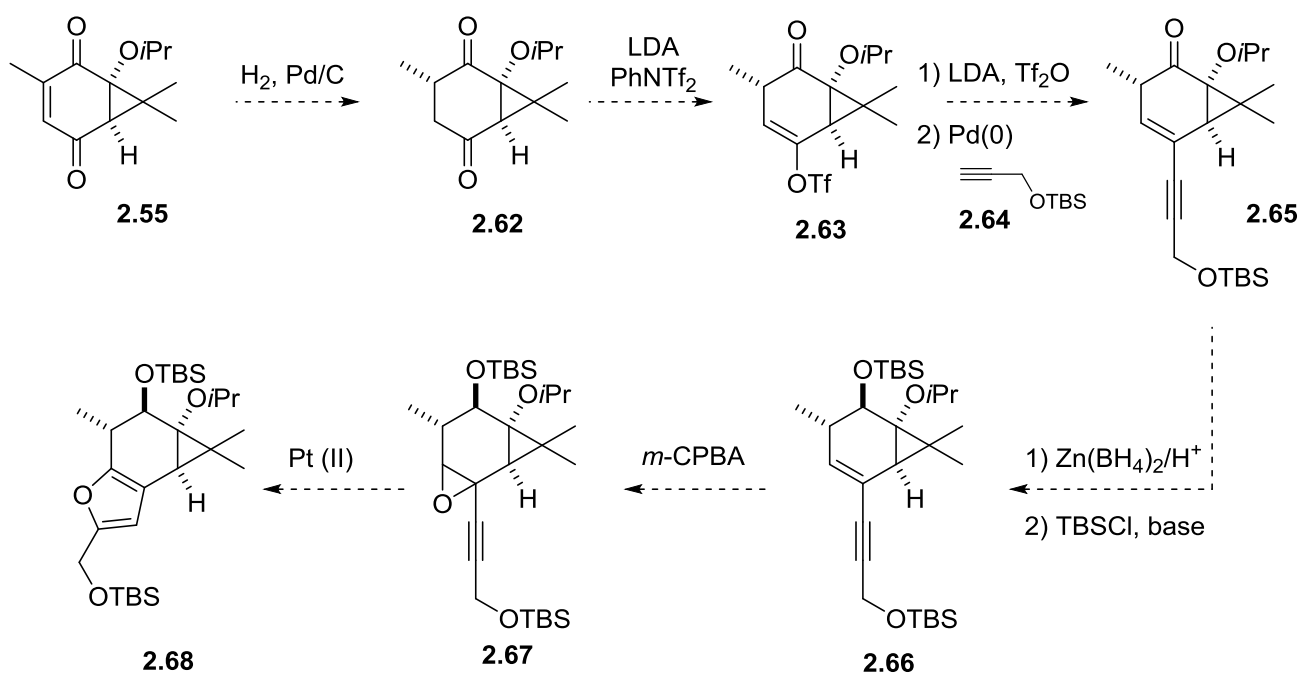


Scheme 2.22 Harwood's synthesis of CD-ring system of phorbol.

With a powerful approach to the key intermediate **2.54**, the journey was continued so as to gain new ground in the advancement towards the right hand fragment.

2.6 Ring C: Reduction Studies

As outlined in the retrosynthetic analysis (scheme 2.1) it was envisaged that in the forward direction double bond reduction of advanced intermediate **2.55** could be performed under a number of conditions utilising reagents such as Mg/MeOH,⁹² Stryker's reagent⁹³ or classical hydrogenation conditions. The latter was, however, not desirable due to the following reason. Triflation of the resulting enol would prepare the system for Sonogashira coupling of **2.63** with readily available protected propargyl alcohol **2.64**. A reduction/protection sequence at C-12 followed by epoxidation and metal mediated ring closure should ultimately provide **2.68**.

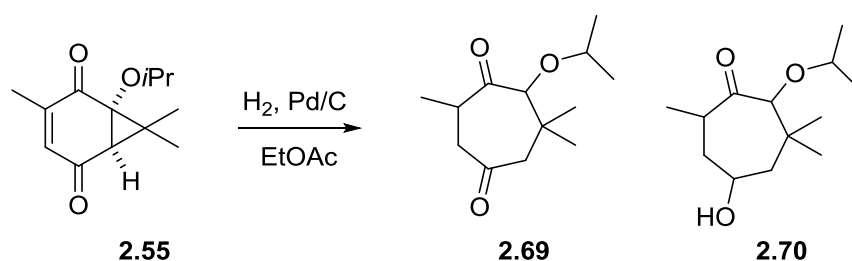


Scheme 2.23 Proposed route to the right hand fragment 2.68.

Due to literature precedents of similar systems undergoing ring opening upon exposure to Pd/C, the first attempts were focused on utilising magnesium in methanol (table 2.7, entry 1) as this has been reported to be a mild method for the reduction of α,β -unsaturated double bonds in the presence of

isolated alkenes. However, the system was unreactive under these conditions. The same situation was faced with Stryker's reagent (entry 2).

Forced by these results it was decided to investigate hydrogenation conditions (entries 3-6) driven by the benefit a successful outcome would offer. This bold move was motivated by the possibility to perform flow hydrogenations utilising an H-Cube® continuous flow reactor, which allows precise control over a number of parameters such as temperature and flow rate and catalyst exposure time. For comparison reasons studies began by investigating hydrogenation under classical conditions. Treating **2.55** under classical hydrogenation conditions afforded, as expected, ring-opened product **2.69** along with traces of alcohol **2.70** (scheme 2.24).



Scheme 2.24 Hydrogenation studies on 2.55.

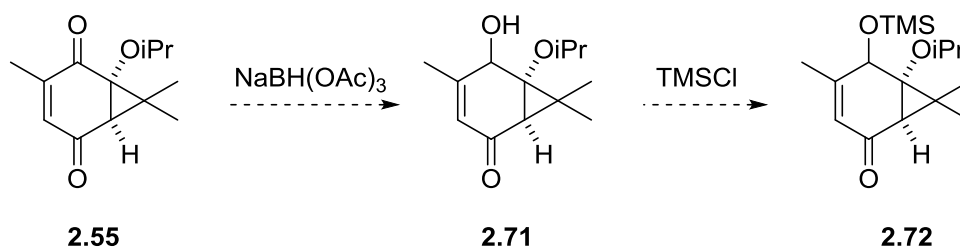
Next, a series of hydrogenations under flow conditions were performed. It was found that catalyst exposure time (flow rate of 3 mL/min vs. 1 mL/min) had no effect on the outcome of the reaction. Furthermore, utilising extremely mild conditions involving presaturation of the palladium catalyst with hydrogen were investigated.

<i>Entry</i>	<i>Conditions</i>	<i>Product</i>
1	Mg, MeOH	No reaction
2	Stryker's reagent	No reaction
3	Pd/C, H ₂ (Classic)	2.69 , traces 2.70
4	Pd/C, H ₂ (H-Cube®)	2.69 , traces 2.70
5	Pd/C, H ₂ + pyridine (Classic, H-Cube®)	2.69 , traces 2.70
6	Lindlar®, H ₂ (H-Cube®)	2.69 , traces 2.70

Table 2.7 Condition screening for the reduction of 2.55.

Using the adsorbed hydrogen on the catalyst as the only hydrogen source affected the same transformation to afford **2.69** and traces of **2.70**. Poisoning the catalyst with pyridine (entry 5) or using Lindlar® catalyst (entry 6) unfortunately did not change the course of the reaction.

Having failed to directly reduce the double bond it was envisaged that reducing the more hindered ketone at C-12 and protection of the resultant alcohol would afford a more stable system by removing the conjugation ultimately reducing the strain of the three-membered ring D (scheme 2.25). Accordingly, attempts were made at reducing the C-12 ketone employing $\text{Zn}(\text{BH}_4)_2$ as the reducing agent.⁹⁴ In the event of over-reduction, i.e. reduction at C-12 and C-8, respectively, selective mild re-oxidation could lead to the desired product **2.72**. The advantage of utilising $\text{Zn}(\text{BH}_4)_2$ lies in the selective anti-reduction of α -hydroxyketones as reported by Nakata *et al.*^{94b} leading to the desired relative configuration.

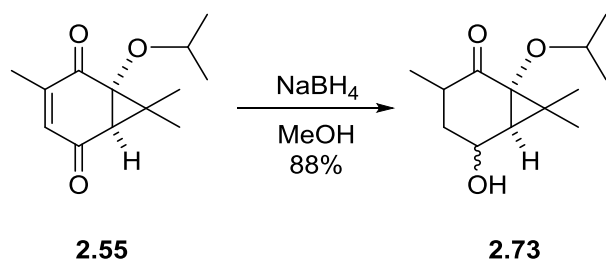


Scheme 2.25 Alternate approach for reduction of the C-ring.

When exposing **2.55** to $\text{Zn}(\text{BH}_4)_2$ in diethyl ether, however, no reaction was observed and starting material was fully recovered. A series of temperatures and exposure times were employed, yet again without success.

In the total synthesis of (+)-phorbol (**1.1**), Wender³⁷ made use of $\text{NaBH}(\text{OAc})_3$ when reducing the C-12 ketone on the tiglane core. This prompted deployment of this methodology to the quinone system **2.55**. Frustratingly, also these attempts were unsuccessful.

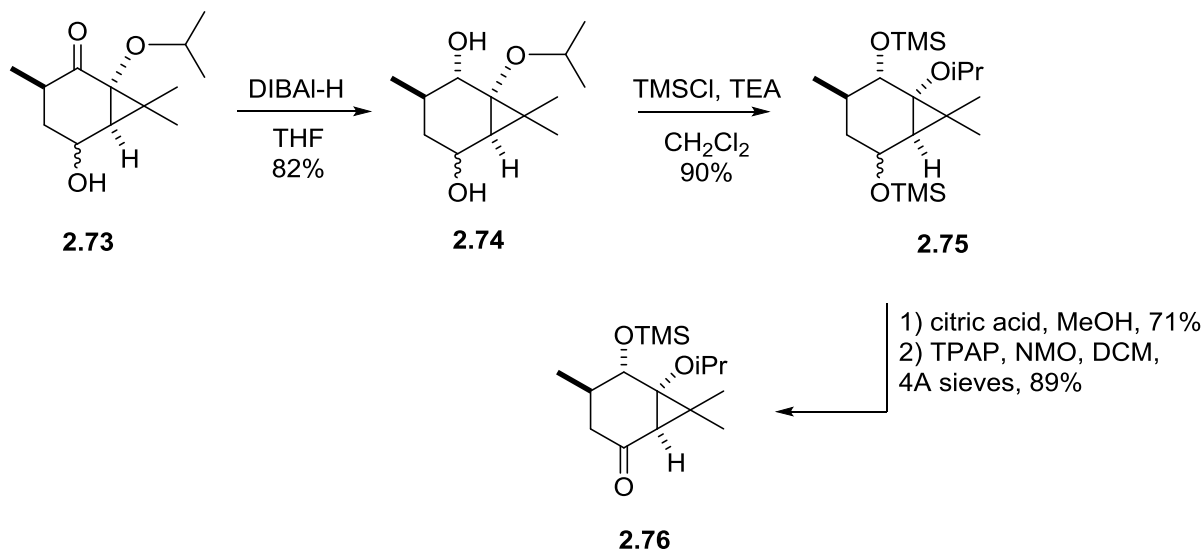
Due to the lacking reactivity of the key intermediate **2.55** towards these mild conditions, a global reduction was attempted in the hope of selectively re-oxidising the less hindered alcohol. To affect this transformation harsher conditions were employed, i.e. NaBH_4 as the reducing agent.



Scheme 2.26 Reduction studies to 2.55 utilising NaBH₄.

Even under these more forcing conditions, ketone at C-12 remained unaltered. Instead two consecutive reductions, namely a 1,4 and a 1,2-reduction, occurred to afford **2.73**. Re-oxidation of the resultant alcohol utilising tetrapropylammonium ruthenate (TPAP) was partially successful. However, it was plagued by oxidative reinsertion (i.e. oxygen) of the undesired olefinic bond.

Moving to the more powerful reducing agent DIBALH, the diol **2.74** was successfully obtained in 82% yield which was globally protected to afford disilyl ether **2.75** in 90% yield. Selective deprotection utilising citric acid in methanol followed by oxidation under standard conditions using TPAP/NMO then afforded the desired ketone **2.76** in 63% yield over 2 steps.



Scheme 2.27 Synthetic pathway to ketone 2.76.

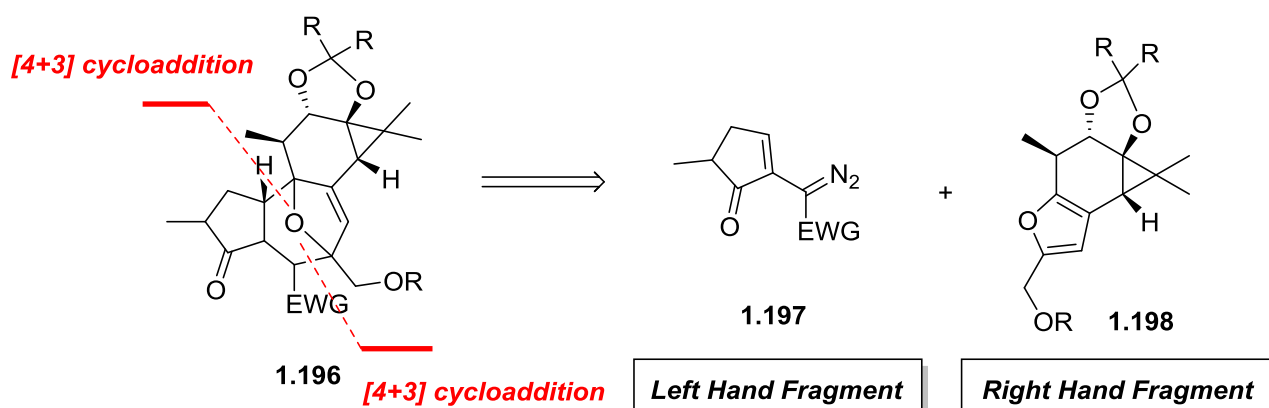
Due to time limitations further work on this system as outlined in scheme 2.23 is currently underway in the Williams laboratory performed by Dr Sharon Chow. Thus, with the right hand

fragment in an advanced state it was important to now start investigating the synthesis of the A-ring and the subsequent [4+3] cycloaddition reactions.

3 Synthetic Investigations Towards the Construction of the Left Hand Fragment

3.1 Introduction

As outlined in chapter 1.11 (scheme 1.21) the retrosynthetic approach to the seven-membered ring of the target molecule (-)-phorbol **1.169** is envisaged to be achieved *via* a formal [4+3] cycloaddition reaction between a diazo compound and a furan.^{63a}



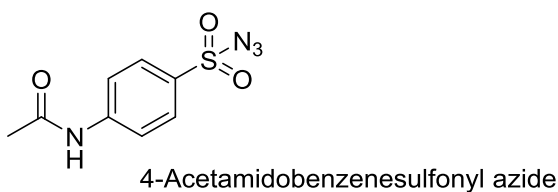
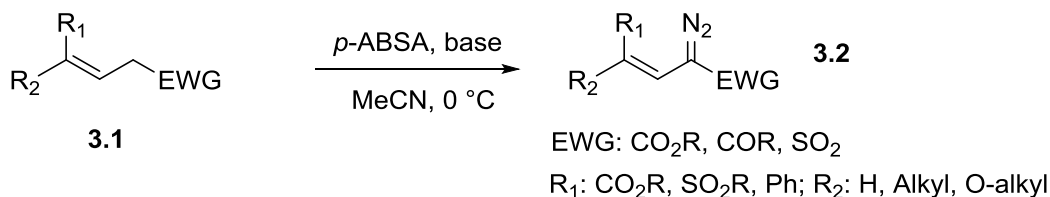
Scheme 3.1 Retrosynthetic leading to LHF and RHF.

Diazo compounds have been shown to be extremely versatile reagents and modern organic chemistry still benefits from the unique versatility of diazocarbonyl compounds ranging from cyclopropanations and C-H insertion to cycloadditions amongst many other useful organic reactions.⁹⁵

3.2 Diazo Transfer Approach

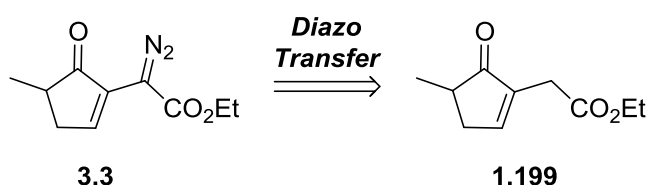
The standard approach to alkenyldiazoacetates of type **3.1** involves the treatment of the corresponding unsaturated ester with diazo transfer reagents such as tosyl azide or more commonly 4-acetamidobenzenesulfonyl azide (*p*-ABSA) in presence of base as shown in scheme 3.2.⁹⁶

Diazo Transfer Reaction



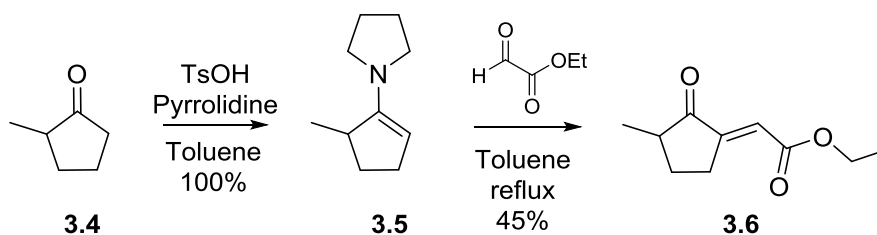
Scheme 3.2 General diazo transfer transformation.

While most of the diazo transfer reactions occur on activated methylene groups of 1,3-dicarbonyls it has been shown that β,γ -unsaturated carbonyl systems such as **1.199** undergo these type of reactions without additional activation.⁹⁷



Scheme 3.3 Synthetic plan for diazo transfer to construct the LHF.

A feasible method to provide the diazo transfer precursor **1.199** was to utilise enamine chemistry described by Barco *et al.*⁹⁸ Enamines are versatile intermediates in organic chemistry and can be easily prepared *via* the reaction of a ketone with secondary amines. *In situ* formation of enamine **3.5** (scheme 3.4) from 2-methylcyclopentanone and pyrrolidine followed by condensation with ethyl glyoxalate affords compound **3.6** bearing an exocyclic double bond.



Scheme 3.4 Forward strategy to diazo transfer precursor 3.6.

Compound **3.6** was characterised *via* ^1H , ^{13}C and 2D COSY correlation spectroscopy. A representation of the latter can be seen in figure 3.1. Methyl group 9 is represented by a doublet signal at 1 ppm while the associated carbon signal shows a resonance at 119.9 ppm in the corresponding ^{13}C NMR spectrum. The correlation between the methyl 9 and proton 2 can be clearly seen from the 2D COSY spectrum (figure 3.1). The exocyclic double bond 5 at a shift of 6.52 ppm shows correlations to two protons at 4-position.

Installation of the double bond at the desired position proved overwhelmingly difficult. Classic double bond isomerisation methods such as acid catalysed isomerisation failed to afford the desired compound **1.199** in acceptable yields.

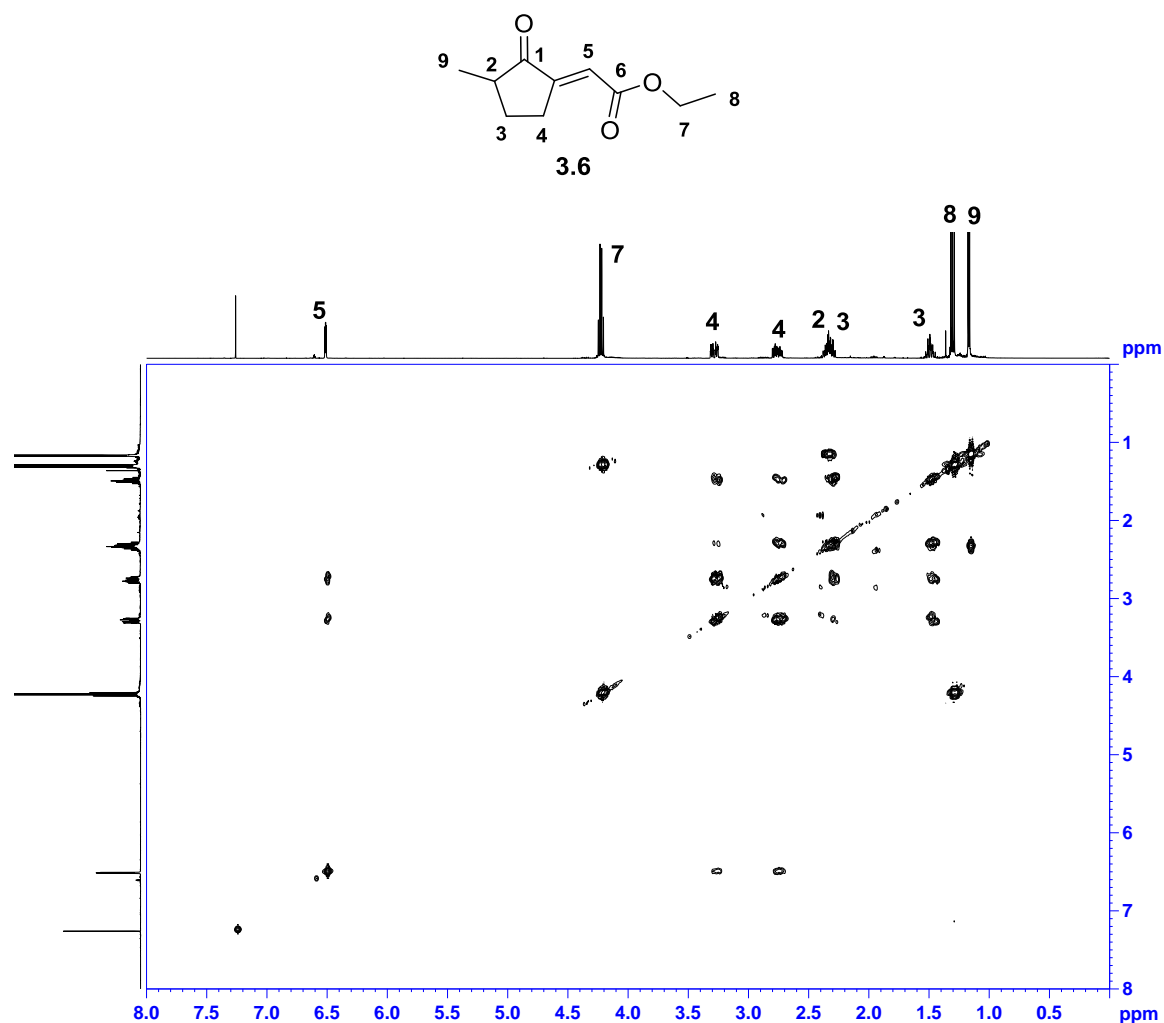
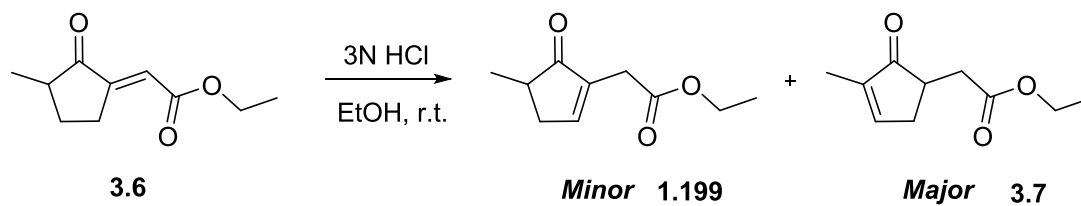


Figure 3.1 2D-COSY spectrum of exocyclic compound 3.6.

The major compound isolated from the double bond isomerisation reaction (scheme 3.5) was **3.7**, which seemed to be the more stable enone. The purification of the obtained products from this reaction was not straightforward using flash chromatography as the three components possessed similar R_f -values on silica.



Scheme 3.5 Double bond isomerisation of 3.6 under acidic conditions.

Initial purification *via* column chromatography followed by Kugelrohr distillation was able to resolve the components to an acceptable degree. As seen in figure 3.2 only a minor amount of **3.7** was present after purification.

The ^1H NMR of **3.6**, **1.199** and **3.7** is shown in figures 3.2 and 3.3. The double bond isomerisation from the exocyclic **3.6** to **1.199** gives rise to a multiplet resonance between 7.30 and 7.22 ppm in comparison to 6.52 ppm. The installation of the $\Delta^{4,5}$ - double bond (**1.199**) correlates to most downfield shift at 7.53 – 7.51 ppm.

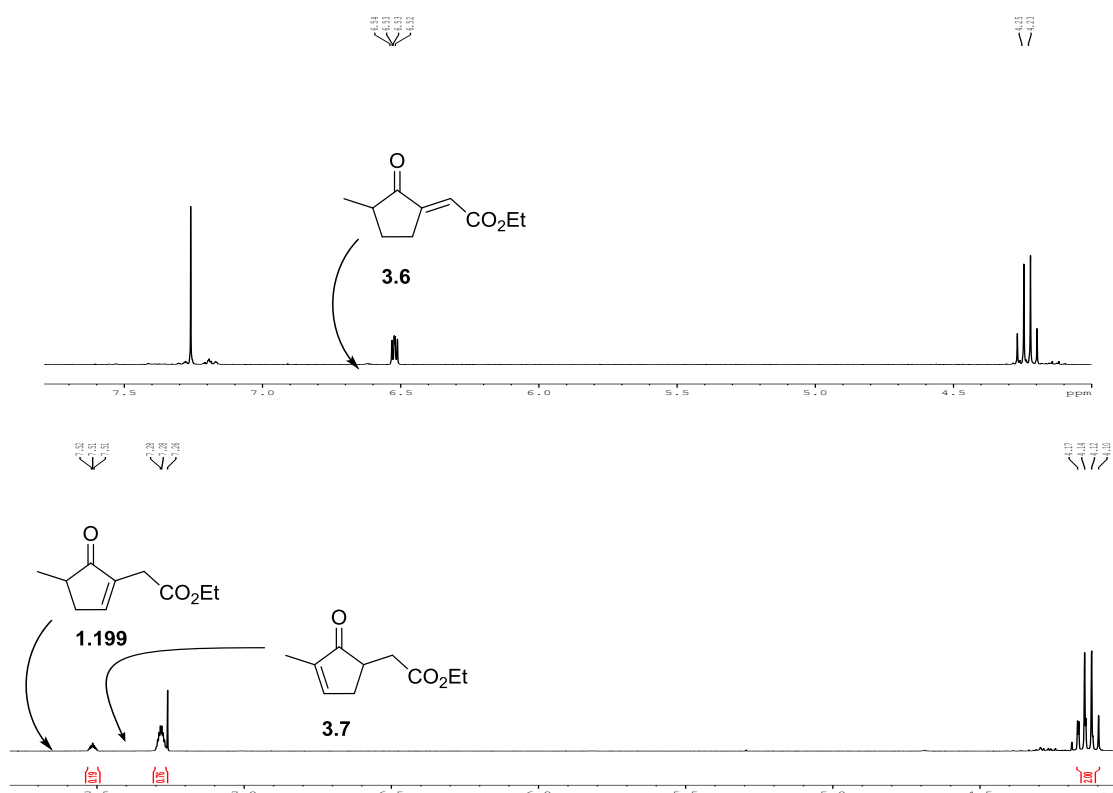
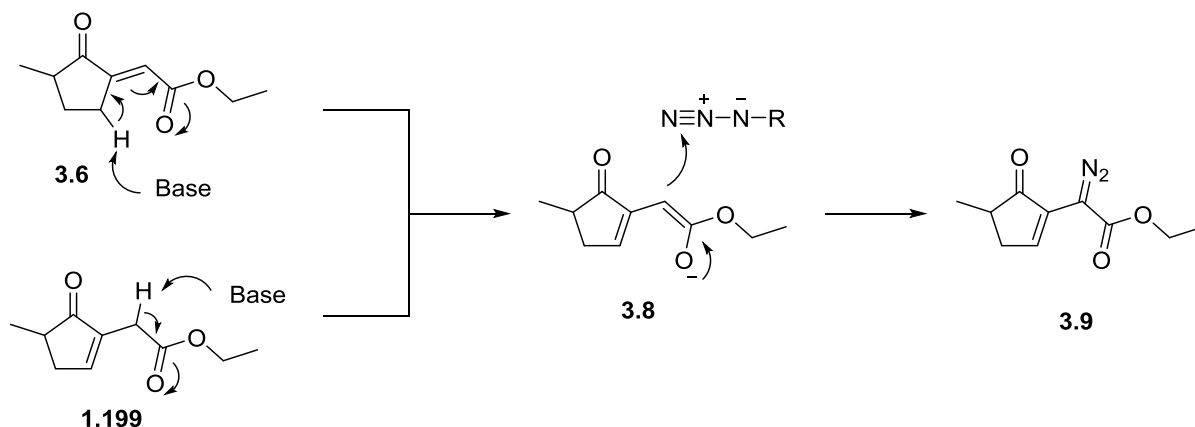


Figure 3.2 Distinction of double bond isomerisation products by ^1H NMR.

Fortunately, sufficient of the desired compound could be obtained in order to further investigate the diazo transfer reaction. Furthermore, exocyclic ester **3.6** was believed to be capable of diazotisation *via* deprotonation at the γ -position followed by reaction of the resulting enol (scheme 3.6). If such a reaction would prove successful the synthesis of **1.199** would be made redundant thus shortening the synthetic sequence.



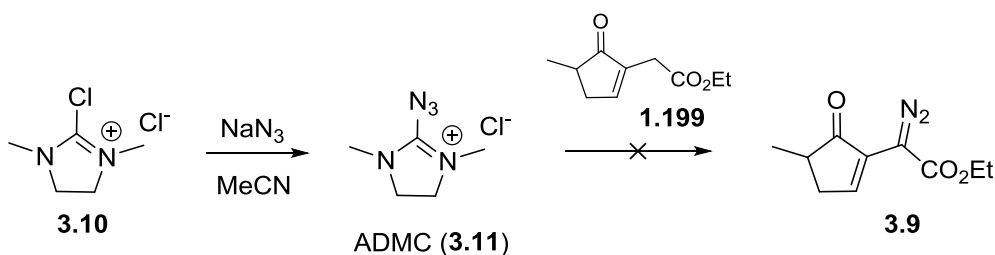
Scheme 3.6 Diazo transfer reaction using either **1.199 or **3.6**.**

Initial attempts at performing the diazo transfer reaction in the presence of tosyl azide and triethylamine (table 3.1, entry 1) failed to give the desired product in both cases. Rather decomposition was observed on prolonged reaction times. In an effort to optimise reaction conditions the stronger base DBU (entry 2) was employed to investigate whether the failure could be accounted for by the lack of enolisation. However, DBU did not achieve an improvement over triethylamine. Unfortunately, reversion to the more reactive diazo transfer reagent *p*-ABSA (entry 3 and 4), was likewise met with the same disappointing outcome.

<i>entry</i>	<i>reagent</i>	<i>base</i>	<i>solvent</i>	<i>product</i>
1	TsN ₃	NEt ₃	MeCN	decomposition
2	TsN ₃	DBU	MeCN	decomposition
3	<i>p</i> -ABSA	NEt ₃	MeCN	decomposition
4	<i>p</i> -ABSA	DBU	MeCN	decomposition
5	ADMC	DBU	MeCN	decomposition
6	ADMH	DBU	MeCN	decomposition

Table 3.1 Screening of diazo transfer reagents and conditions.

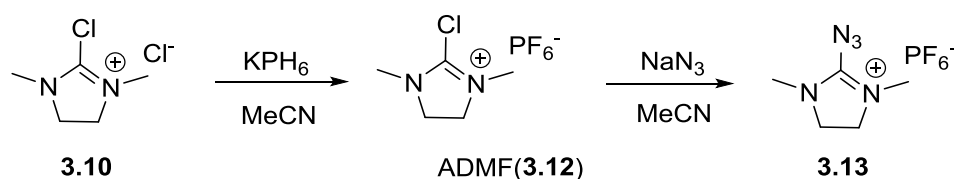
Kitamura *et al.* discovered the utility of 2-azido-1,3-dimethylimidazolinium chloride (ADMC) (**3.11**, scheme 3.7) as a new diazo transfer reagent with a high substrate tolerance, which has since become a highly useful reagent that is now commercially available.⁹⁹ In addition, this newly developed reagent offers the advantage of water soluble by-products, which facilitates the purification process immensely. Accordingly, 2-azido-1,3-dimethylimidazolinium azide **3.11** was formed *in situ* from 2-chloro-1,3-dimethylimidazolinium chloride **3.10** and sodium azide in acetonitrile at 0 °C. Upon addition of **1.199** to the reaction mixture (table 3.1, entry 5-6) no reaction was observed under the given conditions. This could have been due to the well-known sensitivity of ADMC toward traces of moisture.



Scheme 3.7 Diazo transfer with Kitamura's salt ADMC.

To improve upon the hygroscopic nature of ADMC Kitamura *et al.* reported that a counter anion exchange from the chloride to hexafluorophosphate could circumvent this issue and increase the stability of the reagent significantly.^{99b} Thus, counter ion exchange was accomplished in excellent yields using potassium hexafluorophosphate to afford chloride **3.12**. With its improved stability

3.12 could be isolated and further converted to the stable azide **3.31** upon treatment with sodium azide.



Scheme 3.8 Counter-ion exchange for a more stable Kitamura reagent (ADMF).

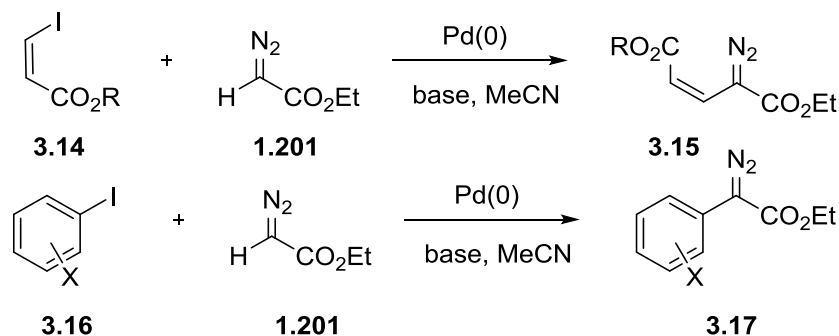
The reaction with **1.199** and the newly prepared diazo transfer reagent was conducted under identical conditions using DBU in acetonitrile (table 3.1, entry 6). Unfortunately, the more stable reagent did not yield the desired compound **3.9**.

Having failed to obtain the left hand fragment *via* this otherwise robust method new avenues were required in which to achieve the synthesis of this key fragment. One such possibility based on the work of Wang *et al.*,¹⁰⁰ which describes direct palladium mediated cross coupling of vinyl and aryl iodides with ethyldiazo acetate.

3.3 Diazo Direct Palladium Cross-Coupling Approach

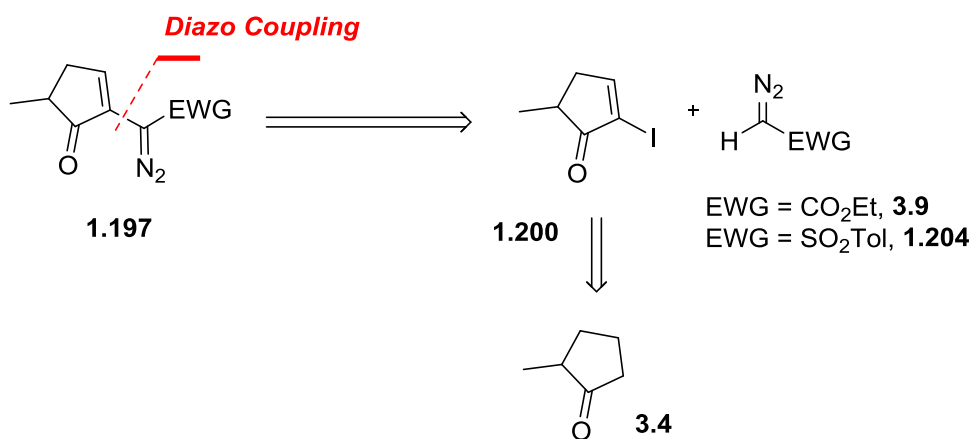
3.3.1 First generation Approach

Wang and co-workers discovered that diazo compounds such as ethyldiazo acetate are sufficiently nucleophilic reagents to facilitate a direct palladium cross coupling in moderate yields. In Wang's work vinyl and aryl iodides were smoothly fused to the corresponding diazoacetates **3.15** and **3.17** (scheme 3.9).



Scheme 3.9 Wang's direct diazo cross-coupling.

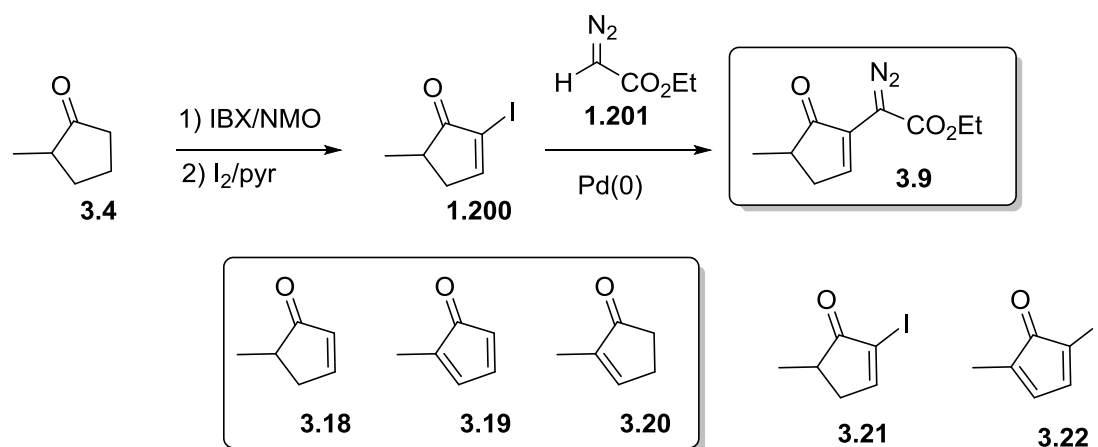
Utilising this new methodology the synthesis of the left hand fragment **3.9** was approached *via* a newly revised strategy. The alternate retrosynthetic analysis of the left hand fragment begins with disconnection of ethyldiazo acetate to generate the necessary precursors for a direct diazo cross coupling as described by Wang *et al.* (scheme 3.8). In turn iodide **1.86** can be synthesised from commercially available 2-methylcyclopentanone **3.4**. Controlling the stereochemistry at C-2 is not necessary as it is eliminated at a later stage in synthesis.



Scheme 3.10 Alternate retrosynthetic analysis of the LHF.

Unfortunately, this methodology could not be directly superimposed. Coupling of ethyl diazoacetate with non-aromatic cyclic iodides such as **1.200** has thus far not appeared in the literature. Nevertheless, it seemed feasible that such a transformation had high probability.

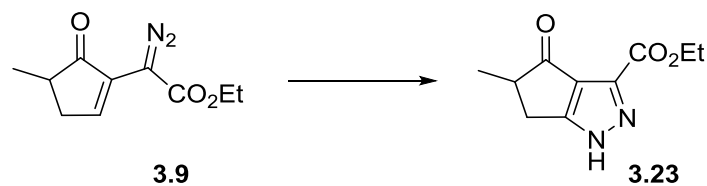
In an attempt to synthesise key fragment **1.200** introduction of the double bond was performed using IBX/NMO⁶⁷ to afford a 2:1:1 mixture of products **3.18**, **3.19** and **3.20** (scheme 3.11).



Scheme 3.11 Alternate forward strategy to the LHF.

Attempts at purifying the desired compound **3.18** *via* atmospheric distillation failed due to the similar physical properties of all compounds. With this in mind it was envisaged that derivatisation of the mixture with iodine would regioselectively afford compound **3.21** and **3.22** facilitating purification *via* silica column chromatography. Unfortunately, compound **1.200** was found to be unstable to silica column chromatography, but sufficient material was obtained in order to investigate palladium coupling. When performing the cross coupling reaction with ethyldiazo acetate, no reaction was observed. Despite repeated attempts under various conditions, treatment of **1.200** with ethyldiazo acetate returned a complex mixture of products.

In an attempt to understand why the palladium coupling was failing the reaction was repeated without attempting further purification. A crude sample was analysed by GC/MS and a peak tentatively assigned to compound **3.23** was observed.



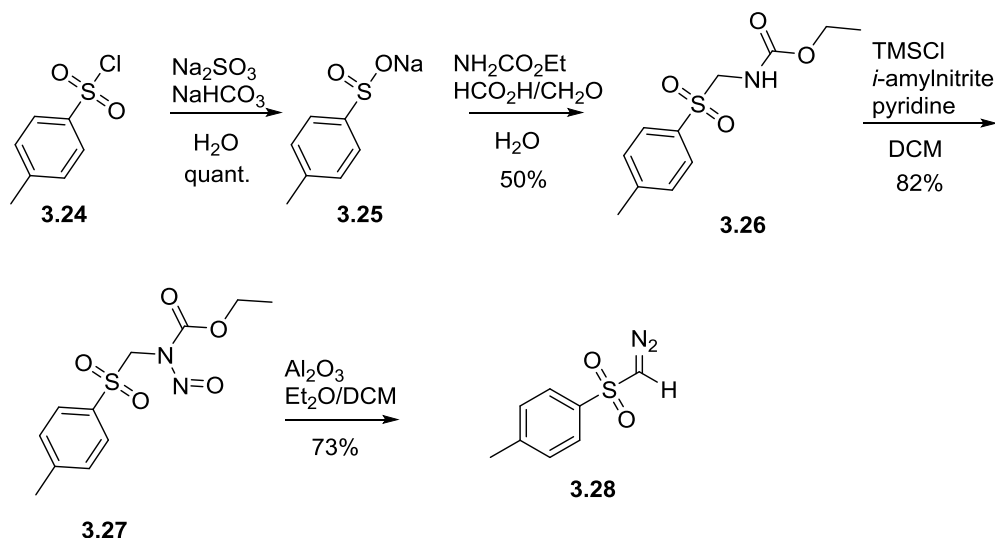
Scheme 3.12 Possible pyrazole formation during diazo formation.

The basis of the structural assignment was maintained by the fact that under mass spectrometry electron ionisation conditions diazo compounds tend to decompose to the corresponding carbenes. As loss of nitrogen from the molecular ion was not observed the conclusion was drawn that under the reaction conditions spontaneous cyclisation occurs to afford the more stable pyrazole **3.23** as previously reported.¹⁰¹ Thus, the complex nature of the mixture in combination with low conversion and the unexpected spontaneous cyclisation of the diazo compound proved fatal to this approach and as such it was abandoned.

In a separate approach the effect of tosyl diazomethane **3.29** as an electron withdrawing group was briefly investigated in an attempt to circumvent the aforementioned difficulties (scheme 3.13). As an added advantage the removal of a sulfone moiety can be achieved in a more straightforward manner in contrast to that of an ester (i.e. mild removal with Na/Hg). This would possibly allow a smoother transition at a later stage of the synthesis by removal of this handle once construction of the seven-membered ring had been achieved. Thus, the synthesis of tosyl diazomethane **3.28** was undertaken (scheme 3.13).

3.4 Synthesis of Tosyl diazomethane

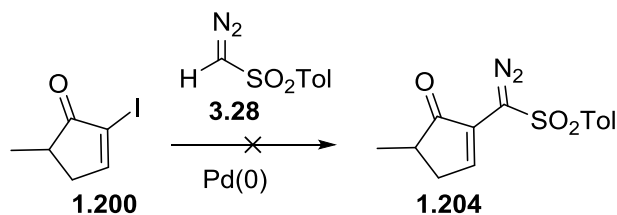
Following the route reported by Corey *et al.*⁷⁵ the synthesis of **3.28** was started with commercially available tosyl chloride **3.24**. The chloride **3.24** was converted to **3.25** by treatment with an aqueous equimolar mixture of sodium sulfate and sodium hydrogen carbonate.



Scheme 3.13 Synthesis of tosyl diazomethane **3.28**.

Synthesis of ester **3.26** was achieved by exposure of **3.25** to an aqueous mixture of urethane, formic acid and formaldehyde. Subsequent nitrosation gave rise to compound **3.27** in 82% yield. The title diazo compound **3.28** was then obtained upon treatment of **3.27** with aluminium oxide in dichloromethane in 73% yield.

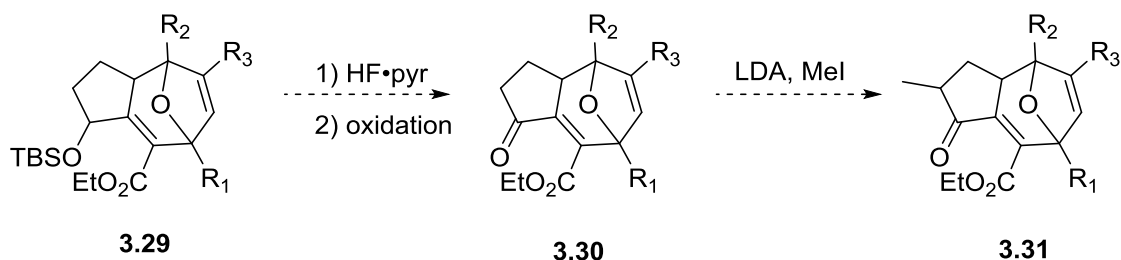
With the synthesis of **3.28** completed further attempts in trying to achieve the synthesis of the left hand fragment **1.204** could be undertaken. Treating 2-iodocyclopentenone with tosyl diazomethane (**3.28**) utilising Wang's conditions (i.e. DBU, $\text{Pd}(\text{PPh}_3)_4$, $n\text{Bu}_4\text{NBr}$) unfortunately, afforded the same outcome as previously observed with ethyldiazo acetate. Screening a variety of different conditions did not lead to the desired compound forcing a re-evaluation of the synthetic strategy.



Scheme 3.14 Initial direct diazo coupling of 1.200 to 3.28.

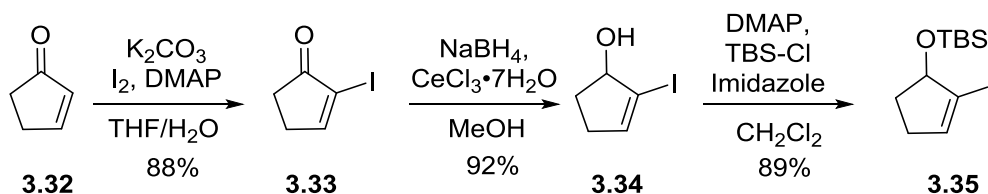
3.4.1 Second Generation Approach

Reflecting upon the experience with this system it was quickly realised that the methyl group at C-2 contributed to additional by-products by affording a competitive pathway to a more stabilised alkene **3.7** (scheme 3.5). The methyl group could easily be introduced at a later stage in the total synthesis as it is situated alpha to the C-3 carbonyl moiety (compound **1.169**, scheme 2.1). This could be achieved *via* deprotection/oxidation sequence to afford ketone **3.30** as outlined in scheme 3.15. Subsequent enolisation under standard conditions followed by quenching with MeI would arrive at the C-2 methyl ketone **3.31** as desired.



Scheme 3.15 Possible introduction of the C-2 methyl group.

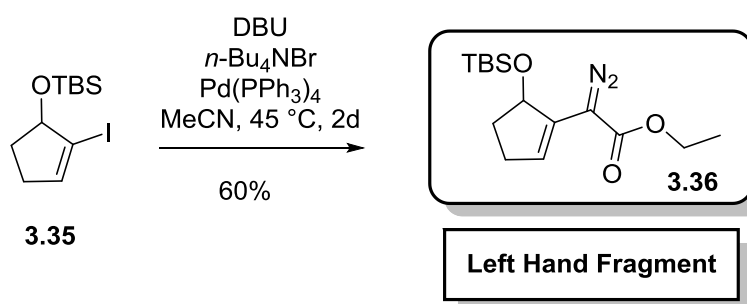
Furthermore, the necessity to derail pyrazole formation prompted further simplification of the cyclopentene ring ultimately arriving at **3.32** which was chosen as a starting material.



Scheme 3.16 Second generation approach to the coupling precursor 3.35.

The synthetic sequence began with α -halogenation under standard aqueous conditions for enones to afford **3.33** in 88% yield. Luche reduction followed by TBS protection gave rise to the coupling precursor **3.35** in an overall yield of 72% over three steps. The significantly improved approach now made it synthetically feasible to proceed with a thorough investigation towards the direct diazo cross coupling reaction.

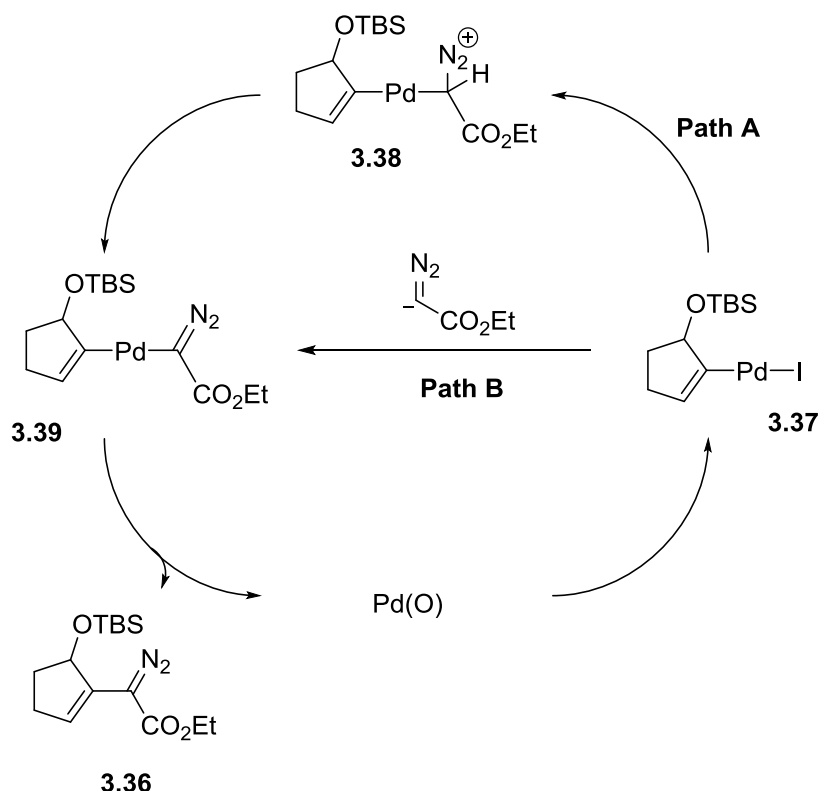
While initial attempts in utilising NEt_3 and $\text{Pd(PPh}_3)_4$ in MeCN failed to give the desired product, increasing the basicity of the amine by the use of DBU in combination with a slight increase in temperature (45 °C) ultimately afforded a desired left hand fragment **3.36**.



Scheme 3.17 Successful synthetic route to the LHF.

The reaction is highly concentration dependent, requiring as long as 48 hours while dilute, reducing to just 12 hours when starting with a more concentrated solution. To the best of our knowledge this represents the first example of a diazo coupling utilising a cyclic vinyl iodide.

A possible mechanistic explanation of the direct diazo coupling is depicted in figure 3.18. Wang *et al.*¹⁰⁰ suggested two different pathways for the construction of such systems. Oxidative addition of the palladium source to the substrate followed by diazo anion substitution affords **3.39** (Path B). Alternatively, **3.39** is believed to be formed *via* the coordination of the ethyldiazo acetate anion to **3.37** to form complex **3.38** from which proton is removed by base (Path A).



Scheme 3.18 Plausible mechanism for the direct diazo coupling to afford 3.36.

Compound **3.36** was characterised *via* ^1H , ^{13}C NMR spectroscopy, IR, and GC/MS analysis. In order to obtain a full carbon spectra, extended acquisition and delay times had to be applied. The ^{13}C key resonances are shown in figure 3.3 with the C-7 carbonyl resonating at 166.4 ppm, the alkene moiety C-4 at 132.1 ppm and C-1 resonating at 78 ppm. Despite variations in NMR data acquisition, a sufficiently strong signal of the C-6 quaternary carbon could not be obtained to prove conclusively, most likely due to the nitrogen quadrupole effect. A weaker signal at 44 ppm could be obtained and was tentatively assigned to the C-6 carbon. However, strong evidence is obtained from IR measurements of the presence of the diazo functionality (figure 3.4).

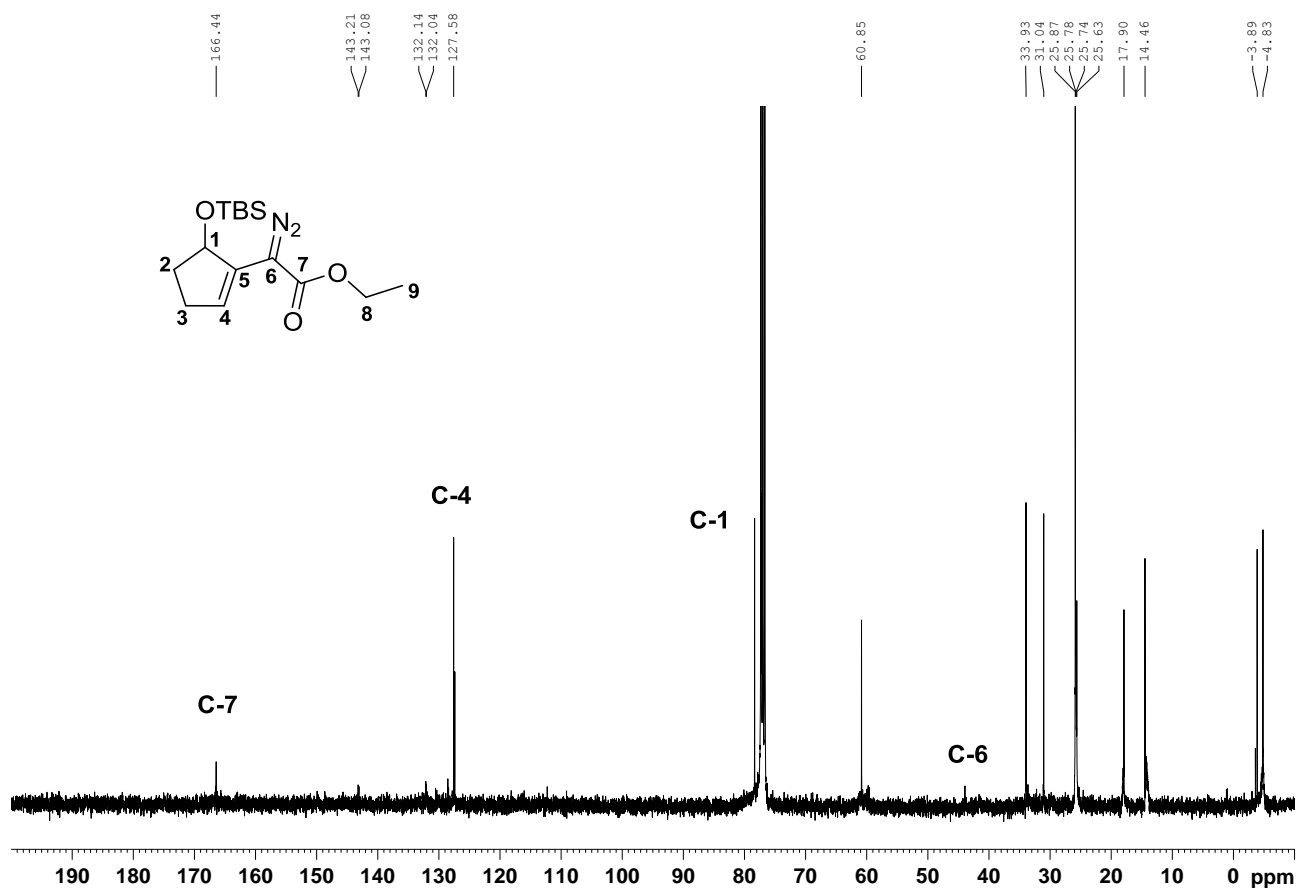


Figure 3.3 ^{13}C key resonances of compound 3.36.

The FTIR spectrum of the Left Hand Fragment **3.36** exhibits a broad absorption band at 2085 cm^{-1} that is attributed to the diazo stretch of the molecule while ethyldiazo acetate itself exhibits a broad absorption band slightly shifted at 2107 cm^{-1} (figure 3.4)

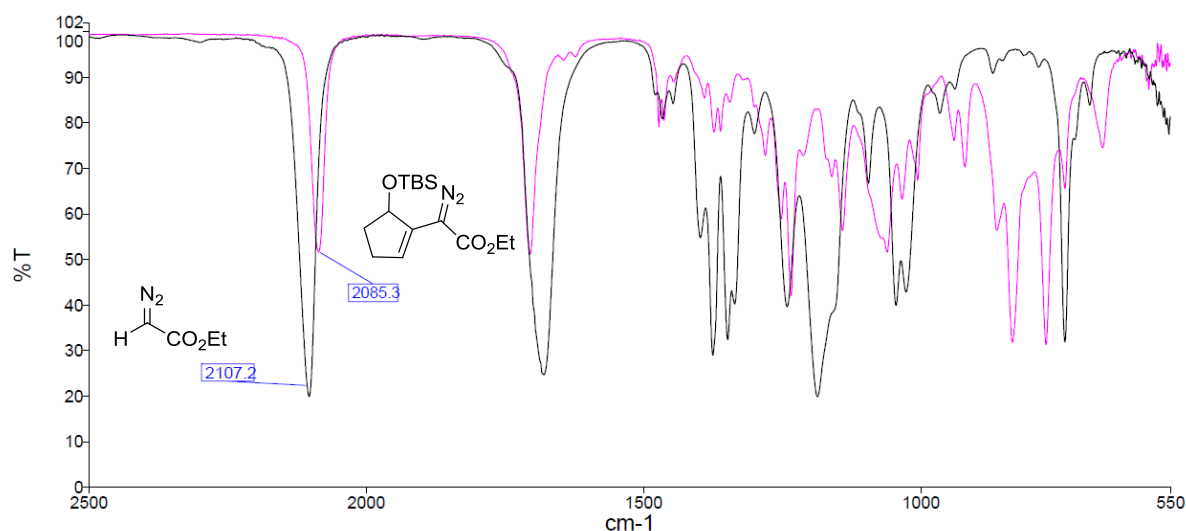


Figure 3.4 Diazo stretch comparison between 3.36 and ethyldiazo acetate.

Moreover, characterisation using GC/MS under electron ionisation (EI) conditions showed the loss of nitrogen while low resolution electrospray ionisation (LRESI) mass measurements showed a mass of m/z 333 which corresponds to $[M+Na]$. In contrast to our previous discussions in regard to spontaneous cyclisation of **3.9** to pyrazole **3.23** (scheme 3.12) a direct comparison of the GC/MS spectra (figure 3.5) confirms our suspicions thus justifying the new simplified approach.

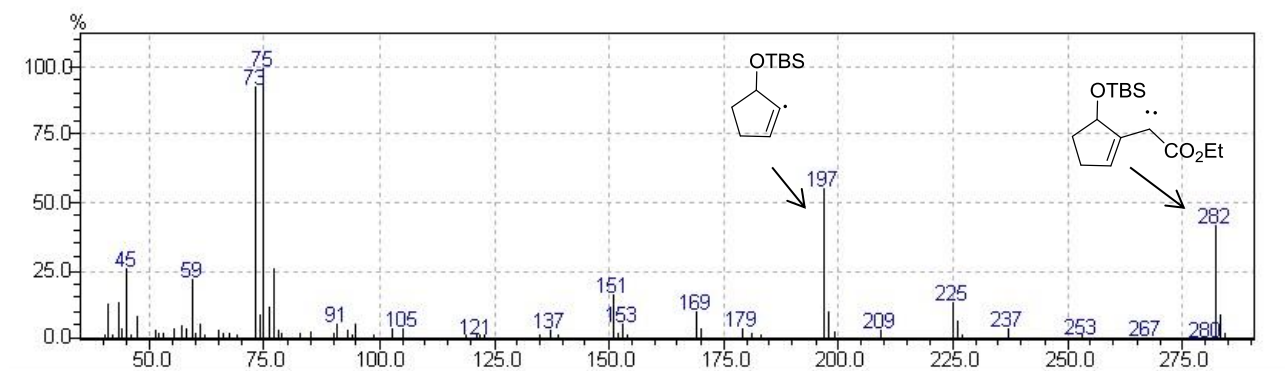
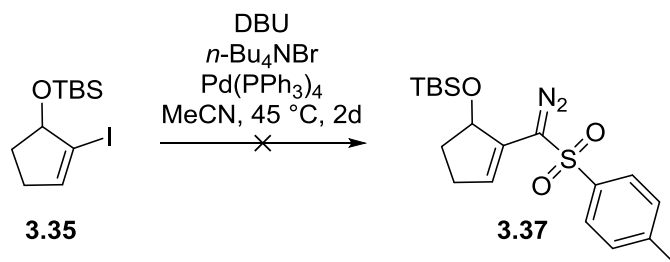


Figure 3.5 GC/MS fragmentation pattern of compound 3.36.

For reasons mentioned previously the viability of tosyl diazomethane **3.28** as the coupling partner was investigated. Performing the palladium catalysed cross-coupling reaction under identical conditions to that of **3.36** proved unsuccessful. Likewise, a change in catalyst to the more reactive $Pd(dba)_2$ did not alter the outcome of the reaction.



Scheme 3.19 Direct diazo coupling between 3.35 and 1.204.

With the left hand fragment complete the key transformation could be addressed in the construction of the seven-membered ring B of (-)-phorbol **1.169**. The following chapter outlines a model study of the left hand fragment with a variety of furans to assess the viability of the proposed approach.

4 Studies Towards Seven-Membered Ring Formation

4.1 Introduction

Seven-membered rings are ubiquitous in biologically active natural products such as frondosin B,¹⁰² (\pm) tremulenolide A,¹⁰³ engelerin A¹⁰⁴ and phorbol esters.¹⁰⁵ In addition, a considerable amount of carbocyclic seven membered rings are also found in pharmaceuticals and FDA approved drugs such as colchicine¹⁰⁶ with a wide variety of pharmacological properties. Still, only a handful of methodologies are known to date to access highly functionalised cycloheptadiene systems. More common methods to form seven-membered rings in the last decade included: ring closing metathesis (ene-ene and ene-yne metathesis),¹⁰⁷ cyclisation reaction, ring expansion and cycloaddition reactions including the utilisation of Diels-Alder, [4+3], [5+2] and [2+2+2] reactions.

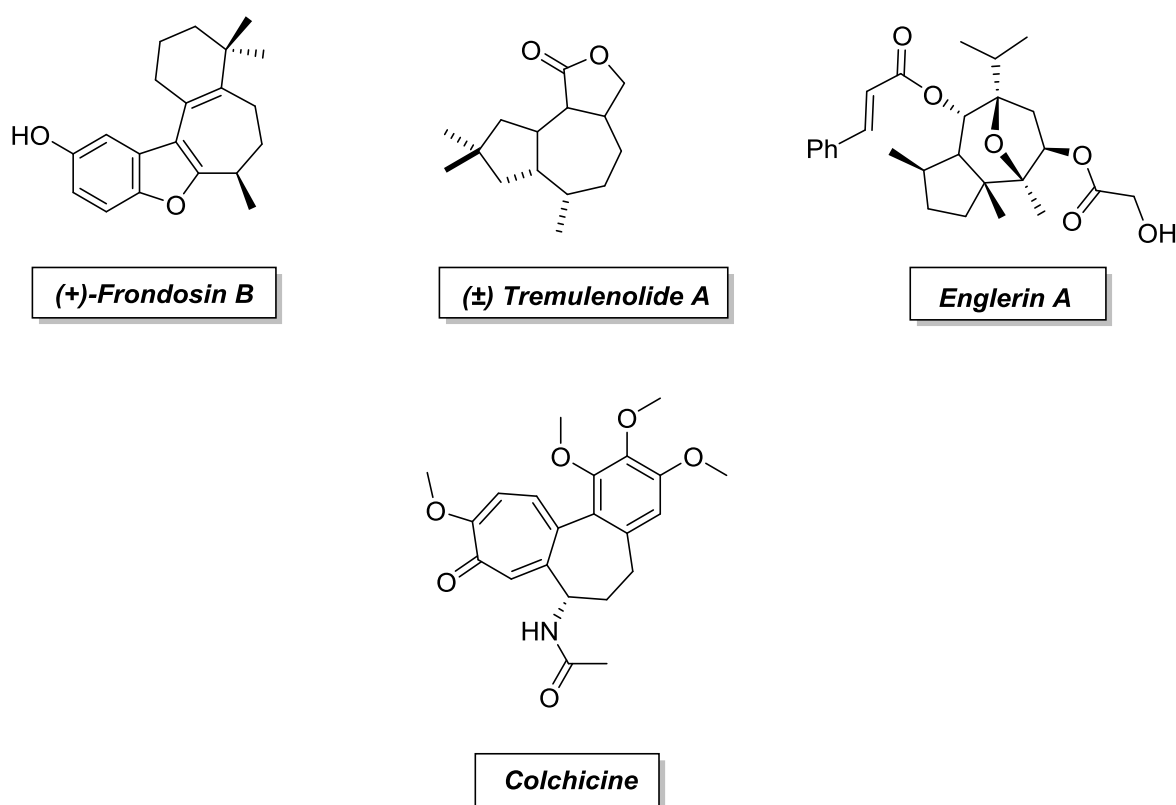


Figure 4.1 General representation of natural products containing seven-membered ring cores.

4.2 Ring-Closing Metathesis

Among the most utilised methodologies of recent times in modern synthetic chemistry is ring-closing metathesis.¹⁰⁷ This approach is particularly useful as it provides convenient access to various ring-size carbocycles and has been widely studied as a C-C bond formation methodology. Tungsten complexes were the first catalysts used for the reaction with acyclic olefins and despite working nicely, they were quite sensitive. Schrock *et al.*¹⁰⁸ introduced in 1990 the first synthesis and use of molybdenum imido alkylidene complexes (figure 4.2) that have shown to possess a wider substrate tolerance and a greater tendency to be reduced than the Schrock catalysts.¹⁰⁹ Another breakthrough was achieved by Grubbs *et al.*¹¹⁰ with the introduction of ruthenium based carbene complexes. The first generation catalyst did not provide the level of activity compared to Schrock catalysts. However, the applicability in natural product synthesis could not be denied. A second generation Grubbs' catalyst was introduced demonstrating an air and moisture stable catalyst with a higher activity than the first generation catalysts.

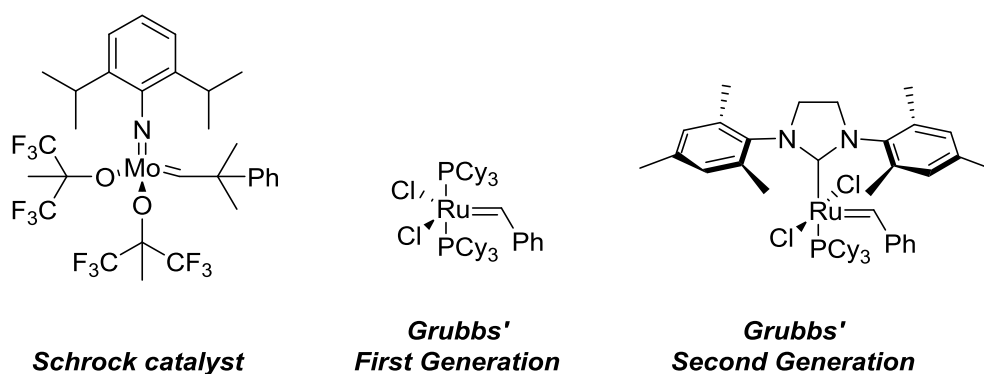
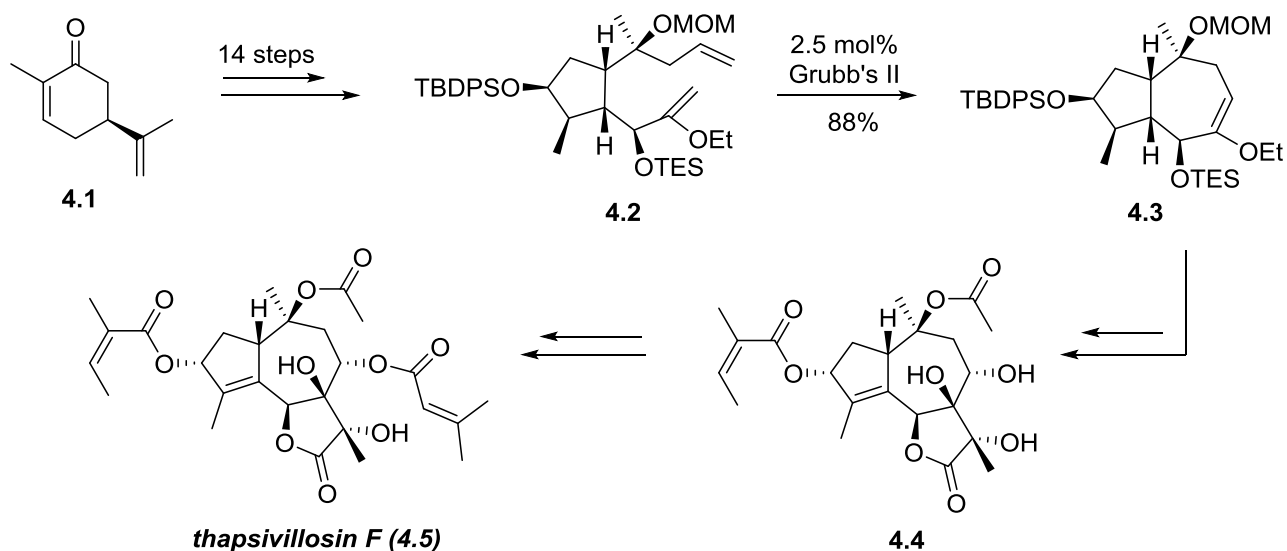


Figure 4.2 Common catalysts for ring-closing metathesis.

An elegant application of the Grubbs' catalyst was demonstrated by Ley *et al.* in the total synthesis of thapsigargin from (*S*)-carvone.¹¹¹ Preparation of precursor **4.2** was accomplished in 14 steps followed by the ring closing metathesis utilising the second generation Grubbs' catalyst to afford **4.3** in 88% yield. Further synthetic manipulations provided triole **4.4** which serves as a precursor to a number of thapsigargin derivatives including thapsivillosin F, nortrilobolide and trilobolide.



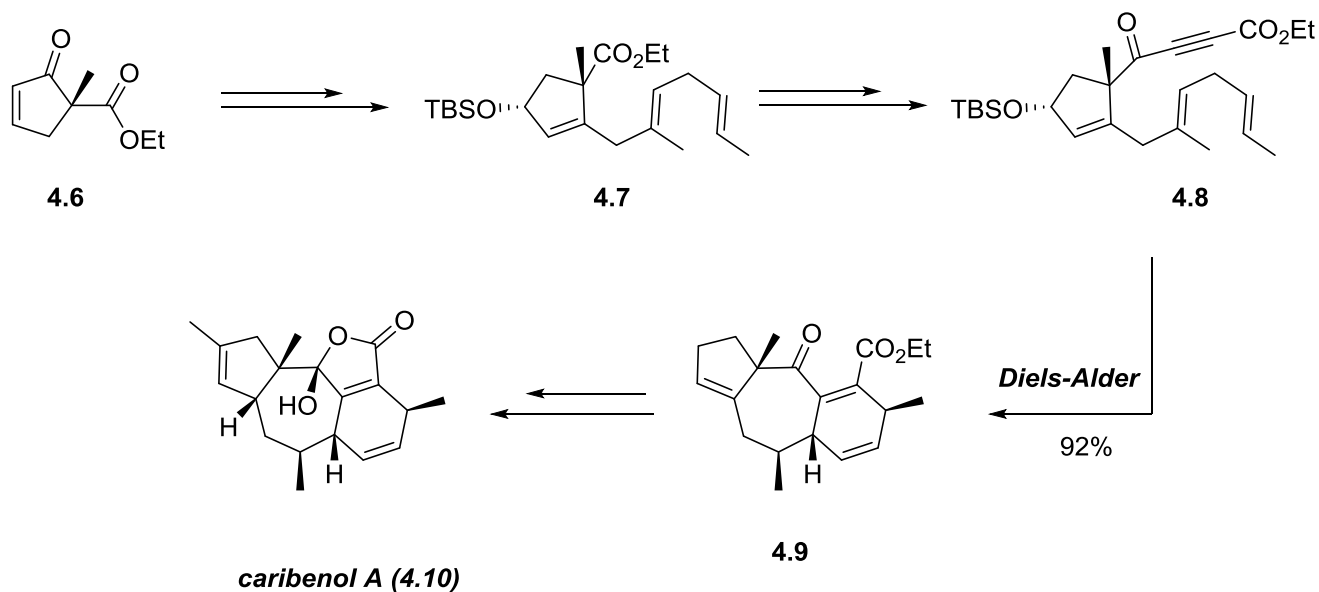
Scheme 4.1 Ley's total synthesis of thapsivillosin F 4.5.

Ley's approach to this family shows clearly the strength of the ring-closing metathesis in accessing five out of the total 17 members of the thapsigargin family.

4.3 Diels-Alder reaction

Diels-Alder reactions are more commonly known for the synthesis of cyclohexane rings *via* the reaction of a diene system and an alkene.¹¹² When used as an intramolecular approach access to seven-membered rings can be achieved. Elegant examples of this approach to natural products comprising a seven-membered ring core include the asymmetric total synthesis of caribenol A¹¹³ and Chen's total synthesis of (+)-echinopines A.¹¹⁴

In the former case intermediate **4.7** was prepared in four steps from cyclopentenone **4.6**. Following this, cycloaddition precursor **4.8** was synthesised in a 6 step synthetic sequence and an overall yield of 62%. The subsequent intramolecular Diels-Alder reaction was then performed utilising 2,6-di-*tert*-butyl-4-methylphenol (BHT) catalytically to afford the desired adduct in 92 % yield.



Scheme 4.2 Total synthesis of caribenol A (4.10).

4.4 [4+3]Cycloaddition reaction

The [4+3] cycloaddition reaction has become a powerful tool for the construction of seven-membered rings over the last decade and has found widespread application in natural product synthesis, including the synthesis of englerin A,¹¹⁵ (+)-frondosin B,¹¹⁶ (+)-barekol¹¹⁷ and (+)-barekoxide¹¹⁷ to mention a few.

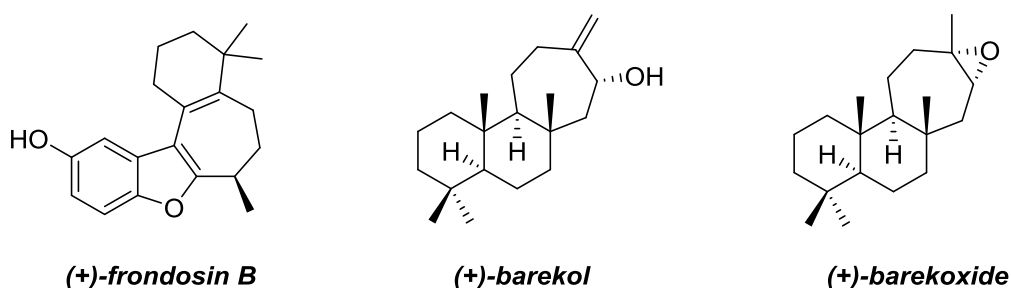


Figure 4.3 General representation of natural products containing seven-membered rings formed *via* [4+3] cycloaddition reaction.

4.4.1 Rhodium-catalysed formal [4+3] Cycloaddition reaction

One of the most versatile reactions in this regard is the formal [4+3] cycloaddition reaction of stabilised diazo compounds with substituted dienes.^{63b,95a} Diazo compounds have been exploited for their utility in the formation of stabilised donor/acceptor carbenes *via* metal catalysed decomposition; a methodology that has been widely applied in modern organic chemistry after its discovery by Davies *et al.*^{63b,118} In combination with rhodium catalysts, especially rhodium (II) tetracarboxylates, these carbenes have proven to be extremely useful in affording a variety of important intermediates for the synthetic organic chemist. The key to this success lies in the realisation that the substitution pattern of the carbenes is crucial for their stability and thus their ability to undergo controlled reactions.

Mechanistically construction of the seven-membered ring is a combination of two concomitant steps, namely, cyclopropanation followed by Cope rearrangement. Thus, these reactions are referred to as formal [4+3] cycloaddition reactions.

Three common dirhodium species are shown in figure 4.4. $\text{Rh}_2(\text{DOSP})_4$ and $\text{Rh}_2(\text{PTAD})_4$ capable of undergoing C-H functionalization reactions with high reactivity and selectivity and the achiral $\text{Rh}_2(\text{OPiv})_4$. All three catalysts have proven effective with a wide range of substrates. An added advantage for all of them is their solubility in hydrocarbon solvents thus improving substrate conversion and stereocontrol.

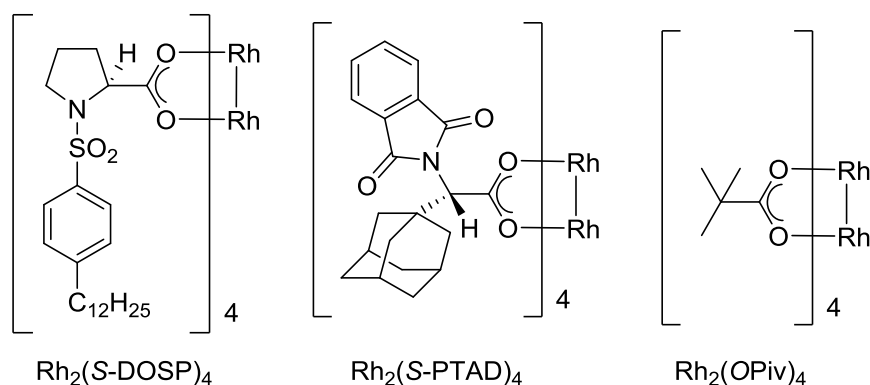
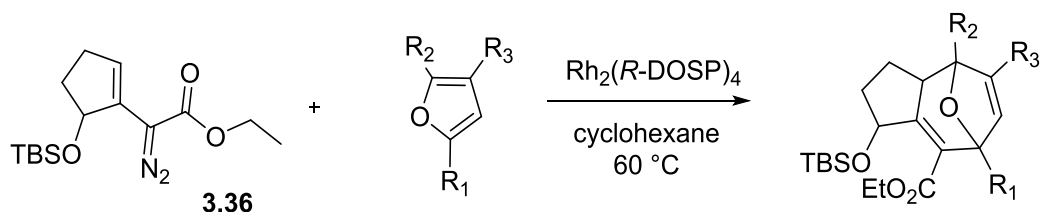


Figure 4.4 Selected rhodium catalysts for the formal [4+3] cycloaddition reaction.

4.5 Model Studies with the Left Hand Fragment

To probe a wide scope of substrates the study began with a number of mono-, di- and trisubstituted furans. Both mono- and disubstituted furans could be obtained *via* commercial sources. However, to widen the scope further model trisubstituted furans were synthesised. The catalyst $\text{Rh}_2(\text{R-DOSP})_4$, was initially chosen due to its versatility.

Table 4.1 outlines the results when treating diazo compound **3.36** with a wide range of furans in cyclohexane at 60 °C. With most furans the reaction yielded moderate to low yields. After extensive screening these conditions were found to be the most favourable.



Entry	Furan	Product Number	Product	Reaction Time, h	Yield, %
1		4.11		1.5	50
2		4.12		1.5	47
3		4.13		2.5	38
4		4.14		1.5	29
5		4.15		1	34

Table 4.1 Model studies of 3.36 with selected furans.

In the case of electron withdrawing substituents at position C-2 and C-3 of the furan (entries 1-3) the yields favoured ester over ketone. This could, however, be due to the poor solubility of 3-acetylfuran (entry 3) in cyclohexane. The position of the ester (C2 or C3) did not influence the yield

of the reaction. Installing a bulky TBS-ether (entry 3) gave a lower yield in comparison to that of the esters. A similar outcome was obtained using 3-bromofuran (entry 5). Using 2-methylfuran as a substrate with a weak electron donating effect of the methyl moiety likewise afforded a lower yield to that of the esters.

A typical representation of the NMR spectrum of the epoxyazulene core can be seen in figure 4.5. The alkene protons Ha and Hc can be seen at 6.60 ppm and 5.57 ppm, respectively. The bridge head proton Hb is situated further upfield at 5.03 ppm. Finally, Hd appears as a broad singlet at 4.97 ppm suggesting an angle in the vicinity of 90 ° to its adjacent protons. In comparison, substituting the methyl function at C-9 to a methyl ester (entry 1) shifts the corresponding signals at Ha-Hc to 6.77, 5.83 and 5.11 ppm respectively. The signal at Hd is unaffected by the substitution at C-9. This latter also holds through in case of the TBS protected substituent (entry 3). However, a multiplet is observed rather than a broad singlet.

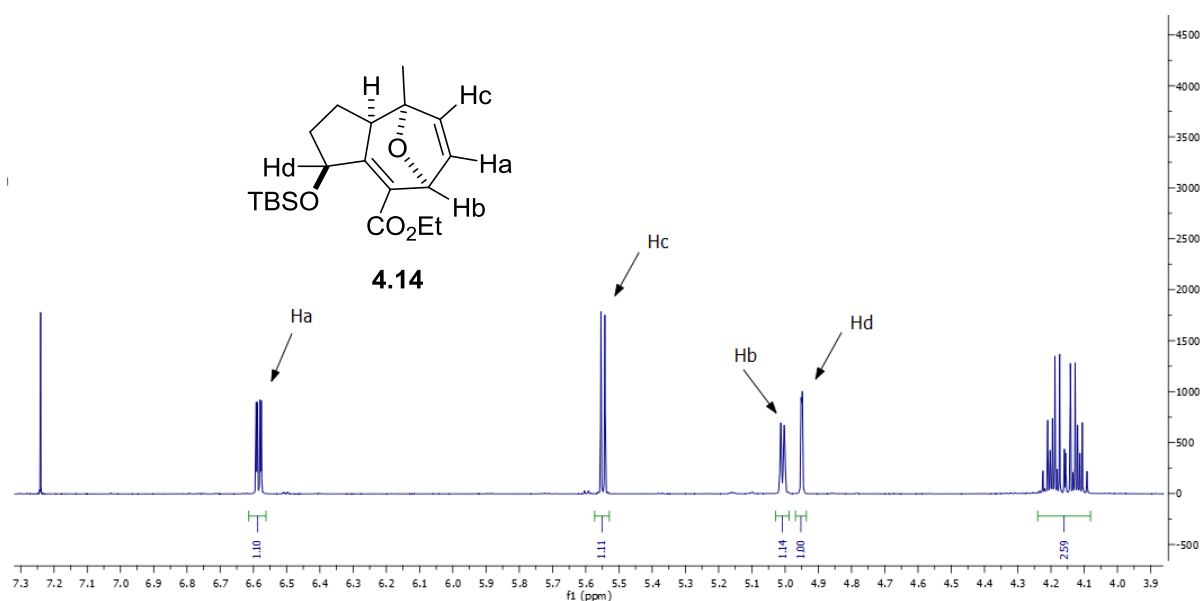
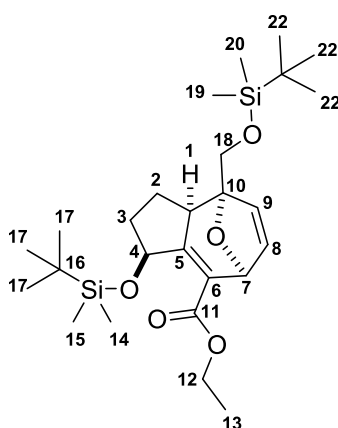


Figure 4.5 ^1H NMR spectrum showing the olefinic protons of cycloaddition product **4.14**.

The relative stereochemistry was confirmed *via* X-ray crystallography. Compound **4.12** (entry 2) readily crystallised from petroleum ether.

Unfortunately by analysing NOE correlation spectra of compounds **4.11** – **4.15**, determination of stereochemistry could not be achieved. As the interspace distance of protons important for

characterisation such as H4 and H1 were shown to be too great for NOE correlations, the relative stereochemistry of these compounds were extrapolated from the crystal data of compound **4.12**. Based on the theory behind $\text{Rh}_2(R\text{-DOSP})_4$ catalysis and the fact that this catalyst was used in all cases shown in table 4.1, such a hypothesis can be expected to be of rather high accuracy. As can be seen in scheme 4.4 orientation of the furan substituents relative to the rhodium carbenoid should remain unaltered, due to the steric demand of the catalyst, for the list of structurally similar furans. A similar assumption, however, cannot be made for the regiochemistry of the reaction. This is of no importance as the connectivity of the product is easily assigned by 2D NMR measurements.

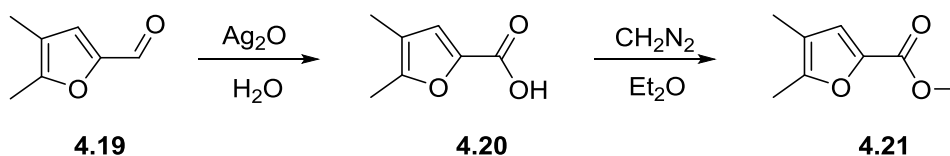


<i>Position</i>	δ_H	<i>Position</i>	δ_H
1	2.78 (dd, $J = 6.6, 13.2$ Hz, 1H)	12	4.24 – 4.11 (m, 2H)
2	1.77 – 1.69 (m, 1H)	13	1.28 (t, $J = 7.1$ Hz, 3H)
	1.14 – 1.13 (m, 1H)		
3	1.77 – 1.69 (m, 1H)	14, 15	0.04 (d, $J = 1.5$ Hz, 6H)
	1.68 – 1.59 (m, 1H)		
4	5.03 – 5.0 (m, 1H)	17	0.91 (s, 9H)
7	5.03 – 5.0 (m, 1H)	18	3.92 (s, 2H),
8	6.64 (dd, $J = 1.7, 5.9$ Hz, 1H)	19, 20	0.09 (s, 6H),
9	5.64 (d, $J = 5.9$ Hz, 1H)	22	0.78 (s, 9H),

Table 4.2 ^1H -NMR data for compound **4.13** (500 MHz, CDCl_3).

Moving on to di- and trisubstituted furans (table 4.3) dihydrobenzofuranone could be commercially obtained, whereas trisubstituted furans (entries 2-3) were synthesised from 1-ethynylcyclohexene⁴ and 4,5-dimethylfuraldehyde, respectively.

Oxidation of aldehyde **4.19** (scheme 4.3) utilising silver (I) oxide to afford acid **4.20** followed by treatment with diazomethane afforded the desired ester **4.21** in excellent yield (97%).



Scheme 4.3 Synthetic strategy to 2-methyl-4,5-dimethyl carboxylate.

With di- and trisubstituted furans (entries 1-3, table 4.3) at hand treatment under identical conditions failed to give the corresponding seven-membered rings. However, recent investigations in the Williams laboratory have proceeded to afford **4.13**, albeit in low yield. Optimisation studies and investigations of both systems are currently ongoing.

⁴ Furan (entry 2, table 4.3) was kindly provided by Dr Sharon Chow

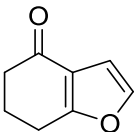
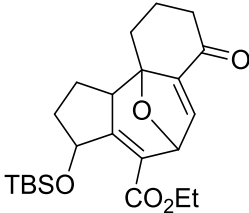
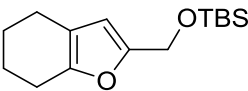
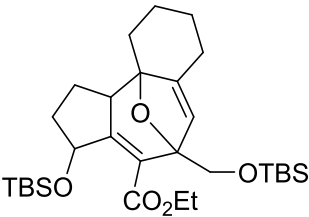
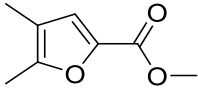
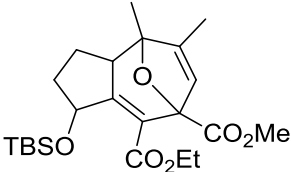
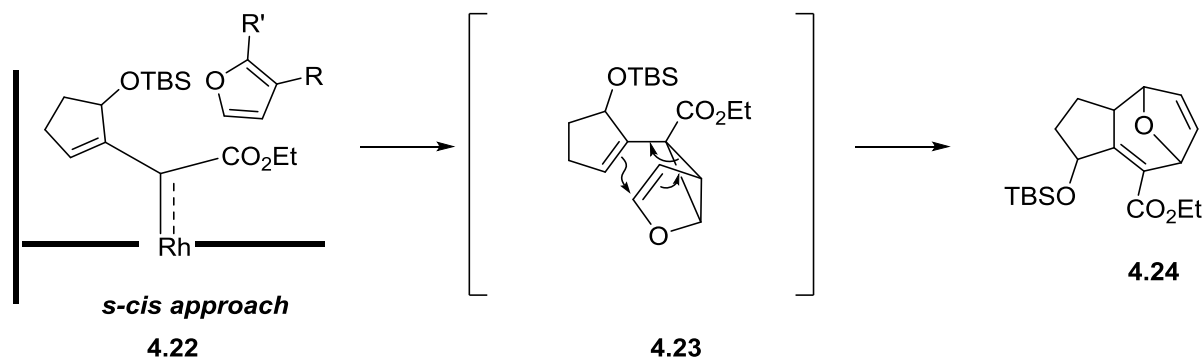
Entry	Furan	Product Number	Product	Reaction Time	Yield
1		4.16		1.5 - 24	-
2		4.17		1.5 - 24	-
3		4.18		1.5 - 24	-

Table 4.3 Cycloaddition studies with di- and trisubstituted furans.

From the experiments above no obvious trend could be observed. This is believed to be the consequence of a number of factors. It is well-known that cyclopropanation is sterically prevented if substrates are highly functionalised. Thus, in regard to trisubstituted furans it is believed that lack of reactivity preventing the cyclopropanation is of steric nature. When stoichiometric amounts of these furans were used, analysis revealed a complex mixture containing unaltered furan. It is believed this arises from decomposition of the carbene in absence of a reaction with the furan. A known competing reaction to that of cyclopropanation is C-H insertion. The lack of products arising from such an event further confirmed suspicions. A brief investigation of chiral catalysts such as $\text{Rh}_2(\text{S-DOSP})_4$ and $\text{Rh}_2(\text{S-PTAD})_4$ revealed no improvement.

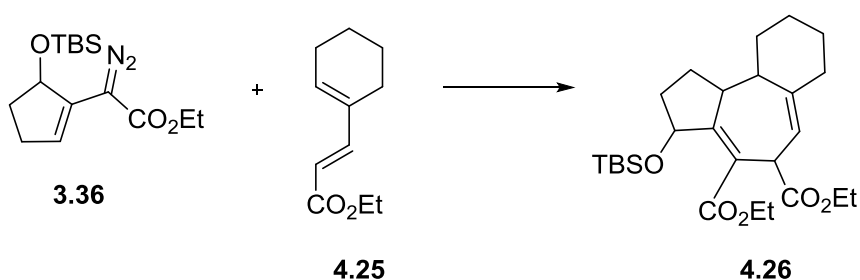
The reported mechanism involves a least hindered approach of the furan to give a cyclopropanated intermediate **4.23** (scheme 4.4). Cope rearrangement of the cyclopropane through a boat transition state then affords the seven-membered ring.



Scheme 4.4 Proposed cycloaddition mechanism.

Although the formation of seven-membered rings from monosubstituted furans were demonstrated with success difficulties were now faced with constructing a trisubstituted seven –membered ring as dictated by the requirements of the retrosynthetic analysis of phorbol.

As an alternative approach reversion back to the [4+3] cycloaddition reaction between a diazo compound and a diene system as previously reported for the total synthesis of (-)-5-*epi*-vibsanin E **1.170** (scheme 1.15). A small scale trial reaction involving the left hand fragment **3.36** was reacted with diene **4.25** using $\text{Rh}_2(\text{S-PTAD})_4$ in hexanes at -27°C . Monitoring the reaction with GC/MS revealed a mass of m/z 390 tentatively assigned to the desired product. Current investigations by the Williams group are aimed on improving upon these results.

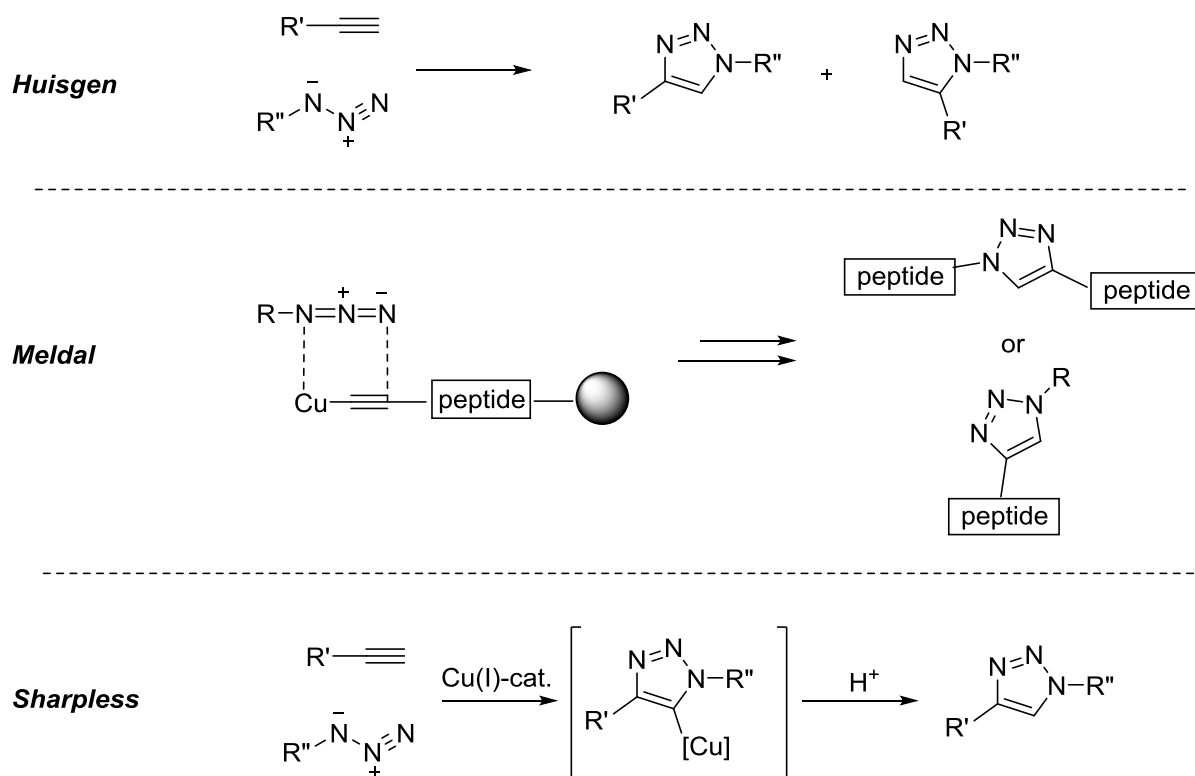


Scheme 4.5 Fallback strategy to the tiglane core.

4.6 Triazole Cycloadditions with Furans

4.6.1 Introduction

1,2,3-Triazoles have long been known for their versatility in organic synthesis. Huisgen was the first to investigate the scope of the 1,3-dipolar cycloaddition reaction between dipolarphiles such as alkynes or alkenes with 1,3-dipoles such as azides and nitrileoxides to give a five-membered heterocycle *via* a concerted mechanism.¹¹⁹ The cycloaddition between an alkyne and an organic azide results in the formation of a triazole. However, under the conditions employed by Huisgen *et al.* this reaction proceeded with poor regioselectivity affording a mixture of 1,4- and 1,5-substituted triazoles (scheme 4.6).



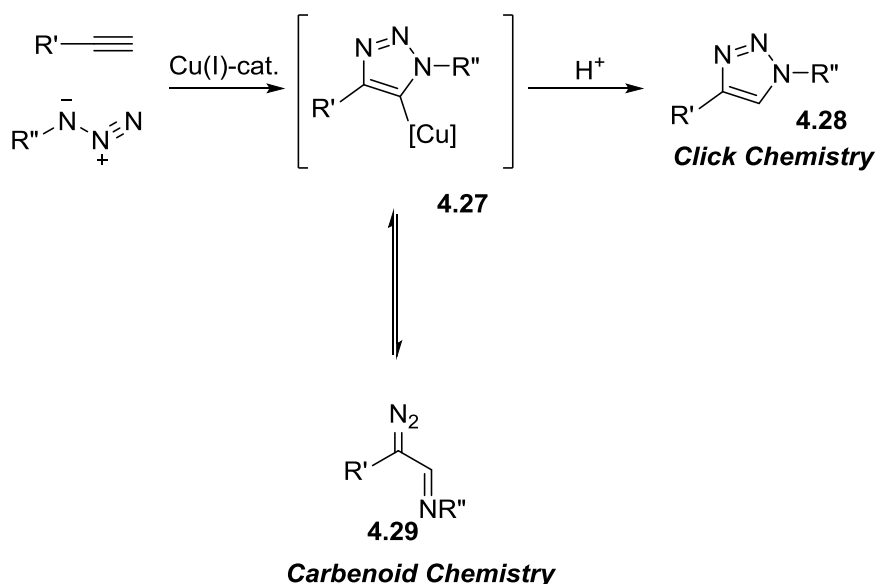
Scheme 4.6 Huisgen 1,3-dipolar cycloaddition vs. Sharpless.

This lack of regioselectivity was addressed by Sharpless *et al.*¹²⁰ in 2001 only months after Meldal *et al.*¹²¹ reported a novel regiospecific copper(I) catalysed 1,3-dipolar cycloaddition reaction of terminal alkynes to azides on solid phase and translated this method to primary, secondary and

tertiary alkyl azides, aryl azides, and azido sugar providing an array of 1,4-substituted [1,2,3]-triazoles in peptide backbones. The described method worked in excellent yield and was fully compatible with solid phase peptide synthesis, all amino acids and all protecting groups.¹²²

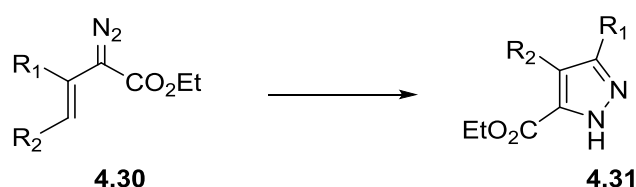
Sharpless' investigations revealed the use of copper (I) as a catalyst to be crucial in obtaining the 1,4-product exclusively with excellent regiocontrol.¹²⁰ Sharpless improved this protocol to be especially useful in what he would refer to as “click chemistry”,¹²³ a methodology described by Sharpless and co-workers as “chemistry that generates substances by joining small units together with heteroatom links”. Furthermore, the term click chemistry refers to what an organic chemist would call “ideal reactions and reaction conditions” including readily available starting materials, non-sensitive substrates, high yields, excellent scope and generation of by-products that can be easily removed by filtering or flash chromatography.

The intermediate formed in the cycloaddition step can also undergo a ring-chain isomerism leading to diazoimine **4.29**. This isomerisation was noted at the time, but it was not until 2009 that Fokin *et al.* showed its usefulness in rhodium carbenoid chemistry.¹²⁴ He showed successfully that *in situ* formed diazoimine decomposes in presence of metals to form azavinyl carbenes that can undergo a wide variety of C-H functionalization reaction.



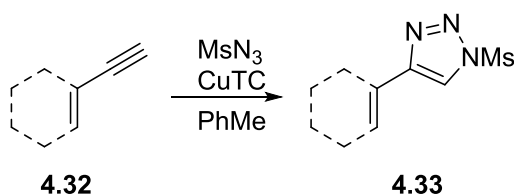
Scheme 4.7 Isomerisation to diazoimine and resulting carbenoid chemistry.

Rhodium stabilised carbenes have been widely studied and applied in C-H activation and C-H insertion processes in synthetic organic chemistry and have shown to possess diverse reactivity as discussed in previous chapters. Formation of these carbenes occurs *via* decomposition of diazo compounds in the presence of rhodium. However, the synthesis of diazo compounds is limited to the extent that a robust synthetic route to all alkenyldiazoacetate types has not been established. Furthermore, upon diazo transfer spontaneous cyclisation of the corresponding diazo species can occur to afford pyrazoles **4.31** (scheme 4.8). This phenomenon was also observed as previously discussed in the synthesis of the left hand fragment (scheme 3.10)



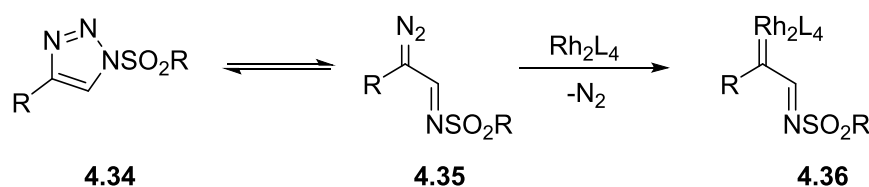
Scheme 4.8 Pyrazole formation of alkenyldiazoacetates.

This of course limits the rhodium carbene formation to a certain extent and for quite some time researchers were seeking alternatives to diazo compounds in order to expand the scope of rhodium carbenoid chemistry. 1,2,3-Sulfonyl triazoles were known in the literature to act as masked diazo compounds.^{124c} However, it was not until Fokin and co-workers reported a straightforward synthesis of these triazoles *via* the copper(II) catalysed azide/alkyne cycloaddition reaction utilising copper(I) thiophene-2-carboxylate and azide to afford the desired triazole (**4.33**) in good to excellent yield (scheme 4.9).^{124b}



Scheme 4.9 Fokin's synthesis of 1,2,3-sulfonyl triazole 4.33.

Triazoles were thus found to serve as precursors to reactive and reasonably stable azavinyl carbenes (**4.36**). Fokin and co-workers have demonstrated the strength of these compounds in their utilisation of a wide variety of transformations (figure 4.6).¹²⁵ It was found that in particular triazoles bearing a sulfonyl group at the N1 position undergo “ring chain isomerism” to the diazoimine **4.35** more easily.



Scheme 4.10 Azavinyl carbene formation.

This is believed to be due to the ring strain between N1 and N2 being perturbed by sulfonyl assisted weakening. Decomposition of the generated diazoimine in the presence of a rhodium catalyst results in the formation of a metal carbene which undergoes C-H-activation and C-H-insertion reactions. Figure 4.6 is a good representation of the inherent diversity of C-H functionalization chemistry.

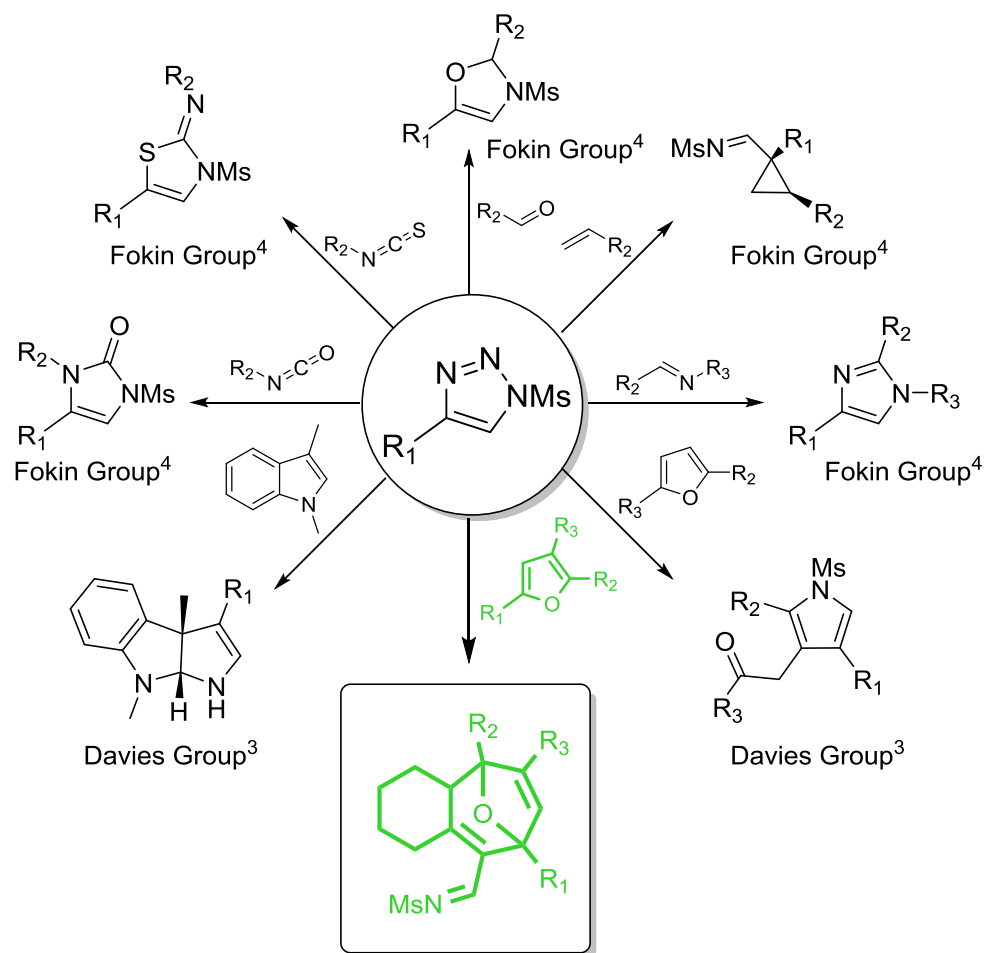
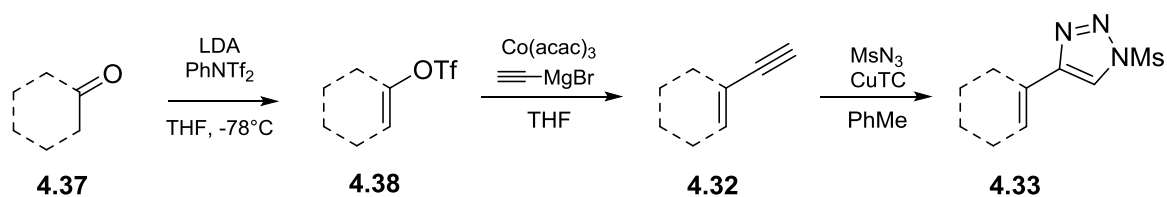


Figure 4.6 Previous synthetic work on 1,2,3-sulfonyl triazoles and proposed reaction with furans.

In regard to seven-membered ring formation it was contemplated whether the scope of this project could be extended by utilising the proposed 1,2,3-sulfonyl triazoles. This would not only lead to a fall-back strategy, but would further add to the advances in this field. To the best of our knowledge, the reaction of 1,2,3-triazoles with furans to obtain the epoxybenzoannulene core has not been reported to date.

Synthesis of the triazoles starts with commercially available ketones. Enolisation/triflation utilising LDA and McMurry's reagent afforded **4.38** in good yields. Subsequent cobalt-catalysed Kumada coupling of **4.38** with ethynylmagnesium bromide provided acetylenes **4.32**. Finally, triazole **4.33** can be synthesised by reaction of **4.32** with mesylazide catalysed by copper thiophene-2-carboxylate (CuTC).¹²⁶



Scheme 4.11 Synthetic route to 1,2,3-sulfonyl triazoles.

Figure 4.7 shows the triazoles synthesised *via* the aforementioned method (scheme 5.6).

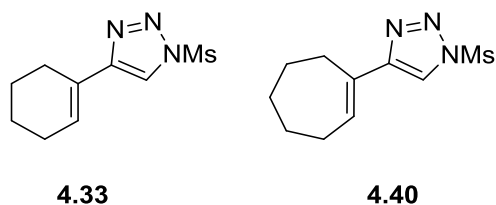


Figure 4.7 Synthesised triazoles.

Our exploratory study started with cyclohexene-triazole **4.33** using the non-chiral catalyst $\text{Rh}_2(\text{OPiv})_4$ and selected furans (entry 1-3, table 4.4). When utilising monosubstituted furans for the cycloaddition reaction (entries 1-2) good yields were obtained. The position and nature of the substituents did not vary the yield significantly.

<i>Entry</i>	<i>Furan</i>	<i>Product Number</i>	<i>Product</i>	<i>Yield</i>
1		4.41		65

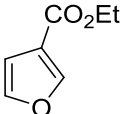
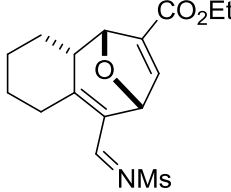
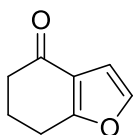
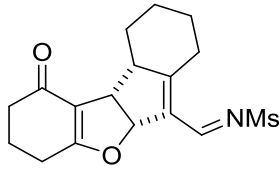
2		4.42		76
3		4.43		72

Table 4.4 Model studies with cyclohexene triazole.

Figure 4.8 shows a crystal structure of compound **4.41** as an ORTEP representation with 30% ellipsoid probability. From the crystal structure the relative stereochemistry has been assigned as depicted in table 4.4 (entry 1). The relative stereochemistry of entry 2 was assigned by analogy.

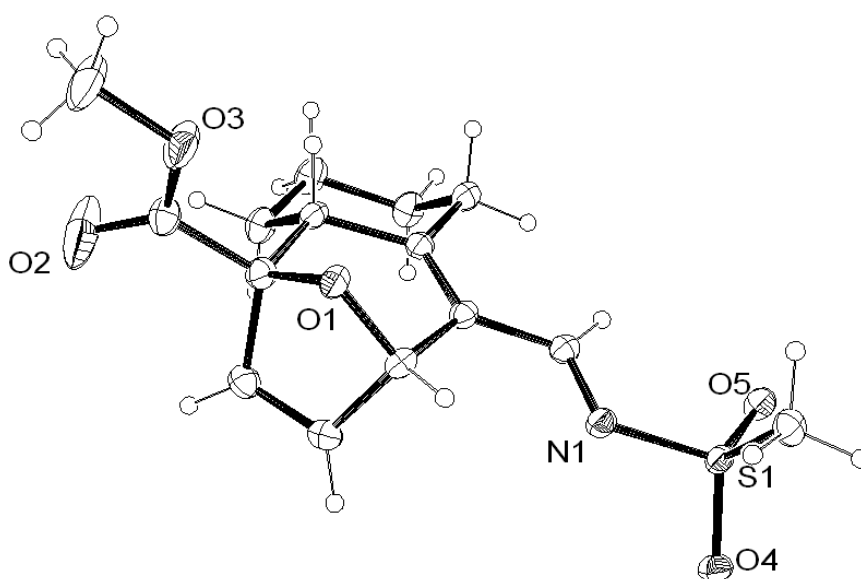
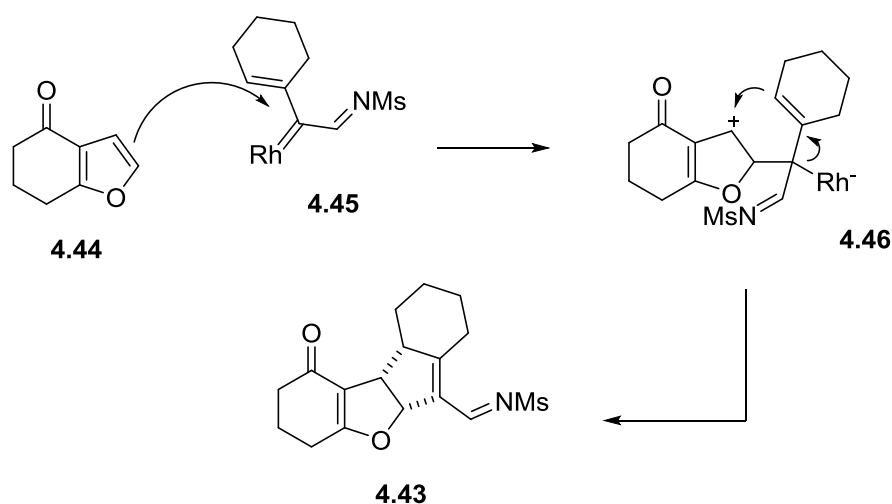


Figure 4.8 ORTEP (30% ellipsoid probability) of compound 4.41.

An unusual tetracyclic product, however, was observed in the rhodium catalysed reaction of dihydrobenzofuranone and triazole **4.33** (entry 3). Interestingly, this reaction leads to a clean [3+2]

cycloaddition reaction with both achiral $\text{Rh}_2(\text{OPiv})_4$ and chiral $\text{Rh}_2(S\text{-nttl})_4$ as the rhodium source to afford **4.43** in 72% yield.

According to literature it is believed that these kinds of products arise from effective charge stabilisation of both the electron-rich dihydrobenzofuranone and the rhodium carbene formed, thus leading to zwitterionic intermediate **4.46** (scheme 4.12).¹²⁷



Scheme 4.12 Plausible mechanistic explanation for the [3+2] cycloaddition reaction of compound 4.43.

This zwitterionic intermediate **4.46** would be expected to be stabilised by the presence of two electron withdrawing oxygens. The loss of rhodium initiates the ring closure from the cyclohexene moiety to the furan portion ultimately leading to the observed tetracyclic compound **4.43**.

As can be seen in figure 4.9 slow hydrolysis of the imine was observed in both the neat sample as well as in CDCl_3 solution upon storage. Upon hydrolysis a shift from a characteristic imine signal at 8.98 ppm to 9.98 ppm can be seen.

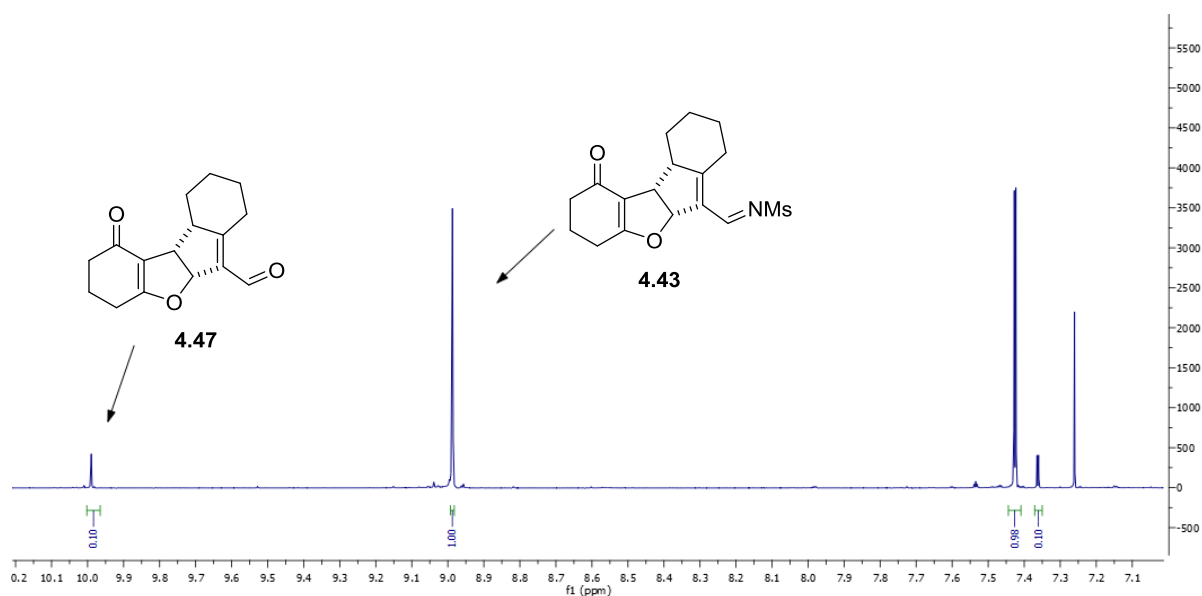


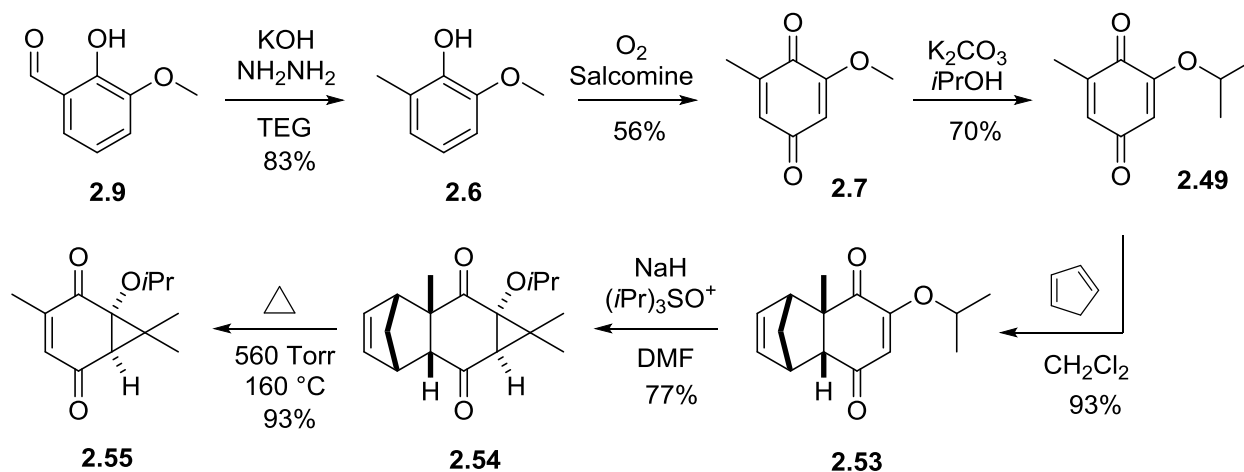
Figure 4.9 ^1H NMR Spectra of the conversion of imine 5.15 to aldehyde 5.19.

5 Conclusion and Future Work

The objective of this thesis was to explore a [4+3] cycloaddition approach to the non-natural (-)-phorbol *via* the fusion of two fragments, namely, a right hand (**1.198**) and a left hand fragment (**1.197**). The justification for attempting the synthesis of non-natural (-)-phorbol **1.169** was driven by biological importance to further understanding the PKC mechanism involved in cancer. The fusion of **1.197** and **1.198** was envisaged to proceed *via* a formal [4+3] cycloaddition utilising rhodium catalysis to afford the seven-membered core of the tigliane skeleton. The results stemming from the synthetic studies herein are summarised in the following text in three separate segments. Firstly, a conclusion and future work section for the right hand fragment is given. Secondly, the left hand fragment and a model study of its application in the proposed formal [4+3] cycloaddition reaction are outlined in a similar manner. Thirdly, a novel approach to seven-membered rings utilising 1,2,3-sulfonyl triazoles with furans is presented.

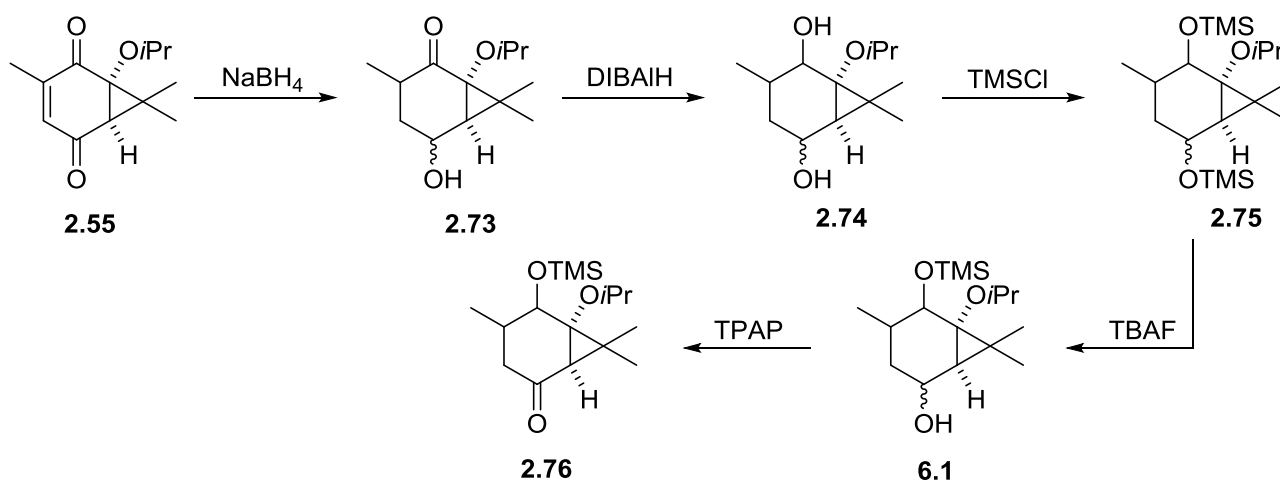
5.1 Right Hand Fragment

In conclusion, advanced intermediate **2.55** was successfully synthesised from commercially available *o*-vanillin in 22% yield over six steps. Successive Wolff-Kishner reduction of *o*-vanillin followed by oxidation of phenol **2.6** afforded quinone **2.7** in moderate yield. A major hurdle in this synthetic sequence was the construction of ring D *via* cyclopropanation of **2.7**. This reaction was plagued by elimination of the methoxy moiety upon treatment with triisopropylsulfoxonium tetrafluoroborate, however, this was overcome by introduction of a more robust alcohol protecting group, i.e. *isopropoxy*.



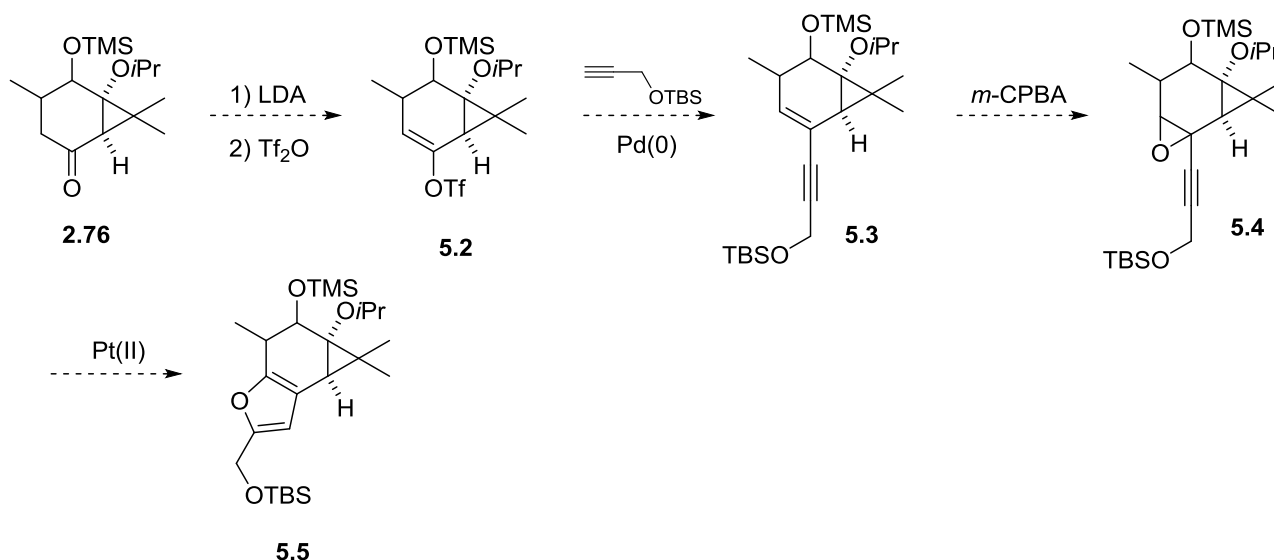
Scheme 5.1 Synthetic route to advanced intermediate 2.55.

In order to prepare this advanced intermediate **2.55** for furan formation reduction of the α,β -unsaturation was necessary. Direct double bond reduction of **2.55** has proven very challenging affording a ring expansion by the opening of the cyclopropane moiety under a variety of conditions. To overcome this ring expansion a three step sequence of reduction/protection/oxidation was successfully employed affording advanced intermediate **2.76**.



Scheme 5.2 Reduction studies on compound 2.55.

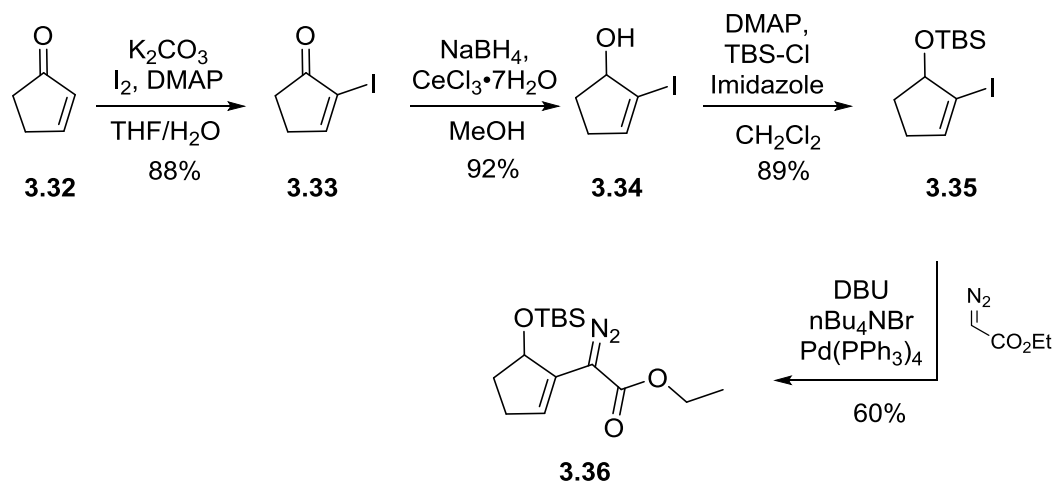
With **2.76** at hand the completion of the right hand fragment can be achieved by triflation of the corresponding C-8 ketone (scheme 5.3) using LDA and triflic anhydride followed by palladium catalysed Sonogashira coupling with a protected propargyl alcohol. Subsequent epoxidation at $\Delta^{8,9}$ -double bond utilising *meta*-chloroperbenzoic acid followed by metal mediated ring closure (Pt, Au, Pd) would provide the desired right hand fragment.



Scheme 5.3 Proposed synthetic route for completion of the RHF.

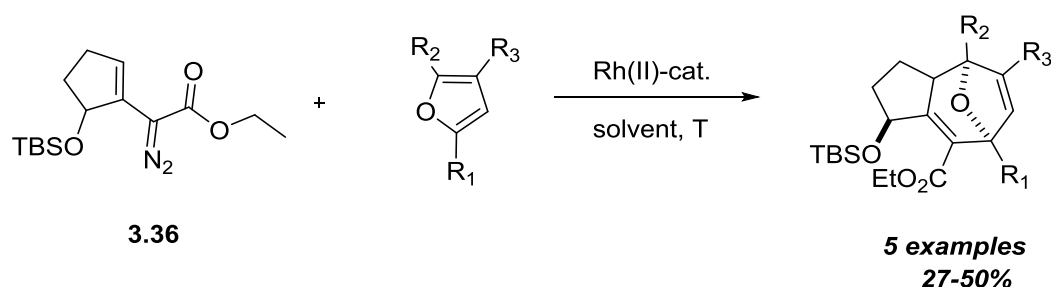
5.2 Left Hand Fragment

In conclusion, a left hand fragment **3.36** was successfully synthesised *via* direct diazo coupling approach between 2-iodocyclopentenone **3.32** and ethyldiazo acetate. A major hurdle in the synthesis was pyrazole formation of alkenyldiazoacetates. In addition, the methyl group that is required for the synthesis of (-)-phorbol **1.169** was dismissed at this stage. α -Halogenation followed by Luche reduction and TBS protection of the resultant alcohol provided **3.35** in 72% over three steps. Diazo coupling between **3.35** and ethyldiazo acetate was accomplished utilising $\text{Pd}(\text{PPh}_3)_4$ and DBU in 60% yield.



Scheme 5.4 Synthetic route to LHF.

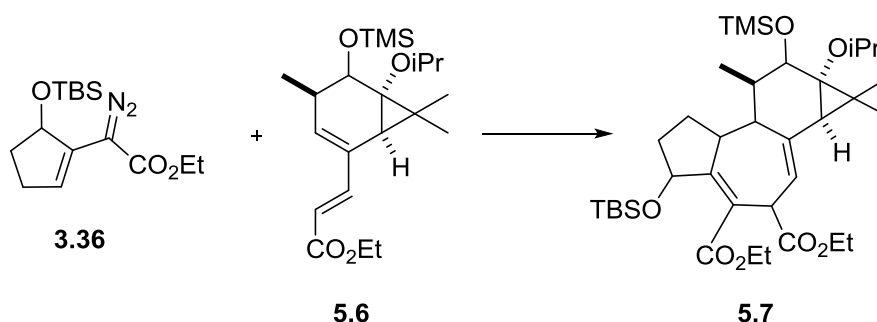
With the successfully synthesised diazo compound **3.36**, initial cycloaddition reactions with mono substituted furans have proven promising. Five examples employing furans with different substitution patterns, i.e. electron withdrawing and electron-donating, have been demonstrated to successfully provide the AB-ring system of our target molecule.



Scheme 5.5 Formal [4+3] cycloaddition reaction between LHF and furans.

Once a viable synthesis of the right hand fragment is in place future studies will be focused at the rhodium catalysed [4+3] formal cycloaddition with newly developed protocols from our collaborators laboratory with left hand fragment as outlined in our retrosynthetic analysis (scheme 1.22).

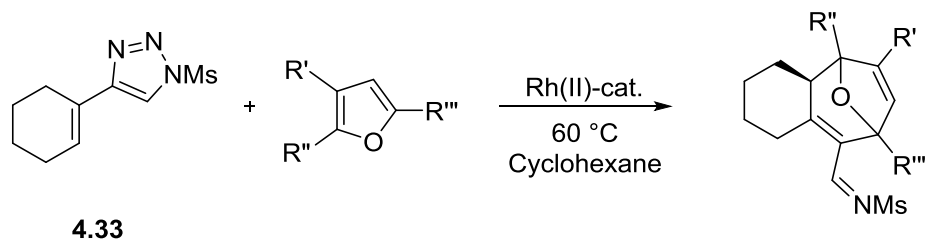
In the event that a reaction between the left and right hand fragments does not occur, a fall-back strategy could be deployed as follows. It is envisaged that in place of a trisubstituted furan as the right hand fragment, the synthesis of diene **5.6** and consequent reaction with diazo compound **3.36** would proceed in parallel with that successfully demonstrated for (-)-5-*epi*-vibsanin E **1.170** by Williams *et al.* As mentioned in chapter 4.5 (page 113) initial investigations with a model diene have been undertaken and have shown promising results, However, optimisation of the reaction conditions has yet to be performed, due to lack of time. Introduction of the tertiary hydroxyl group could then be potentially performed selenium dioxide.



Scheme 5.6 Cycloaddition approach to compound 5.7.

5.3 Triazoles

In conclusion, a novel synthesis has been achieved for the formal [4+3] cycloaddition reaction between 1,2,3-sulfonyl triazole **4.33** and various furans. Building on this novel approach additional triazoles have been synthesised and are being investigated in order to probe the scope of the reaction with regard to the triazole coupling partner. Furthermore, in the unusual case where a [3+2] cycloaddition reaction was observed to afford **5.19** (see chapter **4.6**, scheme 4.12) further studies with the aim to force this reaction over the usually observed [4+3] cycloaddition could hold a novel approach to this type of polycyclic compound.



Scheme 5.7 Formal [4+3] cycloaddition reaction of triazoles and furans.

6 Experimental

6.1 General

6.1.1 Reactions

All reactions were performed in oven dried glassware under a positive pressure of argon unless otherwise stated. All reagents and solvents were dried, distilled or purified before use according to Perrin and Amarego's "Purification of Laboratory chemicals" 3rd edition.¹²⁸

Tetrahydrofuran and toluene were freshly distilled from Na^o/benzophenone. *N,N*-Dimethylformamide, methylene chloride, acetonitrile and cyclohexane were freshly distilled from calcium hydride under argon. Anhydrous *N,N*-diisopropylamine and 1,8-diazabicycloundec-7-ene (DBU) were distilled from calcium hydride under argon and stored over pre-dried sodium hydroxide pellets. *n*-Butyllithium was used as a solution in either hexanes or heptanes. Argon was dried by passing through a drying tube containing 4Å molecular sieves, silica gel beads and Drierites.

6.1.2 Purification

Thin layer chromatography was performed using E. Merck silica gel 60 F254 pre-coated plates. Column chromatography was undertaken on silica gel (Flash silica gel 230-400 mesh). Other chromatographic methods involved using Celite 545®. Petroleum spirit refers to the hydrocarbon fraction with boiling points between 40 – 60 °C.

6.1.3 Characterisation

¹H and ¹³C NMR spectra were recorded on Bruker AV300 (300.13MHz; 75.47MHz), AV400 (400.13MHz; 100.62MHz) and DRX500 (500.13MHz; 125.76MHz) instruments. Coupling constants are given in hertz (Hz) and chemical shifts are reported as δ values in parts-per-million (ppm) with the solvent resonance as the internal standard (¹H-NMR: CDCl₃: δ7.26; acetone-d₆:

δ 2.04; ^{13}C -NMR: CDCl_3 : δ 77.0; acetone- d_6 : δ 29.84 and δ 206.26). Data are reported as followed: chemical shift, multiplicity (s = singlet, br s = broad singlet, d = doublet, t = triplet, q = quartet, quin = quintuplet, sext = sextuplet, sept = septet, m = multiplet), coupling constants (Hz), and integration.

Low resolution electrospray ionisation mass spectrometry measurements (LRESIMS) were recorded in a positive ionisation mode on a Bruker Esquire HCT instrument with a Bruker ESI source.

High resolution electro spray ionization (HRESIMS) accurate mass measurements were recorded in positive ionisation mode on a Bruker MicrOTOF-Q (quadrupole – Time of Flight) instrument with a Bruker ESI source using sodium formate as a reference calibrant.

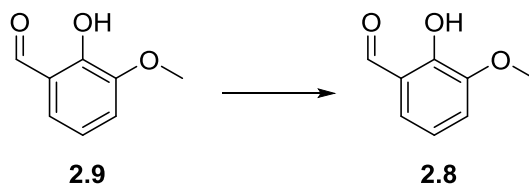
GC/MS data were recorded on a Shimadzu GC-17A VR.3, mass-spectrometer: MS QP5050A, ionisation at 70 eV, column: DB-5ms 30 m 0.25 mm, carrier-gas: He, total flow 32.2 mL/min, column flow 1.3 mL/min, injector temperature: 250 °C, standard program: 2 min at 100 °C, followed by a temperature increase of 16 °C/min and held at 250 °C for 20 min.

Melting points were determined on a DigiMelt Stanford Research Systems melting point apparatus and are uncorrected.

Analytical enantioselective HPLC was performed on an Agilent 1200 series liquid chromatograph (flow rate of 0.5 mL min⁻¹, gradient elution using isopropanol/hexane with the following program: 0 min, IPA/hex 5/95; 4 min, IPA/hex 5/95; 34 min, IPA/hex 40/60; 44 min, IPA/hex 40/60; 46 min, IPA/hex 5/95; 50 min, IPA/hex 5/95) equipped with UV (254 nm) and ALP (Advanced Laser Polarimeter, PDR-Chiral Inc.) detectors and a Chiralpak AD column (4.6 x 250 mm, Daicel Chemical Industries Ltd.).

X-Ray crystallographic data was obtained from the University of Queensland; crystallographic structures were solved by the author using WinGX unless otherwise stated.

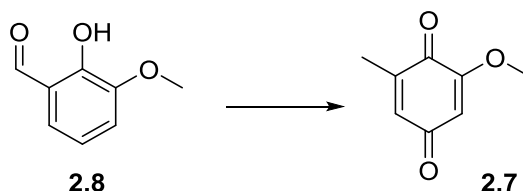
6.2 Experimental Procedures Right Hand Fragment



2-Methoxy-6-methylphenol

Hydrazine hydrate (22.4 mL, 460.08 mmol) was added to a solution of *o*-vanillin (20 g, 131.5 mmol) in triethyleneglycol (100 mL) and the resulting mixture was heated to 110 °C for 10 minutes. Potassium hydroxide pellets (45.7 g, 745.8 mmol) were then added in small portions and the reaction mixture heated to 130 °C overnight. The reaction was quenched with H₂O (20 mL), acidified with conc. HCl to pH 7 and extracted with CHCl₃ (3 x 80 mL). The combined organic layers were washed with brine, dried over Na₂SO₄ and the solvent removed under reduced pressure. Vacuum distillation of the crude oil gave rise to the desired product as white crystals (15 g, 83 %). Spectroscopic data matched that as described in literature.⁷⁰

¹H NMR (300 MHz, CDCl₃) δ 6.76 – 6.69 (m, 3H), 5.68 (br s, 1H), 3.88 (s, 3H), 2.26 (s, 3H)



2-Methoxy-6-methylcyclohexa-2,5-diene-1,4-dione

Oxygen was bubbled through a solution of 2-methoxy-6-methylphenol (15 g, 108.9 mmol) and *N,N'*-bis(salicylidene)ethylenediaminocobalt(II) (3.56 g, 10.9 mmol) in dry DMF (70 mL) over night. The resulting mixture was poured onto ice and the crude product was filtered off. The filtrate was continuously extracted with Et₂O (5 x 70 mL). The organic layers were dried over MgSO₄ and concentrated *in vacuo* yielding a brown solid. The combined products were purified *via* flash column chromatography (ethyl acetate / petroleum ether = 1:1) and further recrystallised from

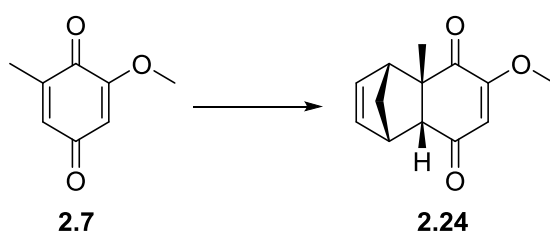
ethanol to afford the titled compound as a bright yellow solid (9.3 g, 56 %). Spectroscopic data matched that as described in literature.⁷⁰

m.p. 148 °C – 149 °C

¹H NMR (300 MHz, CDCl₃) δ 6.55 – 6.53 (m, 1H), 5.88 (d, J = 2.5 Hz, 1H), 3.82 (s, 3H), 2.07 (d, J = 1.5 Hz, 3H)

¹³C NMR (400 MHz, CDCl₃) δ 187.4, 182.4, 158.8, 143.6, 133.8, 107.3, 56.3, 15.5

HRMS (EI) Calculated for C₈H₈NaO₃: 175.0366; Found: 175.0359



(1*S*,4*R*,4*aS*,8*aR*)-6-Methoxy-4*a*-methyl-1,4,4*a*,8*a*-tetrahydro-1,4-methanonaphthalene-5,8-dione

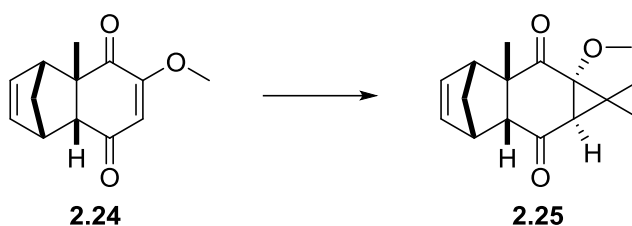
(*S*)-(-)-*o*-Tolyl-CBS-oxazaborolidine (0.5 mL, 0.031 mmol) was diluted with anhydrous CH₂Cl₂ (0.125 mL, 0.02M solution) and cooled to -40°C under an argon atmosphere. A freshly prepared 1M solution of AlBr₃ in anhydrous CH₂Br₂ was then added dropwise, whereby a strong orange colour was observed immediately. After stirring the solution at -40°C for 30 minutes, the mixture was cooled to -78°C and quinone **2.7** dissolved in anhydrous CH₂Cl₂ (1.972 mmol, 0.2M) was added followed by the addition of freshly distilled cyclopentadiene (7.89 mmol). The reaction mixture was then stirred at that temperature for 5 hours, after which complete conversion to product was observed *via* TLC. The reaction was quenched with methanol (2 mL) and the solvent concentrated under reduced pressure yielding a brown oil that was purified *via* column chromatography (ethyl acetate/petroleum spirit = 1:3) to afford the titled compound **2.24** as a yellow solid (85%, 87% ee, *rt* = 19.8min). Spectroscopic data matched that as described in literature.⁷¹

m.p. 81°C – 82°C

¹H NMR (300 MHz, CDCl₃) δ 6.12 (dd, J = 2.8, 5.6 Hz, 1H), 6.02 (dd, J = 2.8, 5.6 Hz, 1H), 5.89 (s, 1H), 3.71 (s, 3H), 3.42 (br s, 1H), 3.12 (br s, 1H), 2.84 (d, J = 3.8 Hz, 1H), 1.68 (d, J = 9.0 Hz, 1H), 1.55 (d, J = 9.0 Hz, 1H), 1.48 (s, 3H)

¹³C NMR (400 MHz, CDCl₃) δ 198.5, 197.6, 162.5, 137.5, 135.2, 113.9, 57.7, 56.4, 53.8, 52.7, 48.7, 46.5, 26.5

X-Ray Data: (see Appendix 8.2)



(1a*S*,1a*S*,3*R*,6*S*, 6a*R*, 7a*R*)-1a-Methoxy-1,1,2a-trimethyl-1a,2a,3,6,6a,7a-hexahydro-1*H*-3,6-methanocyclopropa[*b*]naphthalene-2,7-dione

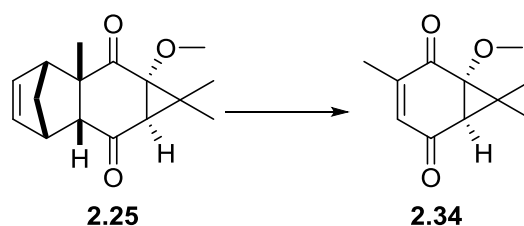
Triisopropylsulfoxonium tetrafluoroborate **2.30** (199 mg, 0.80 mmol) was added in one portion to a stirring suspension of NaH (31 mg, 1.28 mmol) in dry DMF (4 mL) at 0 °C under an argon atmosphere. The reaction mixture was stirred for 5 minutes before dropwise addition of Diels-Alder adduct **2.24** (70 mg, 0.32 mmol) as a solution in dry DMF (0.5 mL). The cooling bath was removed and the reaction mixture warmed to room temperature. On completion – monitored by TLC – the reaction mixture was quenched with saturated NH₄Cl (5 mL) and extracted with EtOAc (3 x 15 mL). The combined organic layers were dried over MgSO₄ and the solvent removed under reduced pressure yielding a brown oil, which was purified *via* column chromatography (ethyl acetate/petroleum spirit = 5:1) to afford the titled compound as a yellow oil (12 mg, 14%).

¹H NMR (300 MHz, CDCl₃) δ 6.25 (dd, J = 2.9, 5.6 Hz, 1H), 6.18 (dd, J = 2.9, 5.6 Hz, 1H), 3.45 (br s, 1H), 3.24 (s, 3H), 3.18 (br s, 1H), 2.56 (d, J = 4.2 Hz, 1H), 1.96 (s, 1H), 1.63 (dt, J = 1.8, 9.3 Hz, 1H), 1.46 (s, 3H), 1.42 (dt, J = 1.8, 9.3 Hz, 1H), 1.30 (d, J = 10.0 Hz, 6H)

¹³C NMR (500 MHz, d₆-benzene) δ 208.2, 204.1, 137.4, 136.9, 77.0, 58.9, 58.5, 57.0, 53.3, 51.1, 47.1, 46.9, 34.1, 26.4, 23.1, 19.4

HRMS (EI) Calculated for C₁₆H₂₀NaO₃: 283.1305; Found: 283.1297

X-Ray Data: (see Appendix 8.2)



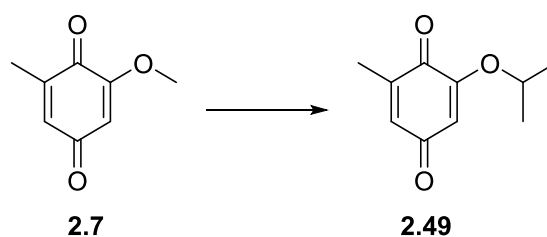
(1*S*,6*R*)-1-Methoxy-3,7,7-trimethylbicyclo[4.1.0]hept-3-ene-2,5-dione

The retro Diels-Alder reaction was performed by heating compound **2.25** (10 mg, 0.04 mmol) at 143°C at 530 Torr using a Kugelrohr apparatus. Compound **2.25** was placed in the terminal 5 mL round bottom flask of a triple bulb (5 mL each) Kugelrohr short path distillation apparatus. The glassware assembly was connected to a vacuum pump (530 Torr) and placed into a Kugelrohr oven preheated to 140°C with one bulb remaining outside for cooling with dry ice. The yellow residual oil in the terminal bulb was then washed with Et₂O and the solvent removed under reduced pressure to afford the titled compound as a yellow oil (6.2 mg, 84%)

¹H NMR (300 MHz, CDCl₃) δ 6.51 – 6.48 (m, 1H), 3.37 (s, 3H), 2.33 (d, J = 1.81 Hz, 1H), 2.04 (d, J = 1.53 Hz, 3H), 1.40 (s, 3H), 1.32 (s, 3H)

¹³C NMR (400 MHz, CDCl₃) δ 195.1, 194.0, 149.7, 137.2, 75.6, 57.1, 44.8, 39.3, 23.2, 16.7, 16.2

HRMS (EI) Calculated for C₁₁H₁₄NaO₃: 217.0835; Found: 217.0839



2-Isopropoxy-6-methylcyclohexa-2,5-diene-1,4-dione

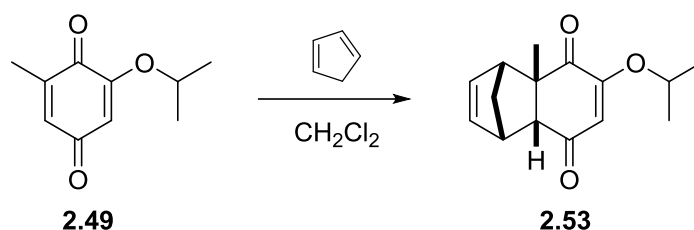
According to a modified procedure of Wurm *et.al.*⁹⁰ methoxyquinone **2.7** (1.5 g, 9.9 mmol) and sodium acetate (3 g) were dissolved in dry *isopropanol* (90 mL) and refluxed for 5 hours. Prolonged hours should be avoided due to disubstitution of the *isopropyl* group. The reaction mixture was

concentrated to dryness and purified *via* column chromatography (ethyl acetate / petroleum ether = 1 : 5) to afford the titled compound as a yellow solid (0.8 g, 44%).

¹H NMR (300 MHz, CDCl₃) δ 6.52 – 6.50 (m, 1H), 5.83 (d, J = 2.4 Hz, 1H), 4.45 (sept, J = 6.0 Hz, 1H), 2.05 (d, J = 1.7 Hz, 3H), 1.39 (d, J = 6.0 Hz, 6H)

¹³C NMR (400 MHz, CDCl₃) δ 187.8, 182.8, 157.0, 143.7, 133.5, 107.8, 72.3, 21.1, 15.6

HRMS (EI) Calculated for C₁₀H₁₂NaO₃: 203.0827; Found: 203.0824



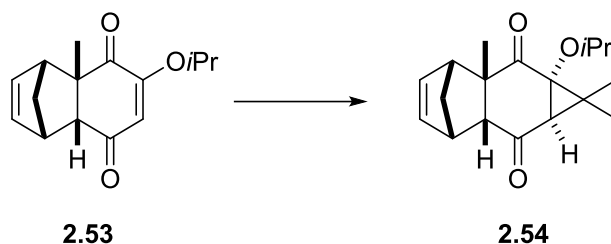
(1*S*,4*R*,4*aS*)-6-Isopropoxy-4*a*-methyl-1,4,4*a*,8*a*-tetrahydro-1,4-methanonaphthalene-5,8-dione

Quinone **2.49** (220 mg, 1.22 mmol), was dissolved in dichloromethane (10 mL) and freshly cracked cyclopentadiene (1.5 mL, 18.33 mmol) was added in one single portion at room temperature. The resulting mixture was stirred at ambient temperature overnight. The crude residue was purified *via* column chromatography (ethyl acetate / petroleum ether = 5:1) to afford the titled compound as a yellow oil (278 mg, 93%).

¹H NMR (300 MHz, CDCl₃) δ 6.12 (dd, J = 2.9, 6.1 Hz, 1H), 6.03 (dd, J = 2.9, 6.1 Hz, 1H), 5.86 (s br, 1H), 4.35 (sept, J = 6.0 Hz, 1H), 3.42 (s br, 1H), 3.10 (s br, 1H), 2.82 (d, J = 3.8 Hz, 1H), 1.67 (dt, J = 1.7, 9.2 Hz, 1H), 1.59 (s, 3H), 1.54 (dt, J = 1.7, 9.2 Hz, 1H), 1.47 (s, 3H), 1.34 (dd, J = 4.4, 6.1 Hz, 6H)

¹³C NMR (400 MHz, CDCl₃) δ 198.8, 197.8, 160.8, 137.5, 135.1, 114.6, 72.3, 57.5, 53.9, 48.7, 46.4, 26.5, 21.0

X-Ray Data: (see Appendix 8.2)



(1a*S*,2a*S*,3*R*,6*S*,6a*R*,7a*R*)-1a-Isopropoxy-1,1,2a-trimethyl-1a,2a,3,6,6a,7a-hexahydro-1*H*-3,6-methanocyclopropa[*b*]naphthalene-2,7-dione

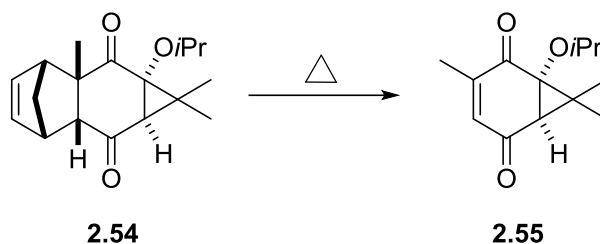
Triisopropylsulfoxonium tetrafluoroborate **2.30** (404 mg, 1.53 mmol) was added in one portion to a stirring suspension of NaH (98 mg, 2.44 mmol) in dry DMF (15 mL) at 0 °C. The reaction mixture was stirred for 5 minutes before drop wise addition of Diels-Alder adduct **2.53** (150 mg, 0.61 mmol) as a solution in dry DMF (1 mL). The cooling bath was removed and the reaction mixture warmed to room temperature. On completion – monitored by TLC – the reaction mixture was quenched with saturated NH₄Cl (5 mL) and extracted with EtOAc (3 x 30 mL). The combined organic layers were dried over MgSO₄ and the solvent removed under reduced pressure yielding a brown oil, which was purified *via* column chromatography (ethyl acetate/petroleum spirit = 5:1) to afford the titled compound as a yellow oil (124 mg, 70%).

¹H NMR (500 MHz, CDCl₃) δ 6.23 (m, 2H), 3.68 (sept, *J* = 6.0 Hz, 1H), 3.50 (m, 1H), 3.21 (m, 1H), 2.59 (d, *J* = 4.2 Hz, 1H), 2.14 (s, 1H), 1.68 – 1.65 (m, 1H), 1.49 (s, 3H), 1.44 (dt, *J* = 1.7, 9.3 Hz, 1H), 1.31 (s, 3H), 1.30 (s, 3H), 1.26 (d, *J* = 6.0 Hz, 3H), 1.02 (d, *J* = 6.0 Hz, 3H)

¹³C NMR (500 MHz, CDCl₃) δ 210.3, 206.4, 137.4, 137.0, 76.2, 72.6, 59.0, 58.4, 53.1, 51.0, 48.2, 47.4, 33.9, 26.9, 23.7, 23.5, 22.9, 19.5

HRMS (EI) Calculated for C₁₈H₂₄NaO₃: 311.1618; Found: 311.1630

X-Ray Data: (see Appendix 8.2)



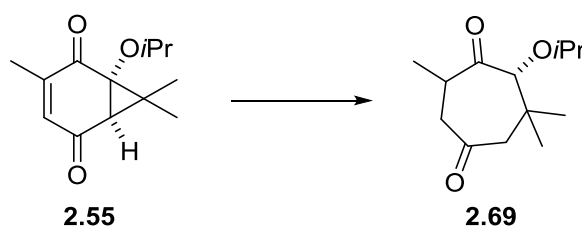
(1*S*,6*R*)-1-Isopropoxy-3,7,7-trimethylbicyclo[4.1.0]hept-3-ene-2,5-dione

The retro Diels-Alder reaction was performed by heating compound **2.54** (127 mg, 0.49 mmol) at 161°C at 500 Torr using a Kugelrohr apparatus. Compound **2.54** was placed in the terminal 10 mL round bottom flask of a triple bulb (10 mL each) Kugelrohr short path distillation apparatus. The glassware assembly was connected to a vacuum pump (500 Torr) and placed into a Kugelrohr oven preheated to 140°C with one bulb remaining outside for cooling with dry ice. The yellow residual oil in the terminal bulb was then washed with Et₂O and the solvent removed under reduced pressure to afford the titled compound as a yellow oil (83%)

¹H NMR (500 MHz, CDCl₃) δ 6.51 – 6.50 (m, 1H), 3.75 (sept, J = 6.2 Hz, 1H), 2.43 (d, J = 1.8 Hz, 1H), 2.04 (d, J = 1.8 Hz, 3H), 1.38 (s, 3H), 1.28 (s, 3H), 1.18 (d, J = 6.2 Hz, 3H), 1.16 (d, J = 6.2 Hz, 3H)

¹³C NMR (400 MHz, CDCl₃) δ 195.7, 194.2, 149.5, 137.0, 73.6, 72.9, 45.4, 38.3, 23.4, 23.2, 22.7, 16.4, 16.3

HRMS (EI) Calculated for C₁₃H₁₈NaO₃: 245.1148; Found: 245.1146



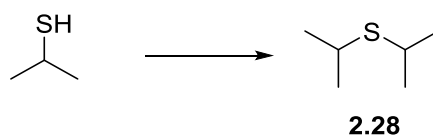
(7*R*)-7-Isopropoxy-2,6,6-trimethylcycloheptane-1,4-dione

Hydrogenation was performed on the H-Cube® Hydrogenator using a 10% Pd/C cartridge. A 0.02M solution of **2.55** in ethyl acetate was pumped through the system with a flow rate of 1 mL/min at room temperature. After one cycle the colourless solution was concentrated to dryness

and purified *via* column chromatography (ethyl acetate/petroleum ether = 1:2) to afford the titled compound as a colourless oil.

¹H NMR (500 MHz, CDCl₃) δ 3.68 (s, 1H), 3.57 (sept, J = 6.2 Hz, 1H), 3.06 (t, J = 13.0 Hz, 1H), 2.83 (d, J = 11.9 Hz, 1H), 2.64 – 2.56 (m, 1H), 2.37 – 2.32 (m, 2H), 1.26 (t, J = 7.2 Hz, 2H), 1.25 (d, J = 7.0 Hz, 2H), 1.19 (dd, J = 6.3, 6.3 Hz, 6H), 1.02 (s, 3H), 0.91 (s, 3H)

¹³C NMR (500 MHz, CDCl₃) δ 212.3, 210.1, 92.0, 72.7, 53.8, 45.6, 41.6, 36.3, 26.3, 25.6, 22.9, 21.4, 18.9, 14.2

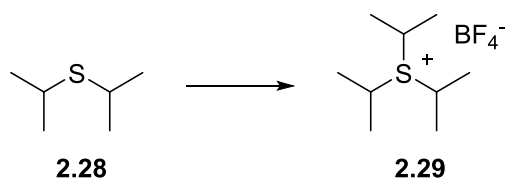


Diisopropylsulfide

Acetone (1 mL, 13.6 mmol) and 2-propanethiol (1.53 mL, 16.32 mmol) were dissolved in dichloromethane (10 mL). A freshly prepared solution of BF₃*H₂O (1eq. of water was added slowly to a cooled solution of BF₃*Et₂O, 1.2 mL) was added and the reaction mixture was stirred for one hour followed by the addition of triethylsilane (2 mL, 13.6 mmol). The resulting cloudy solution was stirred and warmed to room temperature overnight. The solution was then poured onto ice – water and extracted with DCM (3 x 15 mL). The organic layer was washed with water (20 mL), saturated NaHCO₃ (20 mL) and brine (20 mL), dried over MgSO₄ and the solvent was removed under reduced pressure to afford a colourless oil, which was purified *via* distillation giving rise to the titled compound in 25% yield. The spectral data for **2.28** match those reported.^{84a}

¹H NMR (400 MHz, CDCl₃) δ 2.98 (sept, J = 6.7 Hz, 2H), 1.25 (d, J = 6.7 Hz, 12H)

¹³C NMR (400 MHz, CDCl₃) δ 33.4, 23.6

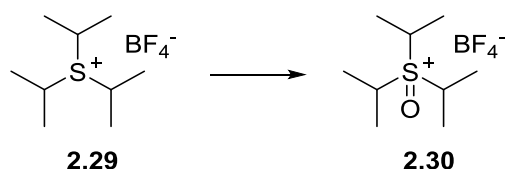


Triisopropylsulfonium tetrafluoroborate

Isopropanol (30 mL, 393.01 mmol) was added to a stirring solution of diisopropylsulfide (5.8 g, 49.14 mmol) and freshly distilled methanesulfonic acid (31.9 mL, 491.4 mmol). The mixture was stirred at 115°C for 3 days resulting in a brown solution which was cooled to room temperature and treated with an excess of HBF₄ (50 mL, 491.4 mmol). The mixture was stirred for further 30 minutes and then washed with H₂O (100 mL) and extracted with CH₂Cl₂ (3 x 100 mL). The organic layer was dried over MgSO₄ and the solvent was removed under reduced pressure to afford the titled compound as cream coloured plates (53%). Spectroscopic data matched that as described in literature.^{84b,129}

¹H NMR (400MHz, d₆-acetone) δ 4.16 (sept, *J* = 6.8 Hz, 3H), 1.67 (d, *J* = 6.8 Hz, 18H)

¹³C NMR (400MHz, d₆-acetone) δ 43.4, 19.8



Triisopropylsulfoxonium tetrafluoroborate

Method A: Ruthenium chloride (1.04 g, 5 mmol) was added to a vigorously stirred solution of 2.29 (3.1 g, 12.5 mmol) in a mixture of MeCN: CCl₄: H₂O = 1: 1: 1.5 (42 mL) and the solution was stirred for 10 minutes. NaIO₄ (18.7 g, 87.5 mmol) was then added in portions and the resulting mixture stirred at room temperature overnight giving rise to a bright yellow suspension which was filtered through a Celite® pad and washed with water (200 mL). To quench the residual RuO₄, methanol (15 mL) was added to the filtrate, whereas a colour change was immediately observed from yellow to dark brown. The water/methanol mixture was then concentrated *in vacuo* and the resulting grey residue suspended in acetone (50 mL), stirred for 20 minutes and filtered. Concentration of the filtrate under reduced pressure gave rise to a yellow oil. The oil was diluted in

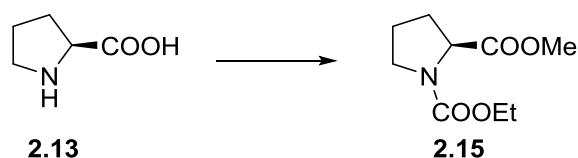
hot methanol (15 mL) and diethyl ether was added dropwise until the solution remained turbid. The mixture was cooled with an ice bath to afford the titled compound as white plates (52%). Spectroscopic data matched that as described in literature.^{84b,129}

Method B: To a solution of triisopropylsulfonium tetrafluoroborate (7.77g, 31.1 mmol) in water (400 mL) at 0 °C was added 2-nitrobenzenesulfonyl chloride (13.9 g, 62.7 mmol) followed by barium hydroxide octahydrate (29.7 g, 94 mmol). The resulting cream suspension was stirred at that temperature for 10 minutes after which H₂O₂ (30% solution in H₂O; 20 mL, 188 mmol) was added over a period of 1 hour. On completion, the resulting mixture was stirred for further 45 minutes at 0 °C after which the cooling bath was removed and the suspension stirred at ambient temperature overnight. The resulting mixture was then filtered through a pad of Celite® and thoroughly washed with water (250 mL). After concentrating the aqueous solution *in vacuo*, the residue was redissolved in dichloromethane, dried over MgSO₄ and filtered again through a pad of Celite® and thoroughly washed with dichloromethane. The filtrate was concentrated to give a beige precipitate. Recrystallization from methanol/diethyl ether gave rise to the desired compound as a white solid (5.54 g, 67%). Spectroscopic data matched that as described in literature.^{84b,129}

¹H NMR (500MHz, *d*₆-acetone) δ 4.69 (sept, *J* = 6.8 Hz, 3H), 1.75 (d, *J* = 6.8 Hz, 18H)

¹³C NMR (500MHz, *d*₆-acetone) δ 53.2, 15.8

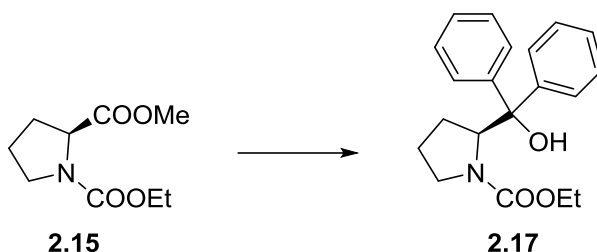
HRMS (EI) Calculated for C₉H₂₁OS⁺: 177.1308; Found: 177.1302



1-Ethyl-2-methyl (*S*)-pyrrolidine-1,2-dicarboxylate

L-Proline (3 g, 26.1 mmol) was dissolved in anhydrous methanol (20 mL) under a positive pressure of argon. Anhydrous K_2CO_3 (3.6 g, 26.1 mmol) was added while maintaining the argon flow and the resulting solution was stirred for 10 minutes. Subsequent addition of ethyl chloroformate (6.2 g, 57.3 mmol) gave rise to a white solution, which was then cooled to 0°C and stirred at that temperature for 8 hours. The solvent was removed under reduced pressure, the residue was suspended in water and extracted with $CHCl_3$ (3 x 60 mL). The organic layer was washed with brine, dried over $MgSO_4$, filtered and concentrated to dryness yielding the desired compound as a yellow oil in 62% yield. The crude product was used in the next step without further purification. The spectral data for **2.15** match those reported in literature.¹³⁰

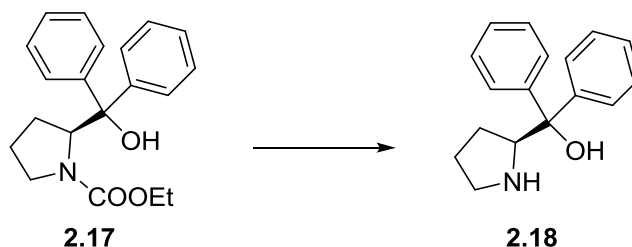
1H NMR (300 MHz, $CDCl_3$) δ 4.45 – 4.25 (m, 1H), 4.23 – 4.0 (m, 2H), 3.72 (d, J = 5.1 Hz, 2H), 3.65 – 3.37 (m, 2H), 2.36 – 2.09 (m, 2H), 2.06 – 1.81 (m, 3H), 1.31 – 1.15 (m, 3H)



Ethyl (*S*)-2-(hydroxydiphenylmethyl)pyrrolidine-1-carboxylate

Compound **2.15** (2.48 g, 12.33 mmol) was diluted in anhydrous THF (20 mL) under an argon atmosphere and cooled to 0°C using an ice/ $NaCl$ bath. The freshly prepared Grignard reagent (4.92 g, 63.7 mmol) was added to the solution *via* cannula and the mixture was stirred at 0°C for 3 hours. On completion the reaction was quenched with saturated NH_4Cl (12 mL), neutralised with 2N HCl and extracted with $CHCl_3$ (3 x 40 mL). The organic layer was washed with brine, dried over $MgSO_4$ and the solvent was removed under reduced pressure to afford the titled compound as an orange oil, which solidified upon standing. The spectral data for **2.17** match those reported in literature.¹³⁰

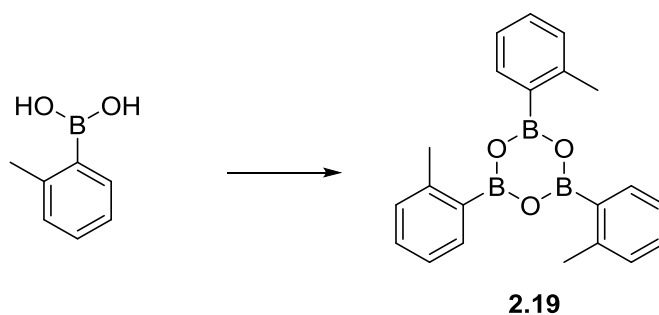
¹H NMR (300 MHz, CDCl₃) δ 7.48 – 7.27 (m, 10H), 4.93 (dd, J = 3.8, 8.8 Hz, 1H), 4.22 – 4.01 (m, 2H), 3.97 – 3.70 (m, 1H), 3.48 – 3.35 (m, 1H), 3.03 – 2.86 (m, 1H), 2.15 – 2.0 (m, 1H), 1.99 – 1.89 (m, 1H), 1.89 – 1.82 (m, 1H), 1.55 – 1.41 (m, 1H), 1.23 (t, J = 7.1 Hz, 3H)



(*S*)-Diphenyl(pyrrolidine-2-yl)methanol

Potassium hydroxide (1.3 g, 22.14 mmol) was added to a methanolic solution of **2.17** (2 g, 6.15 mmol) and the reaction mixture was heated to reflux overnight. After cooling the solution to room temperature, methanol was removed under reduced pressure, the residue suspended in water (20 mL) and the mixture extracted with CHCl₃ (3 x 30 mL). The organic extracts were washed with brine, dried over MgSO₄ and evaporation of the solvent afforded compound **2.18** as a brown oil in 90% yield, which solidified upon standing. The spectral data for **2.18** match those reported in literature.¹³⁰

¹H NMR (300 MHz, CDCl₃) δ 7.54 – 7.28 (m, 10H), 4.55 (dd, J = 5.5, 10.5 Hz, 1H), 3.80 – 3.66 (m, 1H), 3.30 – 3.20 (m, 1H), 2.07 – 1.80 (m, 2H), 1.79 – 1.62 (m, 2H), 1.32 – 1.01 (m, 2H)

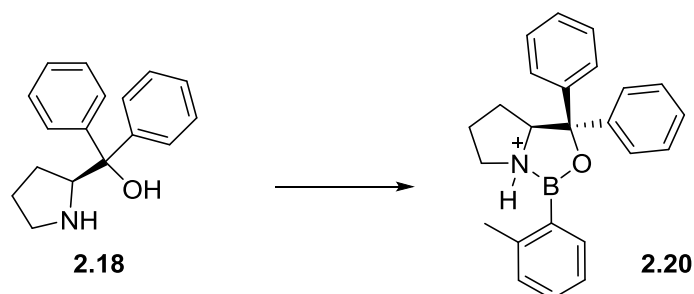


Tri-*o*-tolylboroxine

O-tolylboronic acid (5 g, 36.77 mmol) was charged in a flask equipped with a Dean Stark trap and dehydrated by azeotropic distillation with toluene (3 x 60 mL). After cooling the residue to room

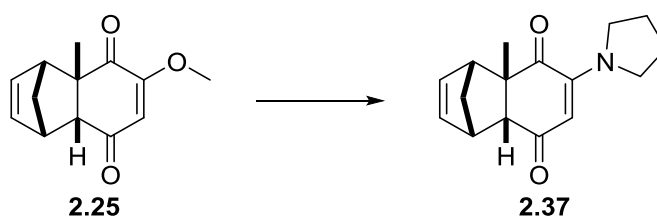
temperature a white solid was formed in quantitative yield that was dried on high vacuum. The spectral data for **2.19** match those reported in literature.¹³⁰

¹H NMR (300 MHz, CDCl₃) δ 8.22 (dd, J = 1.6, 7.4 Hz, 3H), 7.50 (td, J = 1.6, 7.4 Hz, 3H), 7.35 – 7.27 (m, 6H), 2.82 (s, 9H)



(3a*S*)-3,3-diphenyl-1-(*o*-tolyl)hexahydro-1*H*-pyrrolo[1,2-*c*][1,3,2]oxazaborol-7-ium

According to the procedure of Corey *et al.* a 100 mL 2-necked flask equipped with a stir bar, glass stopper and a 50 mL pressure-equalizing funnel (containing a cotton plug and ~10 g of 4Å mol sieve and functioning as a Soxhlet extractor) fitted on top with a reflux condenser and an argon inlet adaptor was charged with compound **2.18** (14.32 mmol), boroxine **2.19** (5.73 mmol) and dry toluene (40 mL). The resulting mixture was refluxed overnight. The reaction mixture was then cooled to 60°C and the addition funnel and the condenser were quickly replaced by a short distillation head. The remaining residue was distilled with toluene (3 x 50 mL) and lastly kept as a solution in toluene under argon.¹³⁰



4a-Methyl-6-(pyrrolidine-1-yl)-1,4,4a,8a-tetrahydro-1,4-methanonaphthalene-5,8-dione

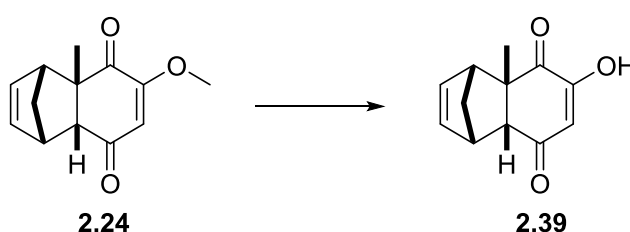
Diels-Alder product **2.25** (99 mg, 0.45 mmol) was suspended in H₂O and pyrrolidine (0.5 mL) was added. The reaction mixture was stirred at room temperature overnight, whereas the titled

compound was formed as a beige precipitate which was filtered and washed with H₂O (48 mg, 41%)

¹H NMR (300 MHz, CDCl₃) δ 6.11 – 6.09 (m, 1H), 6.07 – 6.06 (m, 1H), 5.56 (br s, 1H), 3.42 (br s, 1H), 3.04 (br s, 1H), 2.80 (d, J = 3.8 Hz, 1H), 2.02 – 1.83 (m, 4H), 1.67 – 1.65 (m, 1H), 1.56 – 1.53 (m, 1H), 1.46 (s, 3H)

HRMS (EI) Calculated for C₁₆H₁₉NNaO₂: 280.1308; Found: 280.1310

X-Ray Data: (see Appendix 8.2)



6-Hydroxy-4a-methyl-1,4,4a,8a-tetrahydro-1,4-methanonaphthalene-5,8-dione

Diels-Alder adduct **2.24** (30 mg, 0.21 mmol) was dissolved in a 1M solution of K₂CO₃ in MeOH/H₂O (1:1) and the resulting mixture was heated to reflux overnight. Concentrated hydrochloric acid was then added until a pH of 4 was observed and the reaction mixture was extracted with ethyl acetate (3 x 30 mL), dried over MgSO₄ and the solvent was removed under reduced pressure to afford the titled compound as a beige solid (21 mg, 88%).

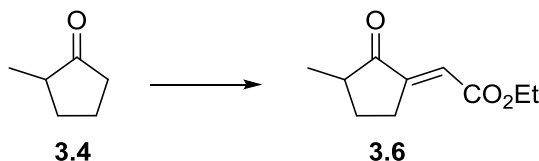
¹H NMR (500 MHz, CDCl₃) δ 6.11 (d, J = 0.8 Hz, 1H), 6.07 (t, J = 1.84 Hz, 2H), 3.46 – 3.42 (m, 1H), 3.13 – 3.10 (m, 1H), 2.88 (d, J = 3.8 Hz, 1H), 1.73 – 1.68 (m, 1H), 1.61 – 1.57 (m, 2H), 1.52 (s, 3H)

¹³C NMR (400 MHz, CDCl₃) δ 200.2, 198.5, 158.2, 136.4, 135.8, 115.2, 58.2, 54.3, 51.4, 49.1, 46.8, 26.0

LRMS (ESI) Calculated for: C₁₂H₁₁O₃ (M-H⁺): 203.08; Found: 202.9

HRMS (EI) Calculated for C₁₂H₁₂O₃Na: 227.0679; Found: 227.0677

6.3 Experimental Procedures Left Hand Fragment



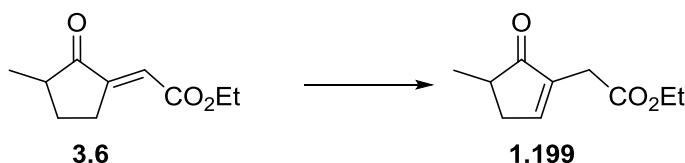
Ethyl (*E*)-2-(3-methyl-2-oxocyclopentylidene)acetate

According to the procedure of Barco *et al.*⁹⁸ a solution of 2-methylcyclopentanone (2 mL, 18.7 mmol), pyrrolidine (3.2 mL, 37.4 mmol) and catalytic amounts of *p*-toluenesulfonic acid in toluene (20 mL) were refluxed using a Dean-Stark trap until no further water was collected. The reaction mixture was cooled to room temperature and ethyl glyoxalate (50% in toluene; 4.5 mL, 21.8 mmol) was added in one portion. The resulting mixture was heated to reflux for further 3 hours until complete conversion to product was observed by TLC. The resulting reaction mixture was cooled to room temperature and 4N HCl (10 mL) was carefully added. The mixture was further stirred for 20 minutes at r.t. and extracted washed with water (3 x 30 mL). The organic layer was dried over MgSO₄ and concentrated in vacuo to afford **3.6** as a crude brown oil, which was purified *via* Kugelrohr distillation to afford the titled compound as a yellow oil (1.2 g, 45 %).

¹H NMR (300 MHz, CDCl₃) δ 6.52 (dd, $J = 3.6, 3.6$ Hz, 1H), 4.23 (q, $J = 7.0$ Hz, 2H), 3.35 – 3.24 (m, 1H), 2.84 – 2.70 (m, 1H), 2.41 – 2.26 (m, 2H), 1.58 – 1.43 (m, 1H), 1.31 (t, $J = 7.0$ Hz, 3H), 1.18 (d, $J = 6.7$ Hz, 3H)

¹³C NMR (500 MHz, CDCl₃) δ 208.9, 166.4, 150.8, 119.9, 60.8, 43.8, 28.5, 27.6, 14.2, 14.2

HRMS (EI) Calculated for C₁₀H₁₄NaO₃: 205.0835; Found: 205.0834



Ethyl 2-(4-methyl-5-oxocyclopent-1-en-1-yl)acetate

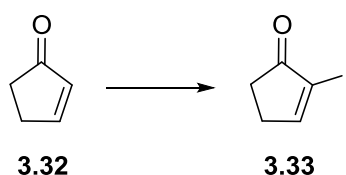
To a solution of **3.6** (0.5 mL, 2.8 mmol) in EtOH (5 mL) was added dilute hydrochloric acid (1M, 0.2 mL) and the resulting mixture stirred at r.t. for 3 hours. The reaction mixture was neutralised by

adding solid NaHCO_3 to the solution. The filtrate was concentrated to dryness and the crude oil purified *via* Kugelrohr distillation to afford the titled compound as a yellow oil (0.1 g, 20%).

^1H NMR (400 MHz, CDCl_3) δ 7.53 – 7.51 (m, 1H), 4.33 – 4.23 (m, 1H), 5.15 (q, $J = 7.1$ Hz, 2H), 3.23 – 3.21 (m, 2H), 2.94 – 2.86 (m, 1H), 2.45 – 2.38 (m, 1H), 2.27 – 2.19 (m, 1H), 1.26 (t, $J = 7.1$ Hz, 3H), 1.19 (d, $J = 7.6$ Hz, 3H)

^{13}C NMR (400 MHz, CDCl_3) δ 210.9, 170.6, 158.8, 137.8, 60.93, 39.5, 35.9, 30.5, 14.1, 13.8

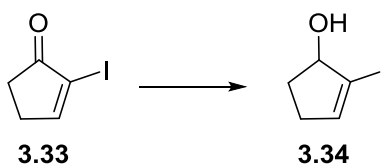
HRMS (EI) Calculated for $\text{C}_{10}\text{H}_{14}\text{NaO}_3$: 205.0835; Found: 205.0834



2-Iodocyclopent-2-en-1-one

Potassium carbonate (396 mg, 2.87 mmol), iodine (909 mg, 3.58 mmol) and DMAP (58 mg, 0.48 mmol) were added to a solution of cyclopentenone (0.2 mL, 2.39 mmol) in a mixture of THF/ H_2O (10 mL, 1:1) at room temperature and the resulting reaction mixture was stirred for 1.5 hours. The mixture was diluted with EtOAc, thoroughly extracted with $\text{Na}_2\text{S}_2\text{O}_3$ and 1N HCl, dried over MgSO_4 and concentrated *in vacuo*. The crude product was purified *via* flash column chromatography (ethyl acetate/dichloromethane, 1:1) to afford the titled compound as a pale yellow solid (300 mg, 60%). Spectroscopic data matched that as described in literature.¹³¹

^1H NMR (500 MHz, CDCl_3) δ 8.02 (t, $J = 2.9$ Hz, 1H), 2.80 – 2.76 (m, 2H), 2.53 – 2.49 (m, 2H)



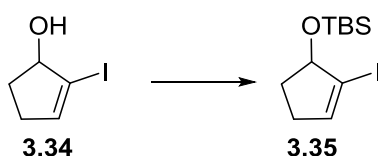
2-Iodocyclopent-2-en-1-ol

A solution of 2-iodocyclopentenone (0.7 g, 3.4 mmol) in MeOH (1 mL) was added to a mixture of $\text{CeCl}_3 \cdot 7\text{H}_2\text{O}$ (1.23 g, 3.4 mmol) in MeOH (10 mL) at 0 °C and stirred for 5 minutes. NaBH_4 (0.15

g, 4.0 mmol) was then added portionwise and the resulting mixture stirred at 0 °C for 1 hour. The cooling bath was removed and the solution stirred for further 60 minutes at ambient temperature. The reaction mixture was quenched with water (10 mL) and the mixture extracted with Et₂O (3 x 20 mL). The combined organic layers were dried over MgSO₄ and concentrated *in vacuo* to give the titled compound as an off white solid (0.4 g, 56 %). Spectroscopic data matched that as described in literature.¹³²

¹H NMR (500 MHz, CDCl₃) δ 6.30 – 6.28 (m, 1H), 4.72 – 4.68 (m, 1H), 2.53 – 2.46 (m, 1H), 2.37 – 2.29 (m, 2H), 1.89 – 1.84 (m, 1H), 1.71 (br s, 1H)

¹³C NMR (500 MHz, CDCl₃) δ 142.6, 100.2, 82.3, 32.8, 31.4



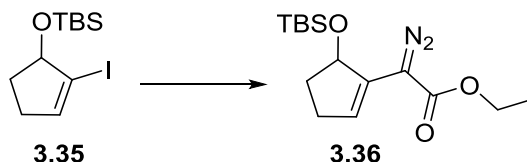
***t*-Butyl[(2-iodocyclopent-2-ene-1yl)oxy]dimethylsilane**

Imidazole (243 mg, 3.6 mmol), DMAP (52 mg, 0.4 mmol) and TBS-Cl (258 mg, 1.7 mmol) were added successively to a solution of **3.34** (300 mg, 1.4 mmol) in dry CH₂Cl₂ (30 mL) and the resulting mixture was stirred at room temperature. Progress was monitored *via* GC/MS and TLC and complete conversion to product was observed after 3 hours. The reaction mixture was quenched with H₂O and extracted with further CH₂Cl₂. The combined organic layers were dried over MgSO₄ and the solvent removed under reduced pressure yielding the desired product as a colourless oil (87 mg, 81 %).

¹H NMR (500 MHz, CDCl₃) δ 6.23 (m, 1H), 4.72 (m, 1H), 2.45 (m, 1H), 2.23 (m, 2H), 1.80 (m, 1H), 0.94 (s, 9H), 0.17 (s, 3H), 0.13 (s, 3H)

¹³C NMR (500 MHz, CDCl₃) δ 141.6, 101.3, 82.3, 32.7, 32.6, 25.9, 25.6, 18.3, -4.4, -4.5

HRMS (EI) Calculated for C₁₁H₂₁INaOSi: 347.0299; Found: 347.0297



Ethyl 2-(5-(*tert*-butyldimethylsilyl)oxy)cyclopent-1-en-1-yl)-2-diazoacetate

The following reaction was performed according to the procedure of Wang *et al.*¹⁰⁰ Ethyl diazoacetate (15% solution in toluene, 0.38 mL, 0.54 mmol), DBU (0.05 mL, 0.33 mmol) and *n*Bu₄NBr (70 mg, 0.22 mmol) were added to a solution of iodocompound **3.35** (70 mg, 0.22 mmol) in dry MeCN (7 mL). Pd(PPh₃)₄ (25 mg, 0.02 mmol) was then added in one portion and the reaction mixture stirred at 45 °C oil bath temperature for 24 hours. Upon completion – progress monitored *via* GC/MS – the solvent was evaporated and the crude oil purified *via* column chromatography (ethyl acetate/petroleum ether, 8:1) to afford the titled compound as a yellow oil (26 mg, 39%).

¹H NMR (500 MHz, CDCl₃) δ 6.22 (m, 1H), 4.94 (m, 1H), 4.26 (q, *J* = 7.0 Hz, 2H), 2.54 (m, 1H), 2.30 (m, 2H), 1.80 (m, 1H), 1.30 (t, *J* = 7.0 Hz, 3H), 0.90 (s, 9H), 0.17 (s, 3H), 0.13 (s, 3H)

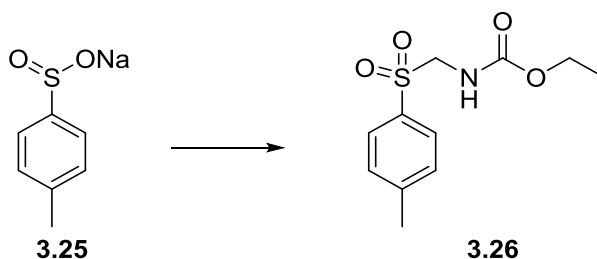
¹³C NMR (500 MHz, CDCl₃) δ 166.4, 127.6, 78.3, 60.8, 33.9, 31.0, 25.8, 17.9, 14.5, - 3.9, - 4.8

GC/MS (EI) *m/z* (%) 282 (M⁺, %), 197, 151, 77, 76, 75, 59, 45

IR (neat, ν_{\max} , cm⁻¹): 2086 (s), 1704 (s), 1234 (s), 1141 (s), 1063 (s), 834 (s), 774 (s)

LRMS (ESI) Calculated for C₁₅H₂₆N₂O₃SiNa: 333.2; Found: 333.1

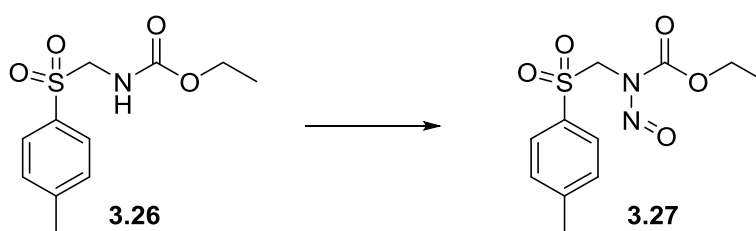
HRMS (EI) Calculated for C₁₅H₂₆N₂O₃SiNa: 333.1605, Found: 333.1598



Ethyl (4-methylphenyl)sulfonamethanecarboxylate

Urethane (5.2 g, 58.4 mmol), formic acid (13.2 mL) and formaldehyde (37 weight % in water, 7 mL) were added to a stirring solution of **3.25** (10.4 g, 58.4 mmol) in water (70 mL) and gently refluxed for 2 hours resulting in a milky solution. The reaction mixture was cooled and the formed precipitate filtered, washed with water and recrystallised from ethanol to afford the titled compound in 50% yield. The spectral data for **3.26** match those reported in literature.⁷⁵

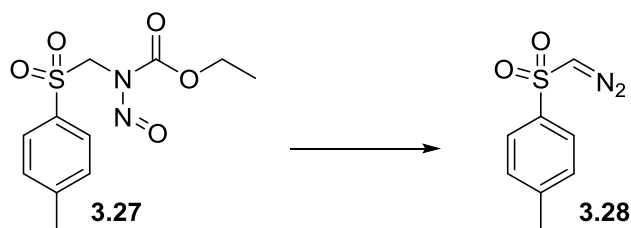
¹H NMR (300 MHz, CDCl₃) δ 7.79 (d, J = 8.31 Hz, 2H), 7.35 (d, J = 8.31 Hz, 2H), 5.55 – 5.47 (m, 1H), 4.54 (d, J = 7.0 Hz, 2H), 3.98 (q, J = 7.0 Hz, 2H), 2.44 (s, 3H), 1.13 (t, J = 7.0 Hz, 3H)



Ethyl nitroso(tosylmethyl)carbamate

Compound **3.26** (4 g, 15.55 mmol) was weighed in under argon and dissolved in dichloromethane (20 mL). The flask was shielded from light and pyridine (1.88 mL, 23.33 mmol), isomalynitrite (3.2 mL, 23.33 mmol) and TMSCl (5.13 mL, 40.43 mmol) were added successively. The reaction mixture was allowed to stir 24 hours at room temperature, whereby complete conversion to product was observed by TLC. The reaction mixture was slowly poured onto a 10% NaHCO₃ solution (180 mL) and stirred for 30 minutes and then extracted with Et₂O (3 x 150 mL). The organic layer was washed with water (200 mL), 1M HCl (200 mL) and brine (200 mL), dried over MgSO₄, filtered and concentrated to dryness yielding a yellow oil, which was triturated with cyclohexane (10 mL) to afford the titled compound as yellow crystals (7.4 g, 49%). The spectral data for **3.27** match those reported in literature.⁷⁵

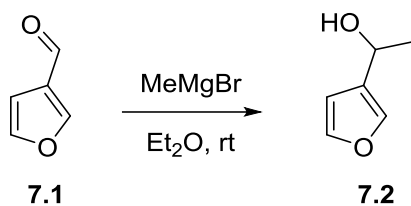
¹H NMR (300 MHz, CDCl₃) δ 7.70 (d, J = 8.4 Hz, 2H), 7.36 (d, J = 8.4 Hz, 2H), 5.12 (s, 2H), 4.52 (q, J = 7.2 Hz, 2H), 2.47 (s, 3H), 1.43 (t, J = 7.2 Hz, 3H)



1-(diazomethyl)sulfonyl-4-methylbenzene

Al_2O_3 (10 g, activated, basic, Brockmann I standard grade, 150 mesh, 58Å) was cooled with an ice/ NaCl bath. Anhydrous diethyl ether (50 mL) was then added and the mixture was stirred for 10 minutes. Compound **3.27** (0.5 g, 1.75 mmol) was then dissolved in anhydrous CH_2Cl_2 (5 mL) and added to the solution at 0°C , whereas the reaction was shielded from light all the time. After stirring the solution at room temperature for 2 hours, complete conversion was observed by TLC, the solution decanted and the Al_2O_3 was washed with further portions of diethyl ether (3 x 20 mL). The solvent was removed under reduced pressure to afford a yellow oil, which solidified upon treatment with cold petroleum ether in a dry ice/acetone bath. The solid was washed with further portions of petroleum ether (3 x 20 mL) to afford the titled compound as a bright yellow solid (250 mg, 73%). The spectral data for **3.28** match those reported in literature.⁷⁵

^1H NMR (300 MHz, CDCl_3) δ 7.76 (d, $J = 8.4$ Hz, 2H), 7.34 (d, $J = 8.4$ Hz, 2H), 5.25 (s, 1H), 2.45 (s, 3H)

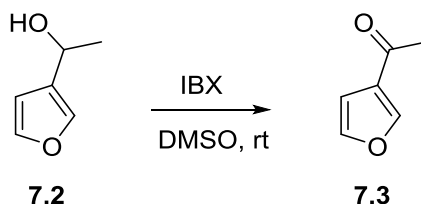


1-(Furan-3-yl)ethan-1-ol

A solution of 3-furaldehyde (1 mL, 11.6 mmol) in anhydrous Et_2O (10 mL) was added to methylmagnesium bromide (3M in Et_2O , 15 mmol) at 0°C under an argon atmosphere. After stirring at the set temperature for one hour the reaction mixture was quenched with H_2O (0.2 mL) and the supernatant layer was decanted. After removing the solvent under reduced pressure, the titled compound was afforded as a yellow oil, which was used in the next step without further purification. Spectral data were in accordance to the literature.¹³³

¹H NMR (400 MHz, CDCl₃) δ 7.38 (d, J = 1.4 Hz, 2H), 6.42 (t, J = 1.4 Hz, 1H), 4.90 – 4.82 (m, 1H), 1.74 – 1.67 (m, 1H), 1.49 (d, J = 6.5 Hz, 3H)

¹³C NMR (400 MHz, CDCl₃) δ 143.3, 138.5, 130.3, 108.5, 63.0, 24.0



1-(Furan-3-yl)ethan-1-one

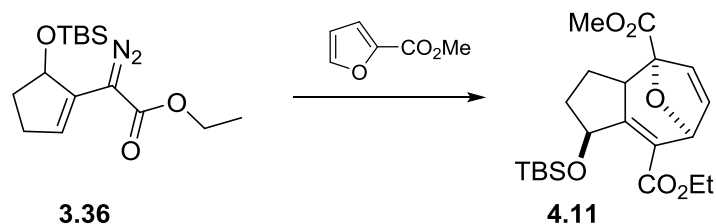
IBX (2.3 g, 8.4 mmol) was added to a solution of 1-(furan-3-yl)ethan-1-ol (0.78 g, 6.9 mmol) in DMSO (10 mL) and the resulting mixture stirred for one hour at ambient temperature. Et₂O (15 mL) was added and the organic layer extracted with NaHCO₃, dried over Na₂SO₄. Removing the solvent under reduced pressure afforded the titled compound as a white solid (0.59 g, 76%). Spectral data were in accordance to the literature.¹³³

¹H NMR (500 MHz, CDCl₃) δ 8.02 – 8.01 (m, 1H), 7.44 (t, J = 1.4 Hz, 1H), 6.77 – 6.76 (m, 1H), 2.44 (s, 3H)

¹³C NMR (500 MHz, CDCl₃) δ 192.4, 147.5, 144.3, 128.1, 108.6, 27.81

6.3.1 General procedure for rhodium catalysed [4+3] cycloaddition reactions of diazo compound 3.36 with furans

Diazo compound **3.36** (1 eq.) was dissolved in dry cyclohexane (0.3 M), furan (3 eq.) was added followed by the addition of Rh₂(*R*-DOSP)₄ (0.01 eq.) in one portion, whereas cease of nitrogen was observed. The reaction mixture was heated to 80 °C oil bath temperature until complete conversion was observed *via* TLC. The solvent was evaporated and the crude mixture purified *via* flash column chromatography (ethyl acetate/petroleum ether = 1 : 5) to afford the titled compound as a slight yellow oil.



8-Ethyl 4-Methyl 1-((*tert*-butyldimethylsilyl)oxy)-2,3,3a,7-tetrahydro-4,7-epoxyazulene-4,8(1*H*)-dicarboxylate

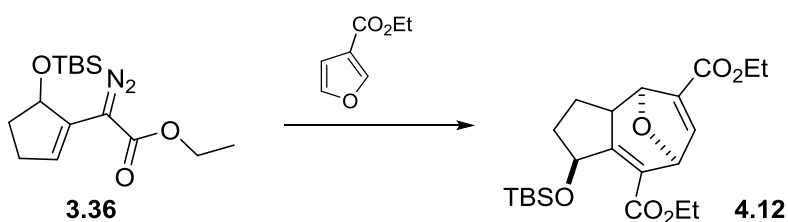
Compound **4.11** was prepared *via* general method 6.3.1 with diazo compound **3.36** (23 mg, 0.074 mmol) and 2-methylfuroate (31 μ l, 0.222 mmol). Purification *via* column chromatography (ethyl acetate/petroleum ether = 1:4) afforded the title compound (15.1 mg, 50%).

¹H NMR (500 MHz, CDCl₃) δ 6.77 (dd, J = 1.7, 5.9 Hz, 1H), 5.83 (d, J = 5.9 Hz, 1H), 5.11 (br s, 1H), 5.03 (d, J = 5.4 Hz, 1H), 4.22-4.16 (m, 2H), 3.86 (s, 3H), 2.85 (dd, J = 6.5, 13.2 Hz, 1H), 1.86 - 1.73 (m, 2H), 1.68 – 1.58 (m, 1H), 1.38 – 1.32 (m, 1H), 1.29 (t, J = 7.0 Hz, 3H), 0.79 (s, 9H), 0.05 (s, 6H)

¹³C NMR (500 MHz, CDCl₃) δ 170.7, 165.1, 154.9, 142.9, 140.7, 130.7, 124.2, 89.4, 78.3, 70.6, 60.3, 52.6, 45.9, 35.3, 25.7, 23.1, 17.9, 14.2, -3.8, -5.3

LRMS (ESI) Calculated for C₂₁H₃₂O₆SiNa: 431.2; Found: 431.1

HRMS (EI) Calculated for C₂₁H₃₂O₆SiNa: 431.1860; Found: 431.1858



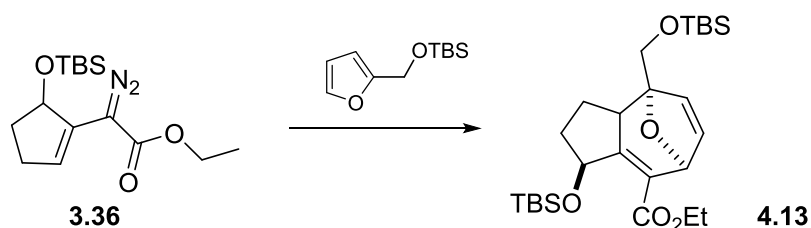
Diethyl 1-((*tert*-butyldimethylsilyl)oxy)-1,2,3,3a,4,7-hexahydro-4,7-epoxyazulene-5,8-dicarboxylate

Compound **4.12** was prepared *via* general method 6.3.1 with diazo compound **3.36** (57 mg, 0.184 mmol) and 3-ethylfuroate (77 μ l, 0.552 mmol). Purification *via* column chromatography (ethyl acetate/petroleum ether = 1:4) afforded the title compound (36.5 mg, 47%).

¹H NMR (500 MHz, CDCl₃) δ 7.45 (d, J = 1.9 Hz, 1H), 5.46 (d, J = 5.8 Hz, 1H), 5.06 (br s, 1H), 5.05 (d, J = 5.3 Hz, 1H), 4.18 (m, 4H), 2.92 (quin, J = 6.5 Hz, 1H), 1.79 (quin, J = 6.5 Hz, 1H), 1.72 (dd, J = 5.9, 13.4 Hz, 1H), 1.60 – 1.53 (m, 2H), 1.30 (t, J = 7.2 Hz, 3H), 1.26 (t, J = 7.2 Hz, 3H), 0.75 (s, 9H), 0.03 (d, J = 4.4 Hz, 6H)

¹³C NMR (500 MHz, CDCl₃) δ 164.9, 163.4, 156.8, 150.1, 131.5, 128.5, 80.7, 77.9, 76.7, 70.6, 60.5, 60.3, 43.4, 35.0, 25.6, 23.7, 17.9, 14.3, 14.2, -3.9, -5.3

HRMS (EI) Calculated for C₂₂H₃₄O₆SiNa: 445.2107; Found: 445.2103

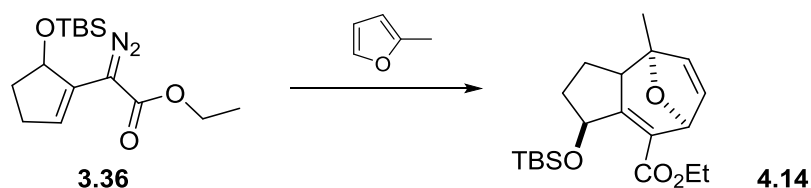


Ethyl 1-(((*tert*-butyldimethylsilyl)oxy)-4-(((*tert*-butyldimethylsilyl)oxy)methyl)-1,2,3,3a,4,7-hexahydro-4,7-epoxyazulene-8-carboxylate

Compound **4.13** was prepared *via* general method 6.3.1 with diazo compound **3.36** (30 mg, 0.097 mmol) and furan (62 μ l, 0.29 mmol). Purification *via* column chromatography (ethyl acetate/petroleum ether = 1:4) afforded the title compound (1.8 mg, 38%).

¹H NMR (500 MHz, CDCl₃) δ 6.64 (dd, J = 1.7, 5.9 Hz, 1H), 5.64 (d, J = 5.9 Hz, 1H), 5.03 – 5.0 (m, 2H), 4.24 – 4.11 (m, 2H), 3.92 (s, 2H), 2.78 (dd, J = 6.6, 13.2 Hz, 1H), 1.77 – 1.69 (m, 2H), 1.68 – 1.59 (m, 1H), 1.28 (t, J = 7.1 Hz, 3H), 0.91 (s, 9H), 0.78 (s, 9H), 0.09 (s, 6H), 0.04 (d, J = 1.5 Hz, 6H)

¹³C NMR (500 MHz, CDCl₃) δ 165.6, 157.0, 141.7, 130.8, 126.0, 90.2, 78.1, 70.6, 66.7, 59.9, 44.7, 35.8, 25.9, 25.7, 22.8, 18.4, 18.0, 14.3, -3.8, -5.2

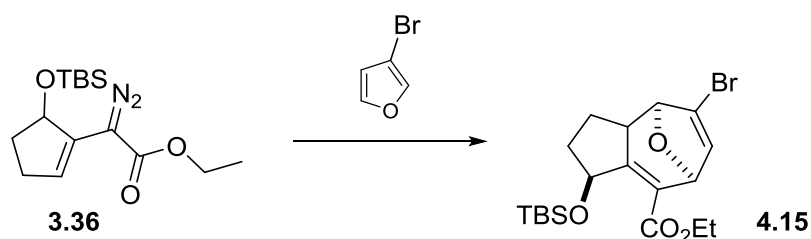


Ethyl-1-((tert-butyldimethylsilyl)oxy)-4-methyl-1,2,3,3a,4,7-hexahydro-4,7-epoxyazulene-8-carboxylate

Compound **4.14** was prepared *via* general method 6.3.1 with diazo compound **3.36** (46 mg, 0.148 mmol) and 2-methylfuran (40 μ l, 0.445 mmol). Purification *via* column chromatography (ethyl acetate/petroleum ether = 1:4) afforded the title compound (1.6 mg, 29%).

^1H NMR (500 MHz, CDCl_3) δ 6.60 (dd, J = 1.7, 5.9 Hz, 1H), 5.57 (d, J = 5.9 Hz, 1H), 5.03 (d, J = 5.2 Hz, 1H), 4.97 (s br, 1H), 4.25 – 4.11 (m, 2H), 2.50 (dd, J = 5.9, 13.0 Hz, 1H), 1.78 – 1.72 (m, 1H), 1.70 – 1.60 (m 2H), 1.56 (s, 3H), 1.28 (t, J = 7.1 Hz, 3H), 1.19 – 1.08 (m, 1H), 0.77 (s, 9H), 0.04 (d, J = 1.5 Hz, 6H)

^{13}C NMR (500 MHz, CDCl_3) δ 165.7, 156.4, 141.2, 131.2, 128.8, 86.7, 77.9, 70.8, 60.0, 49.5, 35.7, 25.7, 23.4, 22.6, 18.0, 14.3, -3.9, -5.3



Ethyl 5-bromo-1-((tert-butyldimethylsilyl)oxy)-1,2,3,3a,4,7-hexahydro-4,7-epoxyazulene-8-carboxylate

Compound **4.15** was prepared *via* general method 6.3.1 with diazo compound **3.36** (28 mg, mmol) and 3-bromofuran (40 μ l, 0.27 mmol). Purification *via* column chromatography (ethyl acetate/petroleum ether = 1:4) afforded the title compound (1.3 mg, 34%).

^1H NMR (500 MHz, CDCl_3) δ 6.72 (d, J = 1.9 Hz, 1H), 5.07 (d, J = 4.7 Hz, 1H), 5.04 (d, J = 5.8 Hz, 1H), 4.91 (d, J = 1.9 Hz, 1H), 4.25 – 4.11 (m, 2H), 2.92 – 2.85 (m, 1H), 1.82 – 1.73 (m, 2H), 1.62 – 1.50 (m, 2H), 1.29 (t, J = 7.3 Hz, 3H), 0.97 (s, 9H), 0.05 (d, J = 3.2 Hz, 6H)

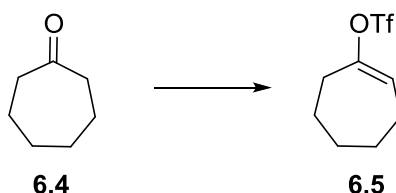
¹³C NMR (400 MHz, CDCl₃) δ 165.0, 155.3, 140.0, 129.6, 115.4, 84.3, 78.0, 70.5, 60.2, 43.1, 35.0, 25.6, 23.7, 17.9, 14.23, -3.8, -5.3

6.4 Experimental Procedures for 1,2,3-sulfonyl triazoles

6.4.1 General procedure for triflation chemistry

Method A: To a solution of diisopropylamine (1.2 eq.) in anhydrous tetrahydrofuran (40 mL) was added drop wise *n*-butyl lithium (1.2 eq., 2M in hexanes) at 0 °C under argon atmosphere. After 30 minutes the reaction mixture was cooled to -78 °C and a solution of ketone in THF (1 eq.) was added dropwise and the resulting mixture was stirred for 2 hours. PhNTf₂ in THF (1 eq.) was then added dropwise and the mixture allowed to warm to room temperature overnight. The resulting reaction mixture was quenched with saturated NH₄Cl (20 mL) and extracted with Et₂O (3 x 80 ml). The combined organic layers were dried over Na₂SO₄ and the filtrate concentrated in vacuo. The residue was passed through a silica plug (100% hexanes to 20% ethyl acetate) to afford the corresponding triflate as a colourless oil.

Method B: LiHMDS (1M; 1.2 eq.) was cooled to -78 °C and a solution of ketone in anhydrous THF (1 eq.) was added dropwise under an argon atmosphere. The resulting mixture was stirred for 1 hour followed by the drop wise addition of PhNTf₂ (1 eq. in THF). The mixture was stirred at -78 °C for another 2 hours and then left to warm to room temperature overnight. The reaction was quenched with saturated NH₄Cl and extracted with pentanes (5 x 70 mL) and 1N HCl (70 mL). The organic layer was dried over Na₂SO₄ and the solvent removed under reduced pressure. The residual oil was purified *via* column chromatography using pure pentanes as the eluent to afford the titled compound as a colourless oil.

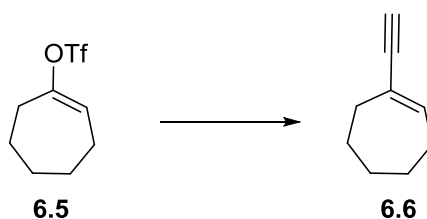


Cyclohept-1-en-1-yl-trifluoromethanesulfonate

Compound **6.5** was prepared *via* method B with cycloheptanone (3 g, 26.8 mmol). Column chromatography was performed with pure petroleum ether to afford the titled compound as a colourless oil (6.1 g, 93%). The spectral data for **6.5** match those reported in literature.¹³⁴

¹H NMR (300 MHz, CDCl₃) δ 5.88 (t, J = 6.6 Hz, 1H), 2.53 – 2.50 (m, 2H), 2.18 – 2.14 (m, 2H), 1.75 – 1.63 (m, 6H)

¹³C NMR (400 MHz, CDCl₃) δ 153.1, 123.1, 119.8, 117.3, 33.2, 29.9, 26.3, 24.8, 24.7



1-Ethynylcyclohept-1-ene

A solution of ethynylmagnesium bromide (0.5M in THF; 160 mL, 80.3 mmol) was warmed to 40 °C and Co(acac)₃ (0.48 g, 1.34 mmol) was added in one portion followed by the addition of triflate (6.53 g, 26.8 mmol). The resulting mixture was stirred for 3 hours until complete conversion to product was observed. Saturated NH₄Cl was added carefully and the mixture extracted thoroughly with pentanes (5 x 70 mL). The combined organic extracts were washed with brine, dried over MgSO₄ and the solvent removed *in vacuo*. The oily residue was purified *via* flash chromatography using petroleum ether as eluent to afford the titled compound as a yellow oil (2.8 g, 88%). The spectral data for **6.6** match those reported in literature.¹³⁴

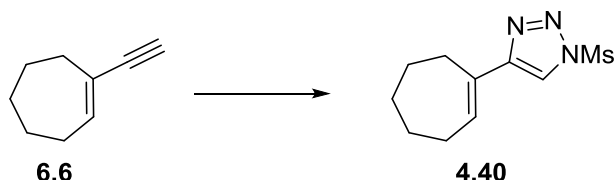
¹H NMR (300 MHz, CDCl₃) δ 6.39 (t, J = 6.8 Hz, 1H), 2.84 (s, 1H), 2.34 (m 1H),

¹³C NMR (400 MHz, CDCl₃) δ 141.6, 125.8, 87.3, 74.2, 33.9, 32.0, 29.1, 26.5, 26.3

6.4.2 General procedure for the CuTC catalysed cycloaddition.

Acetylene (1 mmol, 1eq.) was added to a solution of CuTC (0.1 eq.) in anhydrous toluene and the resulting solution stirred at ambient temperature for 10 minutes. A mesyl azide solution in toluene (1 eq. in 10 mL) was then added drop wise and the resulting mixture stirred at rt overnight. The

solvent was evaporated and the residue purified *via* column chromatography using ethyl acetate / petroleum ether= 1:4 as the solvent system. The orange oil solidified upon standing and was recrystallised at -20 °C from ethyl acetate/petroleum ether to afford the title compound as a white solid.

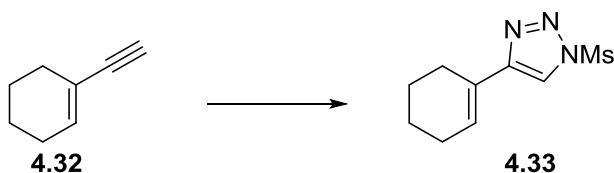


4-(Cyclohept-1-en-1-yl)-1-(methylsulfonyl)-1H-1,2,3-triazole

Compound **4.40** was prepared *via* general method 6.4.2 with acetylene **6.6** (1.3 g, 10.6 mmol). Purification *via* column chromatography (ethyl acetate/petroleum ether = 1:4) and recrystallization from ethyl acetate/petroleum ether afforded the titled compound as a white solid (1.4 g, 54%). Spectral data for compound **4.40** are in accordance with literature.¹²⁶

¹H NMR (500 MHz, CDCl₃) δ 7.91 (s, 1H), 6.82 (t, J = 6.7 Hz, 1H), 3.49 (s, 3H), 2.64 – 2.58 (m, 2H), 2.38 – 2.29 (m, 2H), 1.88 – 1.78 (m, 2H), 1.70 – 1.55 (m, 4H)

¹³C NMR (500 MHz, CDCl₃) δ 150.2, 133.1, 132.2, 117.6, 42.6, 32.0, 30.9, 28.5, 26.5, 26.4, 14.2



4-(Cyclohex-1-en-1-yl)-1-(methylsulfonyl)-1H-1,2,3-triazole

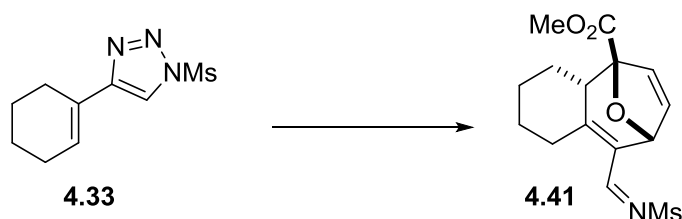
Compound **4.33** was prepared *via* general method 6.4.2. Recrystallization from ethyl acetate/petroleum ether afforded **4.33** in 82% yield. Spectral data for compound **4.33** are in accordance with literature.¹²⁶

¹H NMR (500 MHz, CDCl₃) δ 7.89 (s, 1H), 6.72 (m, 1H), 3.49 (s, 3H), 2.36 – 2.24 (m, 2H), 2.23 – 2.22 (m, 2H), 1.80 – 1.77 (m, 2H), 1.70 – 1.68 (m, 2H)

¹³C NMR (500 MHz, CDCl₃) δ 149.0, 128.1, 125.6, 117.3, 42.6, 26.2, 25.3, 22.2, 22.0

6.4.3 General procedure for rhodium catalysed [4+3] cycloaddition reactions of 1,2,3-sulfonyl triazoles with furans

Furan (3 eq.) was added in one portion to a suspension of triazole in cyclohexane (0.3M solution). Rh(II) catalyst (0.01 eq.) was then added to the mixture and the sample immersed in a 70°C oil bath until starting material appeared to be consumed by TLC analysis. The reaction mixture was concentrated and purified *via* flash column chromatography (ethyl acetate/petroleum spirit = 1:2) to afford the titled compound.



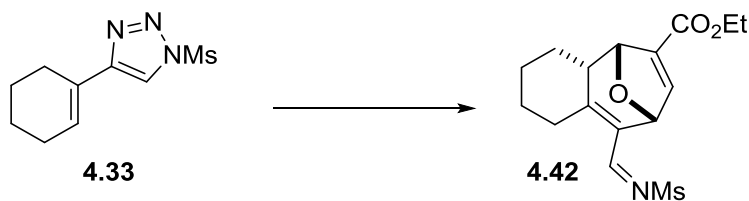
Methyl (*E*)-9-[[[(methylsulfonyl)imino]methyl]-1,2,3,4,4a,8a-hexahydro-5*H*-5,8-epoxybenzo[7]annulene-5-carboxylate

Compound **4.41** was prepared *via* general method 6.4.3 with triazole **4.33** (34.7 mg, 0.153 mmol) and 2-methylfuroate (49 μ l, 0.46 mmol). Purification *via* column chromatography (ethyl acetate/petroleum ether = 1:4) afforded the title compound as pale yellow crystals (32.3 mg, 65% yield).

¹H NMR (500 MHz, CDCl₃) δ 9.02 (s, 1H), 6.64 (dd, J = 2.0, 5.9 Hz, 1H), 6.13 (d, J = 5.9 Hz, 1H), 5.54 (br s, 1H), 3.86 (s, 3H), 3.17 (m, 1H), 3.07 (s, 3H), 2.75 (dd, J = 4.6, 12.9 Hz, 1H), 2.11 – 1.83 (m, 4H), 1.51 – 1.43 (m, 1H), 1.35 – 1.19 (m, 4H)

¹³C NMR (400 MHz, CDCl₃) δ 169.7, 163.6, 139.0, 131.7, 128.2, 88.5, 76.6, 52.8, 43.6, 40.4, 29.8, 27.6, 26.8, 24.9

HRMS (EI) Calculated for C₁₅H₁₉O₅NSNa: 348.0876; Found: 348.0882

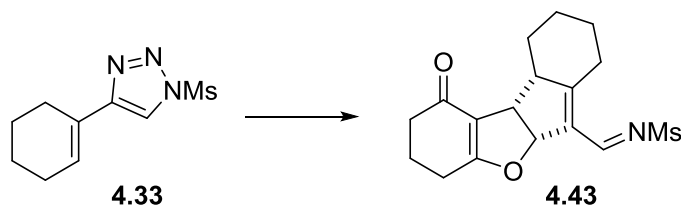


Ethyl (*E*)-9-[[[(methanesulfonyl)imino]methyl]-2,3,4,4a,5,8-hexahydro-1*H*-5,8-epoxybenzo[7]annulene-6-carboxylate

Compound **4.42** was prepared *via* general method 6.4.3 with triazole **4.33** (60 mg, 0.22 mmol) and 3-ethylfuroate (89 μ l, 0.66 mmol). Purification *via* column chromatography (ethyl acetate/petroleum ether = 1:2) afforded the title compound as colourless oil (57 mg, 76% yield).

¹H NMR (500 MHz, CDCl₃) δ 8.98 (br s, 1H), 7.42 (m, 1H), 5.48 (br s, 1H), 5.03 (m, 1H), 4.21 – 4.17 (m, 2H), 3.14 (d, J = 14.0 Hz, 1H), 3.05 (s, 3H), 2.79 – 2.74 (m, 1H), 2.02 – 1.92 (m, 3H), 1.82 – 1.79 (m, 1H), 1.50 – 1.30 (m, 2H), 1.29 – 1.25 (m, 3H), 0.98 – 0.86 (m, 1H)

¹³C NMR (500 MHz, CDCl₃) δ 165.0, 163.5, 163.2, 148.3, 135.6, 130.6, 79.9, 76.4, 60.7, 41.0, 40.3, 29.5, 28.2, 27.7, 25.0, 14.1



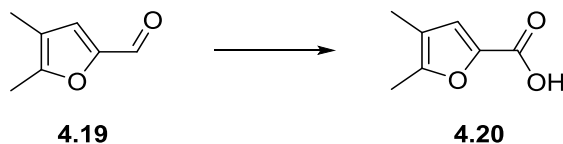
(*E*)-*N*-[(1-oxo-2,3,4,5a,7,8,9,10,10a,10b-decahydro-1*H*-indeno[2,1-*b*]benzofuran-6-yl)methylene]methanesulfonamide

Compound **4.43** was prepared *via* general method 6.4.3 with triazole **4.33** (136 mg, 0.6 mmol) and dihydrobenzofuranone (245 mg, 1.8 mmol). Purification *via* column chromatography (ethyl acetate/hexanes = 5:1) afforded the title compound as a yellow oil (148 mg, 72% yield).

¹H NMR (400 MHz, CDCl₃) δ 8.98 (s, 1H), 6.06 (d, J = 9.6 Hz, 1H), 3.36 (d, J = 8.7 Hz, 1H), 3.12 (s, 3H), 3.07 (d, J = 12.7 Hz, 1H), 2.77 – 2.68 (m, 1H), 2.58 – 2.49 (m, 1H), 2.46 – 2.28 (m, 4H), 2.24 – 2.14 (m, 1H), 2.02 – 1.96 (m, 2H), 1.83 (d, J = 12.7 Hz, 1H), 1.57 – 1.43 (m, 1H), 1.38 – 1.12 (m, 3H)

¹³C NMR (400 MHz, CDCl₃) δ 195.3, 179.2, 176.5, 163.6, 127.7, 116.6, 91.9, 56.6, 46.9, 40.3, 36.5, 28.1, 27.8, 25.3, 24.0, 21.6

HRMS (EI) Calculated for C₁₇H₂₂O₄NS: 336.1259; Found: 336.1275

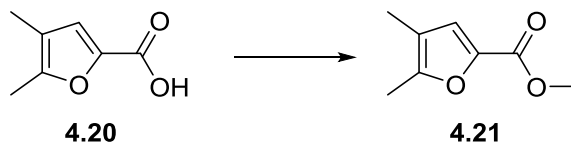


4,5 –Dimethylfuran-2-carboxylic acid

Silver oxide was prepared by adding a NaOH (471 mg, 11.8 mmol) in water (2 mL) to an aqueous solution of silver nitrate (1 g, 5.89 mmol) at 0°C and the resulting mixture was stirred for 10 minutes. Compound **4.19** (0.36 mL, 2.94 mmol) was then added drop wise to the solution and stirred for further 30 minutes. The resulting precipitate was filtered and washed thoroughly with portions of water. The filtrate was acidified with conc. HCl, the resulting precipitate filtered off and washed with water (10 mL) to afford the titled compound as a yellow solid (295 mg, 36%). Spectral data for compound 4.20 are in accordance to literature.¹³⁵

¹H NMR (300 MHz, CDCl₃) δ 7.11 (s, 1H), 2.31 (s, 3H), 2.00 (s, 3H), 1.26 (s, 1H)

¹³C NMR (500 MHz, CDCl₃) δ 163.1, 154.5, 140.6, 123.5, 117.6, 12.0, 9.7

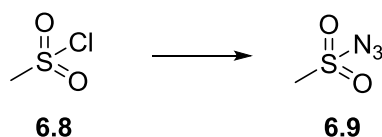


Methyl 4,5-dimethylfuran-2-carboxylate

To a solution of carboxylic acid (20 mg, 0.14 mmol) in diethyl ether (10 mL) was added drop wise a solution of freshly prepared diazomethane in Et₂O. Upon completion - progress was monitored *via* TLC - the reaction mixture was stirred for further 20 minutes open to air followed by evaporation of the solvent to yield the titled compound as an orange oil (20 mg, 91%).

¹H NMR (300 MHz, CDCl₃) δ 6.97 (s, 1H), 3.86 (s, 3H), 2.28 (s, 3H), 1.97 (s, 3H)

¹³C NMR (500 MHz, CDCl₃) δ 159.3, 153.0, 141.5, 121.4, 117.1, 51.7, 11.8, 9.7

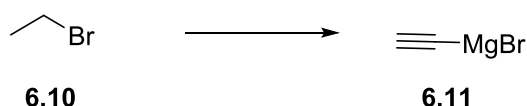


Mesyl azide

Methanesulfonyl chloride (1.4 mL, 17.5 mmol) was dissolved in acetone (15 mL) and NaN_3 (1.7 g, 26.2 mmol) was added portion wise over 30 minutes. The resultant mixture was stirred at ambient temperature for 1 hour. The precipitate was filtered and washed with further portions of acetone; the filtrate was evaporated to give the titled compound as a colourless oil (2 g, 97%).

$^1\text{H NMR}$ (300 MHz, CDCl_3) δ 3.26 (s, 3H)

$^{13}\text{C NMR}$ (500 MHz, CDCl_3) δ 42.8



Ethynylmagnesium bromide solution

According to a procedure of Roy *et al.*¹³⁶ ethyl bromide (16.4 g, 150.1 mmol) was added portion wise to a solution of magnesium (4 g, 165.1 mmol) in THF (150 mL) and an internal temperature of 45 °C was maintained. The resultant mixture was stirred at ambient temperature for further 30 minutes. Acetylene gas was purified by passing the gas through two cold traps (cooled with dry ice/acetone) before bubbling it through the previously prepared ethylmagnesium bromide solution at such a rate to maintain the internal temperature at a maximum of 40 °C. After the exothermic reaction has subsided, the ethynylmagnesium bromide solution was used as such without further purification.

7 References

- (1) Newman, D. J.; Cragg, G. M. *J. Nat. Prod.* **2007**, *70*, 461.
- (2) Henkel, T.; Brunne, R. M.; Müller, H.; Reichel, F. *Angew. Chem. Int. Ed.* **1999**, *38*, 643.
- (3) Newman, D. J. *J. Med. Chem.* **2008**, *51*, 2589.
- (4) Bohm, R.; Flaschentrager, B.; Lendle, L. *Arch. Exp. Pathol. Pharmacol.* **1935**, *177*, 212.
- (5) Berenblum, I.; Lonai, V. *Cancer Res.* **1970**, *30*, 2744.
- (6) Hecker, E. *Cancer Res.* **1968**, *28*, 2338.
- (7) Berenblum, I. *Cancer Res.* **1941**, *1*, 44.
- (8) (a) Ma, D. *Curr. Med. Chem.* **2001**, *8*, 191(b) Goel, G.; Makkar, H. P. S.; Francis, G.; Becker, K. *Int. J. Toxicol.* **2007**, *26*, 279.
- (9) (a) Kupchan, S. M.; Sigel, C. W.; Matz, M. J.; Saenz, R. J. A.; Haltiwanger, R. C.; Bryan, R. F. *J. Am. Chem. Soc.* **1970**, *92*, 4476(b) Handa, S. S.; Kinghorn, A. D.; Cordell, G. A.; Farnsworth, N. R. *J. Nat. Prod.* **1983**, *46*, 123.
- (10) El-Mekkawy, S.; Meselhy, M. R.; Nakamura, N.; Hattori, M.; Kawahata, T.; Otake, T. *Phytochemistry* **2000**, *53*, 457.
- (11) Gonzalez-Guerrico, A. M.; Kazanietz, M. G. *J. Biol. Chem.* **2005**, *280*, 38982.
- (12) Castagna, M.; Takai, Y.; Kaibuchi, K.; Sano, K.; Kikkawa, U.; Nishizuka, Y. *J. Biol. Chem.* **1982**, *257*, 7847.
- (13) (a) Kawahara, Y.; Takai, Y.; Minakuchi, R.; Sano, K.; Nishizuka, Y. *Biochem. Biophys. Res. Commun.* **1980**, *97*, 309(b) Takai, Y.; Kaibuchi, K.; Matsubara, T.; Nishizuka, Y. *Biochem. Biophys. Res. Commun.* **1981**, *101*, 61(c) Nishizuka, Y. *Science (Washington, D. C., 1883-)* **1986**, *233*, 305.
- (14) Nishizuka, Y. *Nature (London)* **1984**, *308*, 693.
- (15) Wender, P. A.; Koehler, K. F.; Sharkey, N. A.; Dell'Aquila, M. L.; Blumberg, P. M. *Proc. Natl. Acad. Sci. U. S. A.* **1986**, *83*, 4214.
- (16) (a) Keck, G. E.; Poudel, Y. B.; Cummins, T. J.; Rudra, A.; Covell, J. A. *J. Am. Chem. Soc.* **2011**, *133*, 744(b) Evans, D. A.; Carter, P. H.; Carreira, E. M.; Charette, A. B.; Prunet, J. A.; Lautens, M. *J. Am. Chem. Soc.* **1999**, *121*, 7540(c) Kageyama, M.; Tamura, T.; Nantz, M. H.; Roberts, J. C.; Somfai, P.; Whritenour, D. C.; Masamune, S. *J. Am. Chem. Soc.* **1990**, *112*, 7407(d) Wender, P. A.; Schrier, A. J. *J. Am. Chem. Soc.* **2011**, *133*, 9228(e) Ohmori, K.; Ogawa, Y.; Obitsu, T.; Ishikawa, Y.; Nishiyama, S.; Yamamura, S. *Angew. Chem., Int. Ed.* **2000**, *39*, 2290(f) Trost, B. M.; Dong, G. *Nature (London, U. K.)* **2008**, *456*, 485.
- (17) (a) Fujiki, H.; Mori, M.; Nakayasu, M.; Terada, M.; Sugimura, T. *Biochem. Biophys. Res. Commun.* **1979**, *90*, 976(b) Fujiki, H.; Mori, M.; Nakayasu, M.; Terada, M.; Sugimura, T.; Moore, R. E. *Proc. Natl. Acad. Sci. U. S. A.* **1981**, *78*, 3872(c) Fujiki, H.; Sugimura, T. *Adv. Cancer Res.* **1987**, *49*, 223.
- (18) (a) Hanks, S. K.; Hunter, T. *FASEB J.* **1995**, *9*, 576(b) Kikkawa, U.; Takai, Y.; Tanaka, Y.; Miyake, R.; Nishizuka, Y. *J. Biol. Chem.* **1983**, *258*, 11442.
- (19) Manning, G.
- (20) Inoue, M.; Kishimoto, A.; Takai, Y.; Nishizuka, Y. *J. Biol. Chem.* **1977**, *252*, 7610.
- (21) McQueen, C. A.; Bond, J.; Ramos, K.; Lamb, J.; Guengerich, F. P.; Lawrence, D.; Walker, M.; Campen, M.; Schnellmann, R.; Yost, G. S.; Roth, R. A.; Ganey, P.; Hooser, S.; Richburg, J.; Hoyer, P.; Knudsen, T.; Daston, G.; Philbert, M.; Roberts, R.; Elsevier.
- (22) (a) Krebs, E. G. In *The Enzymes*; Paul, D. B., Edwin, G. K., Eds.; Academic Press, 1986; Vol. Volume 17(b) *Control by Phosphorylation, Part A: General Features - Specific Enzymes I*.
- (23) Newton, A. C. *J. Biol. Chem.* **1995**, *270*, 28495.

- (24) Newton, A. C. *Biochem. J.* **2003**, 370, 361.
- (25) Griner, E. M.; Kazanietz, M. G. *Nat. Rev. Cancer* **2007**, 7, 281.
- (26) Mochly-Rosen, D.; Das, K.; Grimes, K. V. *Nat. Rev. Drug Discov.* **2012**, 11, 937.
- (27) (a) Buchdunger, E.; Zimmermann, J.; Mett, H.; Meyer, T.; Mueller, M.; Druker, B. J.; Lydon, N. B. *Cancer Res.* **1996**, 56, 100(b) Druker, B. J.; Tamura, S.; Buchdunger, E.; Ohno, S.; Segal, G. M.; Fanning, S.; Zimmermann, J.; Lydon, N. B. *Nat. Med. (N. Y.)* **1996**, 2, 561(c) Capdeville, R.; Buchdunger, E.; Zimmermann, J.; Matter, A. *Nat. Rev. Drug Discov.* **2002**, 1, 493.
- (28) Kerkela, R.; Grazette, L.; Yacobi, R.; Iliescu, C.; Patten, R.; Beahm, C.; Walters, B.; Shevtsov, S.; Pesant, S.; Clubb, F. J.; Rosenzweig, A.; Salomon, R. N.; Van, E. R. A.; Alroy, J.; Durand, J.-B.; Force, T. *Nat. Med. (N. Y., NY, U. S.)* **2006**, 12, 908.
- (29) Rizk, D. A.-F. *CRC Press* **1990**.
- (30) Blumberg, P. M. *Crit. Rev. Toxicol.* **1981**, 8, 199.
- (31) Shao, L.; Lewin, N. E.; Lorenzo, P. S.; Hu, Z.; Enyedy, I. J.; Garfield, S. H.; Stone, J. C.; Marner, F.-J.; Blumberg, P. M.; Wang, S. *J. Med. Chem.* **2001**, 44, 3872.
- (32) (a) Bocklandt, S.; Blumberg, P. M.; Hamer, D. H. *Antiviral Res.* **2003**, 59, 89(b) Biancotto, A.; Grivel, J.-C.; Gondois-Rey, F.; Bettendroffer, L.; Vigne, R.; Brown, S.; Margolis, L. B.; Hirsch, I. J. *J. Virol.* **2004**, 78, 10507(c) Wender, P. A.; Kee, J.-M.; Warrington, J. M. *Science (Washington, DC, U. S.)* **2008**, 320, 649.
- (33) Schmidt, R. J. *Bot. J. Linn. Soc.* **1987**, 94, 221.
- (34) Robinson, D. R.; West, C. A. *Biochemistry* **1970**, 9, 70.
- (35) Hoppe, W.; Brandl, F.; Strell, I.; Roehrl, M.; Gassmann, I.; Hecker, E.; Bartsch, H.; Kreibich, G.; Von, S. C. *Angew. Chem., Int. Ed. Engl.* **1967**, 6, 809.
- (36) Wender, P. A.; Kogen, H.; Lee, H. Y.; Munger, J. D., Jr.; Wilhelm, R. S.; Williams, P. D. *J. Am. Chem. Soc.* **1989**, 111, 8957.
- (37) Wender, P. A.; Rice, K. D.; Schnute, M. E. *J. Am. Chem. Soc.* **1997**, 119, 7897.
- (38) Lee, K.; Cha, J. K. *J. Am. Chem. Soc.* **2001**, 123, 5590.
- (39) Wender, P. A.; Keenan, R. M.; Lee, H. Y. *J. Am. Chem. Soc.* **1987**, 109, 4390.
- (40) Seyferth, D. *Acc. Chem. Res.* **1972**, 5, 65.
- (41) Wender, P. A.; McDonald, F. E. *J. Am. Chem. Soc.* **1990**, 112, 4956.
- (42) (a) Shigeno, K.; Ohne, K.; Yamaguchi, T.; Sasai, H.; Shibasaki, M. *Heterocycles* **1992**, 33, 161(b) Shigeno, K.; Sasai, H.; Shibasaki, M. *Tetrahedron Lett.* **1992**, 33, 4937.
- (43) Sugita, K.; Neville, C. F.; Sodeoka, M.; Sasai, H.; Shibasaki, M. *Tetrahedron Lett.* **1995**, 36, 1067.
- (44) Sodeoka, M.; Uotsu, K.; Shibasaki, M. *Tetrahedron Lett.* **1995**, 36, 8795.
- (45) Uotsu, K.; Sodeoka, M.; Shibasaki, M. *Bioorg. Med. Chem.* **1998**, 6, 1117.
- (46) Wada, R.; Suto, Y.; Kanai, M.; Shibasaki, M. *J. Am. Chem. Soc.* **2002**, 124, 10658.
- (47) Dauben, W. G.; Dinges, J.; Smith, T. C. *J. Org. Chem.* **1993**, 58, 7635.
- (48) Catino, A. J.; Sherlock, A.; Shieh, P.; Wzorek, J. S.; Evans, D. A. *Org. Lett.* **2013**, 15, 3330.
- (49) (a) Hergenbahn, M.; Adolf, W.; Hecker, E. *Tetrahedron Lett.* **1975**, 1595(b) Schmidt, R. J.; Evans, F. J. *Phytochemistry* **1976**, 15, 1778.
- (50) (a) Szallasi, A.; Blumberg, P. M. *Life Sci.* **1990**, 47, 1399(b) Szallasi, A.; Blumberg, P. M. *Neuroscience (Oxford)* **1989**, 30, 515.
- (51) Wender, P. A.; Jesudason, C. D.; Nakahira, H.; Tamura, N.; Tebbe, A. L.; Ueno, Y. *J. Am. Chem. Soc.* **1997**, 119, 12976.
- (52) Murai, K.; Katoh, S.-i.; Urabe, D.; Inoue, M. *Chem. Sci.* **2013**, 4, 2364.
- (53) Winkler, J. D.; Rouse, M. B.; Greaney, M. F.; Harrison, S. J.; Jeon, Y. T. *J. Am. Chem. Soc.* **2002**, 124, 9726.
- (54) Tanino, K.; Onuki, K.; Asano, K.; Miyashita, M.; Nakamura, T.; Takahashi, Y.; Kuwajima, I. *J. Am. Chem. Soc.* **2003**, 125, 1498.

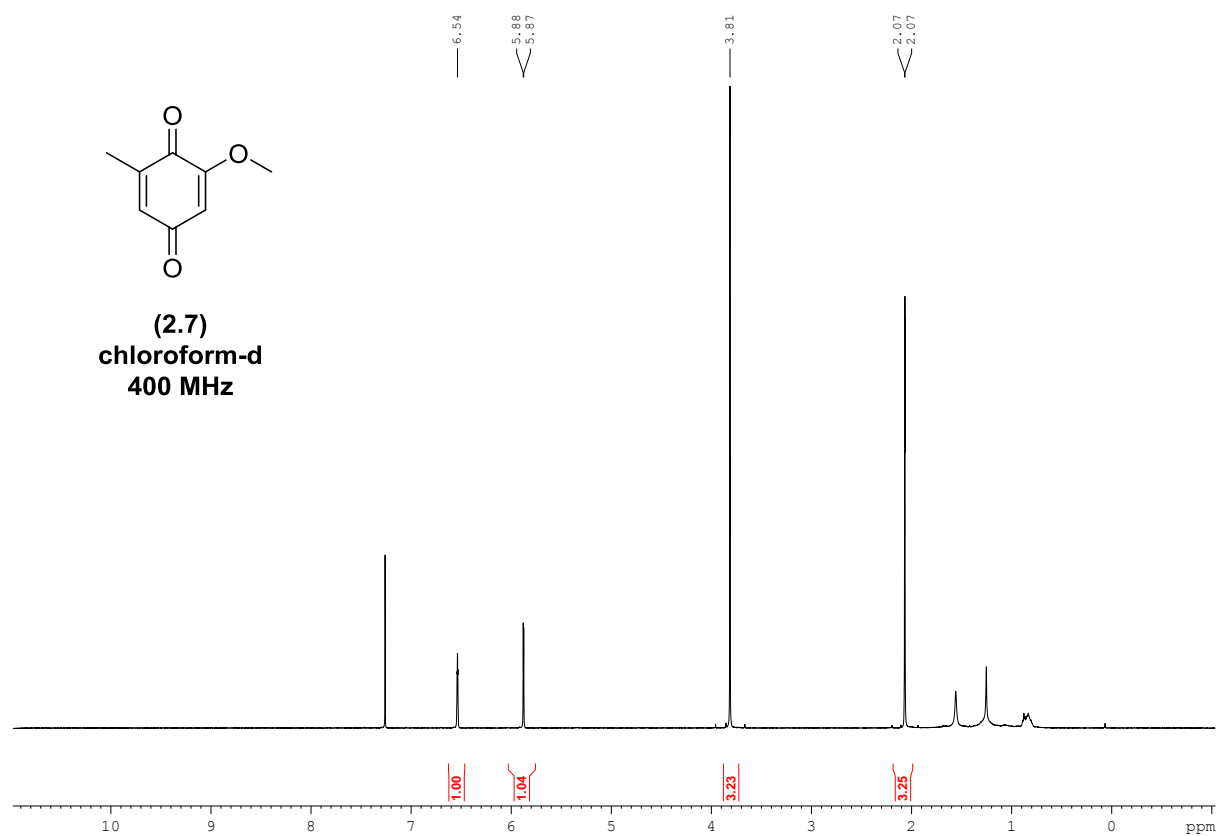
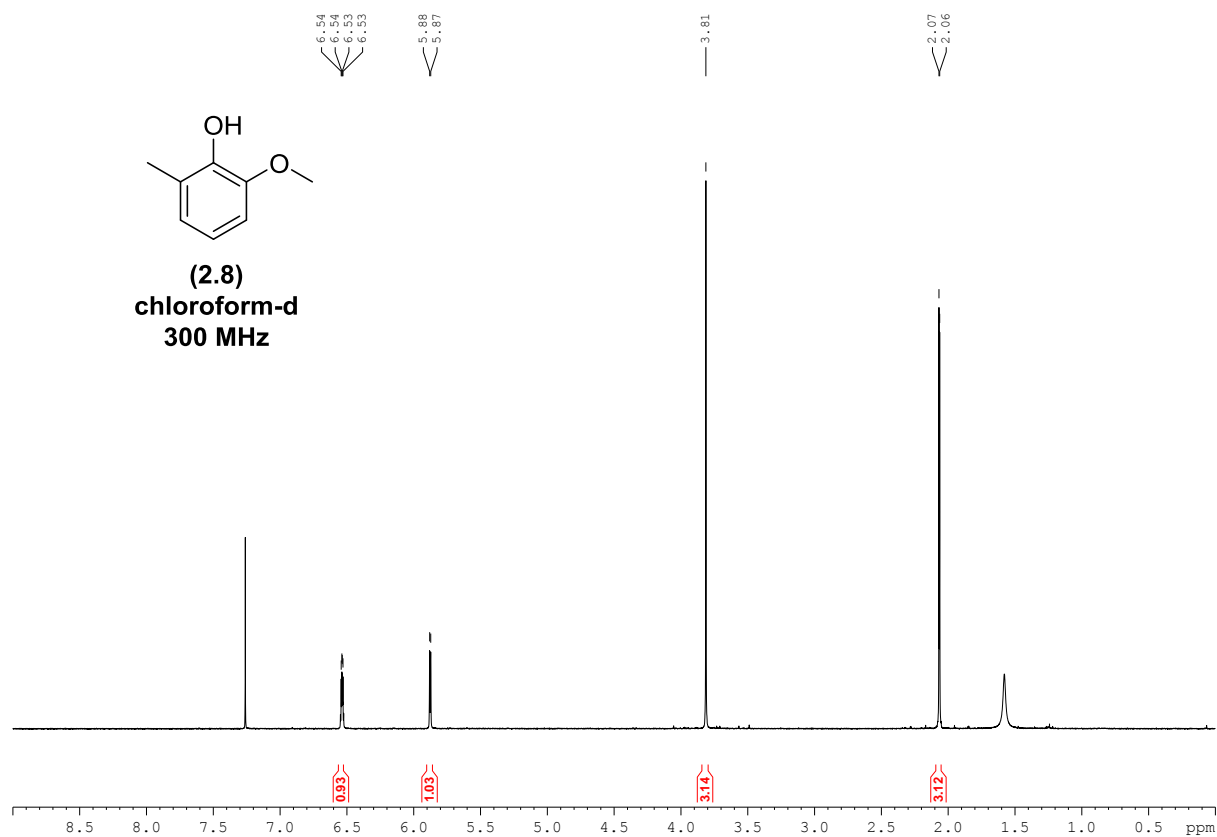
- (55) Nickel, A.; Maruyama, T.; Tang, H.; Murphy, P. D.; Greene, B.; Yusuff, N.; Wood, J. L. *J. Am. Chem. Soc.* **2004**, *126*, 16300.
- (56) Jorgensen, L.; McKerrall, S. J.; Kuttruff, C. A.; Ungeheuer, F.; Felding, J.; Baran, P. S. *Science (Washington, DC, U. S.)* **2013**, *341*, 878.
- (57) (a) Gallen, M. J.; Williams, C. M. *Org. Lett.* **2008**, *10*, 713(b) Chen, A. P. J.; Williams, C. M. *Org. Lett.* **2008**, *10*, 3441(c) Chen, A. P. J.; Muller, C. C.; Cooper, H. M.; Williams, C. M. *Org. Lett.* **2009**, *11*, 3758(d) Schwartz, B. D.; Denton, J. R.; Lian, Y.; Davies, H. M. L.; Williams, C. M. *J. Am. Chem. Soc.* **2009**, *131*, 8329(e) Mak, J. Y. W.; Williams, C. M. *Chem. Commun. (Cambridge, U. K.)* **2012**, 48, 287(f) Mak, J. Y. W.; Williams, C. M. *Eur. J. Org. Chem.* **2012**, 2012, 2001.
- (58) Brogan, J. B.; Zercher, C. K. *J. Org. Chem.* **1997**, *62*, 6444.
- (59) Heim, R.; Wiedemann, S.; Williams, C. M.; Bernhardt, P. V. *Org. Lett.* **2005**, *7*, 1327.
- (60) Mander, L. N.; Sethi, S. P. *Tetrahedron Lett.* **1983**, *24*, 5425.
- (61) Schwartz, B. D.; Williams, C. M.; Bernhardt, P. V. *Beilstein J. Org. Chem.* **2008**, *4*, No. 34.
- (62) Davies, H. M. L.; Loe, O.; Stafford, D. G. *Org. Lett.* **2005**, *7*, 5561.
- (63) (a) Davies, H. M. L. *Tetrahedron* **1993**, *49*, 5203(b) Davies, H. M. L.; Stafford, D. G.; Doan, B. D.; Houser, J. H. *J. Am. Chem. Soc.* **1998**, *120*, 3326.
- (64) Keck, G. E.; Savin, K. A.; Weglarz, M. A. *J. Org. Chem.* **1995**, *60*, 3194.
- (65) Wang, X.; Reisinger, C. M.; List, B. *J. Am. Chem. Soc.* **2008**, *130*, 6070.
- (66) Lautens, M.; Chiu, P.; Ma, S.; Rovis, T. *J. Am. Chem. Soc.* **1995**, *117*, 532.
- (67) Gallen, M. J.; Goumont, R.; Clark, T.; Terrier, F.; Williams, C. M. *Angew. Chem., Int. Ed.* **2006**, *45*, 2929.
- (68) Yoshida, M.; Al-Amin, M.; Shishido, K. *Synthesis* **2009**, 2454.
- (69) Chinchilla, R.; Najera, C. *Chem. Rev. (Washington, DC, U. S.)* **2007**, *107*, 874.
- (70) Stevens, R. V.; Angle, S. R.; Kloc, K.; Mak, K. F.; Liu, Y. X.; Trueblood, K. N. *J. Org. Chem.* **1986**, *51*, 4347.
- (71) Liu, D.; Canales, E.; Corey, E. J. *J. Am. Chem. Soc.* **2007**, *129*, 1498.
- (72) (a) Evans, D. A.; Chapman, K. T.; Bisaha, J. *J. Am. Chem. Soc.* **1984**, *106*, 4261(b) Evans, D. A.; Chapman, K. T.; Bisaha, J. *J. Am. Chem. Soc.* **1988**, *110*, 1238(c) Kagan, H. B.; Riant, O. *Chem. Rev.* **1992**, *92*, 1007.
- (73) Corey, E. J.; Bakshi, R. K.; Shibata, S. *J. Am. Chem. Soc.* **1987**, *109*, 5551.
- (74) Ryu, D. H.; Corey, E. J. *J. Am. Chem. Soc.* **2003**, *125*, 6388.
- (75) Weatherhead-Kloster, R. A.; Corey, E. J. *Org. Lett.* **2006**, *8*, 171.
- (76) Corey, E. J.; Shibata, T.; Lee, T. W. *J. Am. Chem. Soc.* **2002**, *124*, 3808.
- (77) (a) Mathre, D. J.; Jones, T. K.; Xavier, L. C.; Blacklock, T. J.; Reamer, R. A.; Mohan, J. J.; Jones, E. T. T.; Hoogsteen, K.; Baum, M. W.; Grabowski, E. J. J. *J. Org. Chem.* **1991**, *56*, 751(b) Jones, T. K.; Mohan, J. J.; Xavier, L. C.; Blacklock, T. J.; Mathre, D. J.; Sohar, P.; Jones, E. T. T.; Reamer, R. A.; Roberts, F. E.; Grabowski, E. J. J. *J. Org. Chem.* **1991**, *56*, 763.
- (78) Paddon-Row, M. N.; Kwan, L. C. H.; Willis, A. C.; Sherburn, M. S. *Angew. Chem., Int. Ed.* **2008**, *47*, 7013.
- (79) Chen, D. Y. K.; Pouwer, R. H.; Richard, J.-A. *Chem. Soc. Rev.* **2012**, *41*, 4631.
- (80) Lebel, H.; Marcoux, J.-F.; Molinaro, C.; Charette, A. B. *Chem. Rev. (Washington, DC, U. S.)* **2003**, *103*, 977.
- (81) Corey, E. J.; Jautelat, M. *J. Am. Chem. Soc.* **1967**, *89*, 3912.
- (82) Matsuyama, H.; Nakamura, T.; Iyoda, M. *J. Org. Chem.* **2000**, *65*, 4796.
- (83) Corey, E. J.; Chaykovsky, M. *J. Am. Chem. Soc.* **1965**, *87*, 1353.
- (84) (a) Edwards, M. G.; Paxton, R. J.; Pugh, D. S.; Whitwood, A. C.; Taylor, R. J. K. *Synthesis* **2008**, 3279(b) Edwards, M. G.; Paxton, R. J.; Pugh, D. S.; Taylor, R. J. K. *Synlett* **2008**, 521.

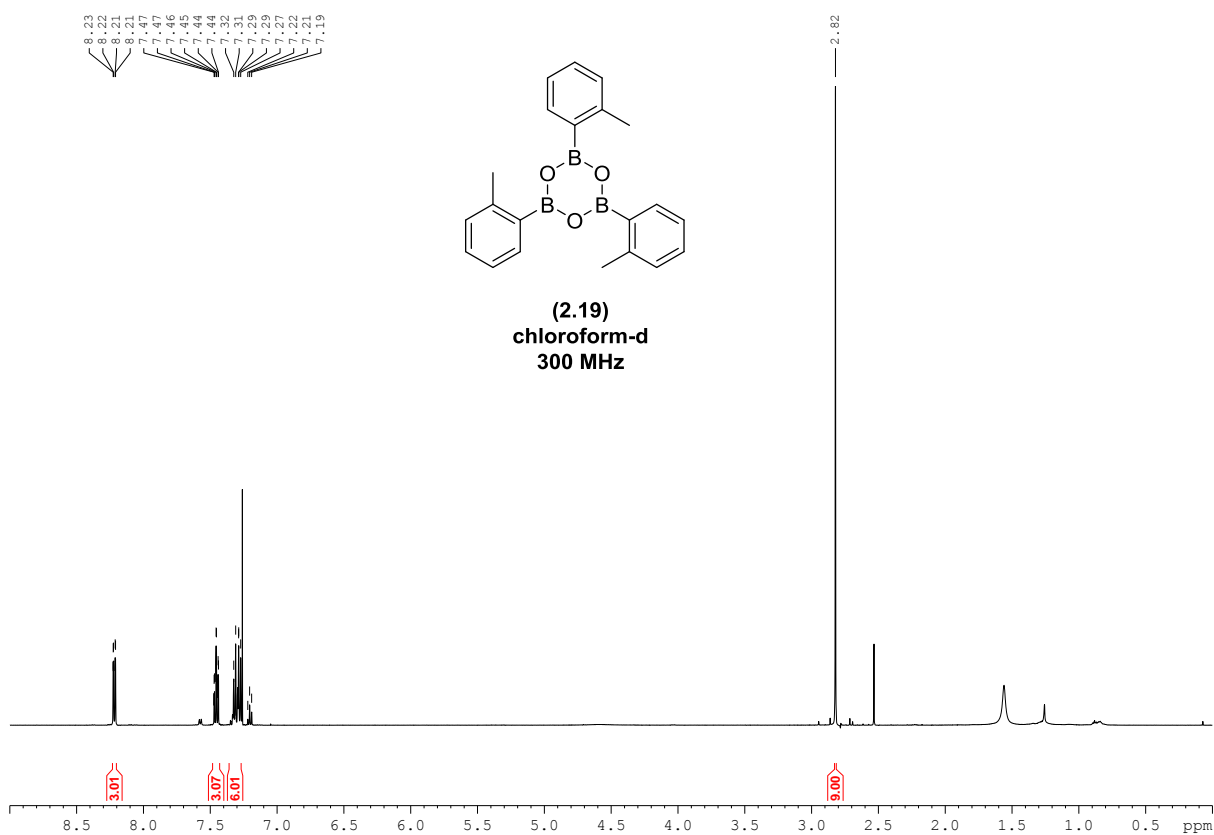
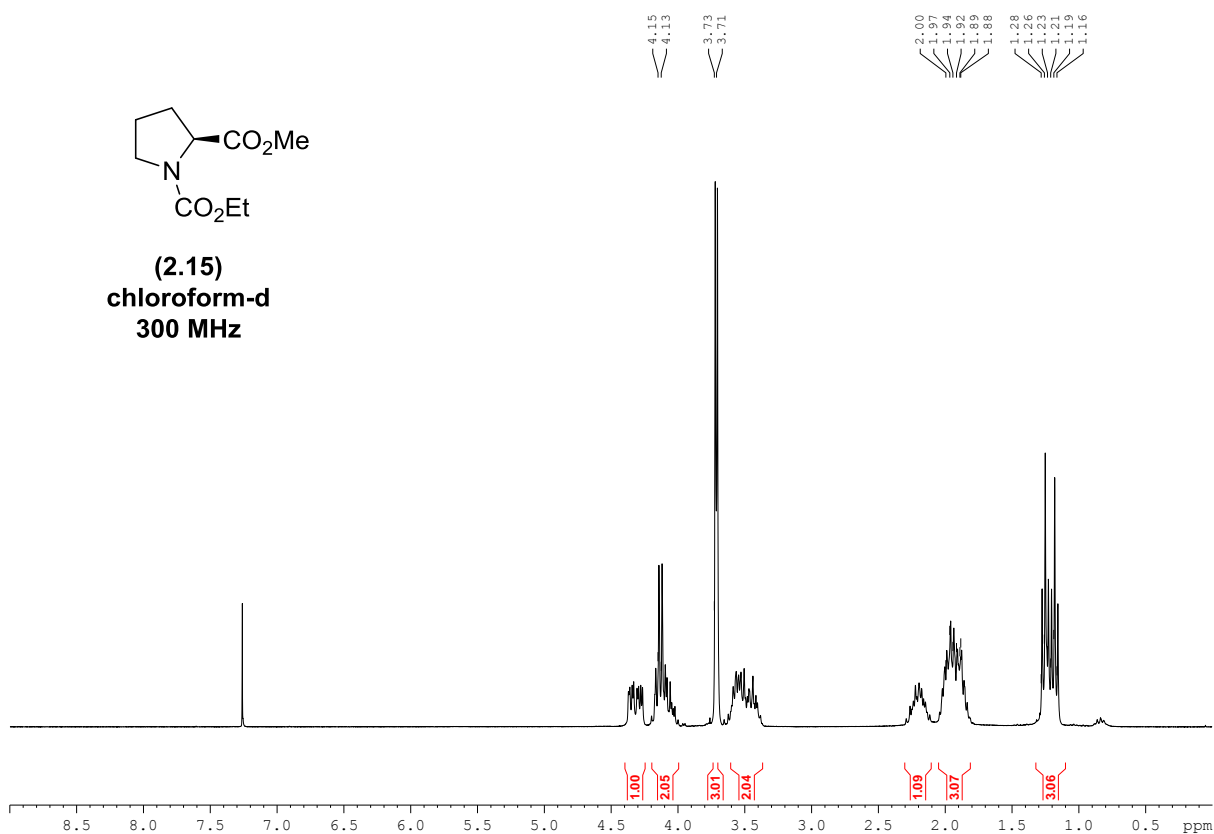
- (85) Simpson, T. H. *J. Org. Chem.* **1963**, 28, 2107.
- (86) Banwell, M. G.; Flynn, B. L.; Stewart, S. G. *J. Org. Chem.* **1998**, 63, 9139.
- (87) Williams, C. M.; Mander, L. N. *Tetrahedron Lett.* **2004**, 45, 667.
- (88) Razafindrabe, C. R.; Aubry, S.; Bourdon, B.; Andriantsiferana, M.; Pellet-Rostaing, S.; Lemaire, M. *Tetrahedron* **2010**, 66, 9061.
- (89) Nicolaou, K. C.; Sasmal, P. K.; Xu, H.; Namoto, K.; Ritzen, A. *Angew. Chem., Int. Ed.* **2003**, 42, 4225.
- (90) Wurm, G.; Gurka, H. J.; Geres, U. *Arch. Pharm. (Weinheim, Ger.)* **1986**, 319, 1106.
- (91) Drew, M. G. B.; Harwood, L. M.; Macias-Sanchez, A. J.; Scott, R.; Thomas, R. M.; Uguen, D. *Angew. Chem., Int. Ed.* **2001**, 40, 2311.
- (92) Lee, G. H.; Youn, I. K.; Choi, E. B.; Lee, H. K.; Yon, G. H.; Yang, H. C.; Pak, C. S. *Curr. Org. Chem.* **2004**, 8, 1263.
- (93) Mahoney, W. S.; Brestensky, D. M.; Stryker, J. M. *J. Am. Chem. Soc.* **1988**, 110, 291.
- (94) (a) Bajwa, N.; Jennings, M. P. *J. Org. Chem.* **2008**, 73, 3638 (b) Nakata, T.; Tanaka, T.; Oishi, T. *Tetrahedron Lett.* **1983**, 24, 2653.
- (95) (a) Davies, H. M. L.; Beckwith, R. E. *J. Chem. Rev. (Washington, DC, U. S.)* **2003**, 103, 2861 (b) Davies, H. M. L.; Denton, J. R. *Chem. Soc. Rev.* **2009**, 38, 3061 (c) Doyle, M. P.; McKervey, M. A.; Ye, T. *Modern Catalytic Methods for Organic Synthesis with Diazo Compounds: From Cyclopropanes to Ylides*; Wiley, 1998.
- (96) Davies, H. M. L.; Yang, J.; Manning, J. R. *Tetrahedron: Asymmetry* **2006**, 17, 665.
- (97) Regitz, M. *Angew. Chem., Int. Ed. Engl.* **1967**, 6, 733.
- (98) Barco, A.; Benetti, S.; Baraldi, P. G.; Simoni, D. *Synthesis* **1981**, 199.
- (99) (a) Kitamura, M.; Tashiro, N.; Okauchi, T. *Synlett* **2009**, 2943 (b) Kitamura, M.; Tashiro, N.; Miyagawa, S.; Okauchi, T. *Synthesis* **2011**, 1037.
- (100) Peng, C.; Cheng, J.; Wang, J. *J. Am. Chem. Soc.* **2007**, 129, 8708.
- (101) Supurgibekov, M. B.; Zakharova, V. M.; Sieler, J.; Nikolaev, V. A. *Tetrahedron Lett.* **2011**, 52, 341.
- (102) Inoue, M.; Frontier, A. J.; Danishefsky, S. J. *Angew. Chem. Int. Ed.* **2000**, 112, 777.
- (103) (a) Ashfeld, B. L.; Martin, S. F. *Org. Lett.* **2005**, 7, 4535 (b) Davies, H. M. L.; Doan, B. D. *J. Org. Chem.* **1998**, 63, 657.
- (104) Radtke, L.; Willot, M.; Sun, H.; Ziegler, S.; Sauerland, S.; Strohmman, C.; Fröhlich, R.; Habenberger, P.; Waldmann, H.; Christmann, M. *Angew. Chem. Int. Ed.* **2011**, 50, 3998.
- (105) Nguyen, T. V.; Hartmann, J. M.; Enders, D. *Synthesis* **2013**, 45, 845.
- (106) Graening, T.; Schmalz, H.-G. *Angew. Chem., Int. Ed.* **2004**, 43, 3230.
- (107) Nicolaou, K. C.; Bulger, P. G.; Sarlah, D. *Angew. Chem., Int. Ed.* **2005**, 44, 4490.
- (108) Schrock, R. R.; Murdzek, J. S.; Bazan, G. C.; Robbins, J.; DiMare, M.; O'Regan, M. *J. Am. Chem. Soc.* **1990**, 112, 3875.
- (109) Schrock, R. R.; Hoveyda, A. H. *Angew. Chem., Int. Ed.* **2003**, 42, 4592.
- (110) (a) Nguyen, S. T.; Johnson, L. K.; Grubbs, R. H.; Ziller, J. W. *J. Am. Chem. Soc.* **1992**, 114, 3974 (b) Schwab, P.; France, M. B.; Ziller, J. W.; Grubbs, R. H. *Angew. Chem., Int. Ed. Engl.* **1995**, 34, 2039.
- (111) Oliver, S. F.; Högenauer, K.; Simic, O.; Antonello, A.; Smith, M. D.; Ley, S. V. *Angew. Chem. Int. Ed.* **2003**, 42, 5996.
- (112) Diels, O.; Alder, K. *Liebigs Ann. Chem.* **1928**, 460, 98.
- (113) Liu, L.-Z.; Han, J.-C.; Yue, G.-Z.; Li, C.-C.; Yang, Z. *J. Am. Chem. Soc.* **2010**, 132, 13608.
- (114) Nicolaou, K. C.; Ding, H.; Richard, J.-A.; Chen, D. Y. K. *J. Am. Chem. Soc.* **2010**, 132, 3815.
- (115) Xu, J.; Caro-Diaz, E. J. E.; Theodorakis, E. A. *Org. Lett.* **2010**, 12, 3708.
- (116) Zhang, J.; Li, L.; Wang, Y.; Wang, W.; Xue, J.; Li, Y. *Org. Lett.* **2012**, 14, 4528.

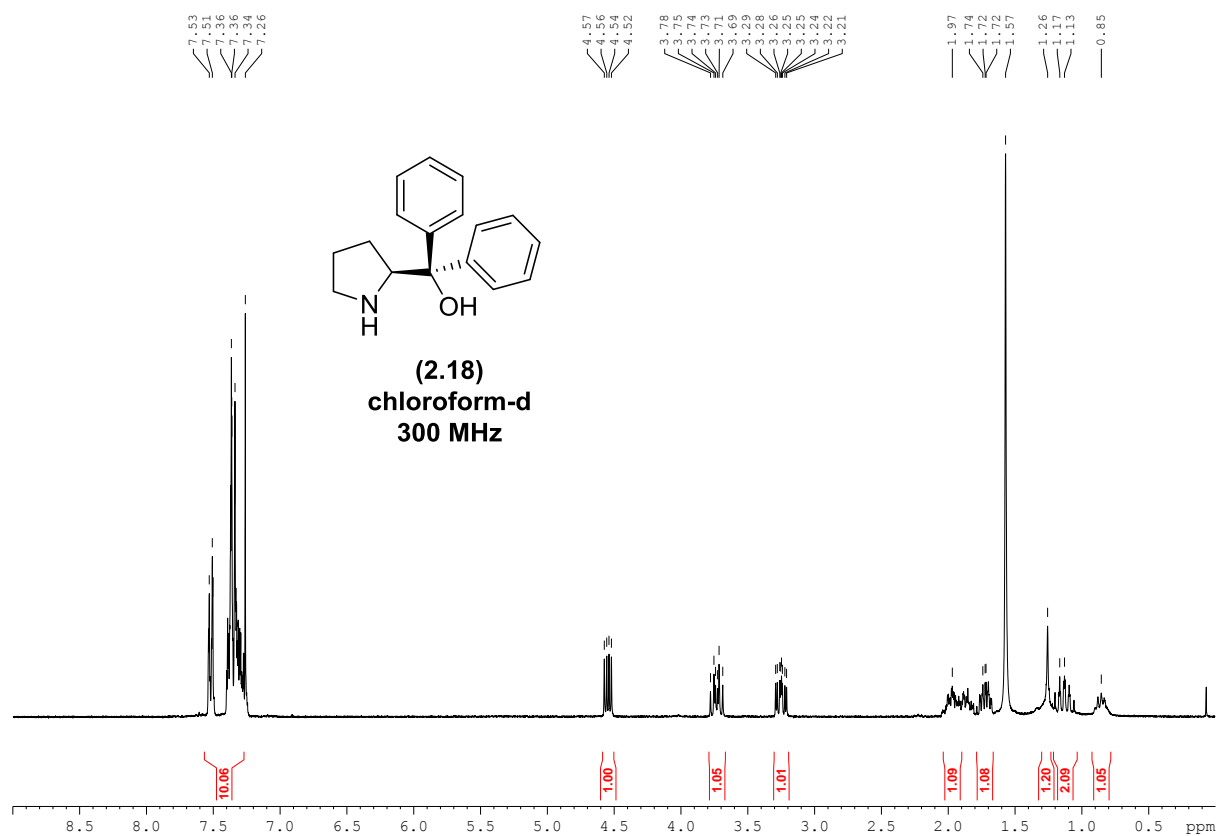
- (117) Lian, Y.; Miller, L. C.; Born, S.; Sarpong, R.; Davies, H. M. L. *J. Am. Chem. Soc.* **2010**, *132*, 12422.
- (118) Reddy, R. P.; Davies, H. M. L. *J. Am. Chem. Soc.* **2007**, *129*, 10312.
- (119) Huisgen, R., 1984; p 1.
- (120) Rostovtsev, V. V.; Green, L. G.; Fokin, V. V.; Sharpless, K. B. *Angew. Chem., Int. Ed.* **2002**, *41*, 2596.
- (121) Tornøe, C. W.; Christensen, C.; Meldal, M. *J. Org. Chem.* **2002**, *67*, 3057.
- (122) Meldal, M.; Tornøe, C. W. *Chem. Rev. (Washington, DC, U. S.)* **2008**, *108*, 2952.
- (123) Kolb, H. C.; Finn, M. G.; Sharpless, K. B. *Angew. Chem. Int. Ed.* **2001**, *40*, 2004.
- (124) (a) Zibinsky, M.; Fokin, V. V. *Angew. Chem., Int. Ed.* **2013**, *52*, 1507(b) Raushel, J.; Fokin, V. V. *Org. Lett.* **2010**, *12*, 4952(c) Chuprakov, S.; Kwok, S. W.; Fokin, V. V. *J. Am. Chem. Soc.* **2013**, *135*, 4652.
- (125) Selander, N.; Worrell, B. T.; Fokin, V. V. *Angew. Chem., Int. Ed.* **2012**, *51*, 13054.
- (126) Parr, B. T.; Davies, H. M. L. *Angew. Chem., Int. Ed.* **2013**, *52*, 10044.
- (127) Davies, H. M. L.; Hedley, S. J. *Chem. Soc. Rev.* **2007**, *36*, 1109.
- (128) Perrin, D. D.; Armarego, W. L. F. *Purification of Laboratory Chemicals. 3rd Ed*; Pergamon Press, 1988.
- (129) Edwards, M. G.; Paxton, R. J.; Pugh, D. S.; Whitwood, A. C.; Taylor, R. J. K. *Synthesis* **2008**, 3279.
- (130) Corey, E. J.; Shibata, T.; Lee, T. W. *J. Am. Chem. Soc.* **2002**, *124*, 3808.
- (131) Krafft, M. E.; Cran, J. W. *Synlett* **2005**, 1263.
- (132) Kim, J.; Bruning, J.; Park, K. E.; Lee, D. J.; Singaram, B. *Org. Lett.* **2009**, *11*, 4358.
- (133) Gryparis, C.; Lykakis, I. N.; Efe, C.; Zaravinos, I.-P.; Vidal, T.; Kladou, E.; Stratakis, M. *Org. Biomol. Chem.* **2011**, *9*, 5655.
- (134) Wulff, W. D.; Peterson, G. A.; Bauta, W. E.; Chan, K.-S.; Faron, K. L.; Gilbertson, S. R.; Kaesler, R. W.; Yang, D. C.; Murray, C. K. *J. Org. Chem.* **1986**, *51*, 277.
- (135) Vegh, D.; Zalupsky, P.; Kovac, J. *Synth. Comm.* **1990**, *20*, 1113.
- (136) Deslongchamps, P.; Roy, B. L. *Can. J. Chem.* **1986**, *64*, 2068.

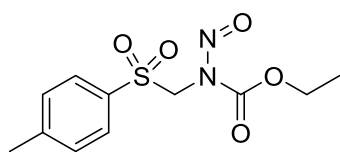
8 Appendix

8.1 Appendix A: Supporting NMR spectra for Chapter 2

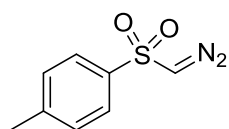
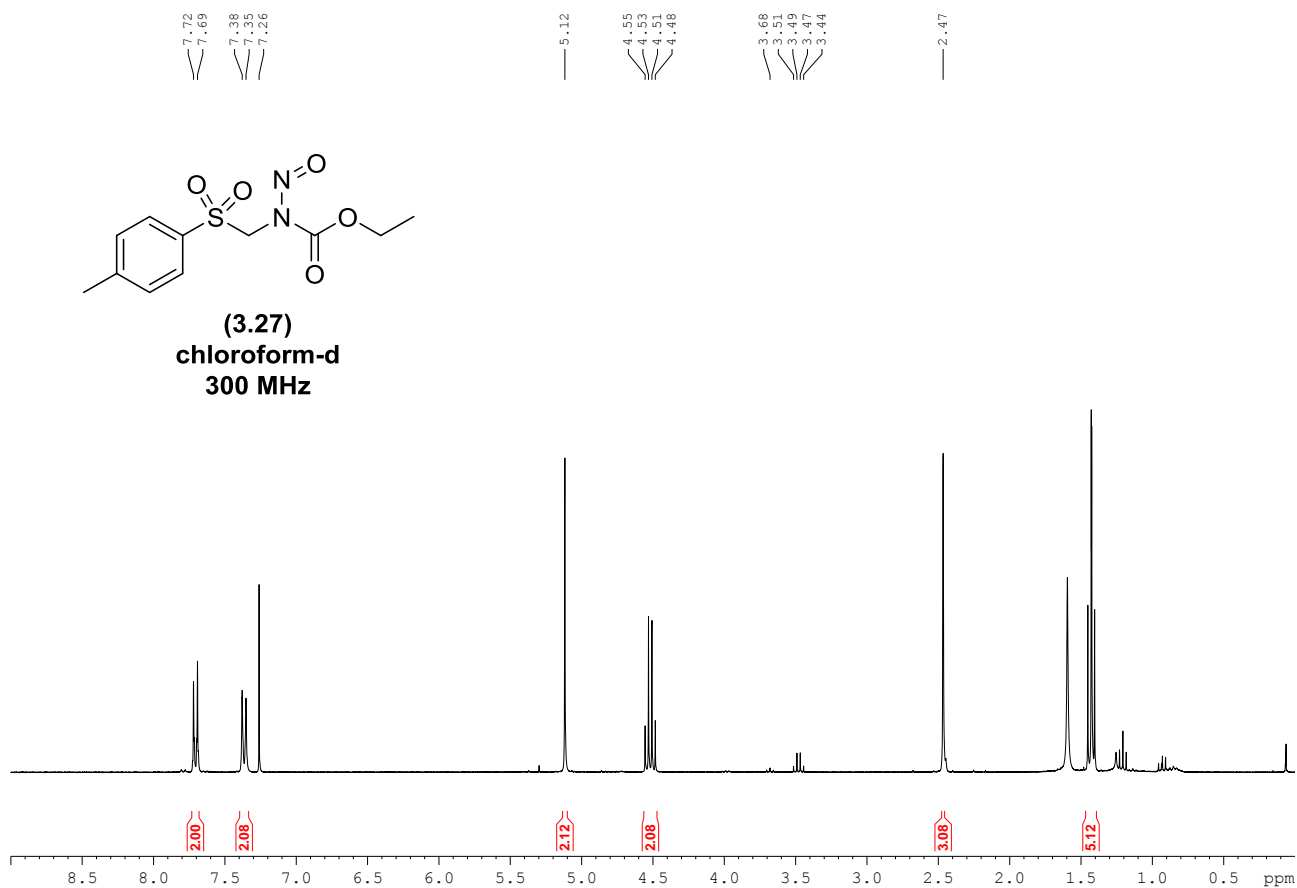




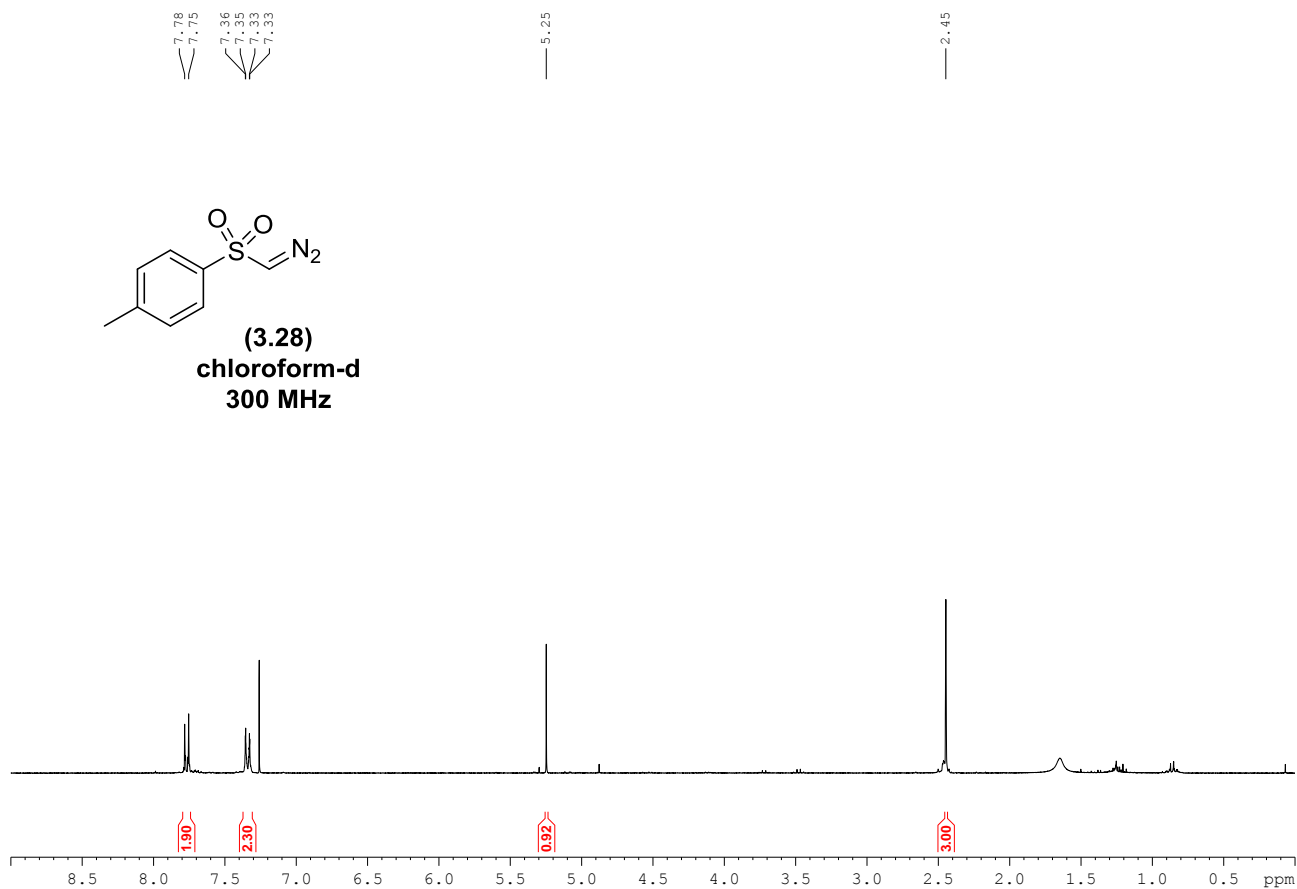


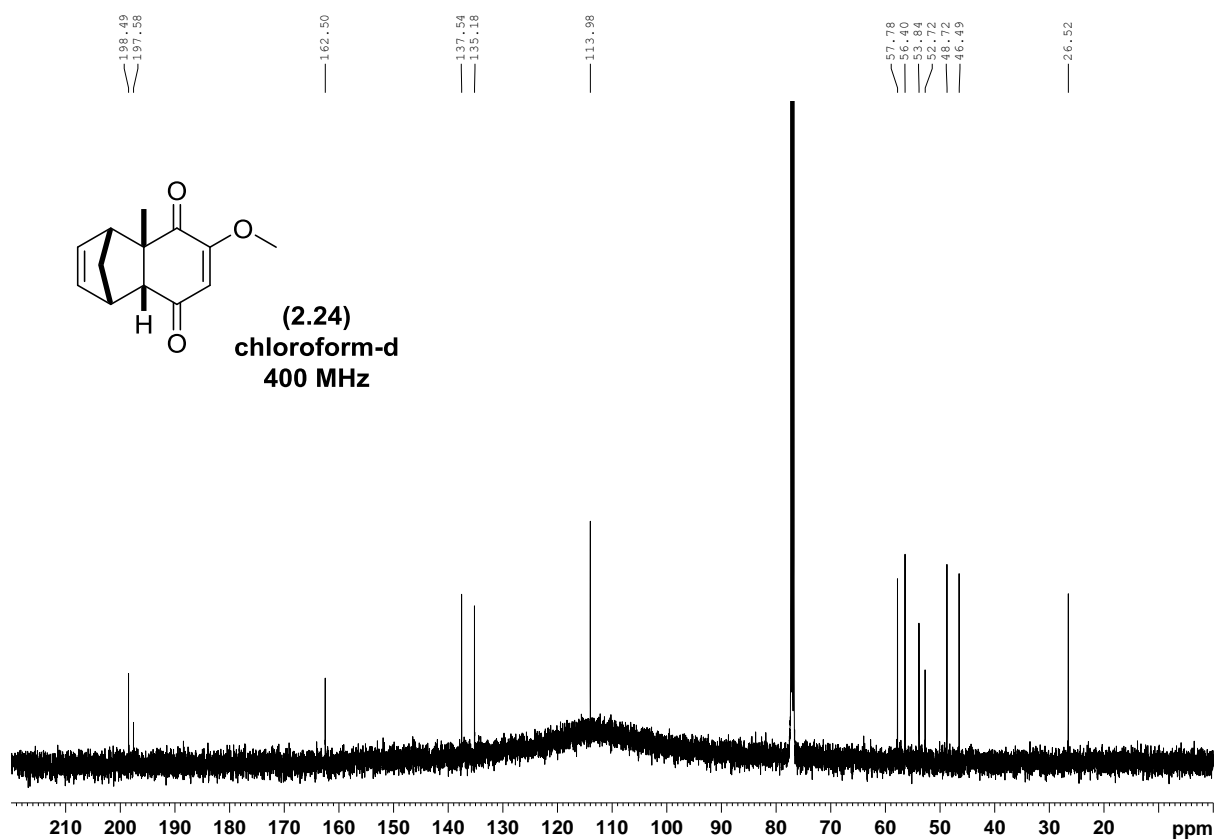
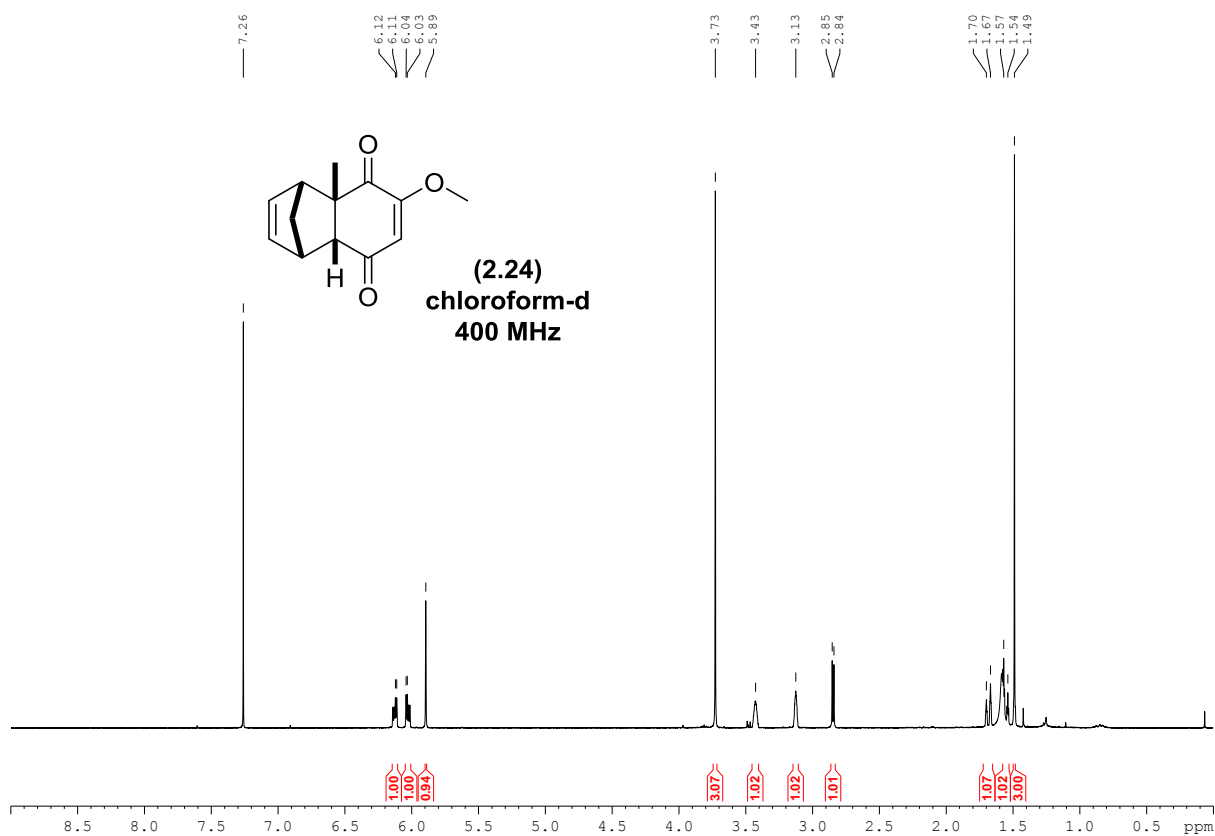


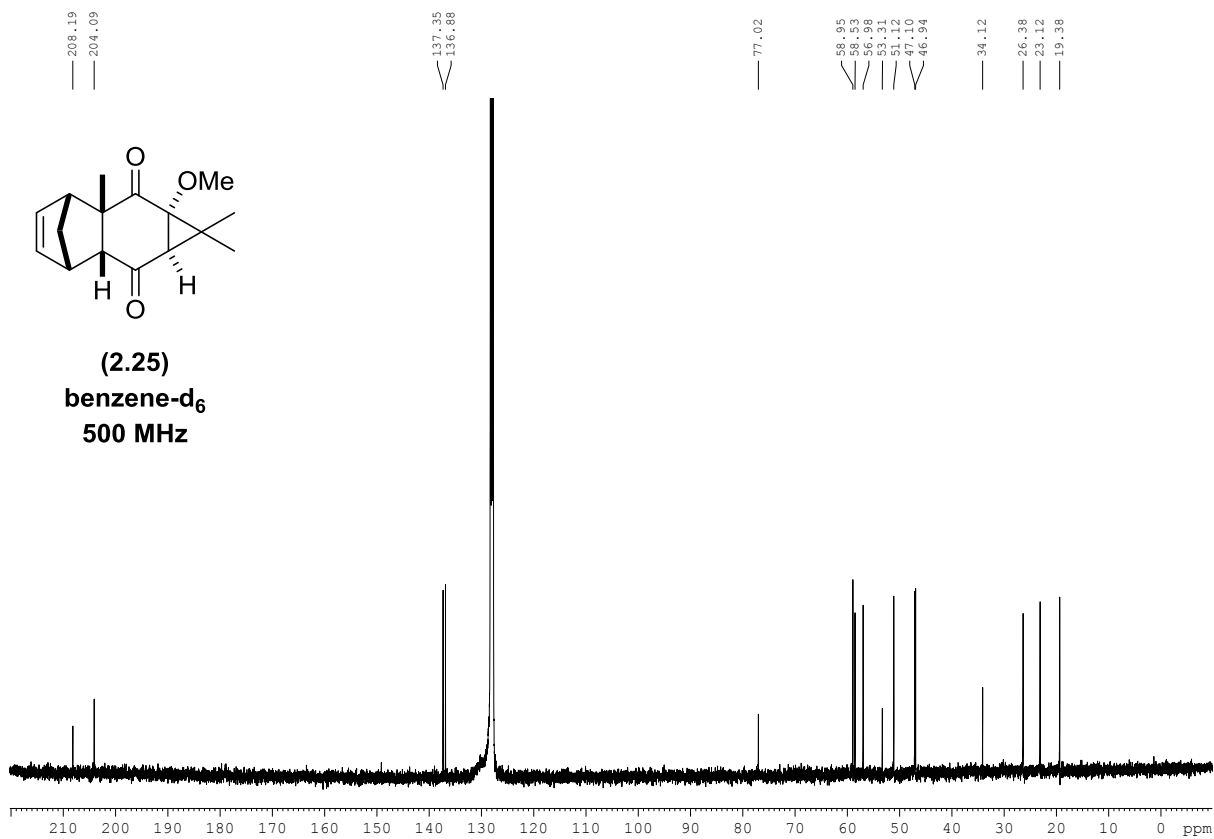
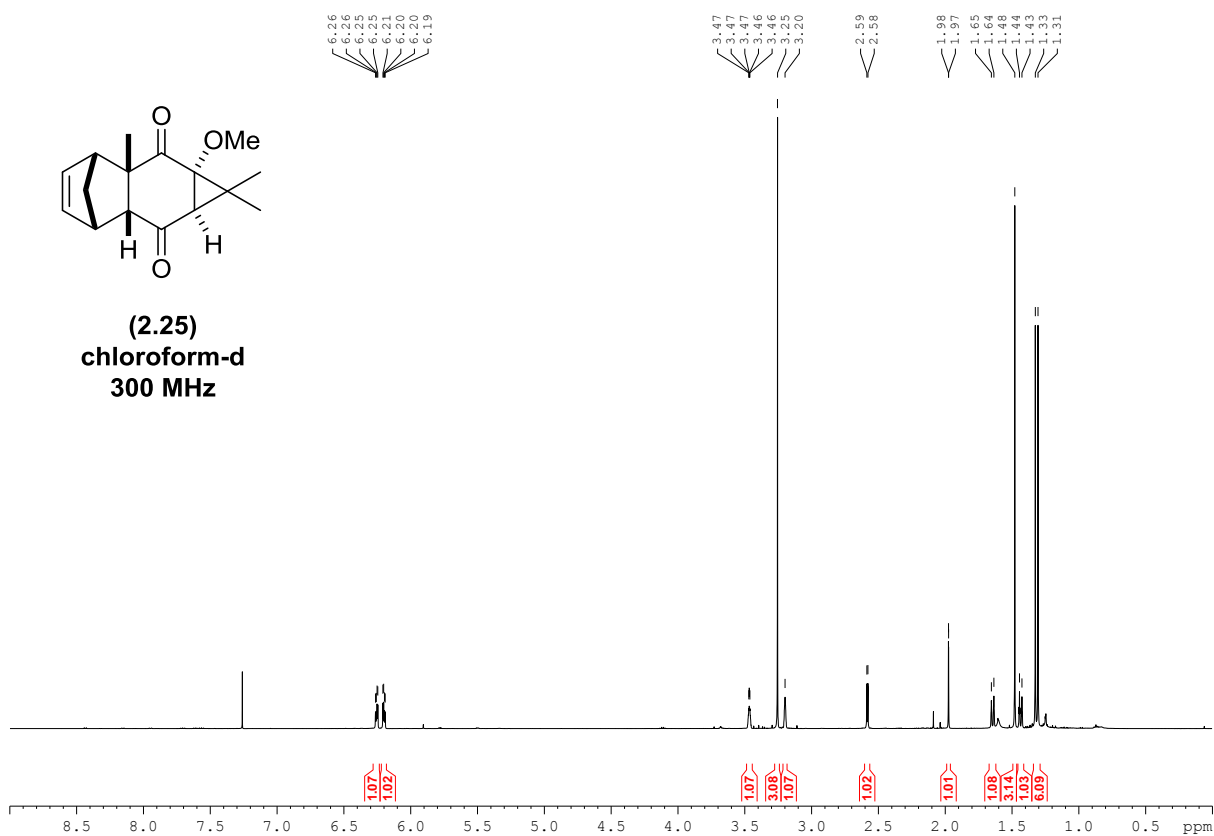
(3.27)
chloroform-d
300 MHz

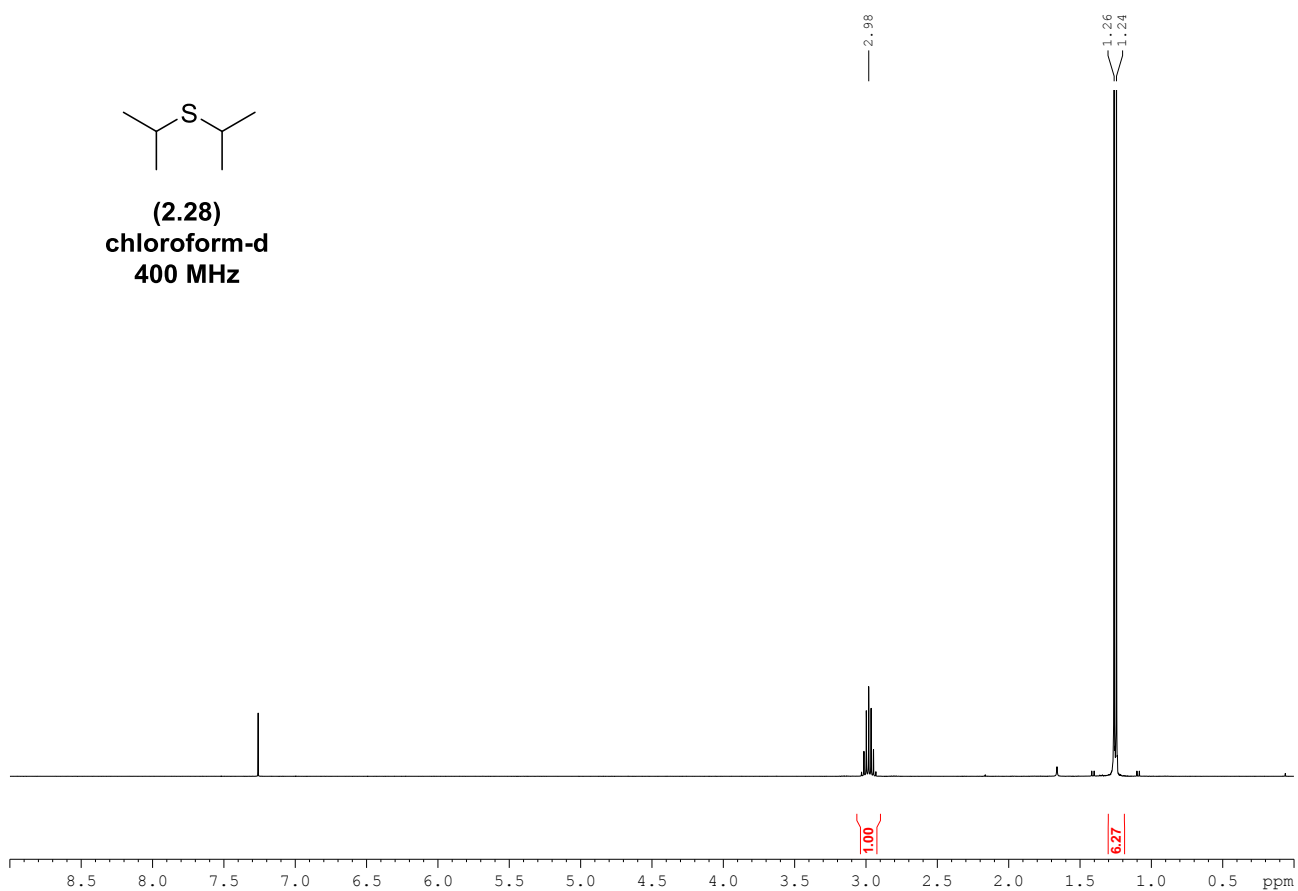
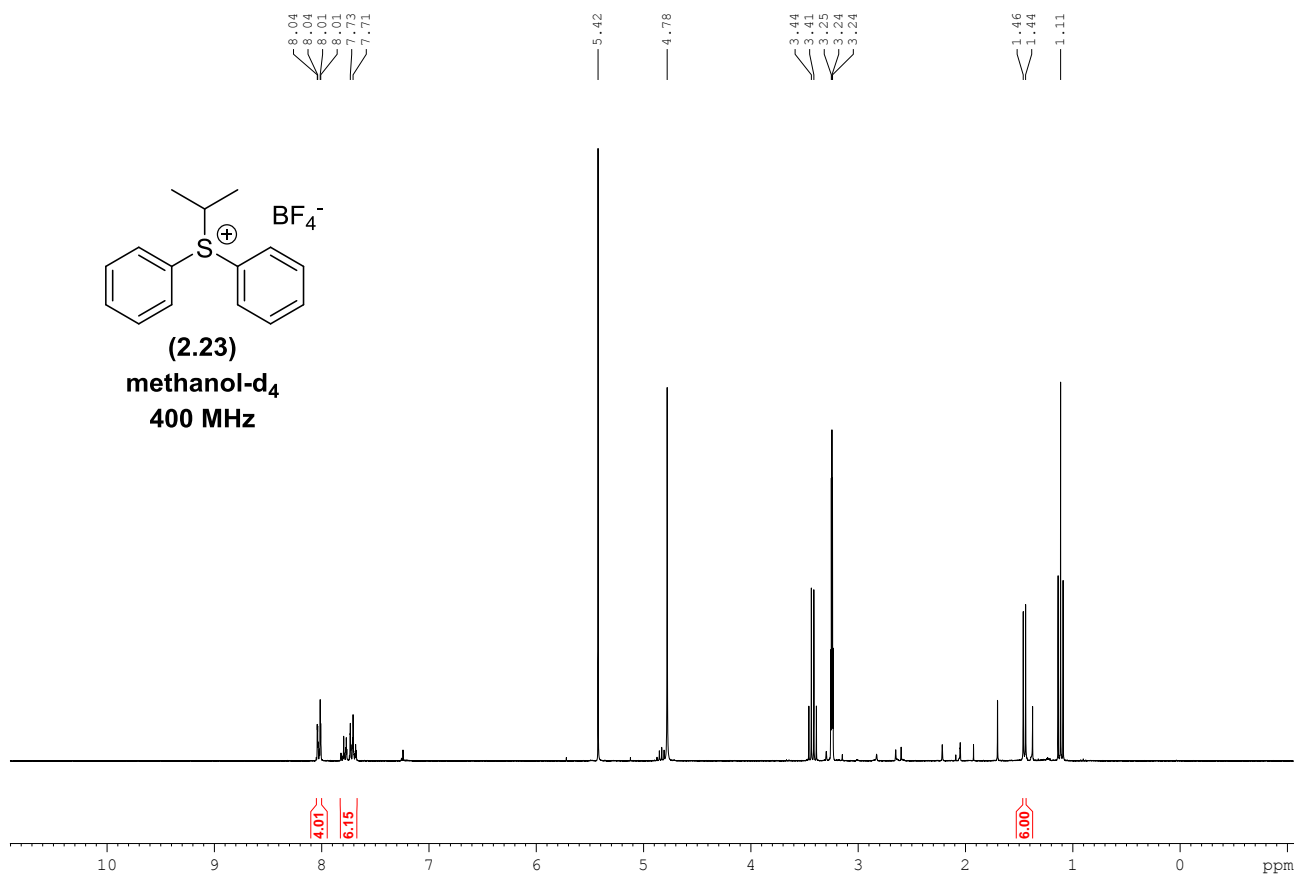


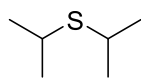
(3.28)
chloroform-d
300 MHz



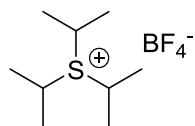
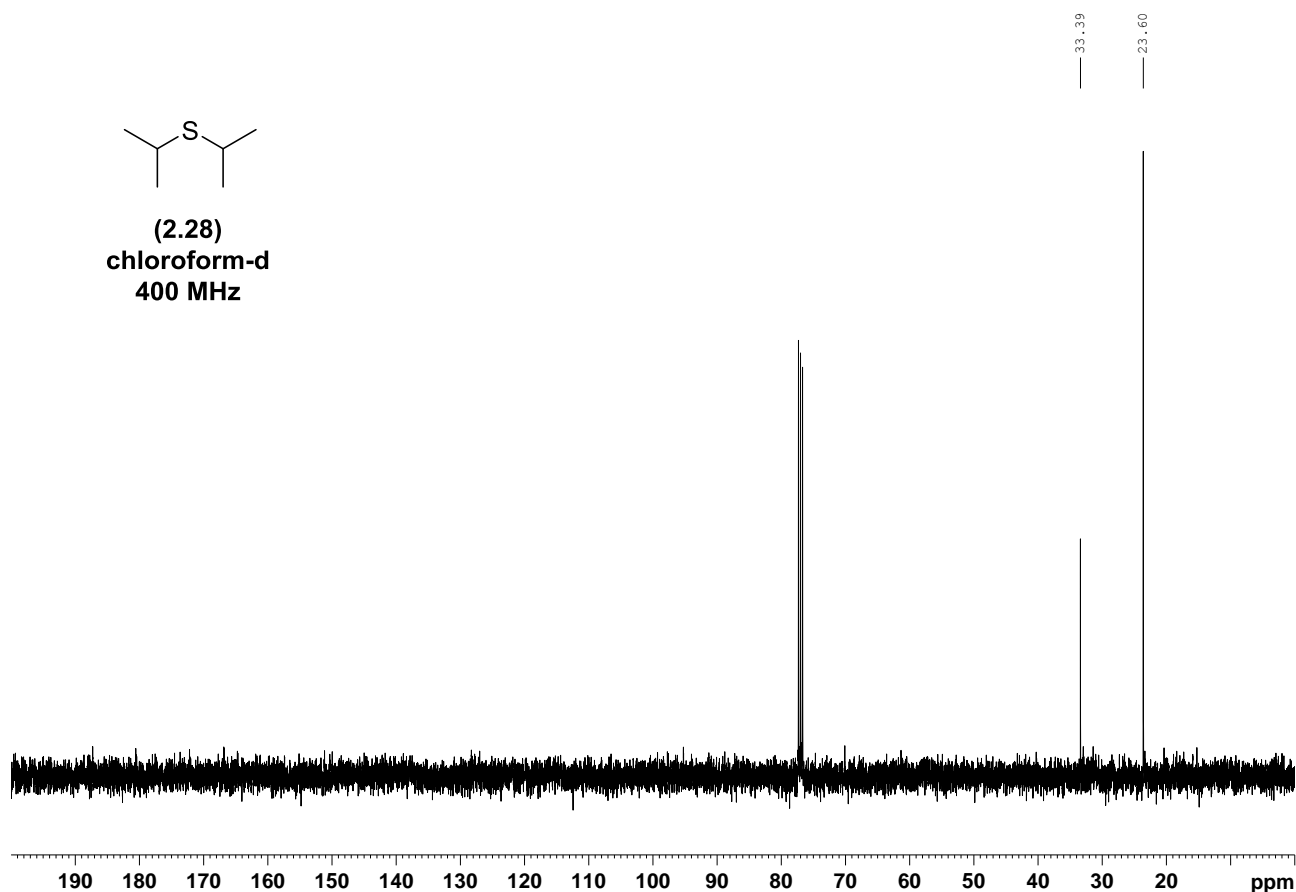




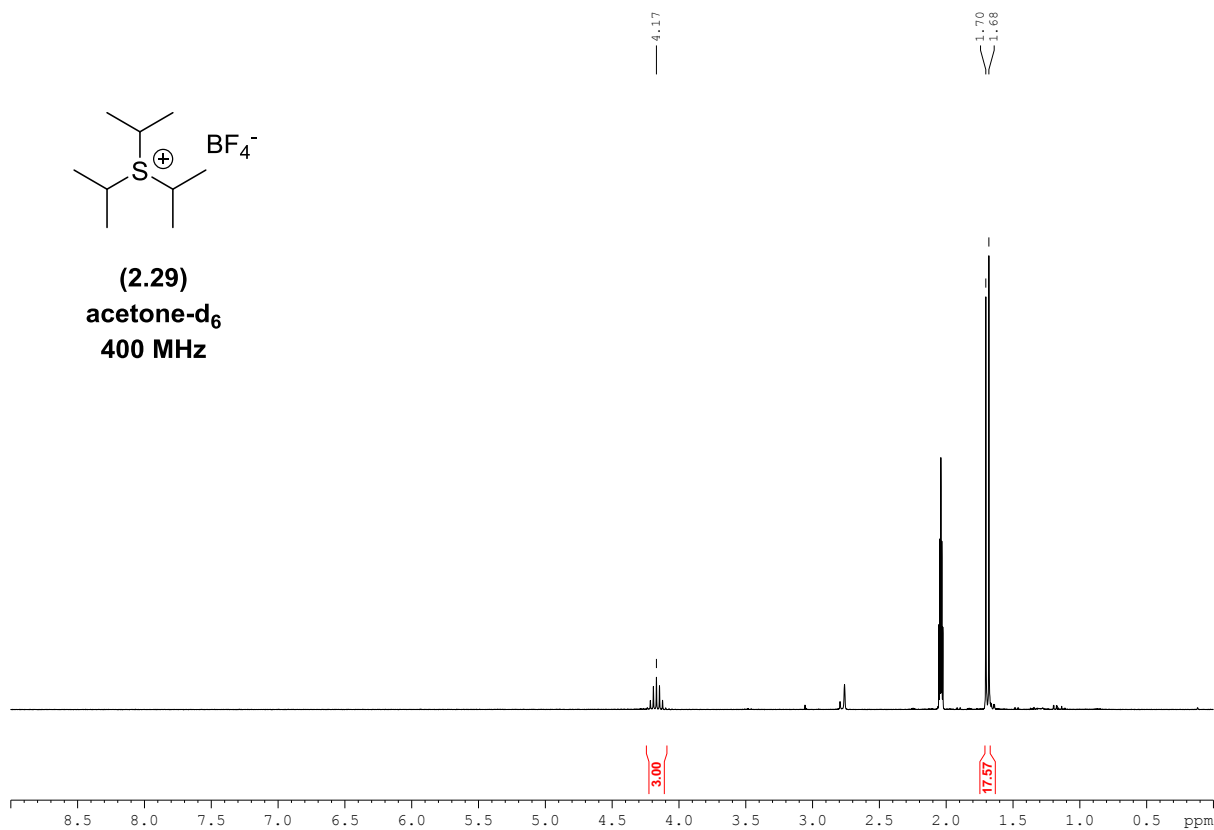


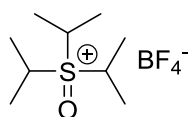


(2.28)
chloroform-d
400 MHz

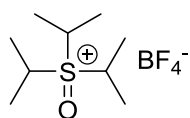
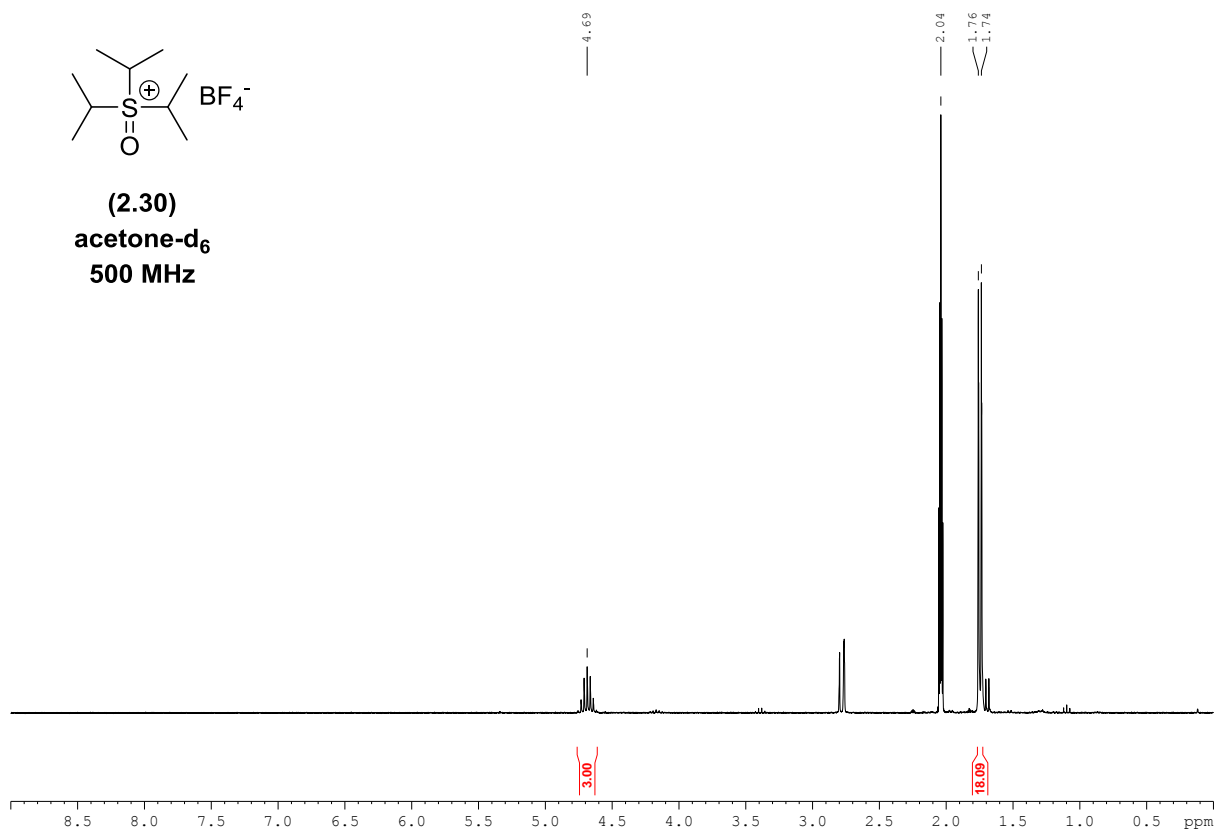


(2.29)
acetone-d₆
400 MHz

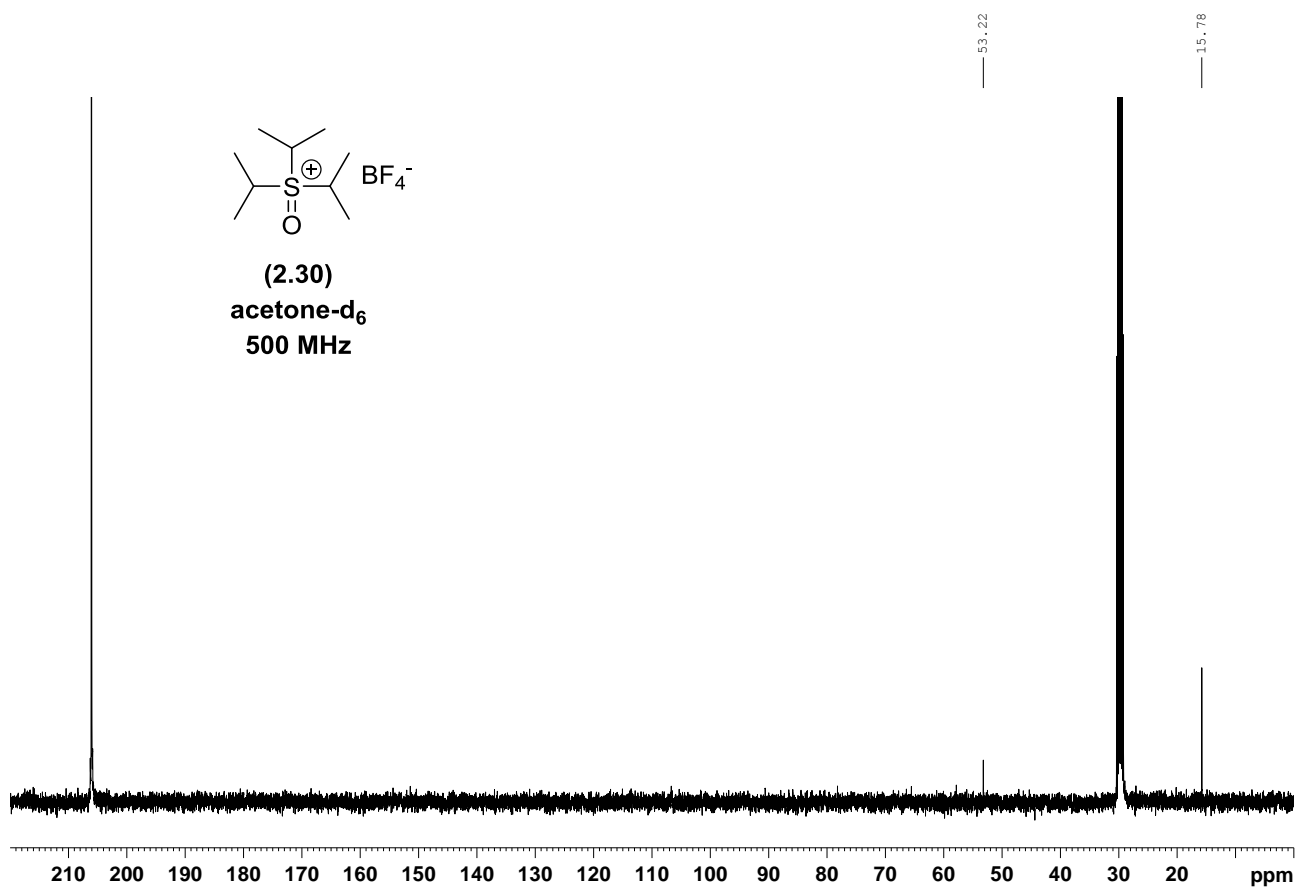


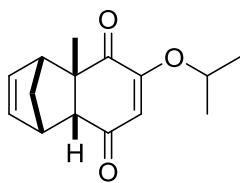


(2.30)
acetone-d₆
500 MHz

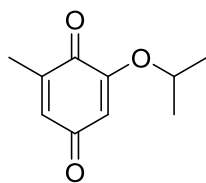
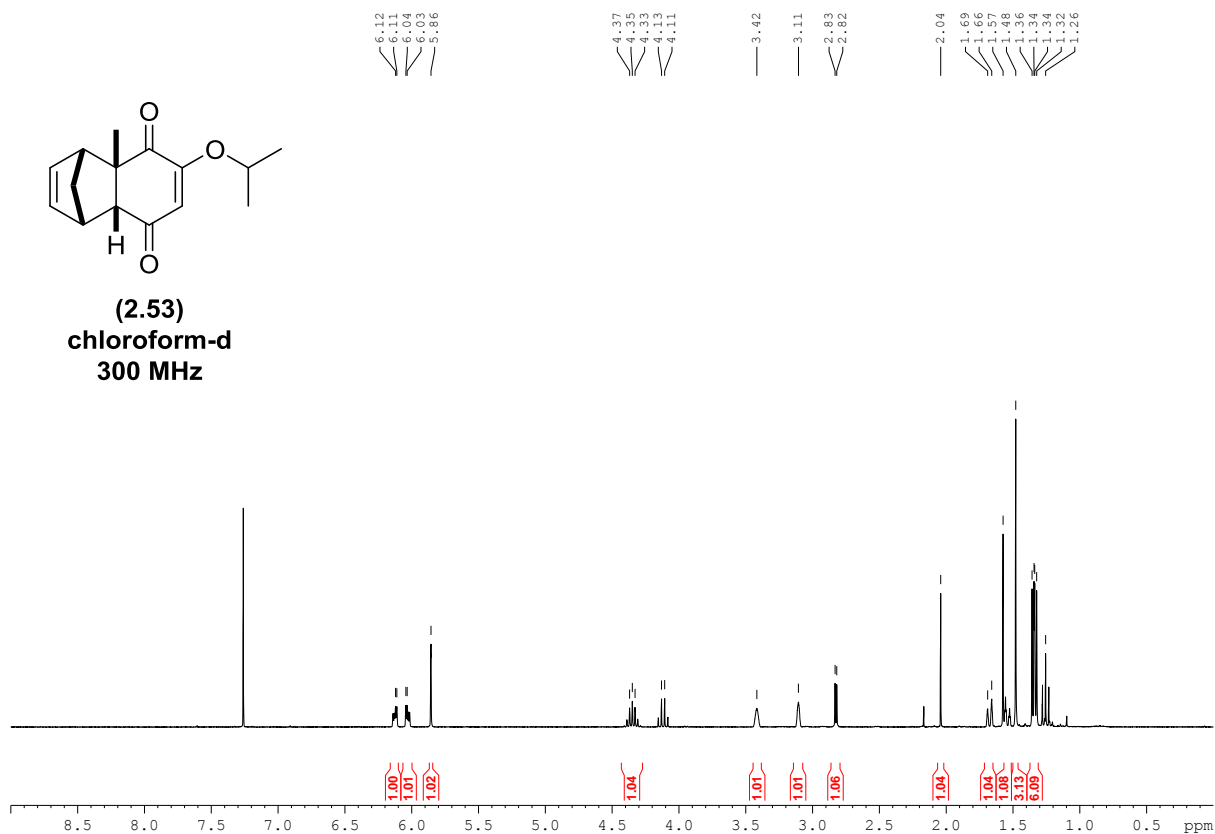


(2.30)
acetone-d₆
500 MHz

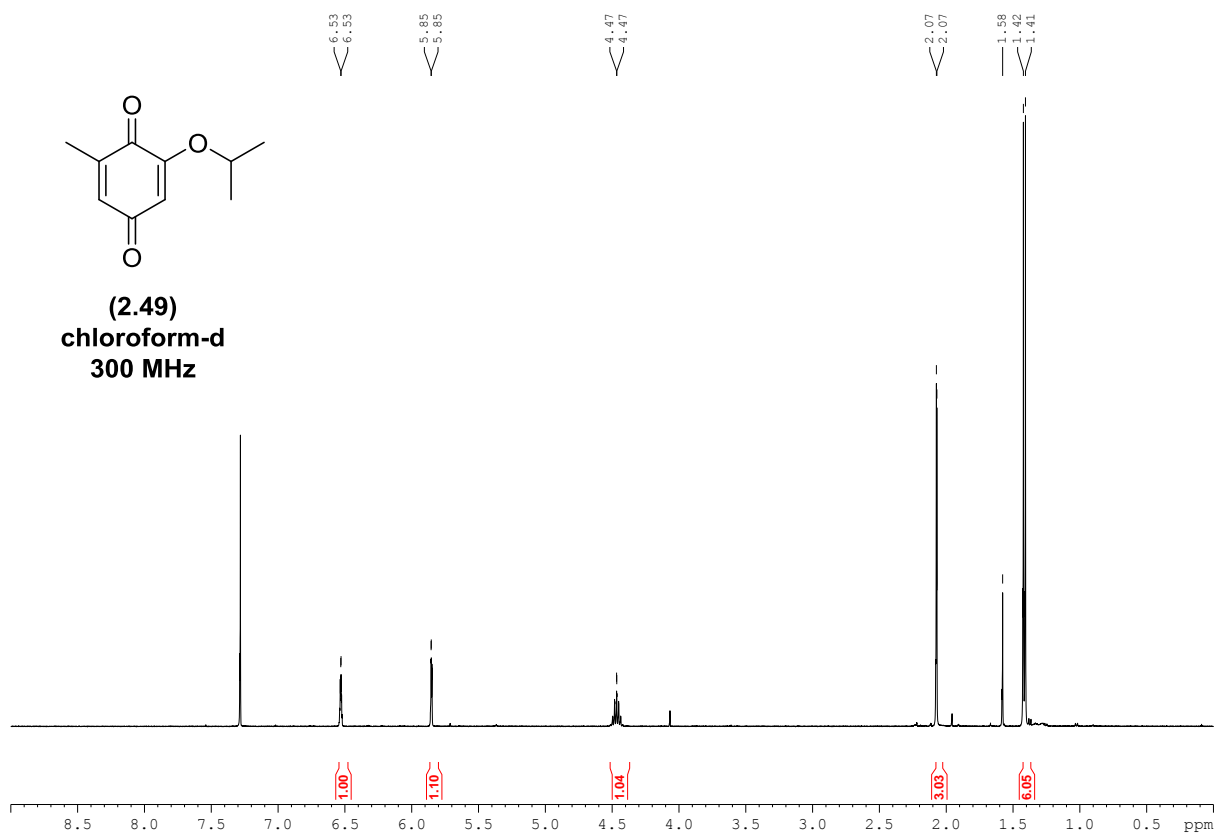


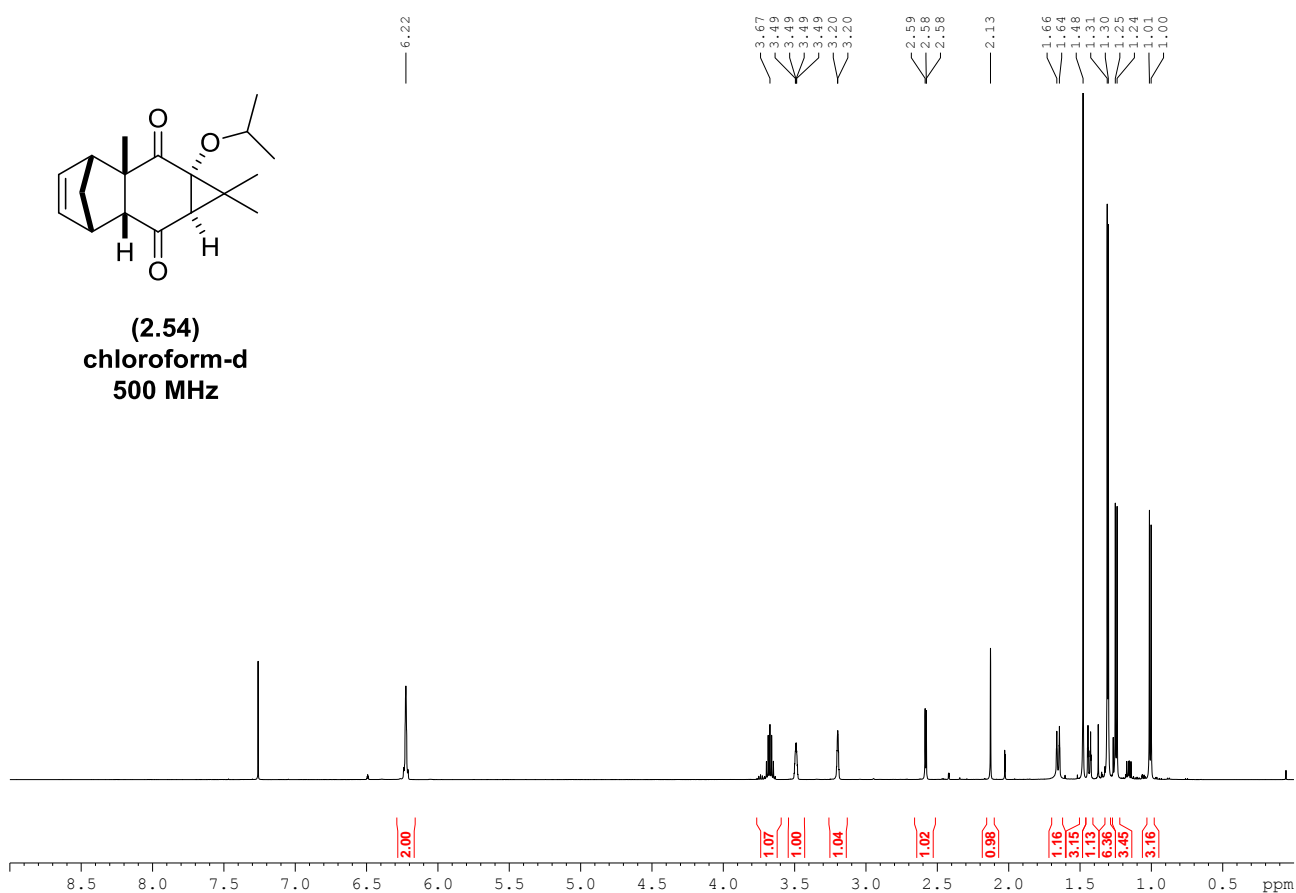
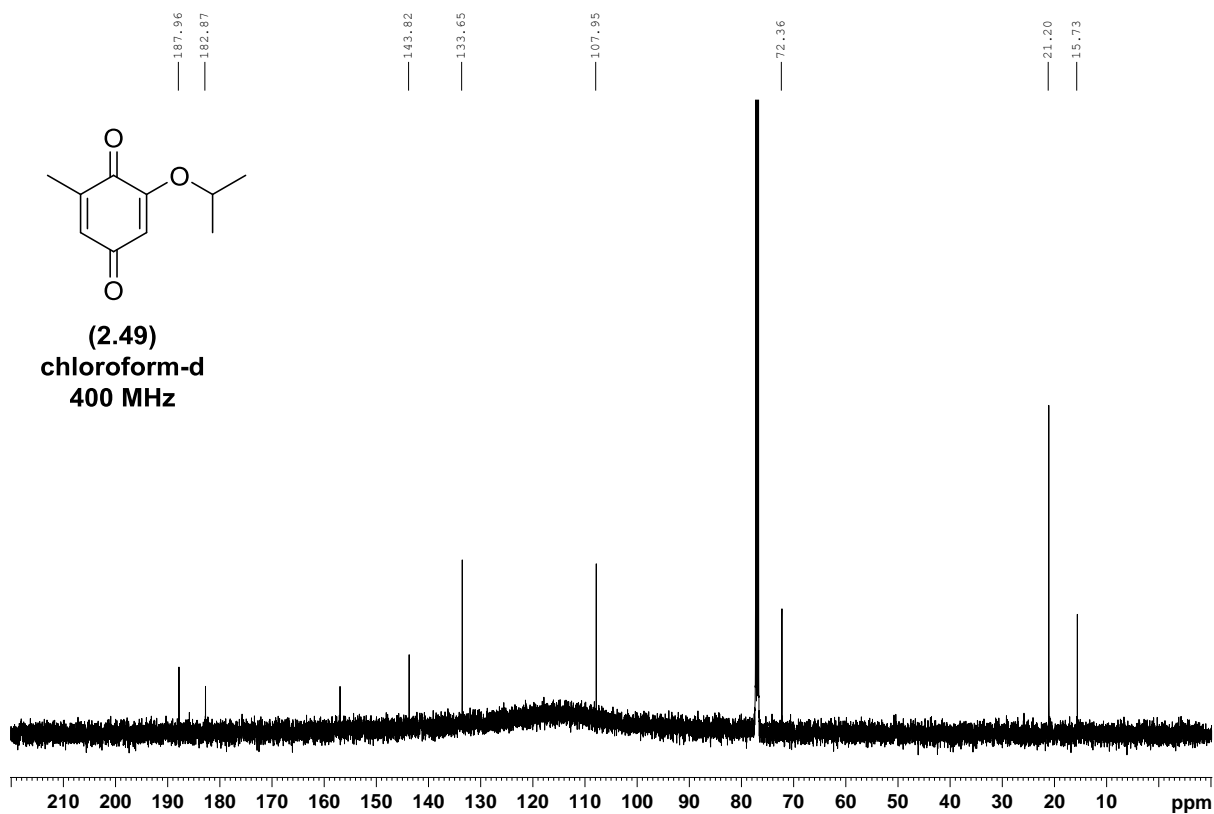


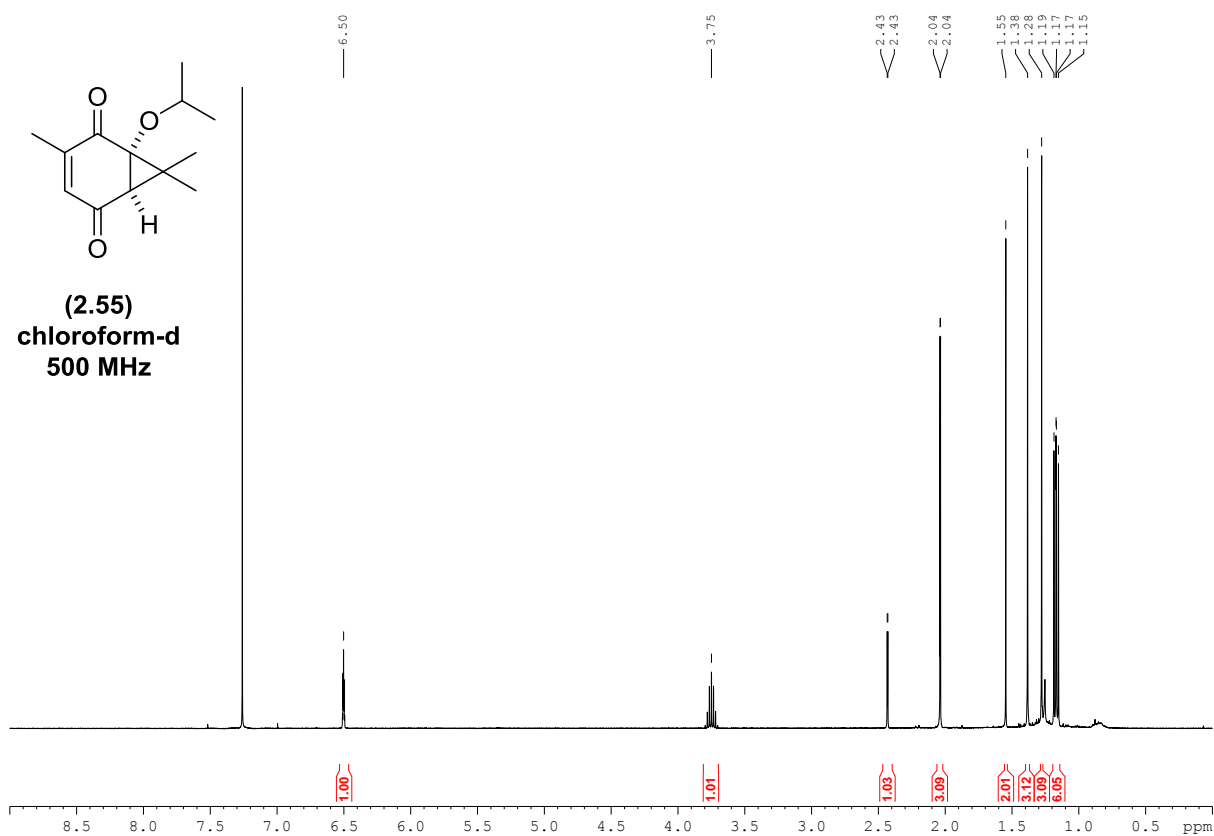
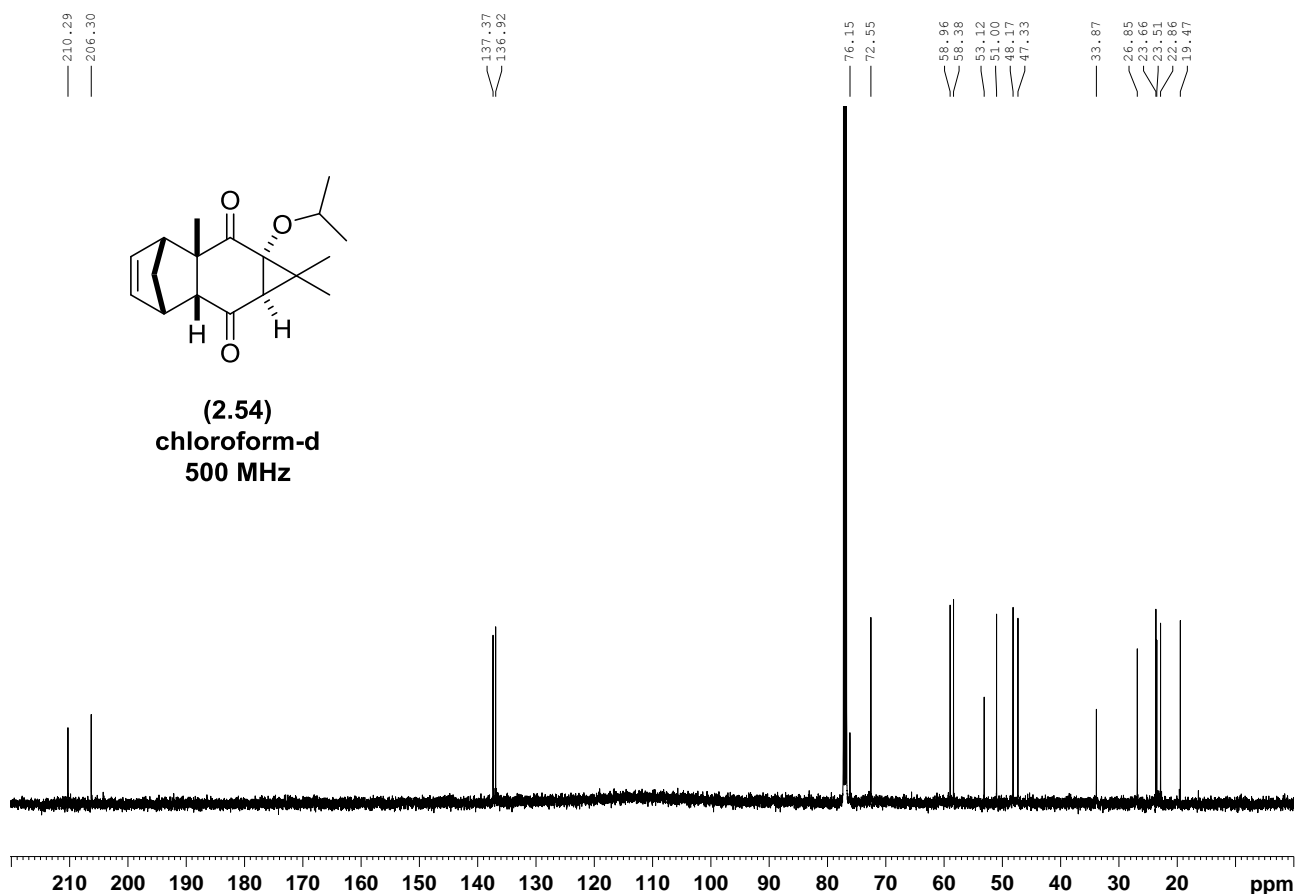
(2.53)
chloroform-d
300 MHz

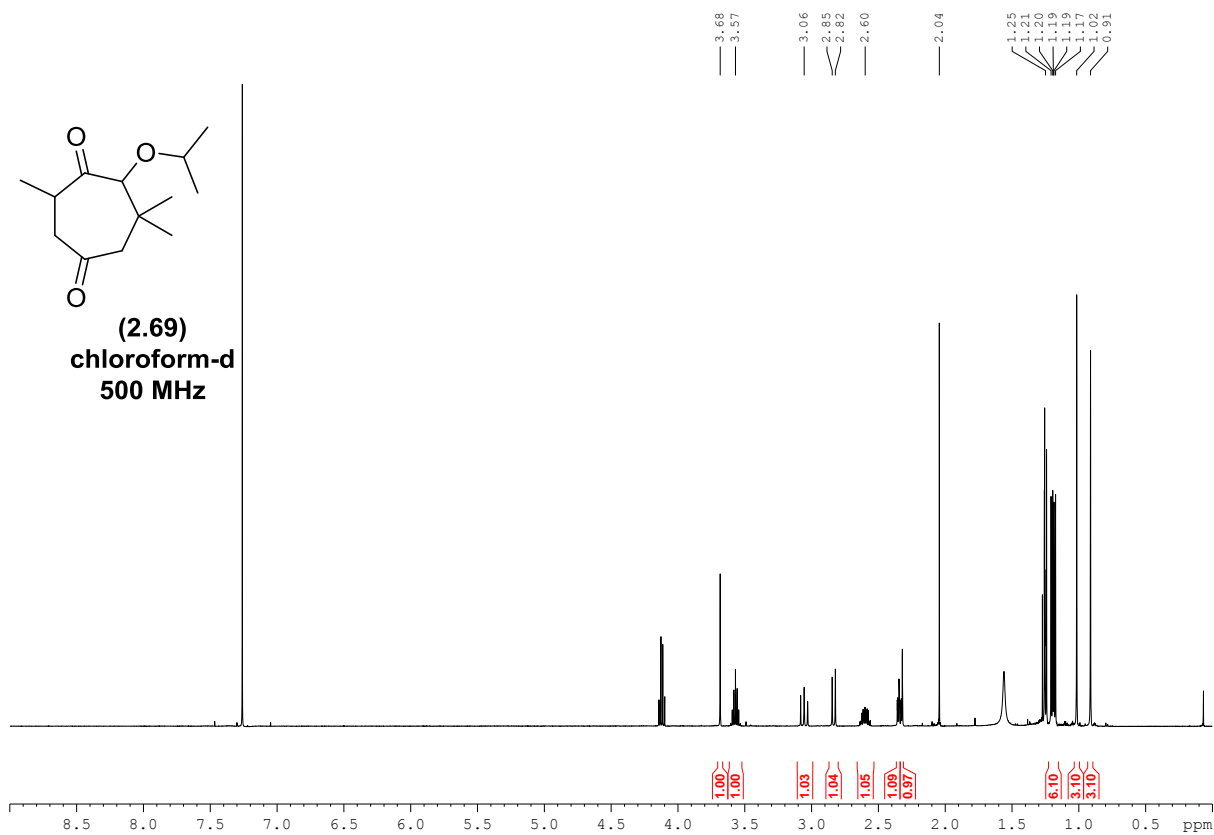
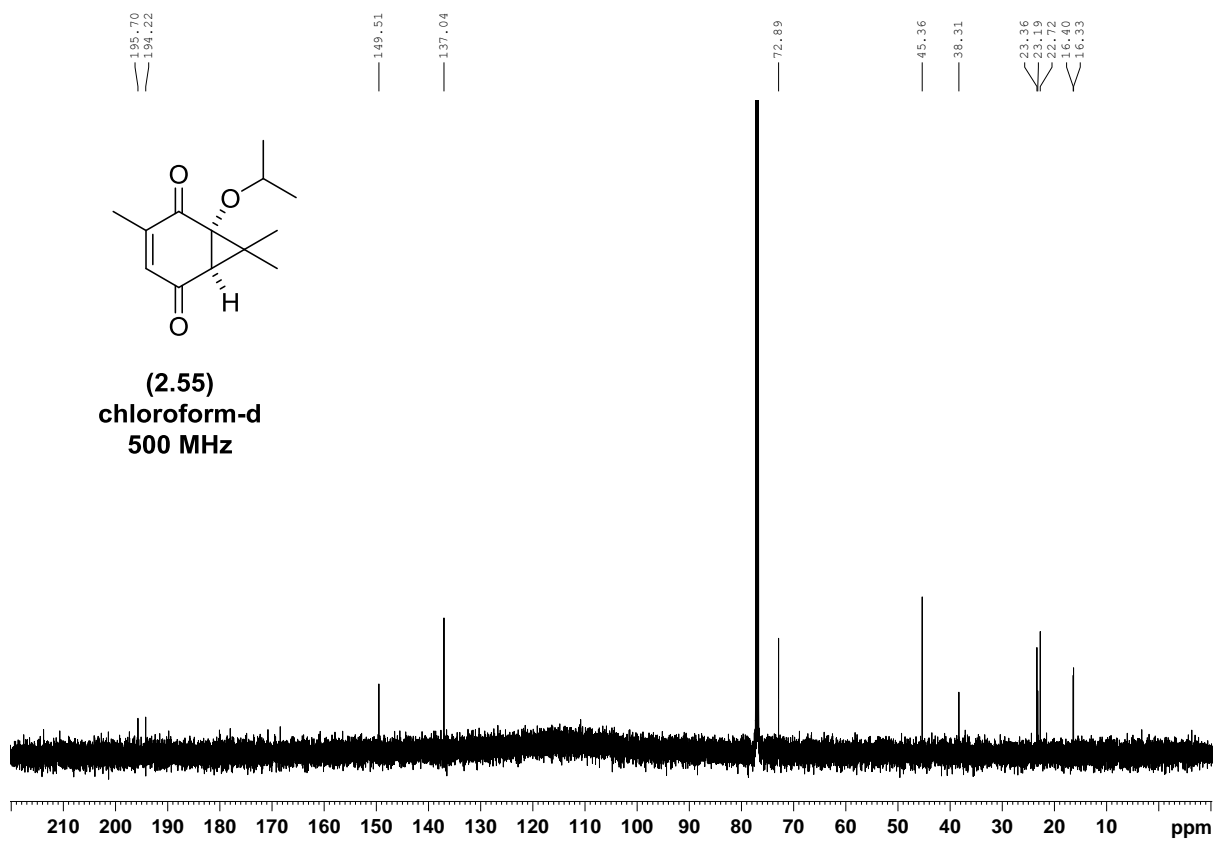


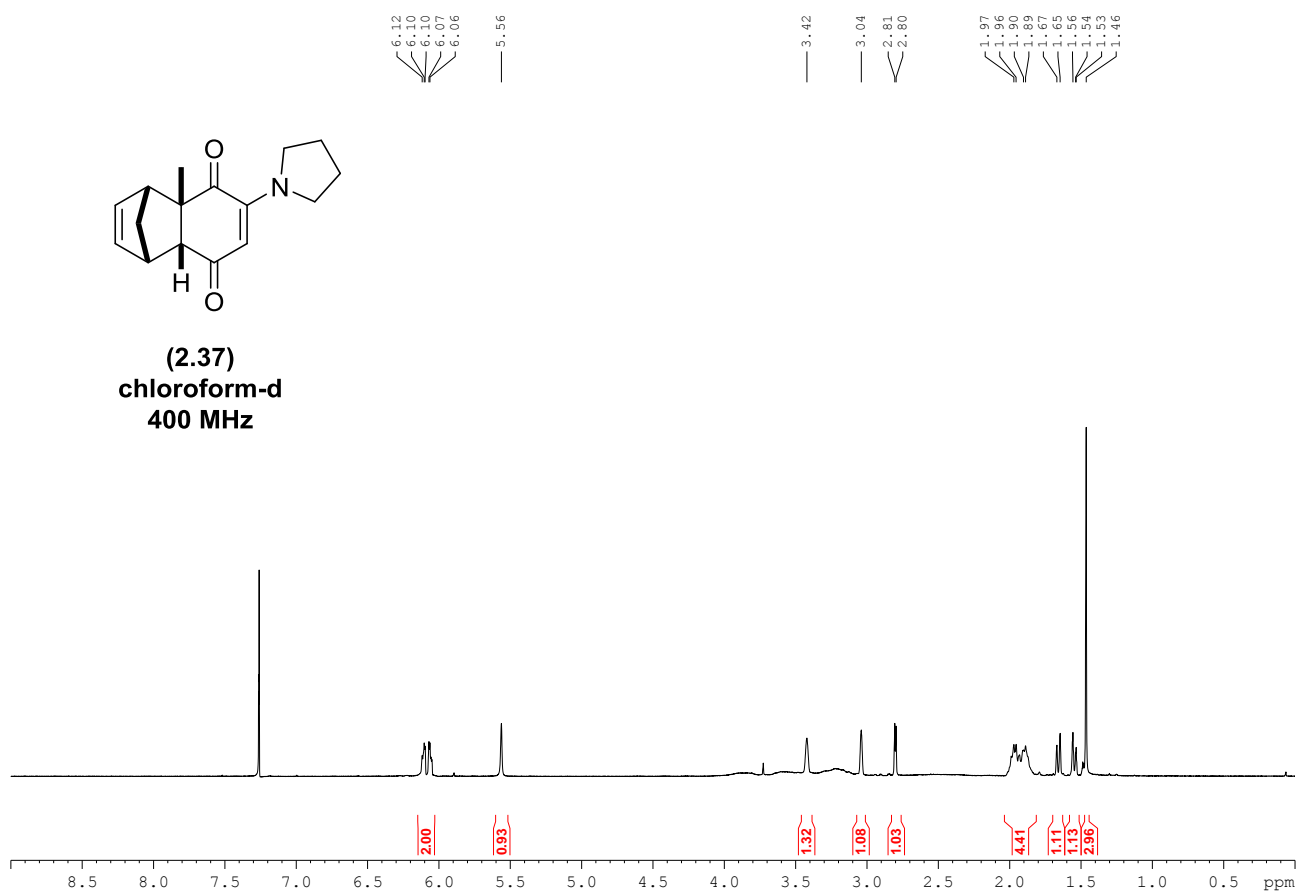
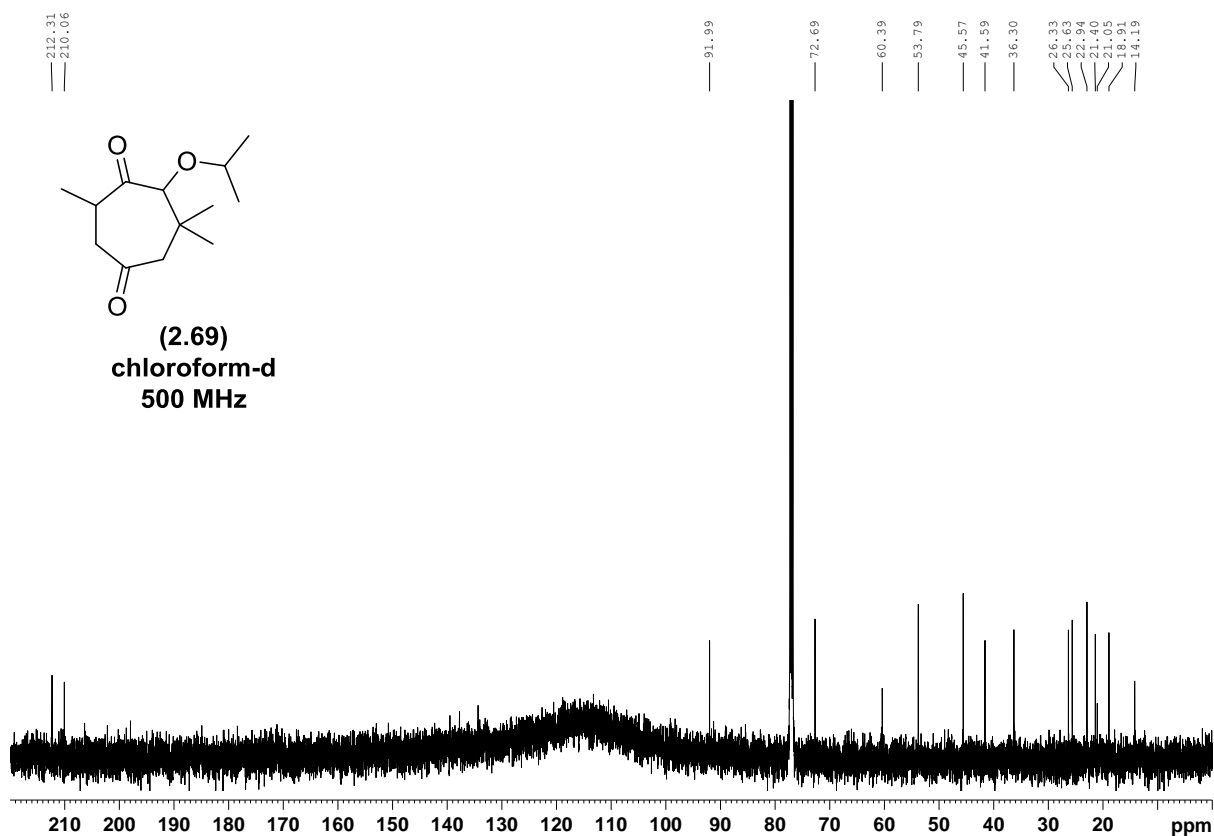
(2.49)
chloroform-d
300 MHz

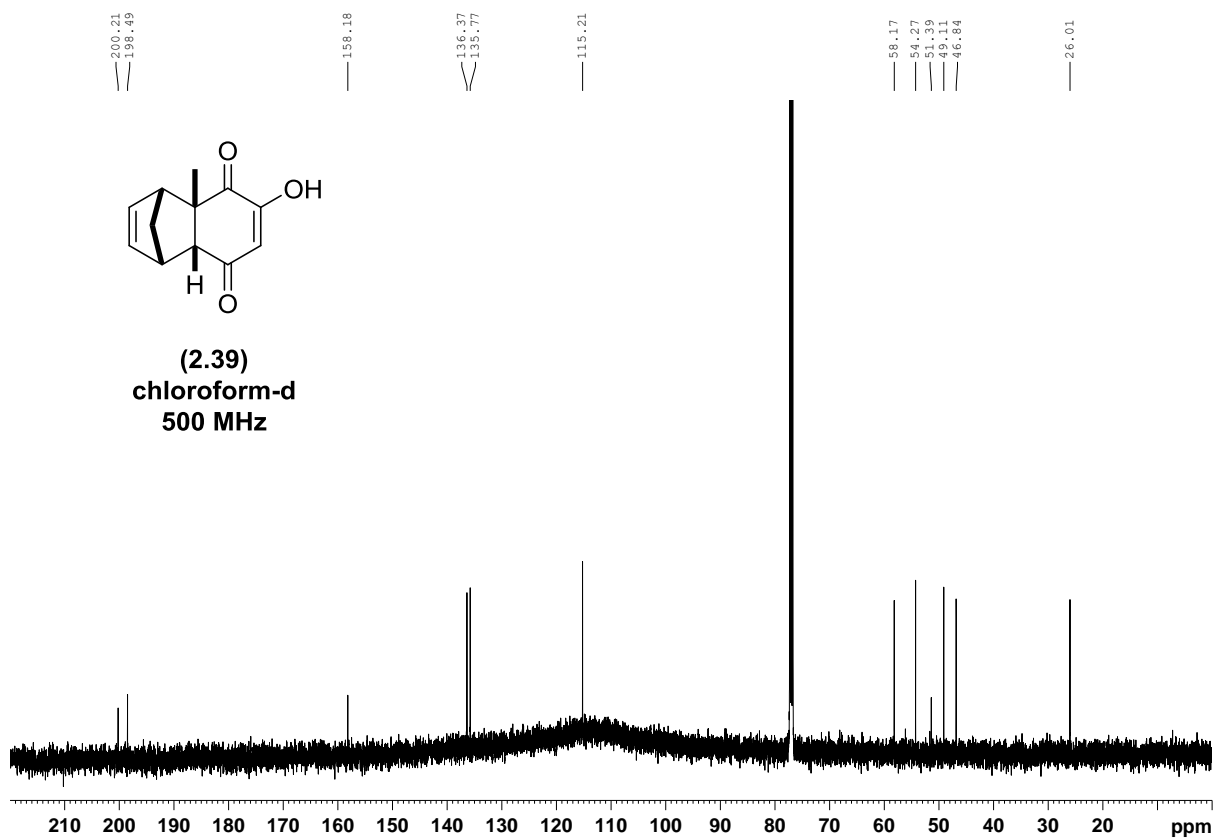
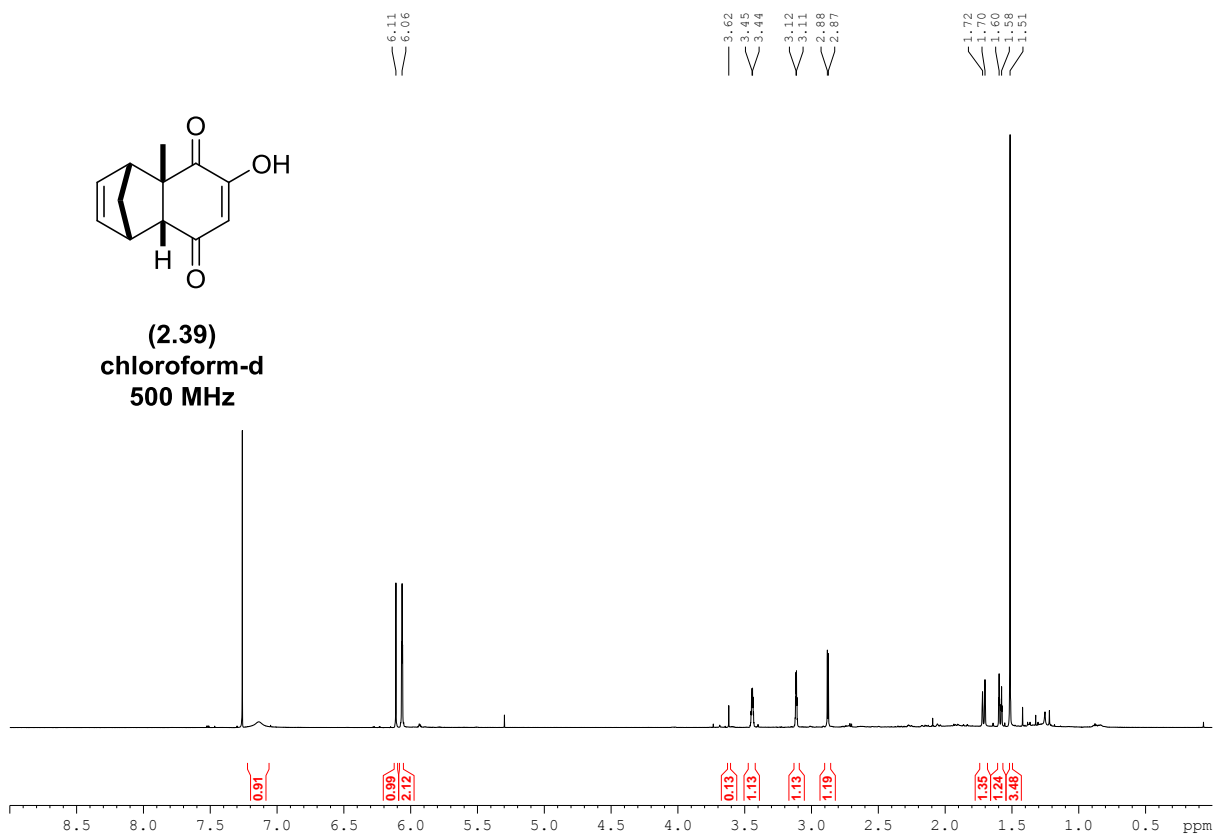




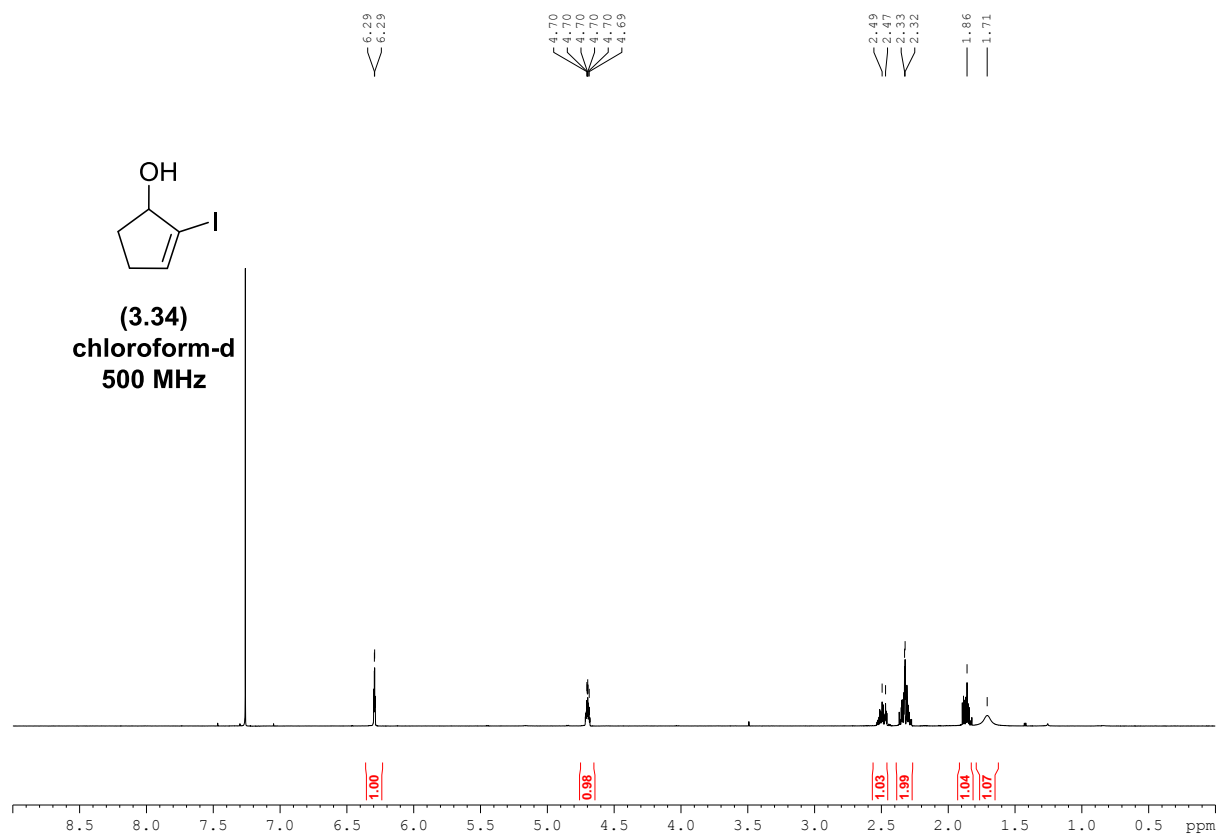
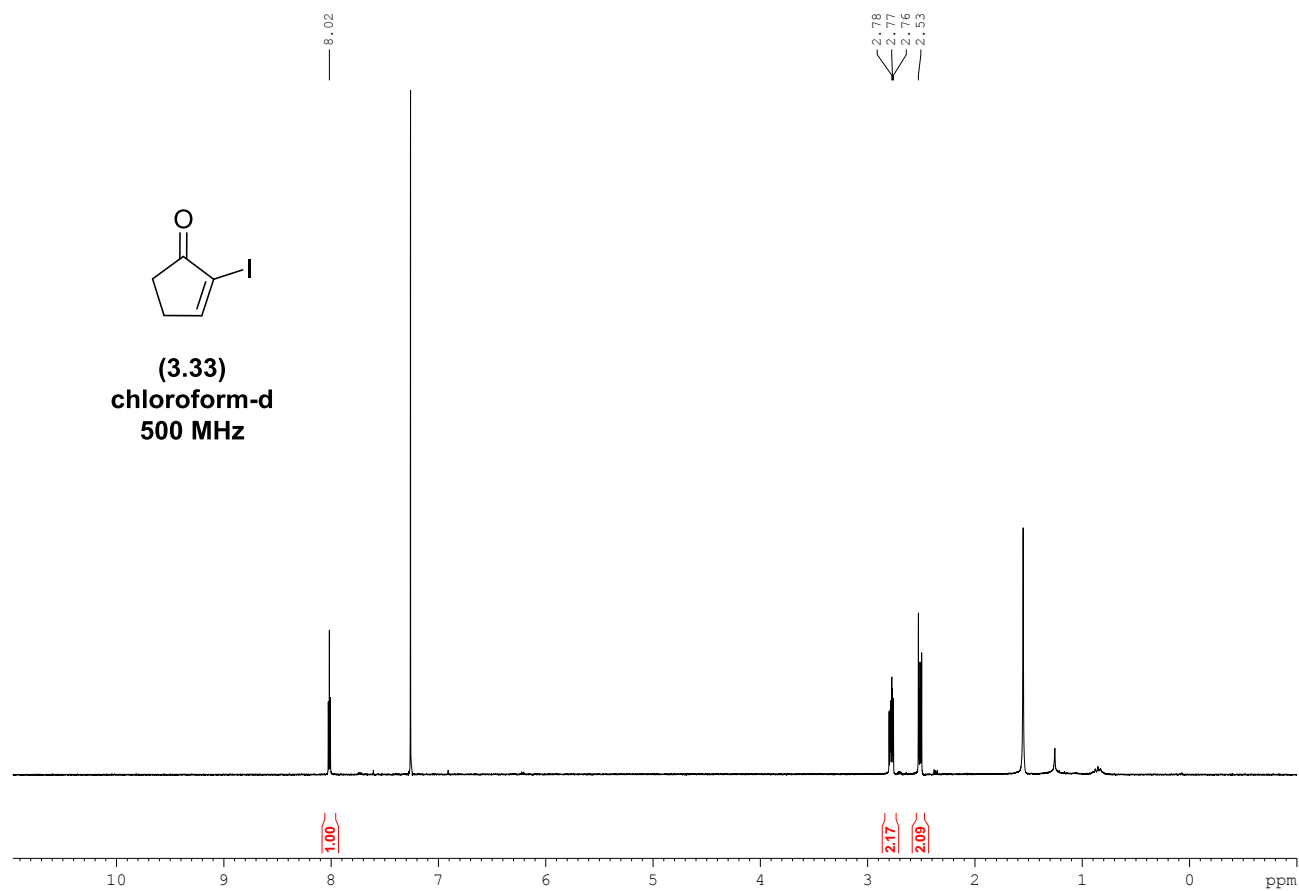


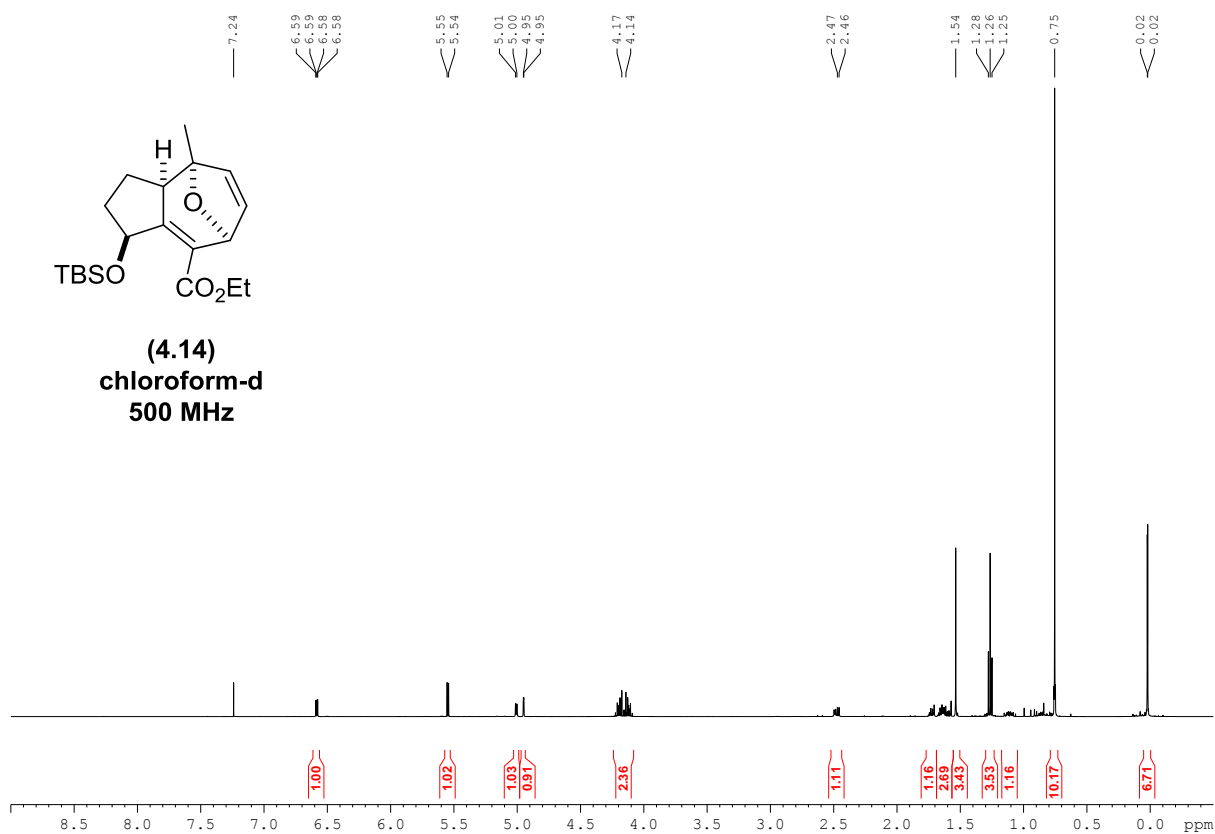
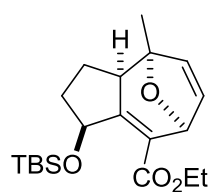
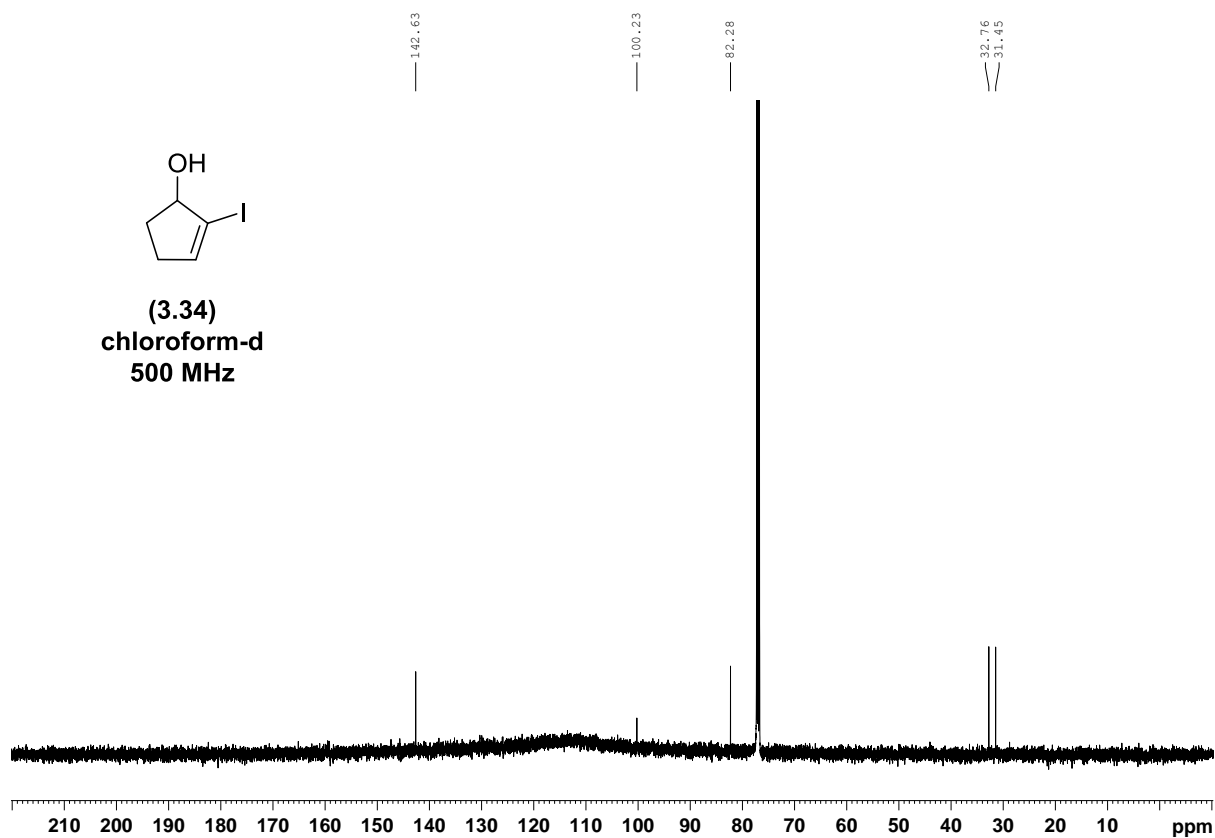
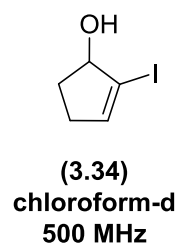


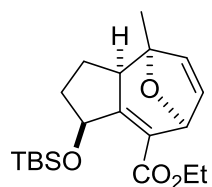




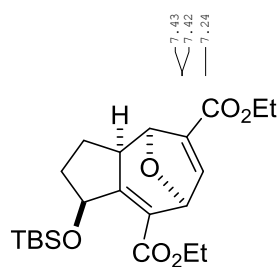
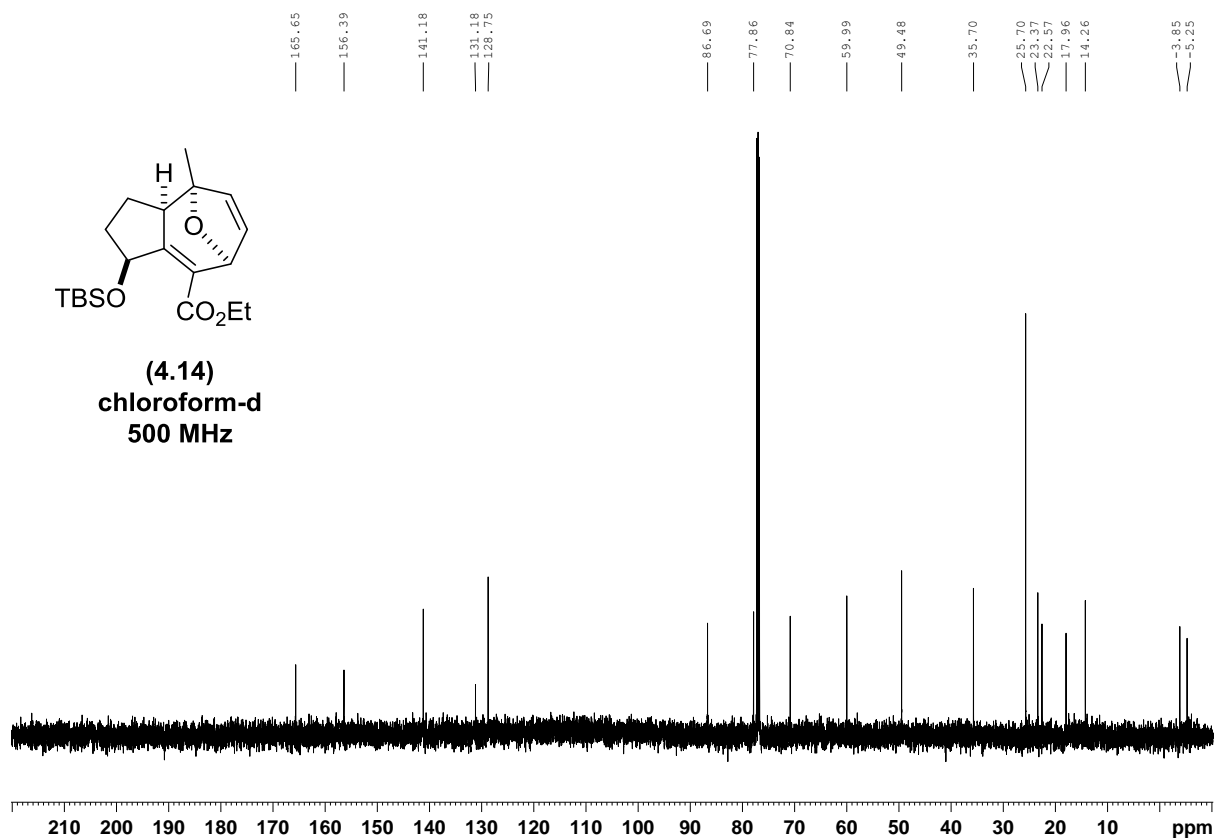
8.2 Appendix B: Supporting NMR Spectra for Chapter 3



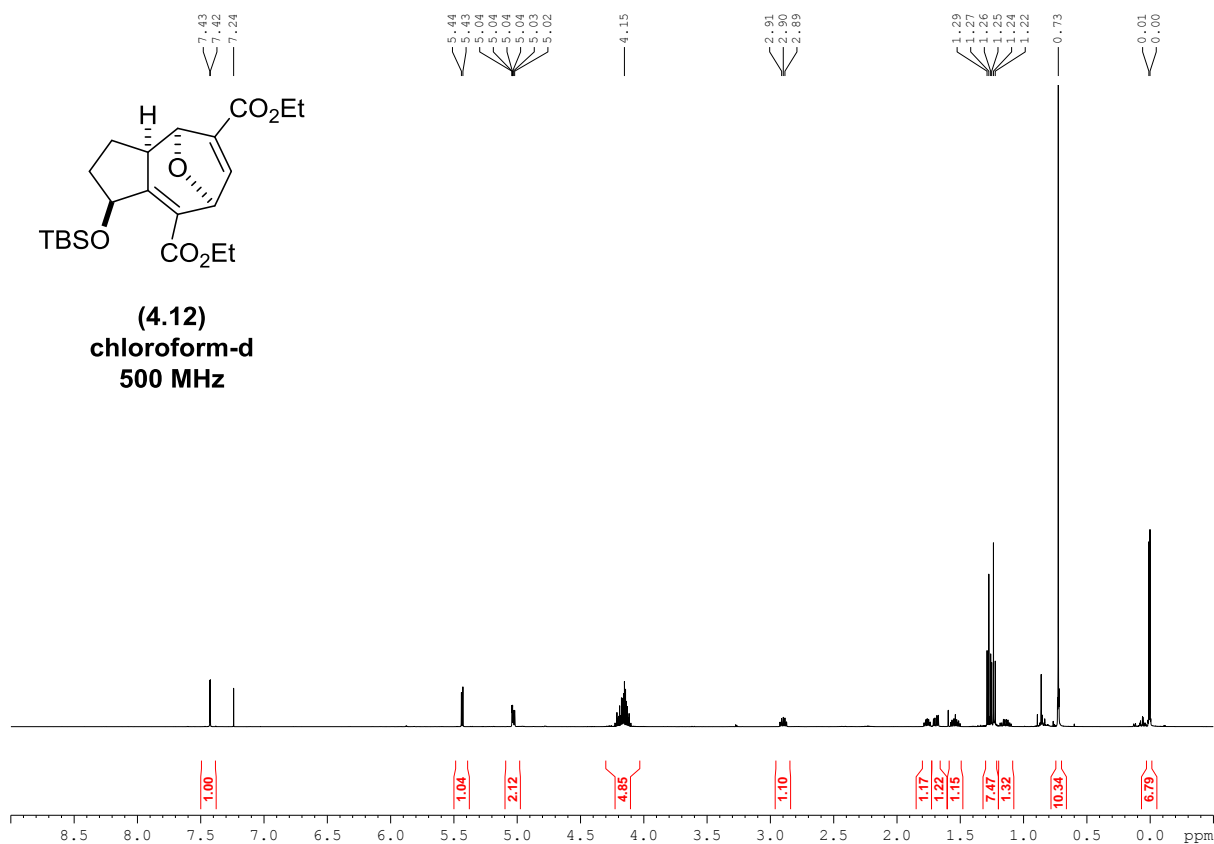


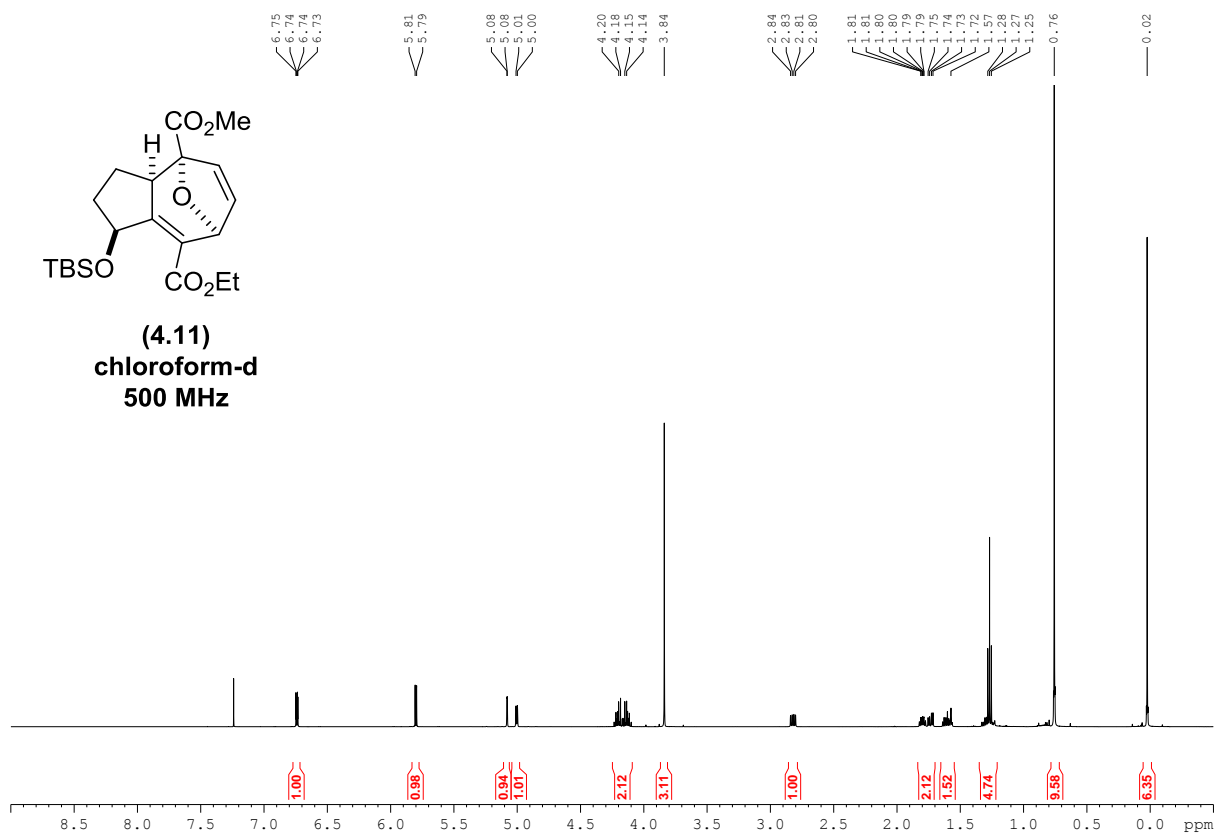
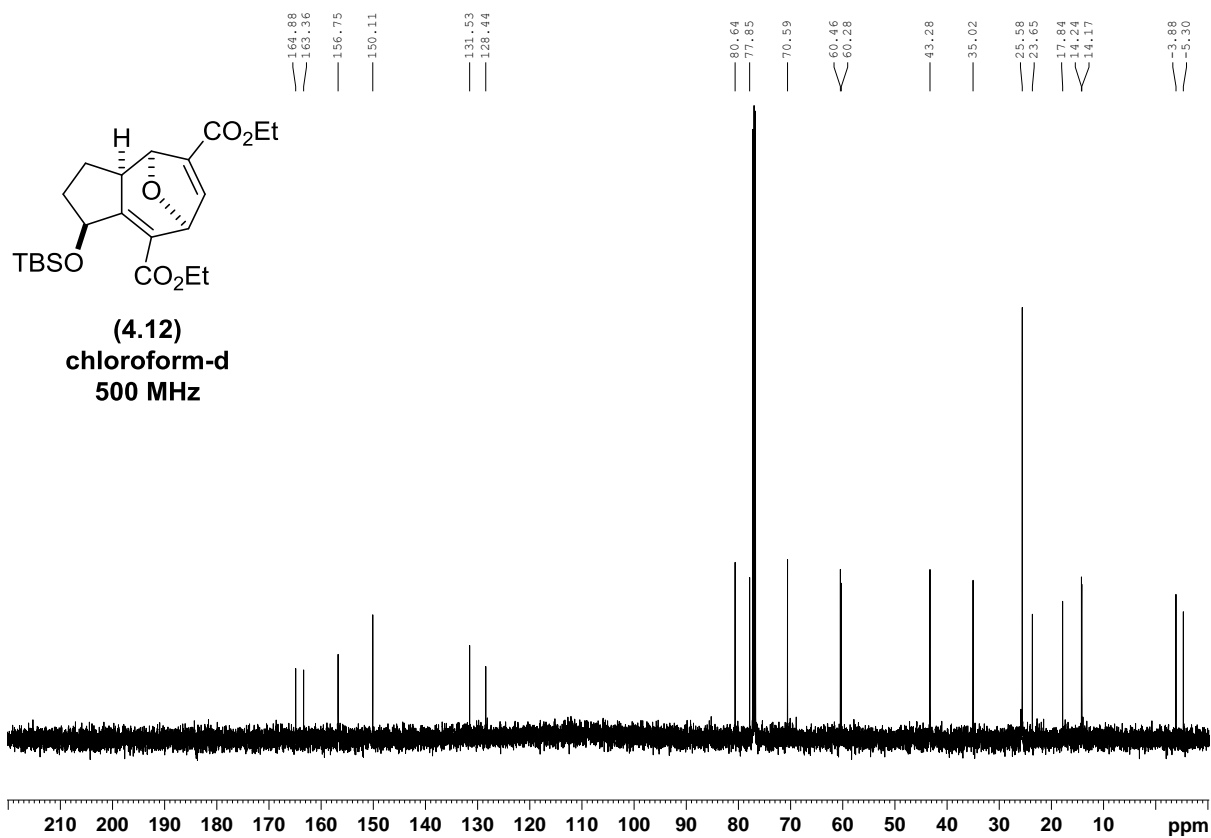


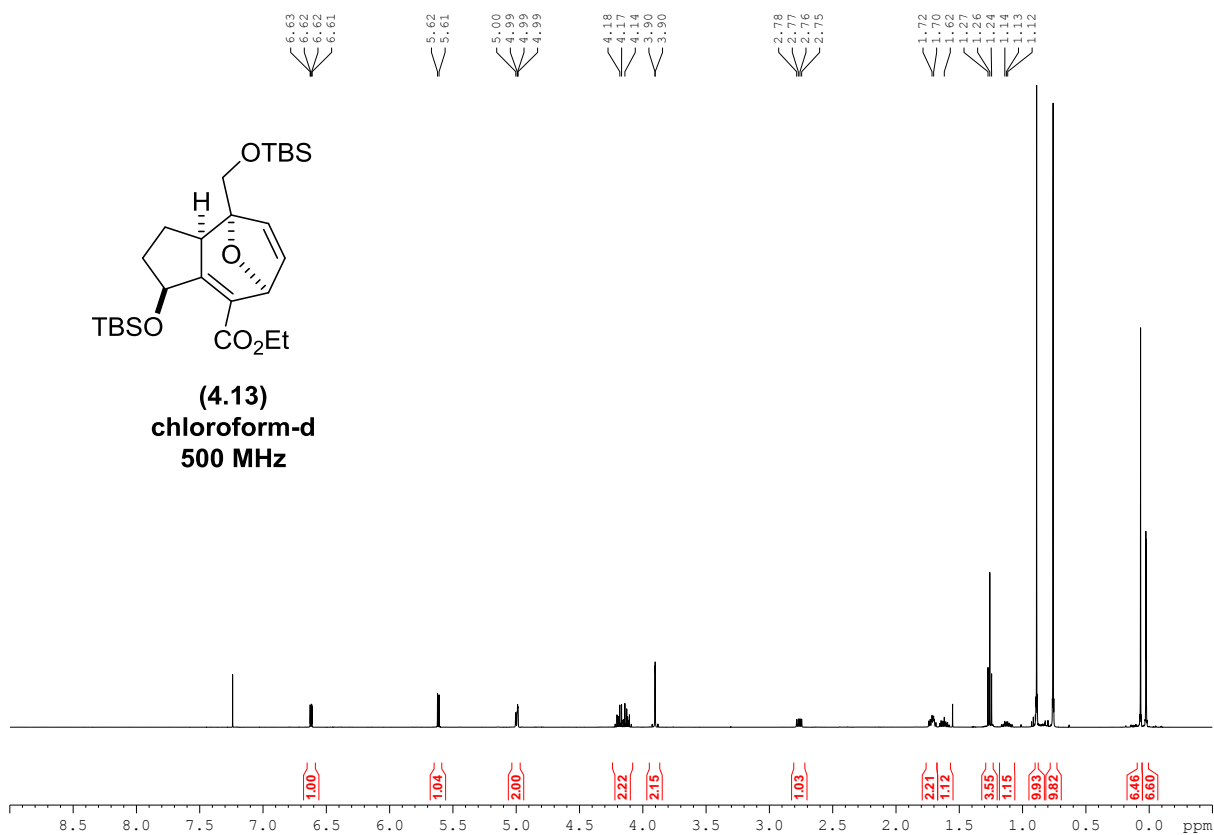
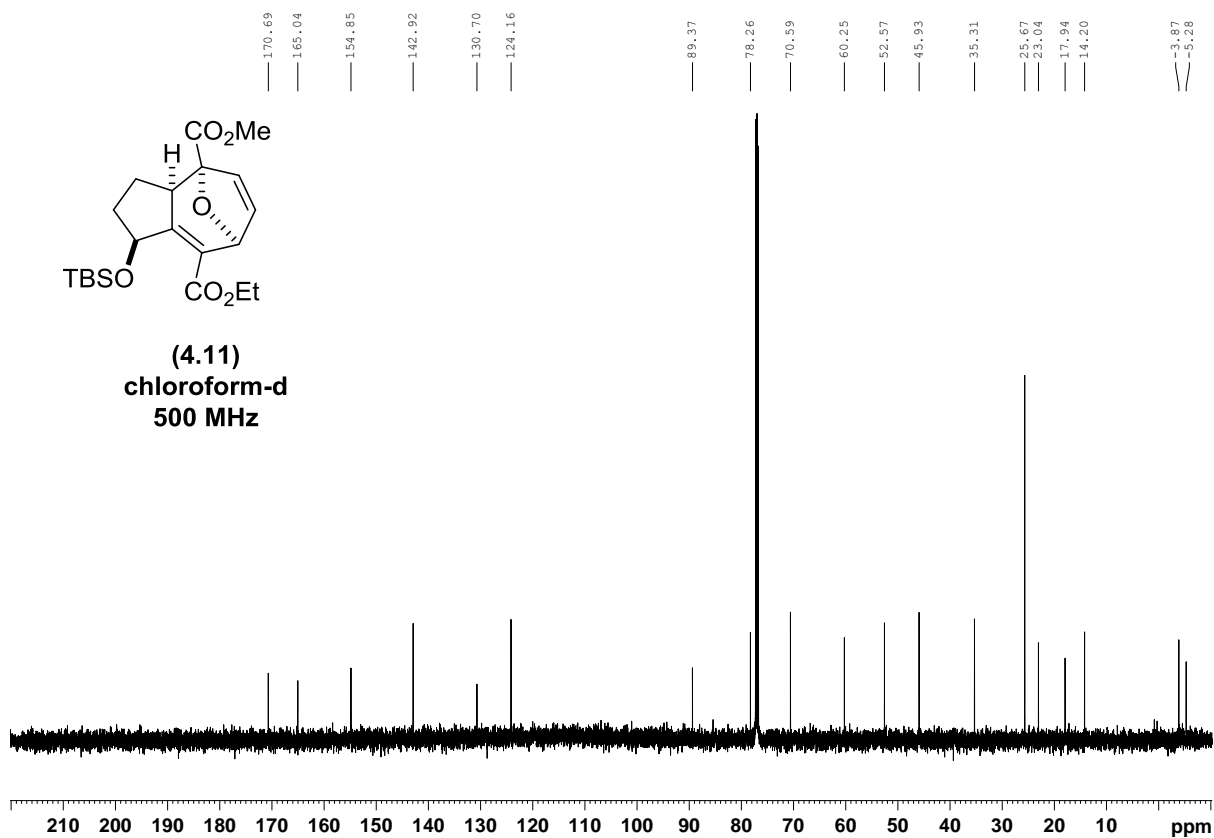
(4.14)
chloroform-d
500 MHz

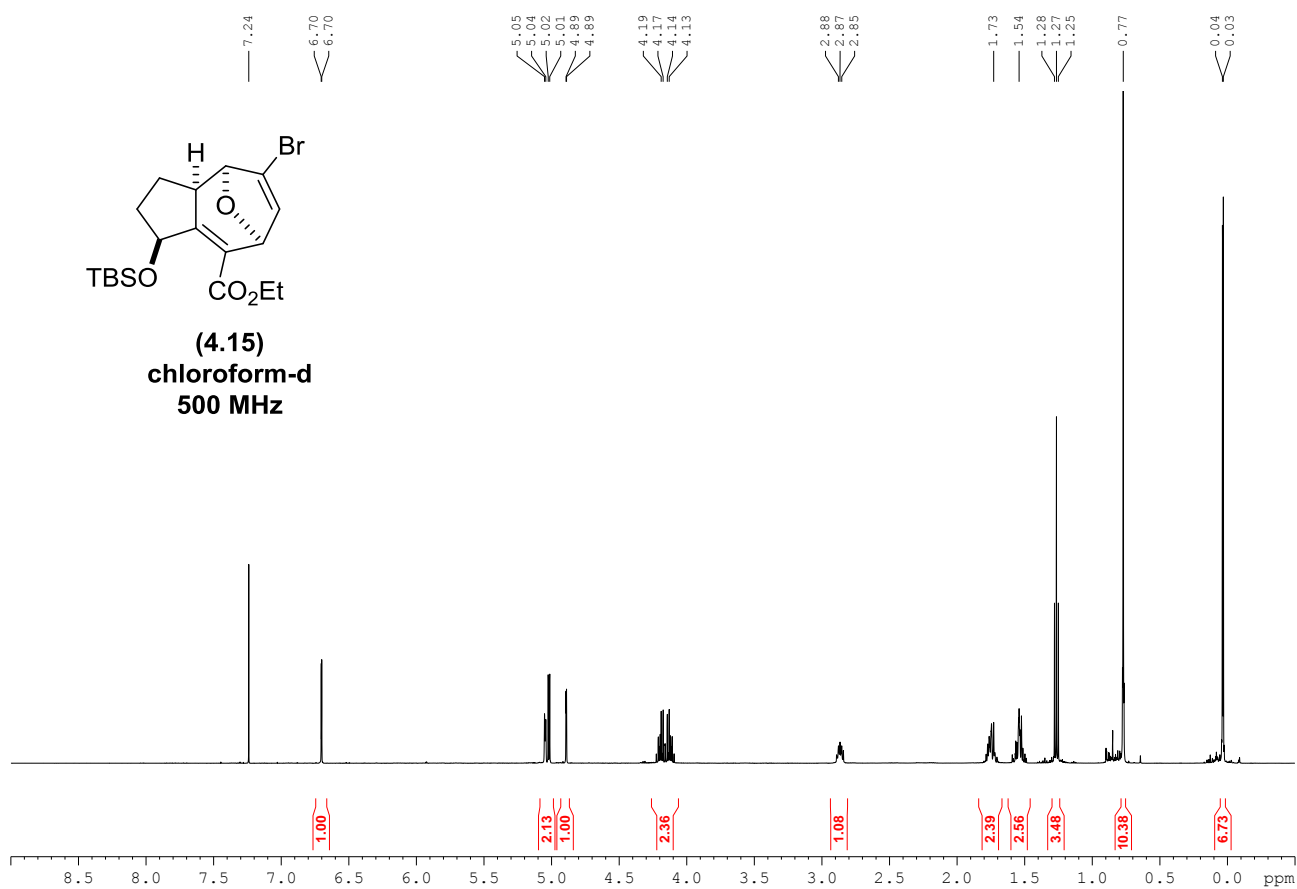
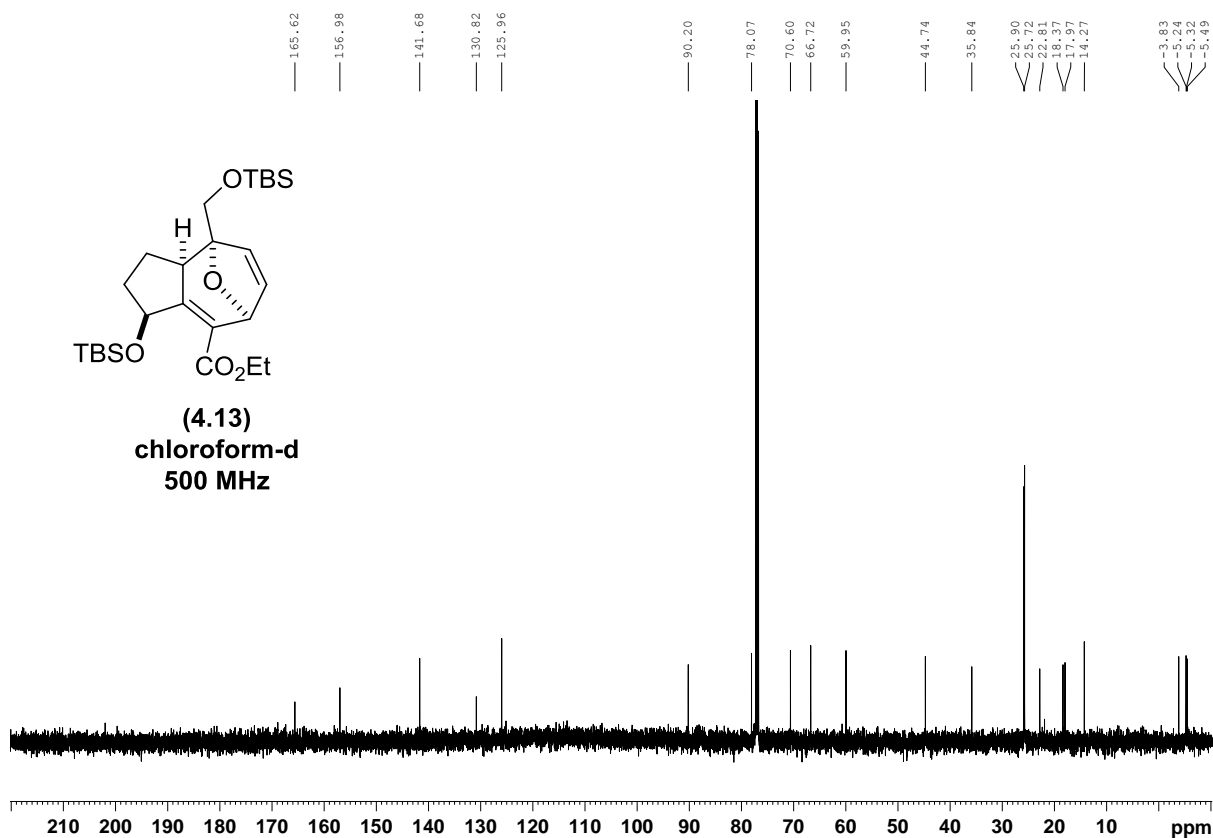


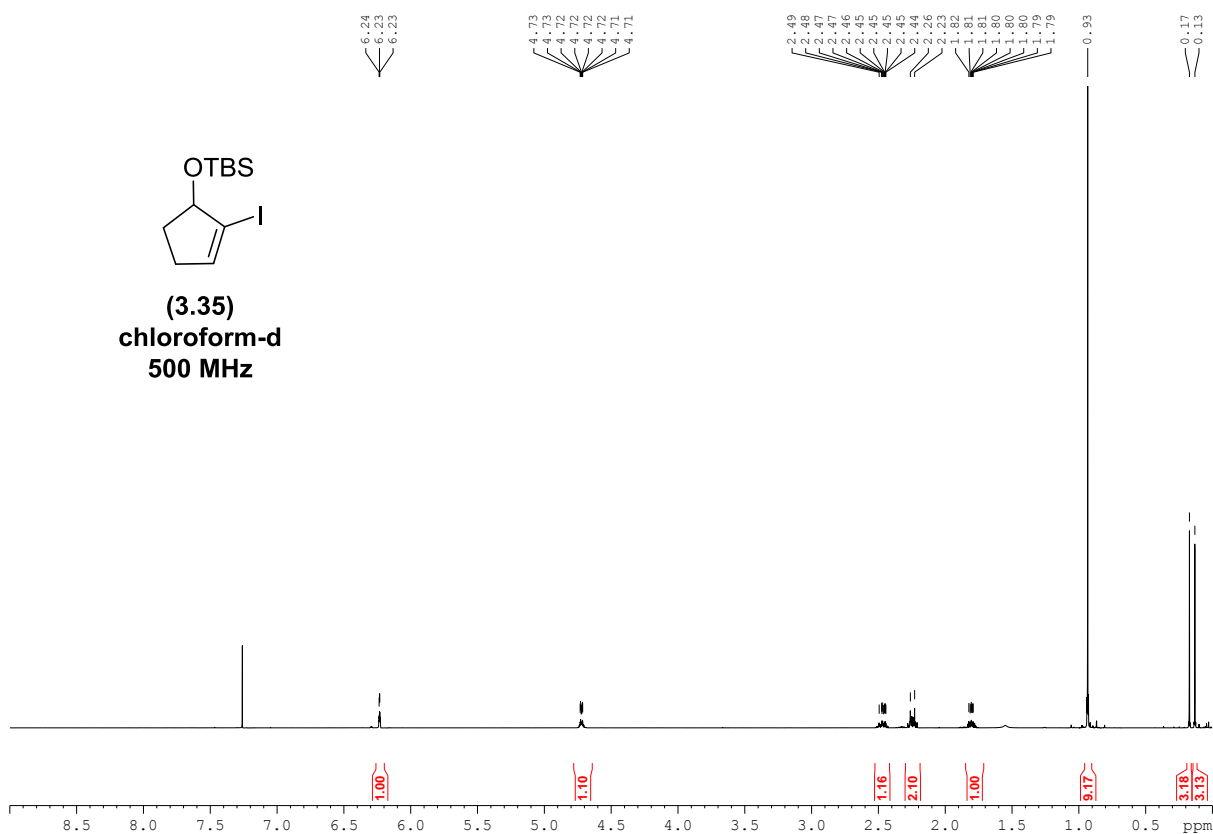
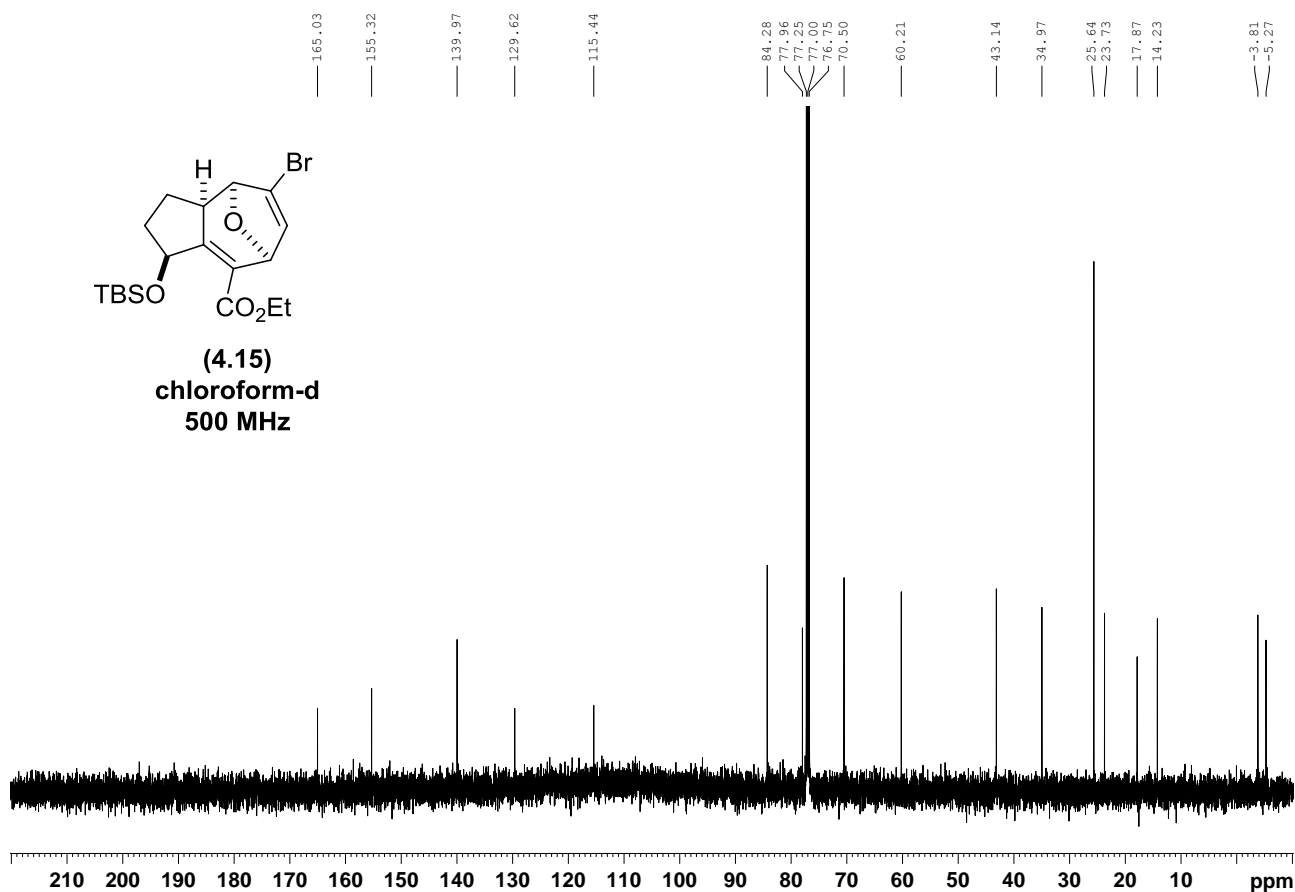
(4.12)
chloroform-d
500 MHz

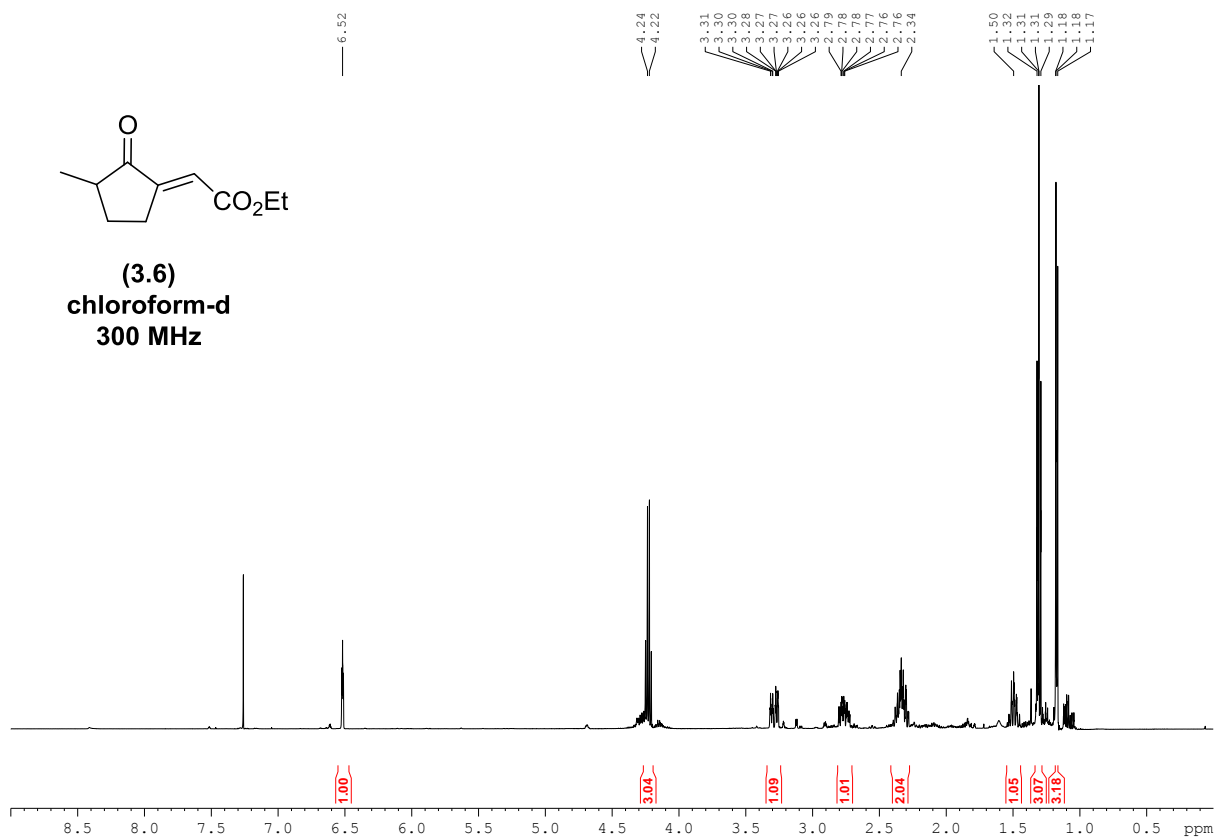
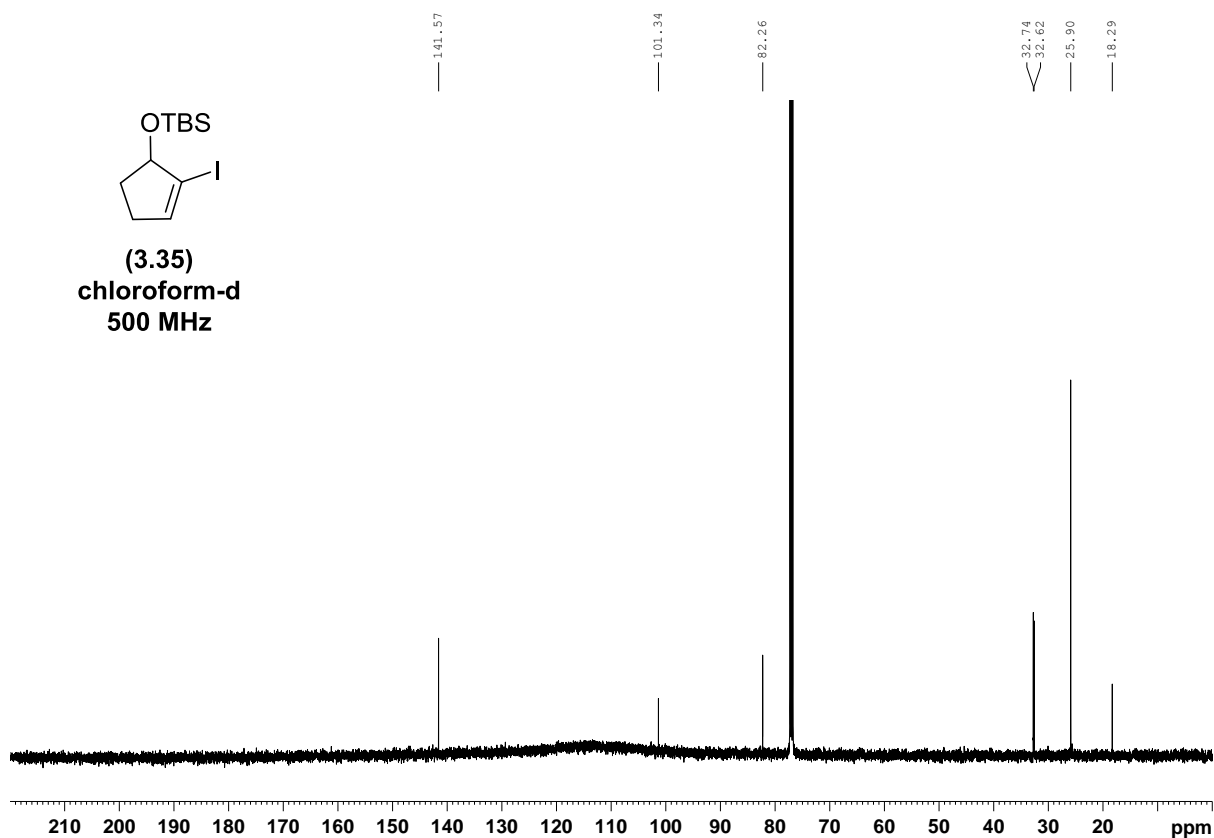


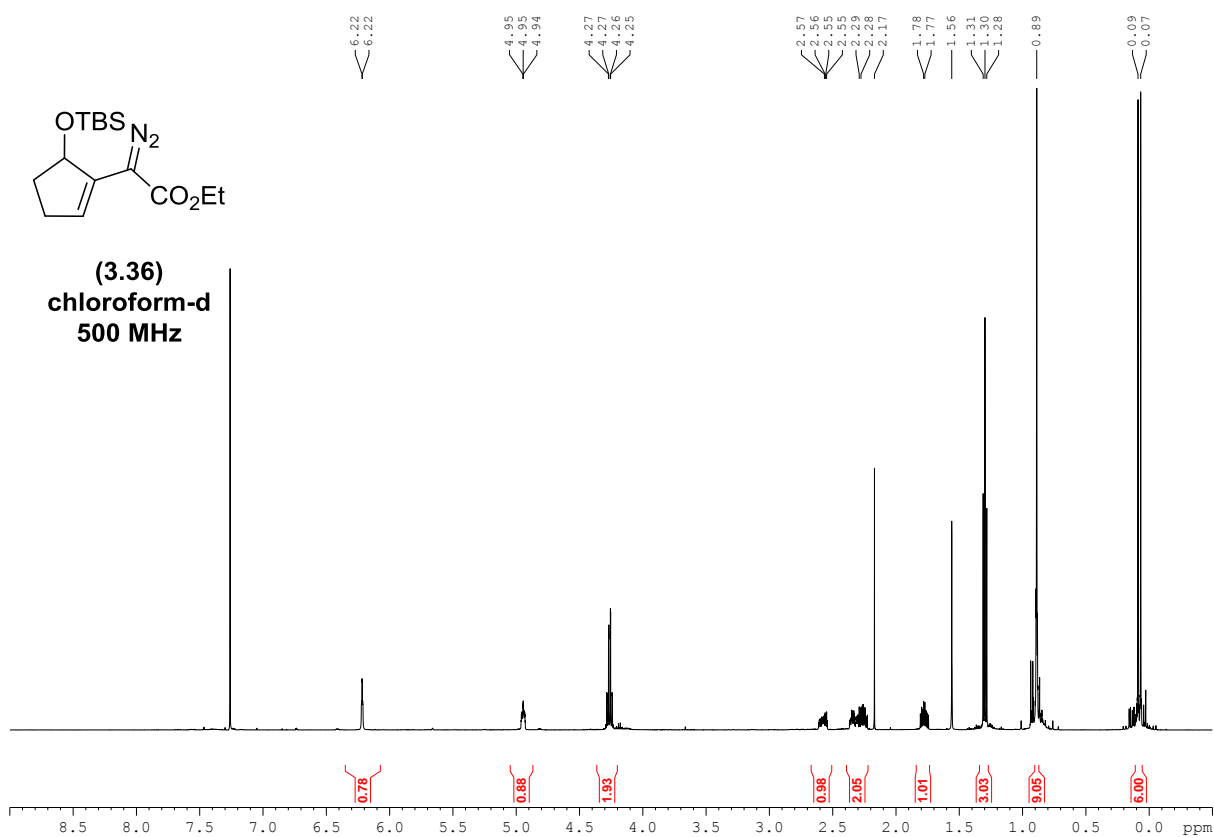
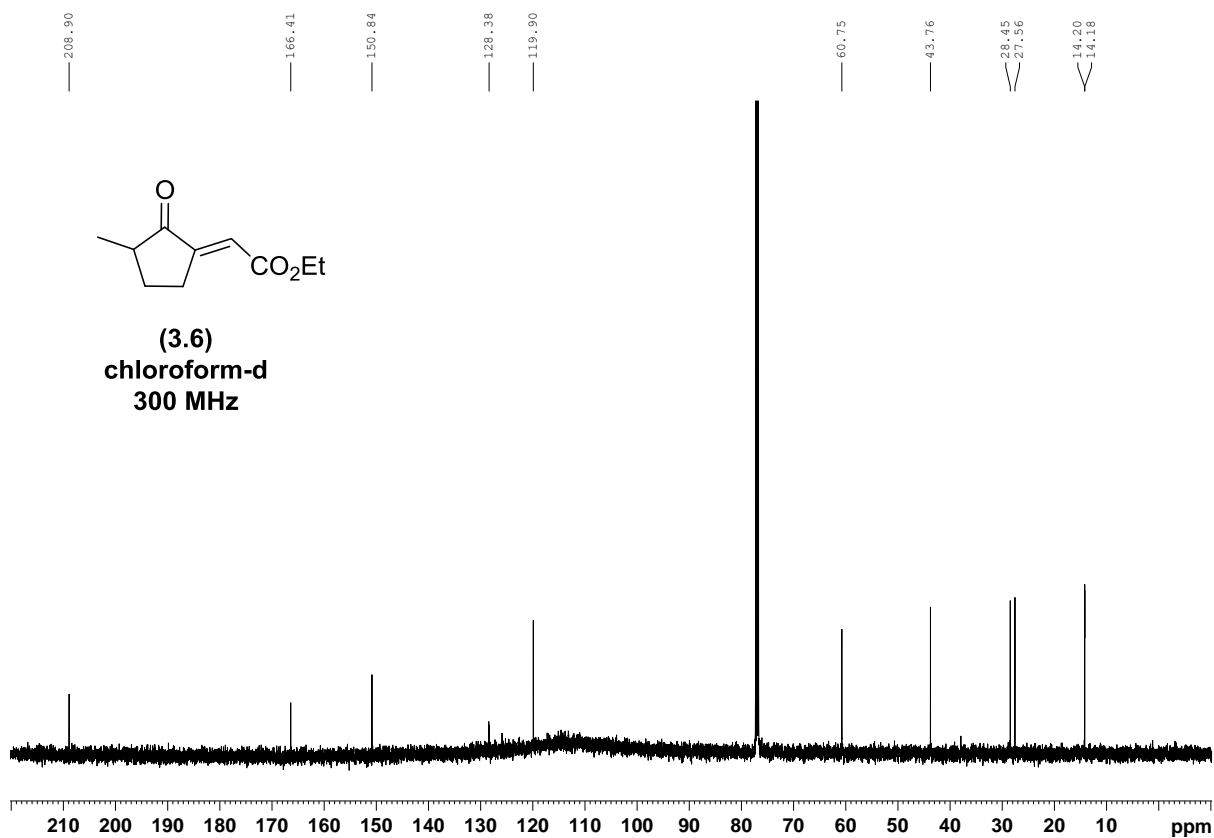


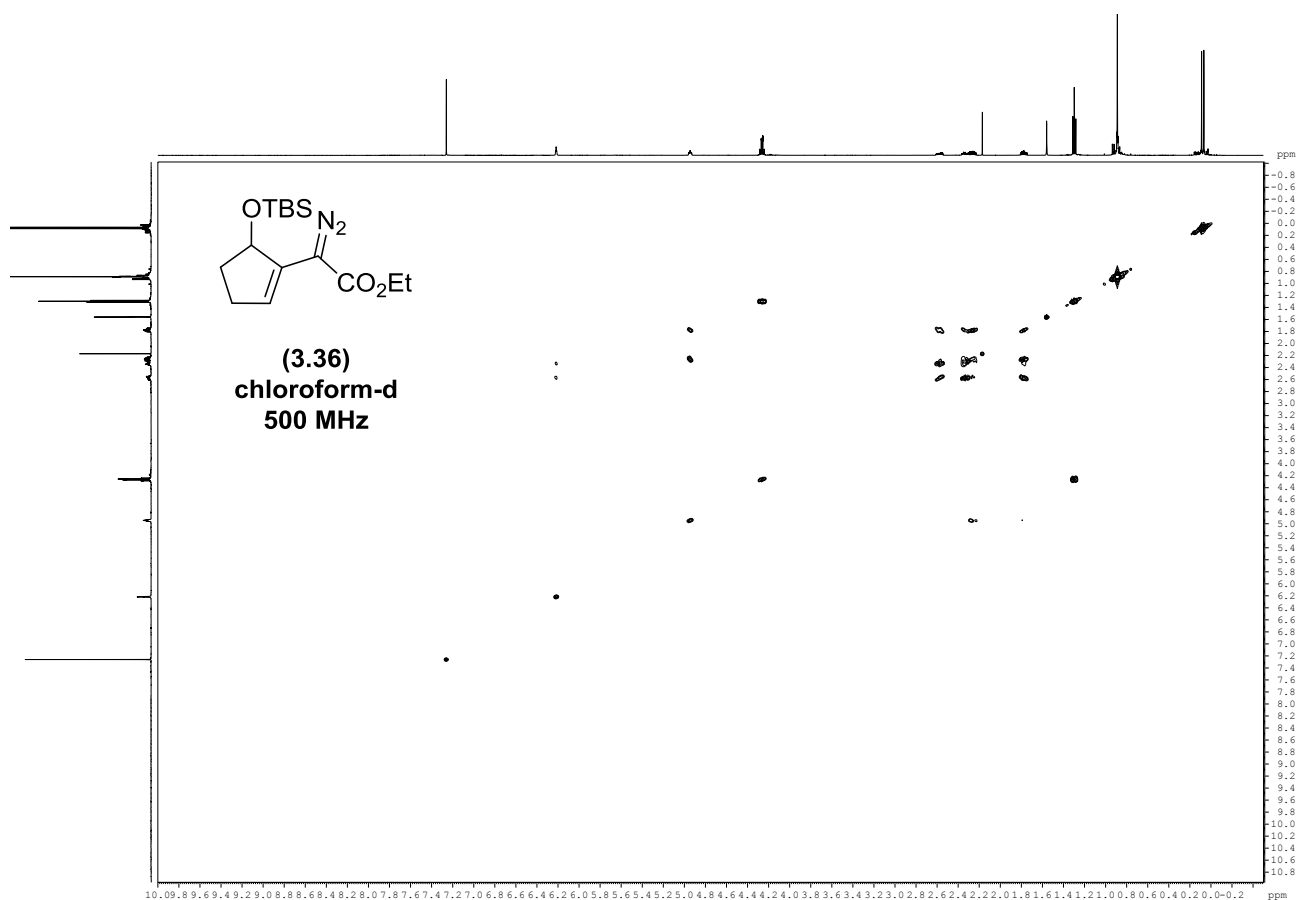
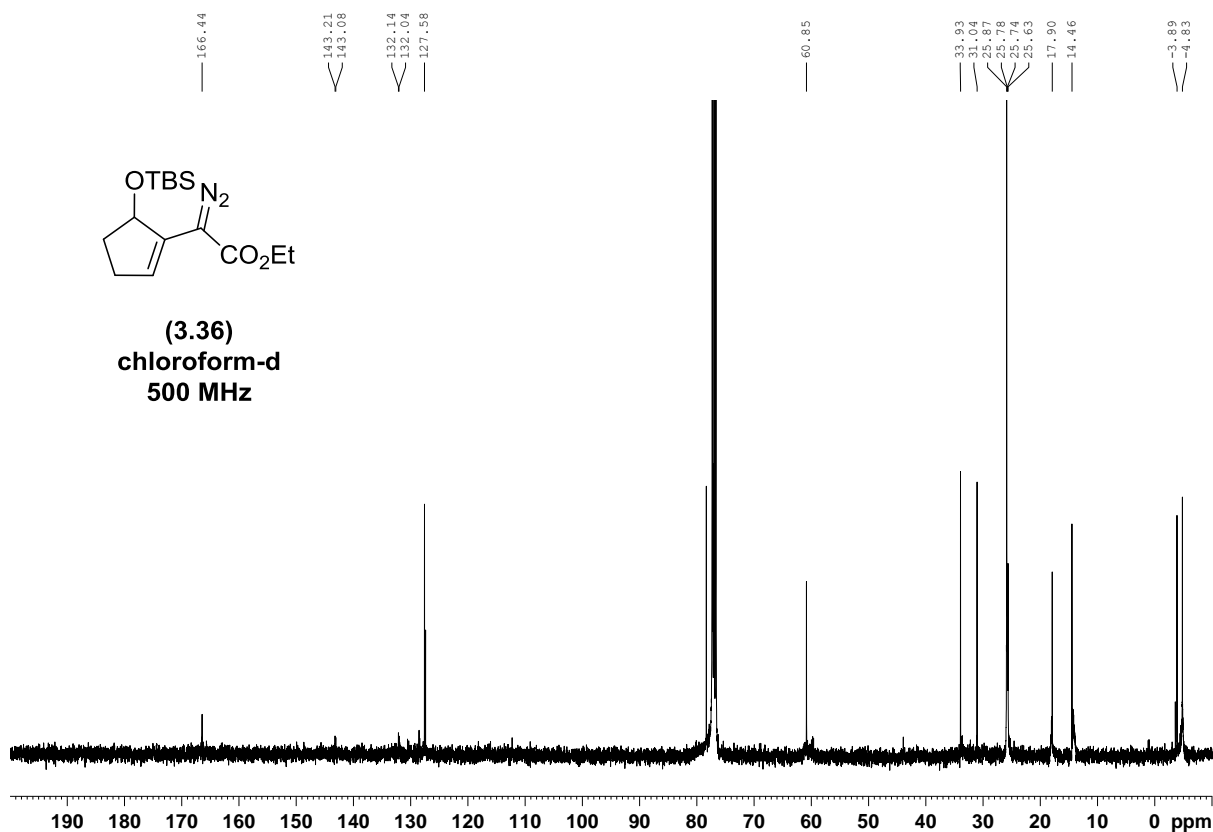


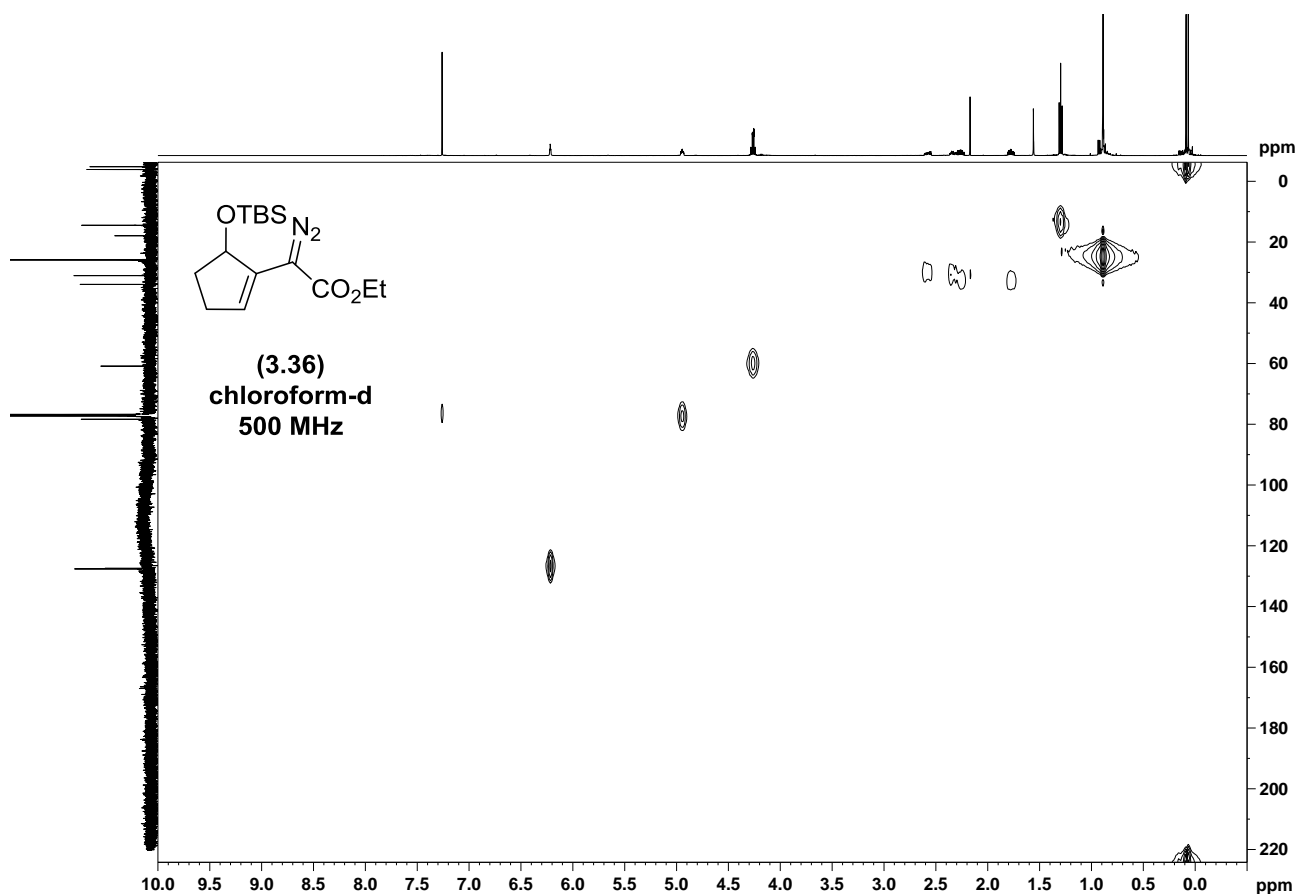












7.29
7.28

4.15
4.12

3.49
3.46

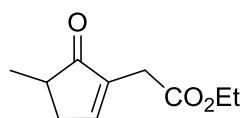
3.22
3.22

2.80

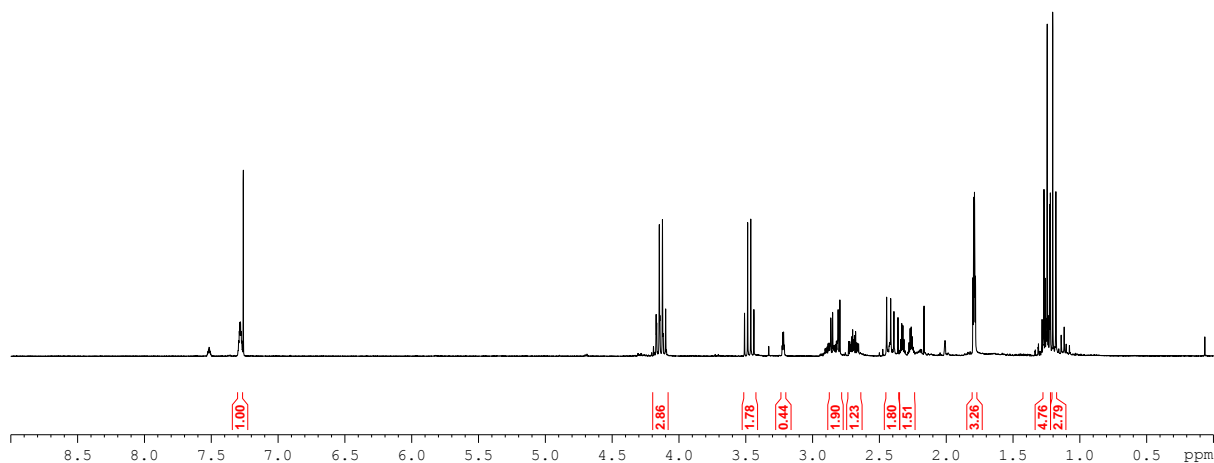
2.45
2.42

1.79
1.79

1.24
1.20



(1.199)
 chloroform-d
 400 MHz



1.00

2.86

1.78

0.44

1.90

1.23

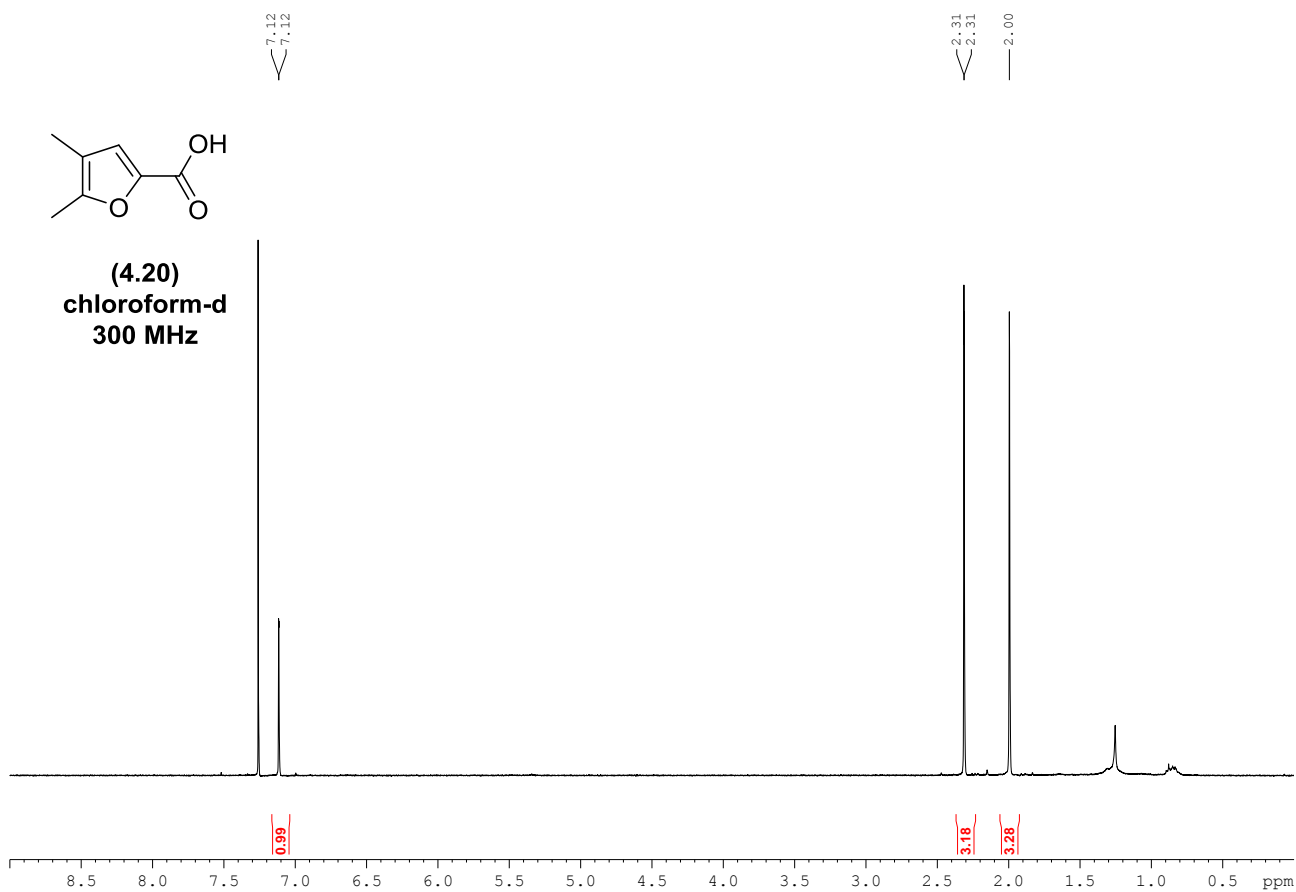
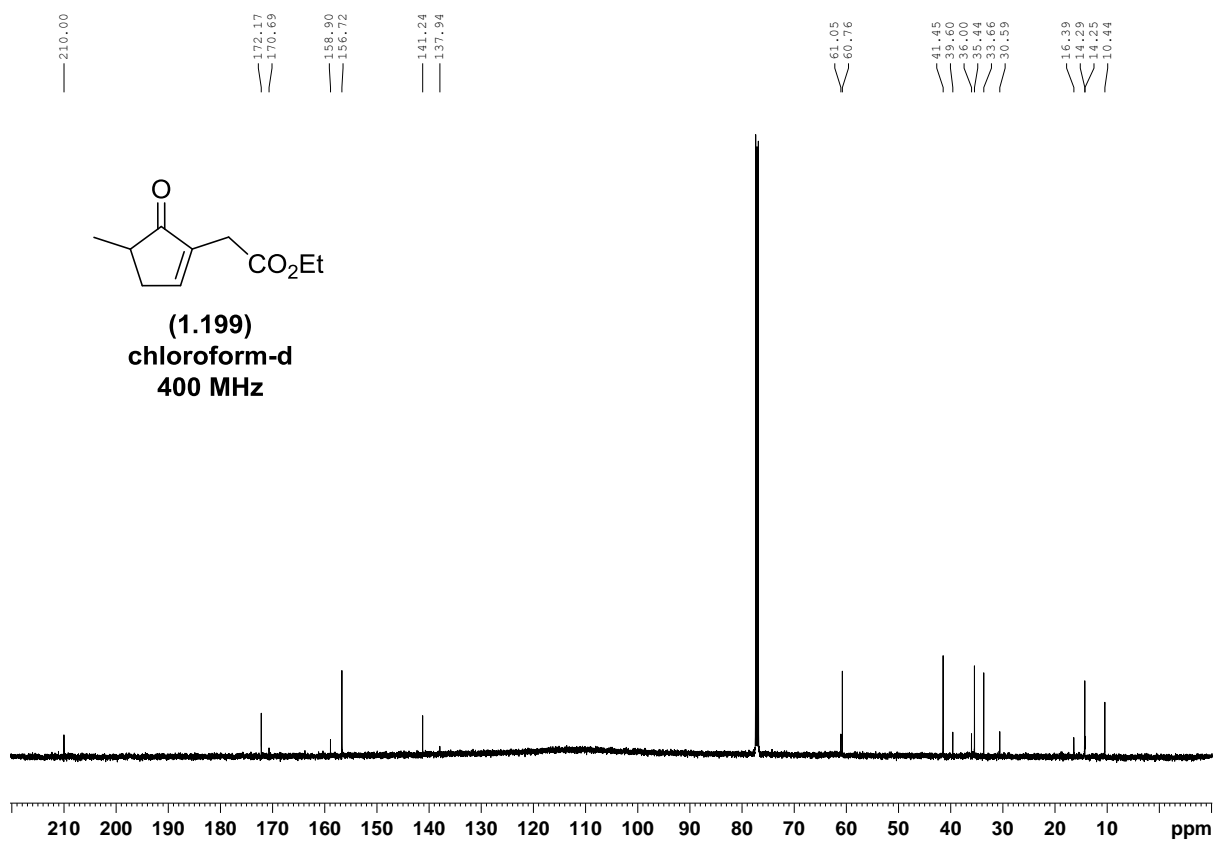
1.80

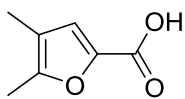
1.91

3.26

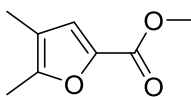
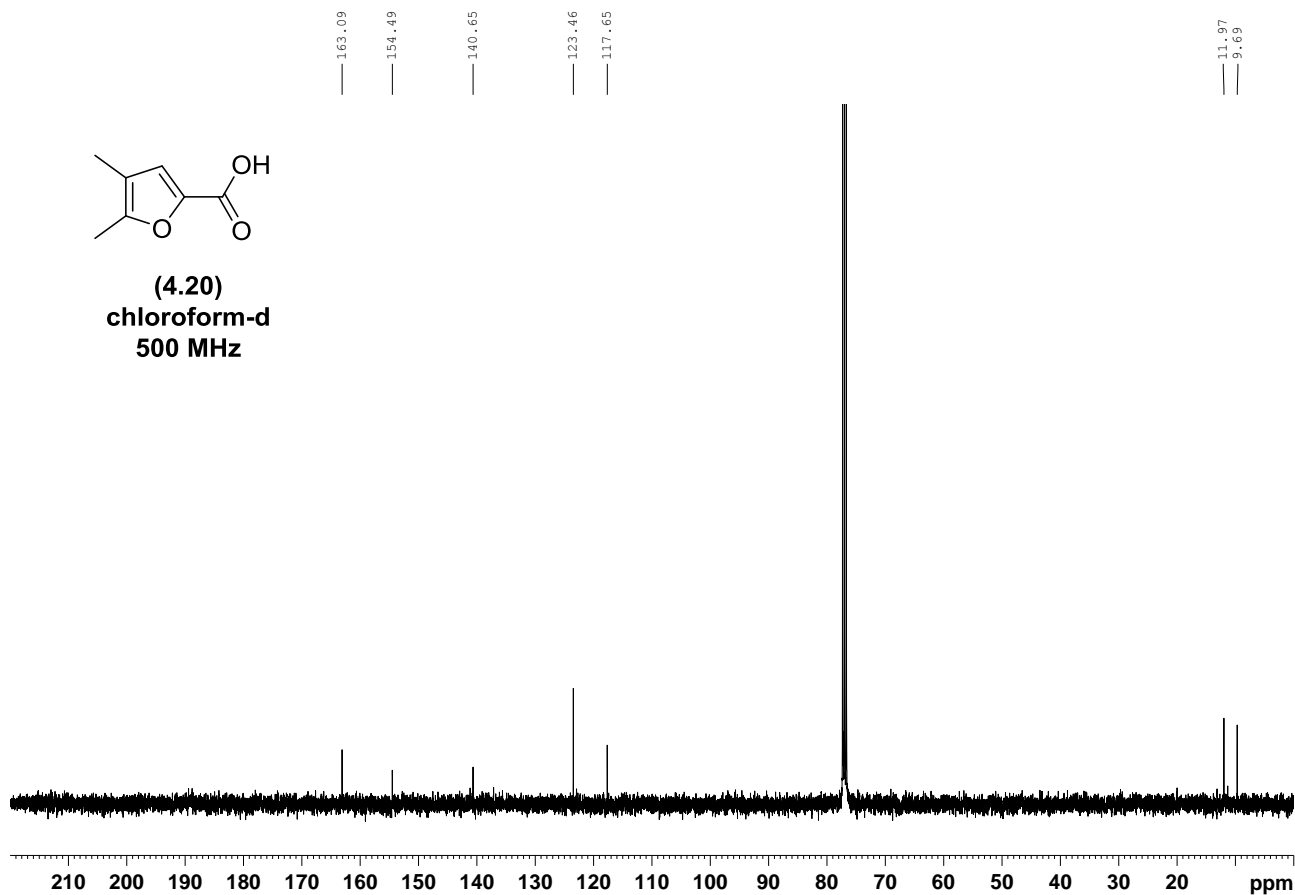
4.76

2.79

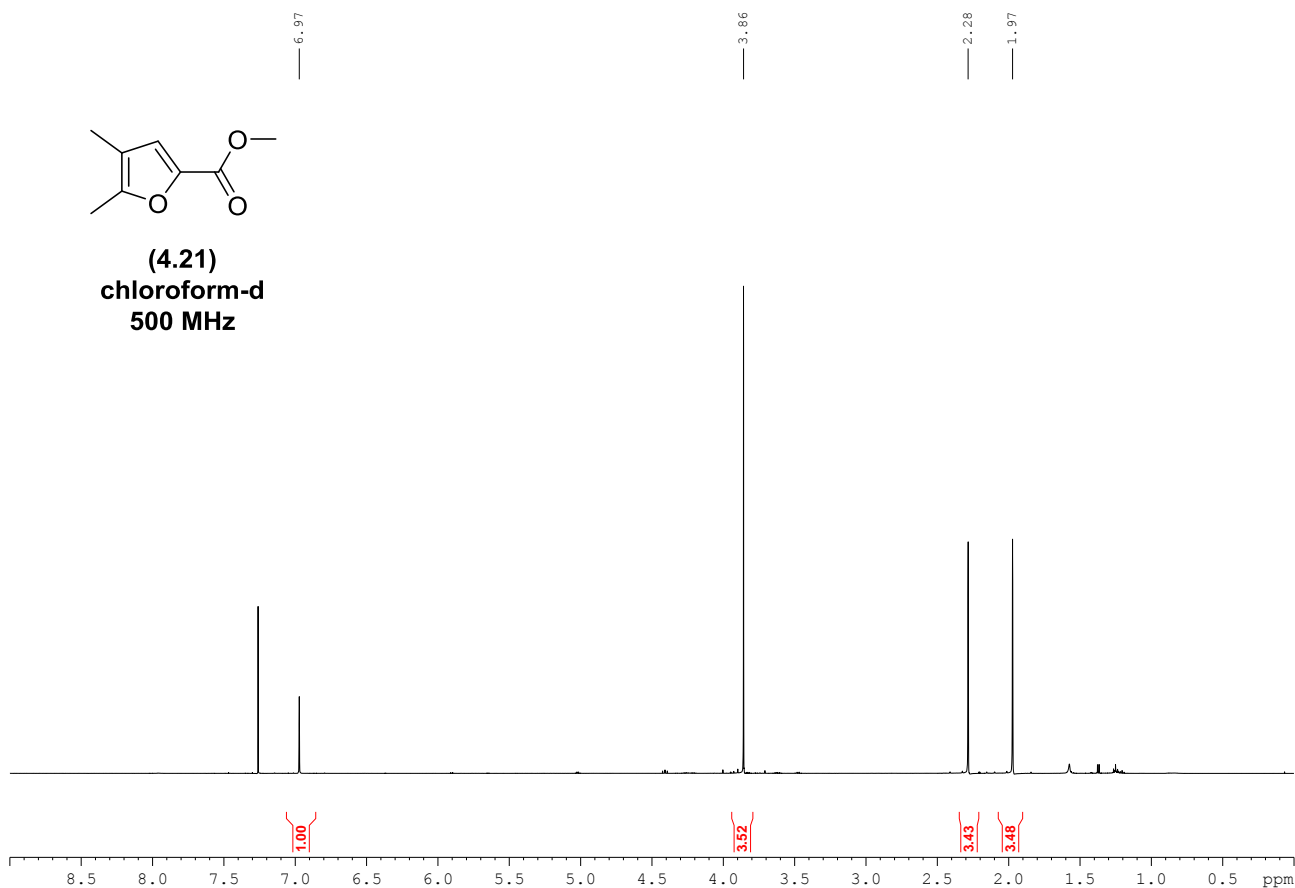


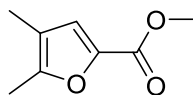


(4.20)
chloroform-d
500 MHz

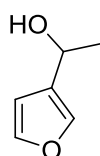
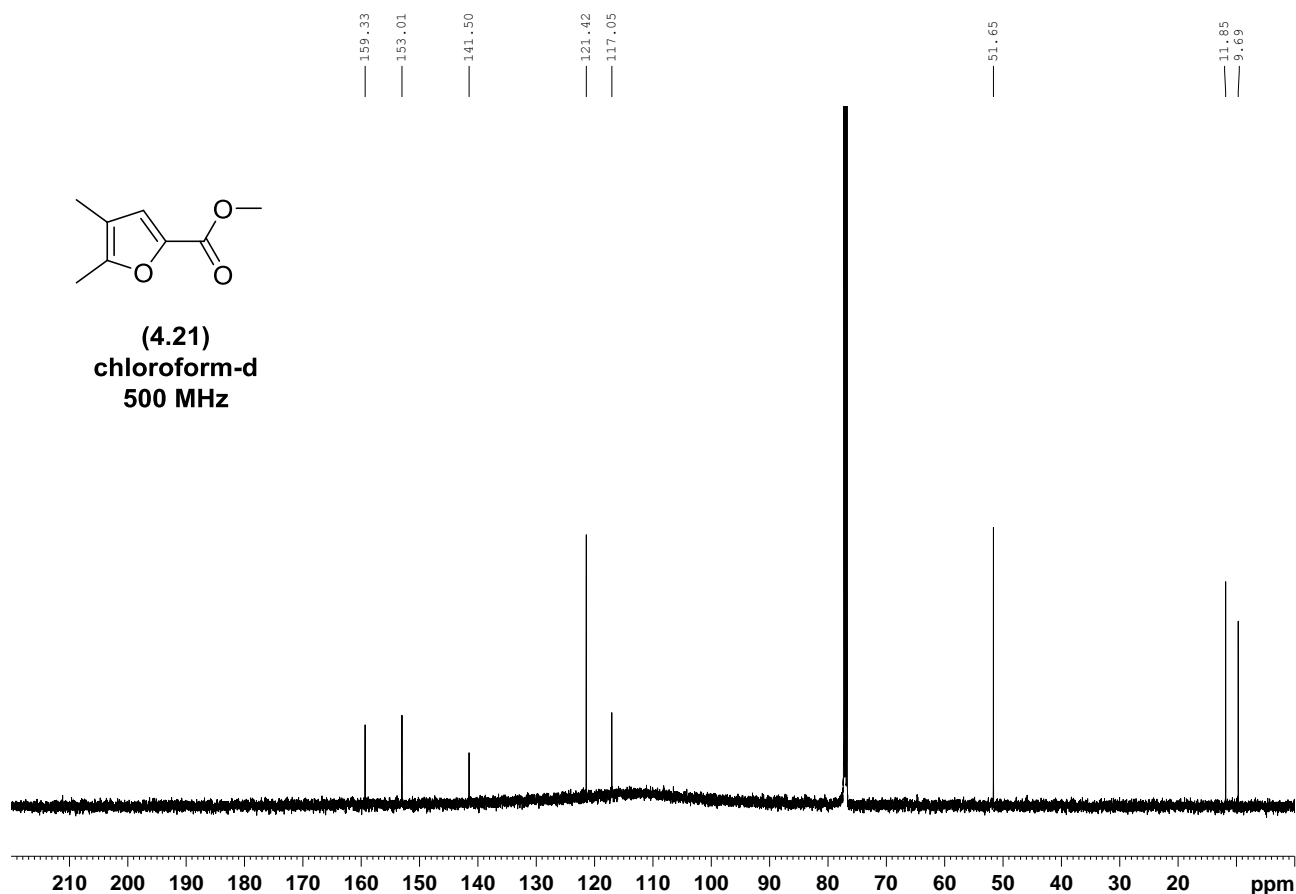


(4.21)
chloroform-d
500 MHz

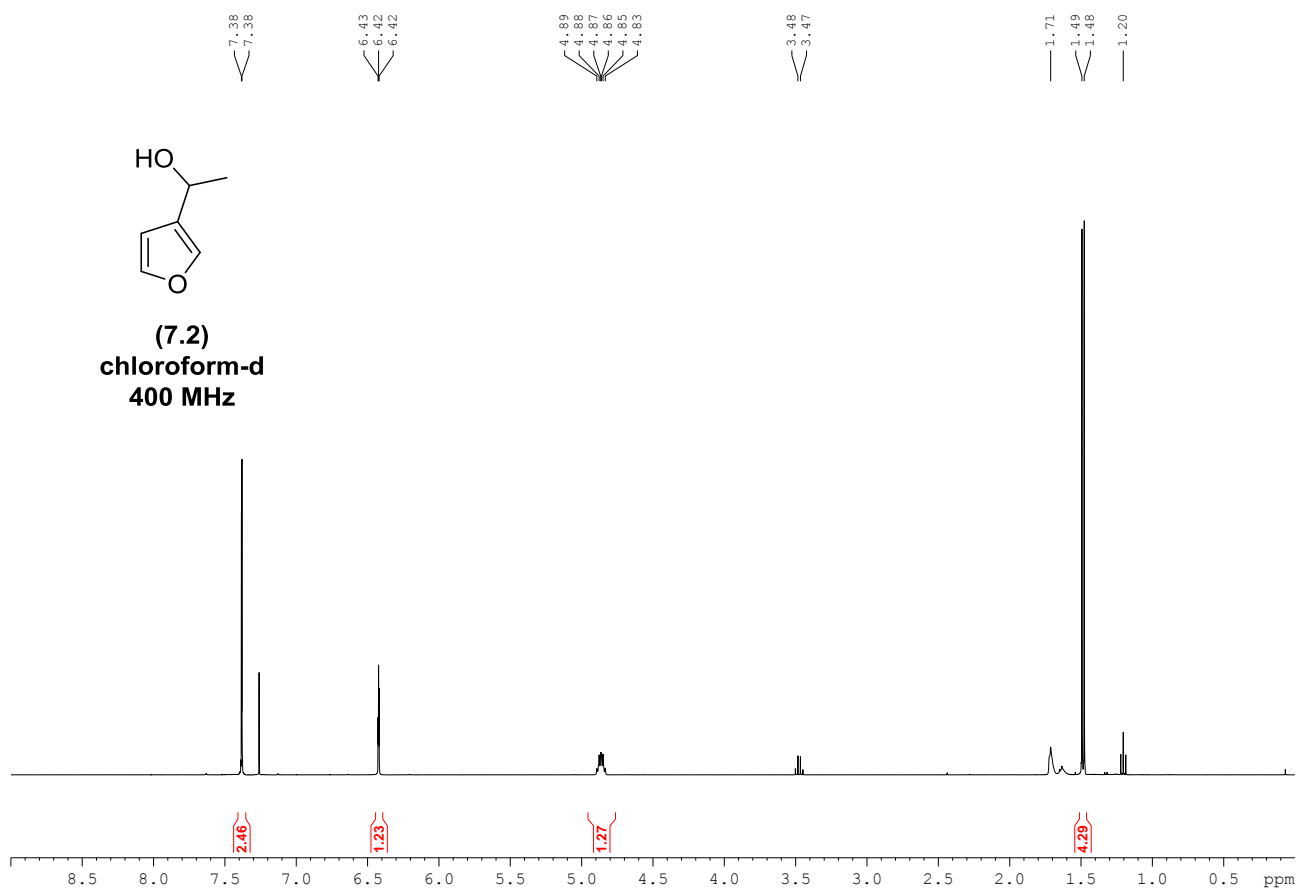


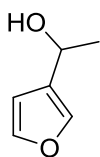


(4.21)
chloroform-d
500 MHz



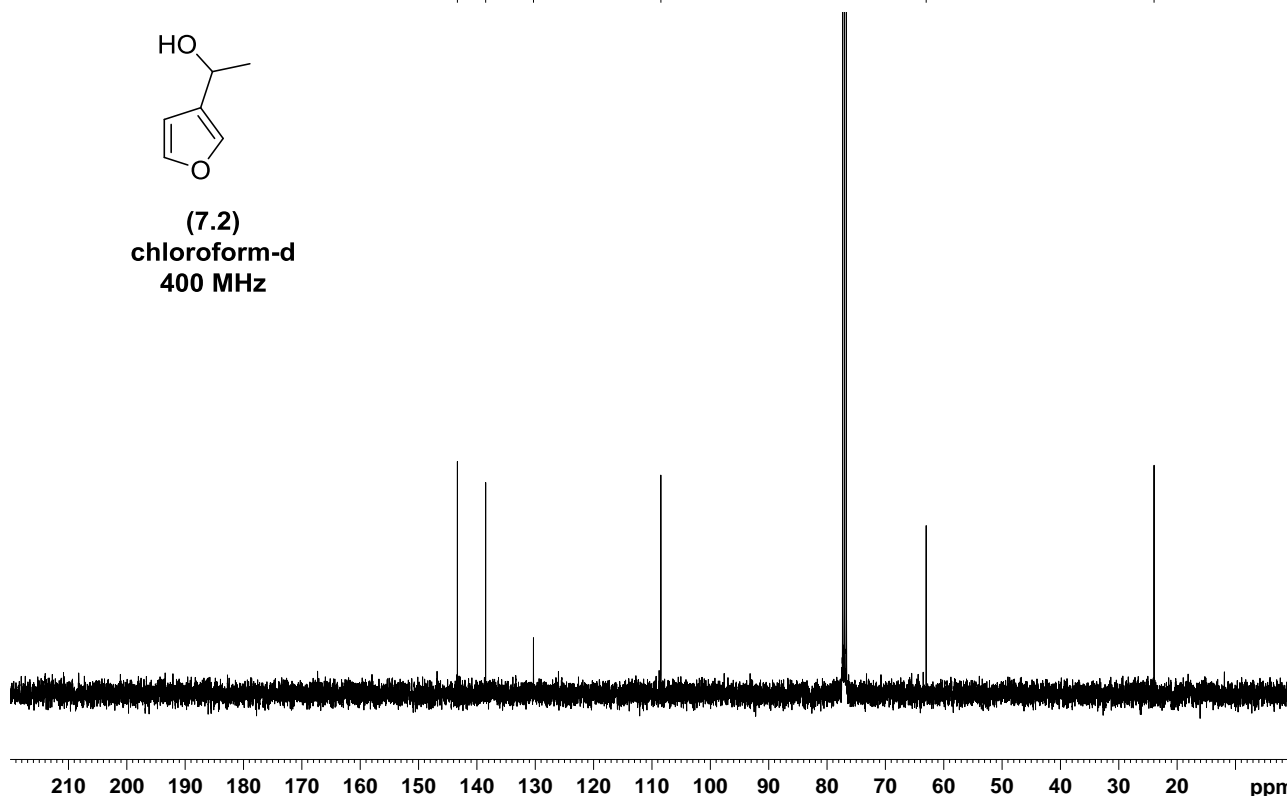
(7.2)
chloroform-d
400 MHz



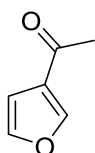


(7.2)
chloroform-d
400 MHz

143.34
138.50
130.30
108.47
63.01
23.96

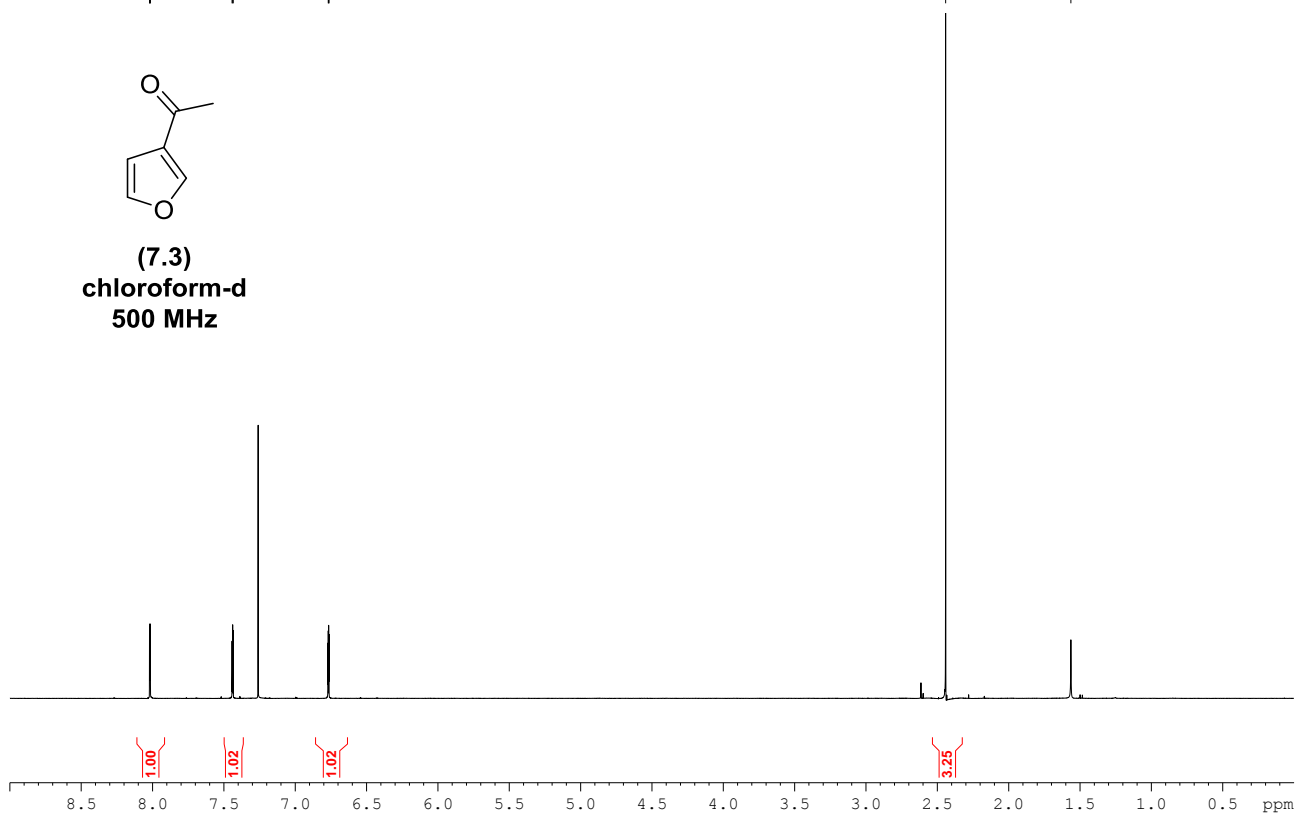


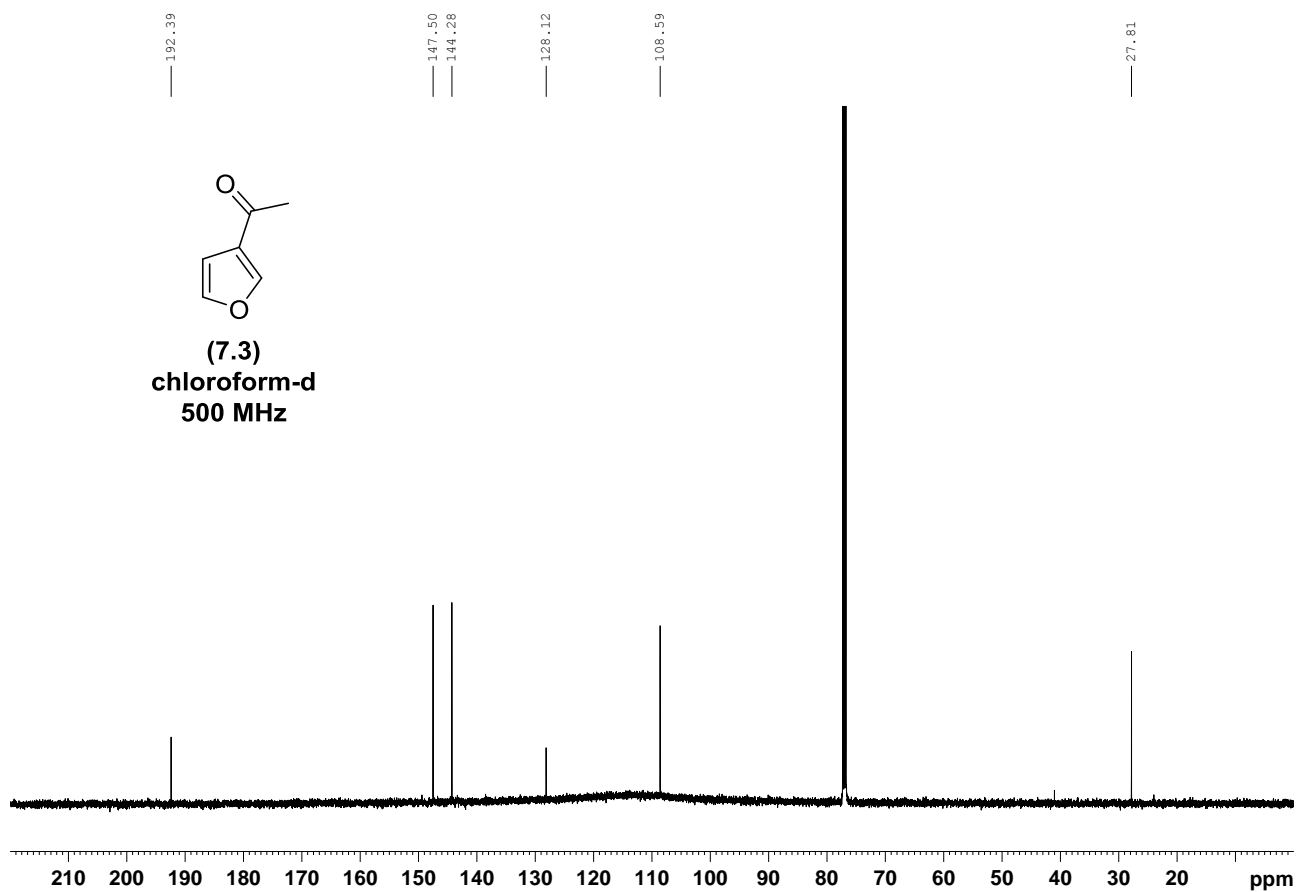
8.02
8.02
8.02
8.02
7.44
7.44
7.43
6.77
6.77
6.76



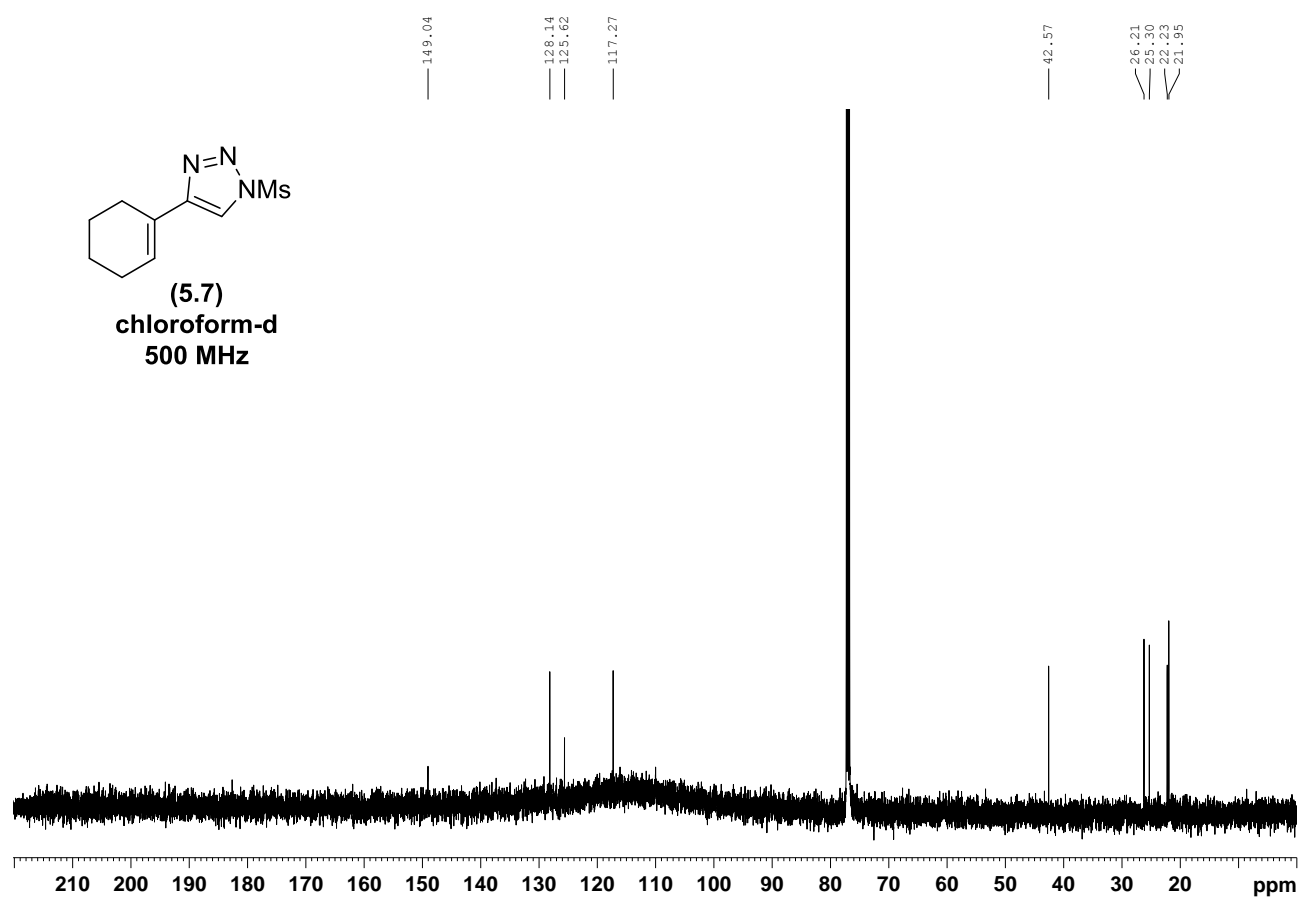
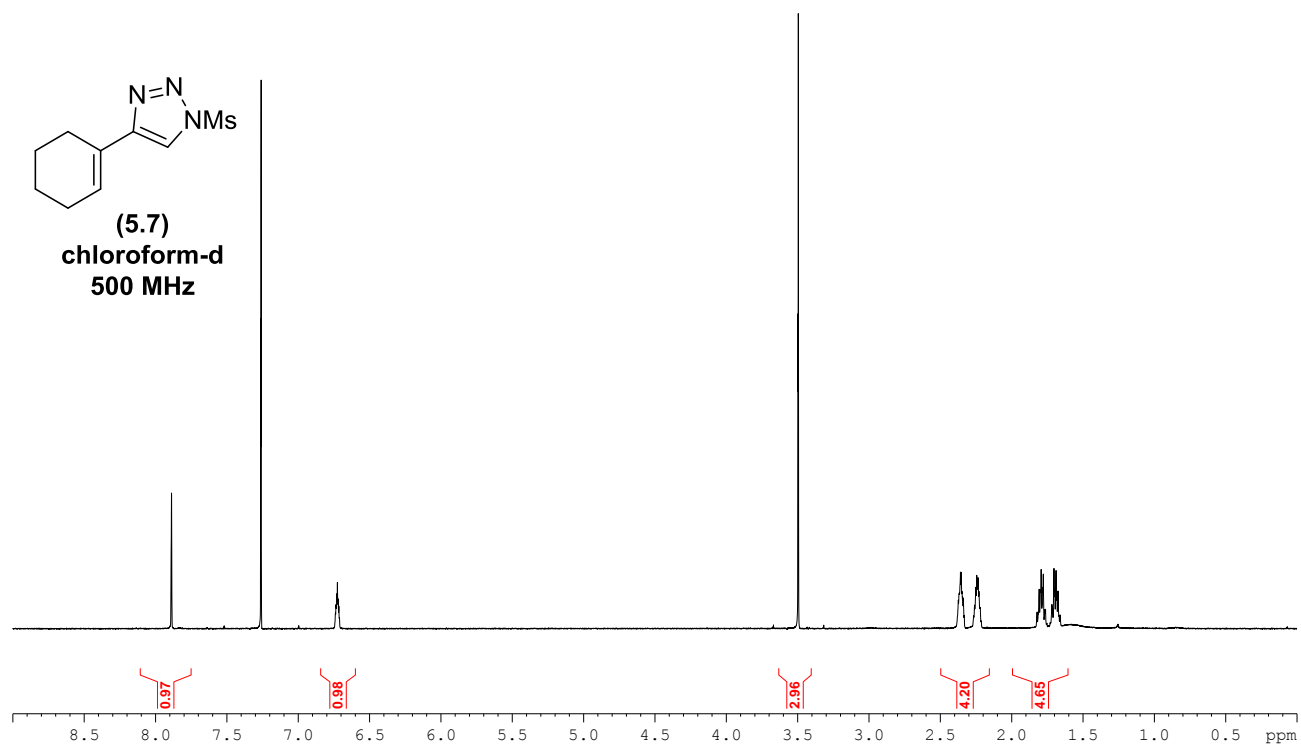
(7.3)
chloroform-d
500 MHz

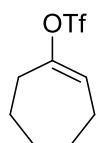
2.44
1.56



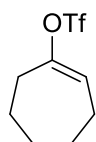
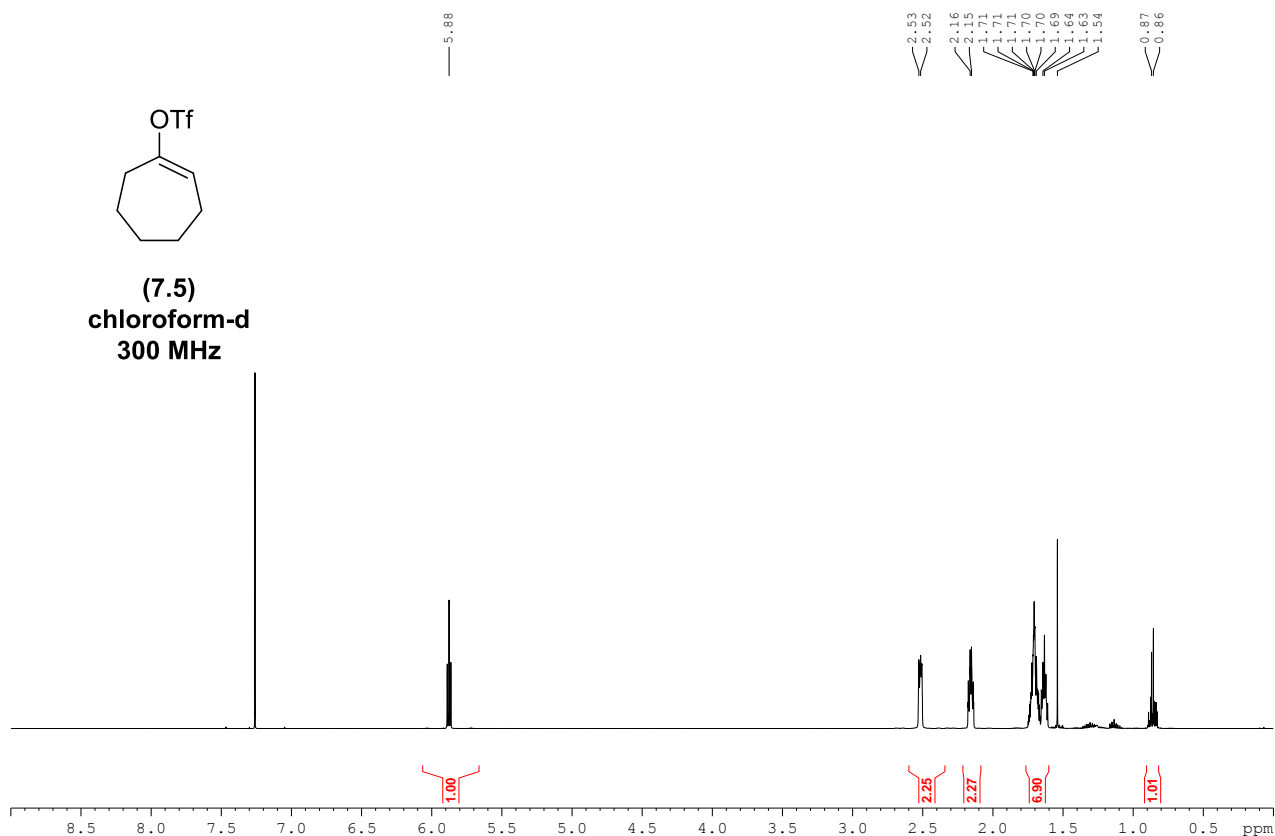


8.3 Appendix C: Supporting NMR Spectra for Chapter 5

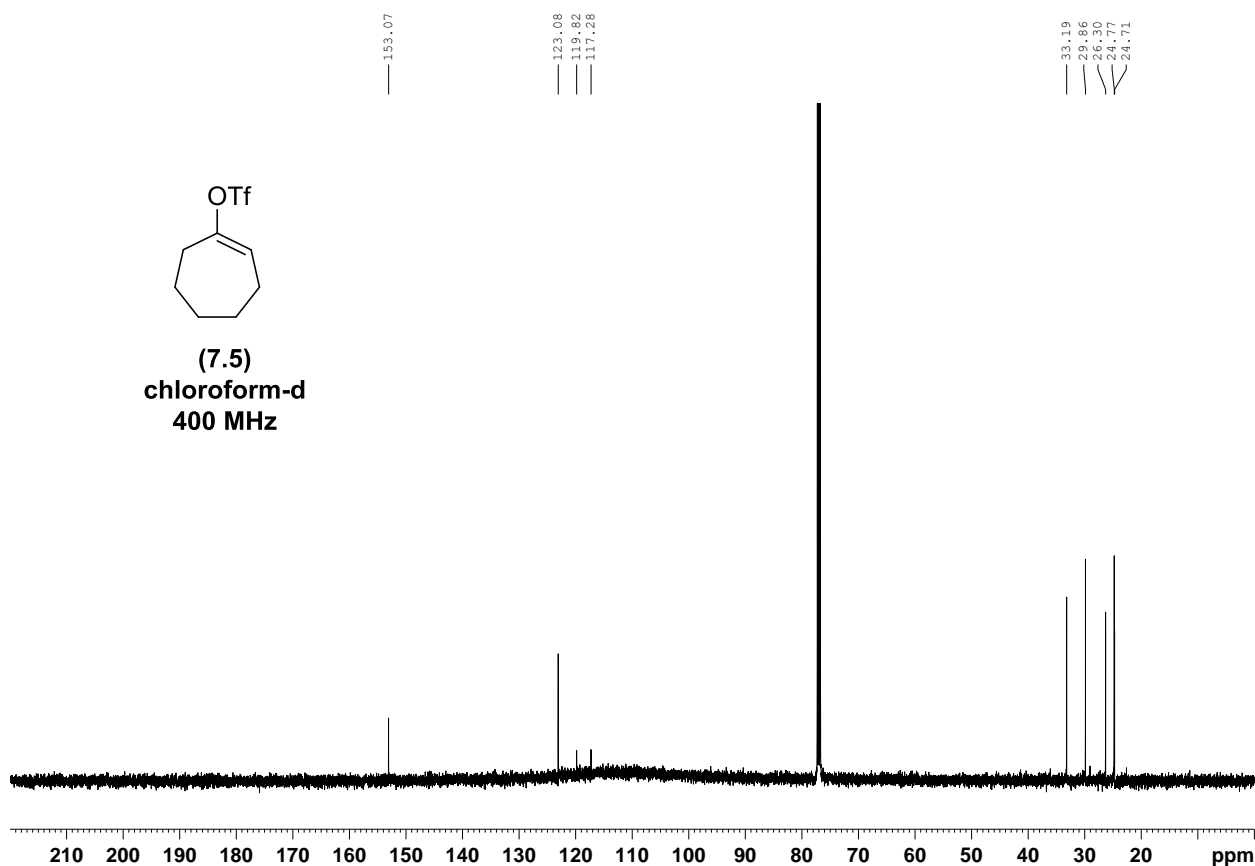


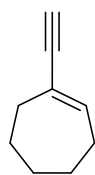


(7.5)
chloroform-d
300 MHz

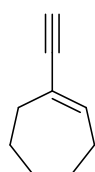
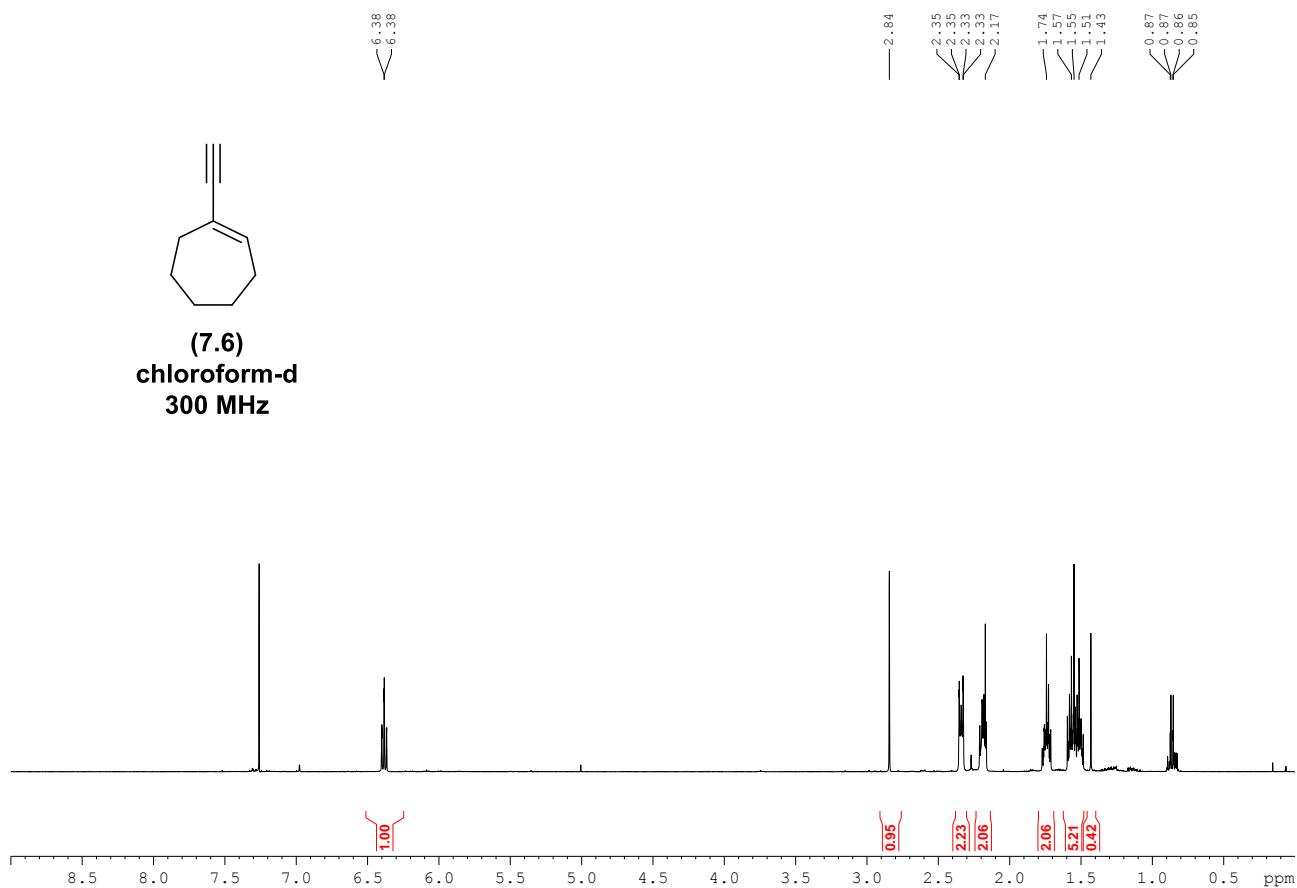


(7.5)
chloroform-d
400 MHz

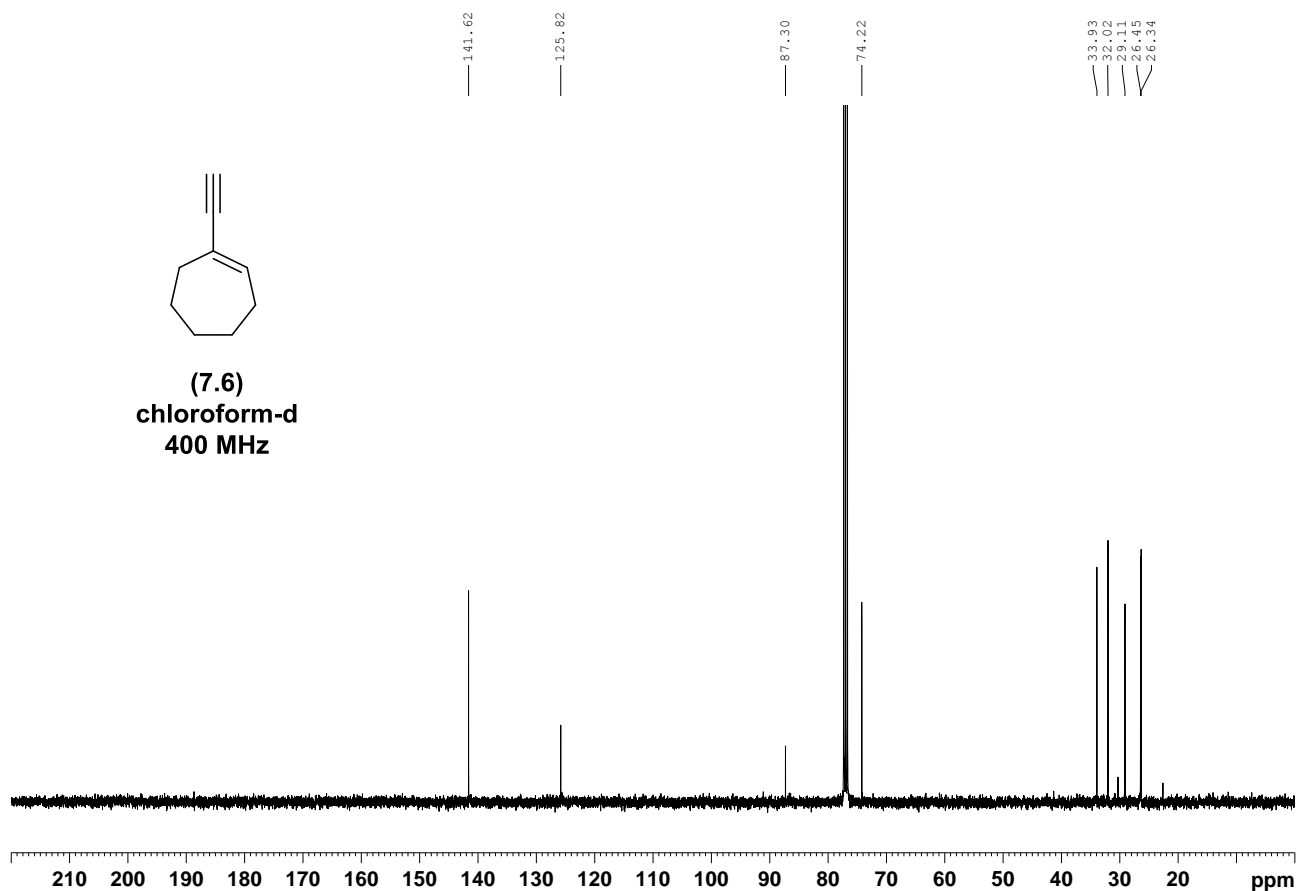


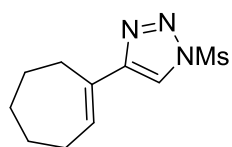


(7.6)
chloroform-d
300 MHz

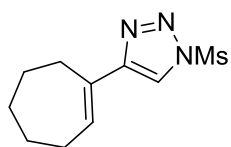
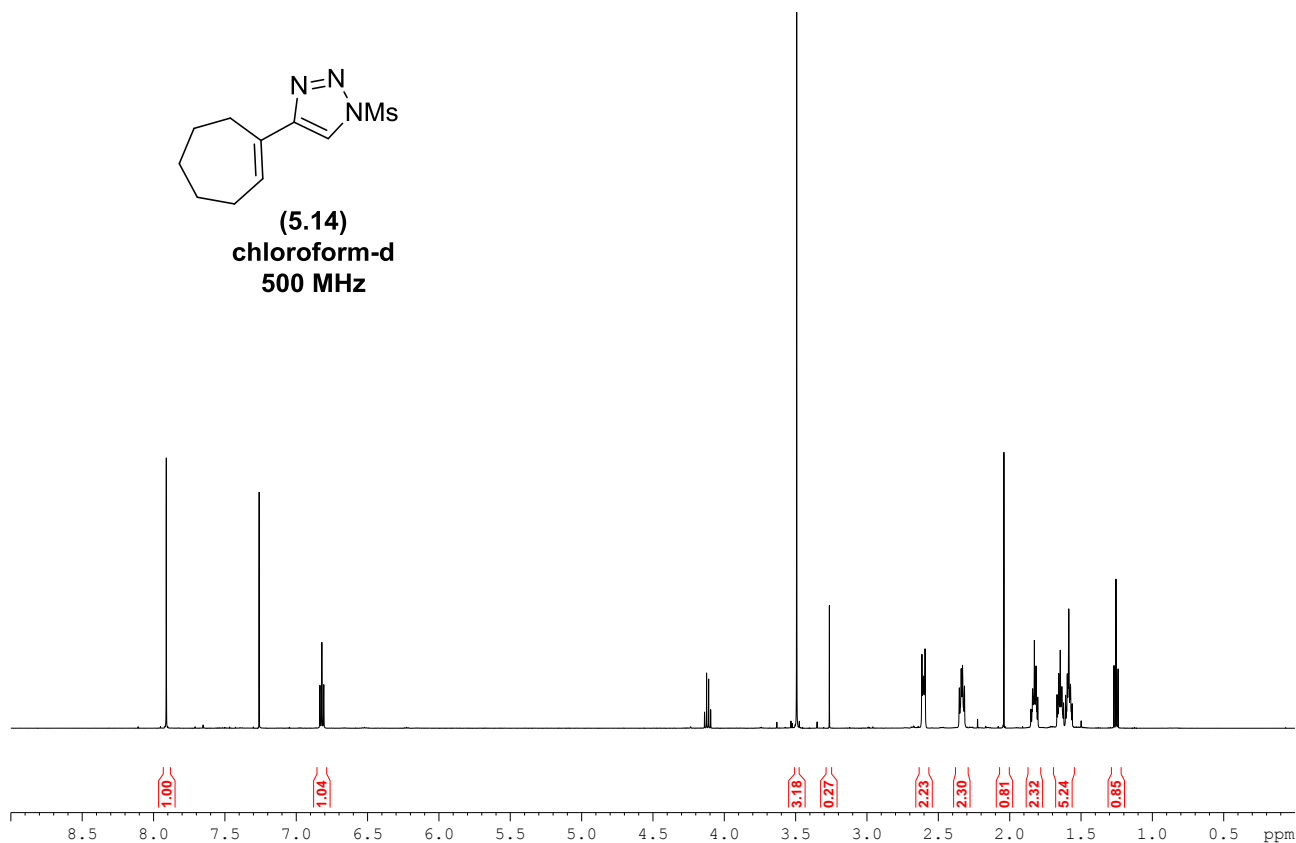


(7.6)
chloroform-d
400 MHz

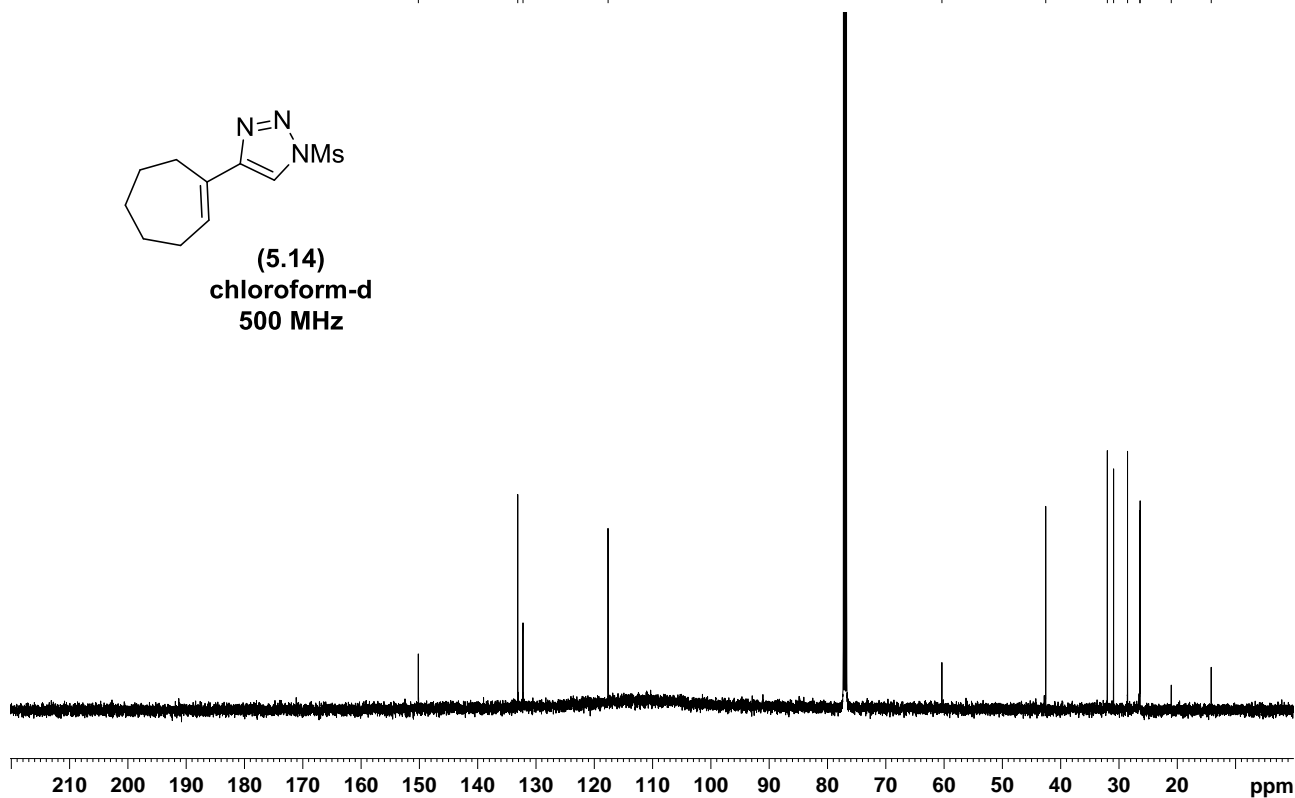


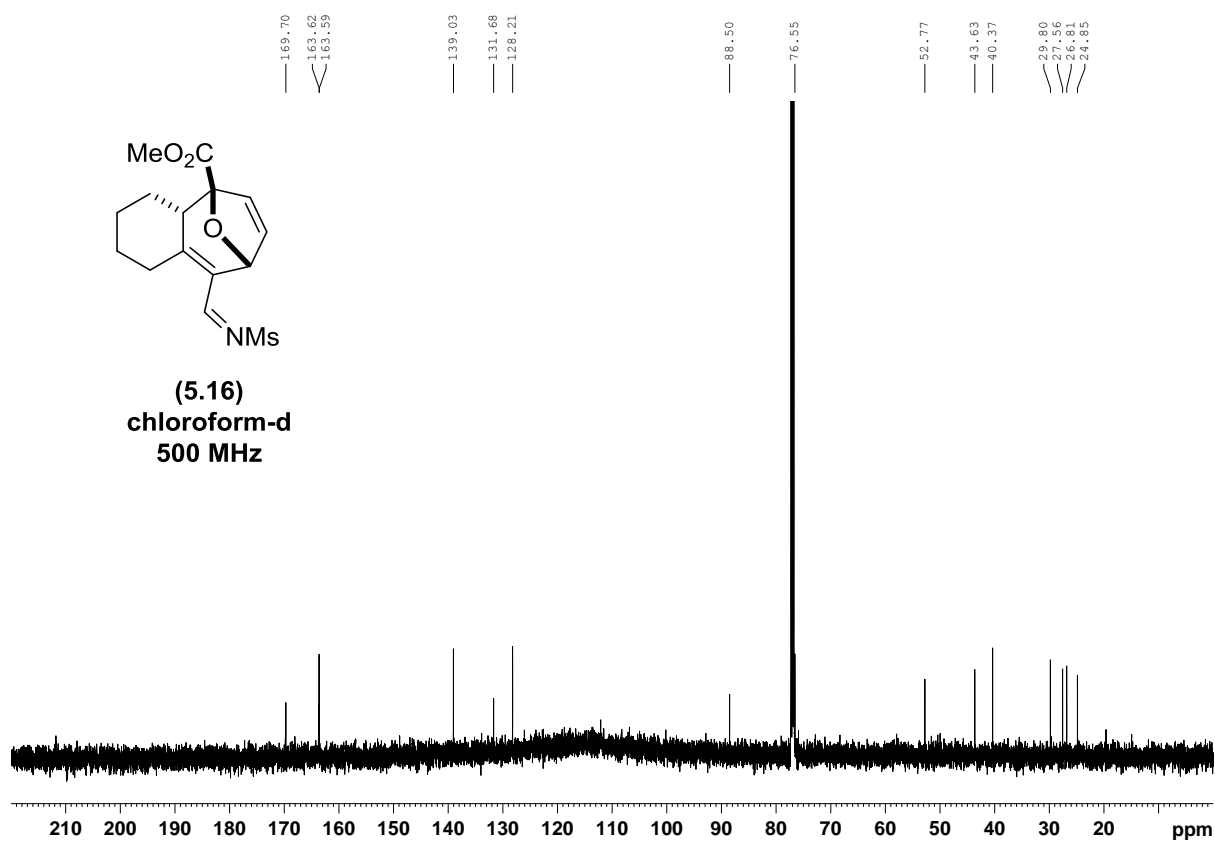
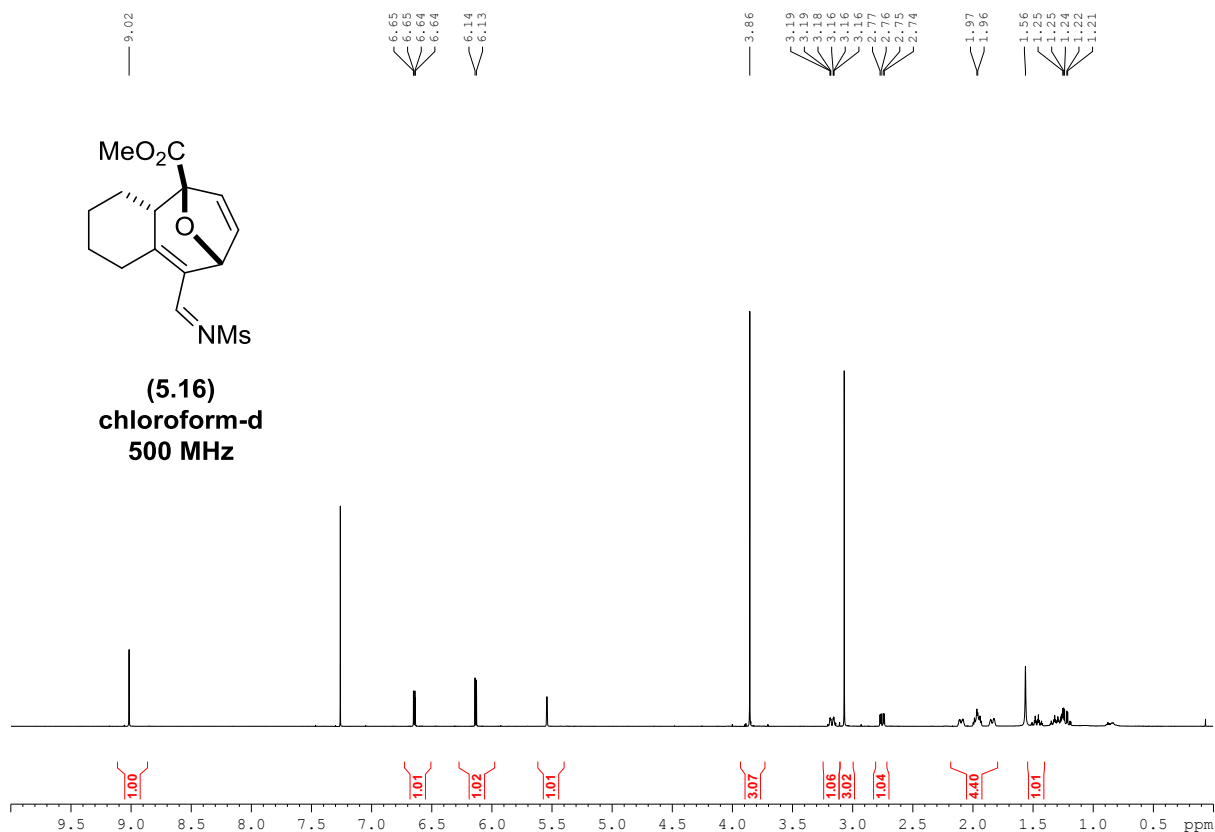


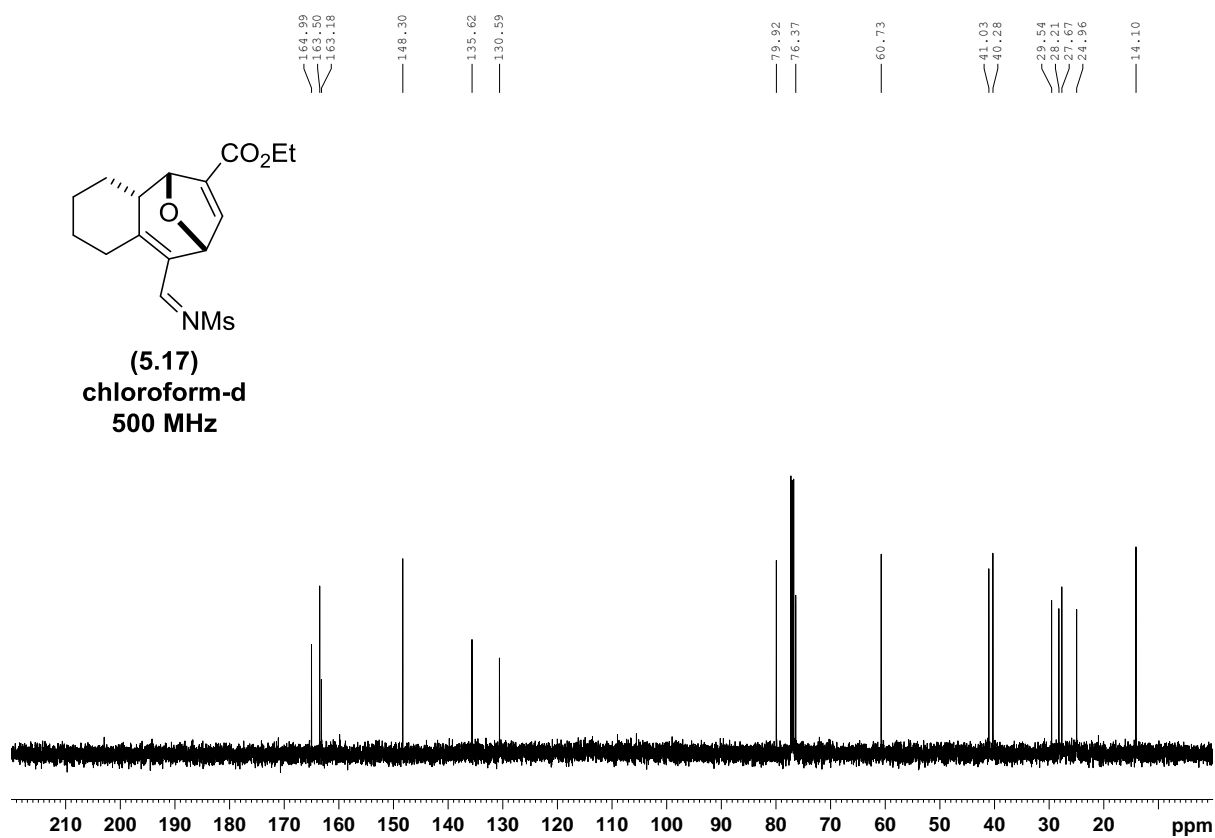
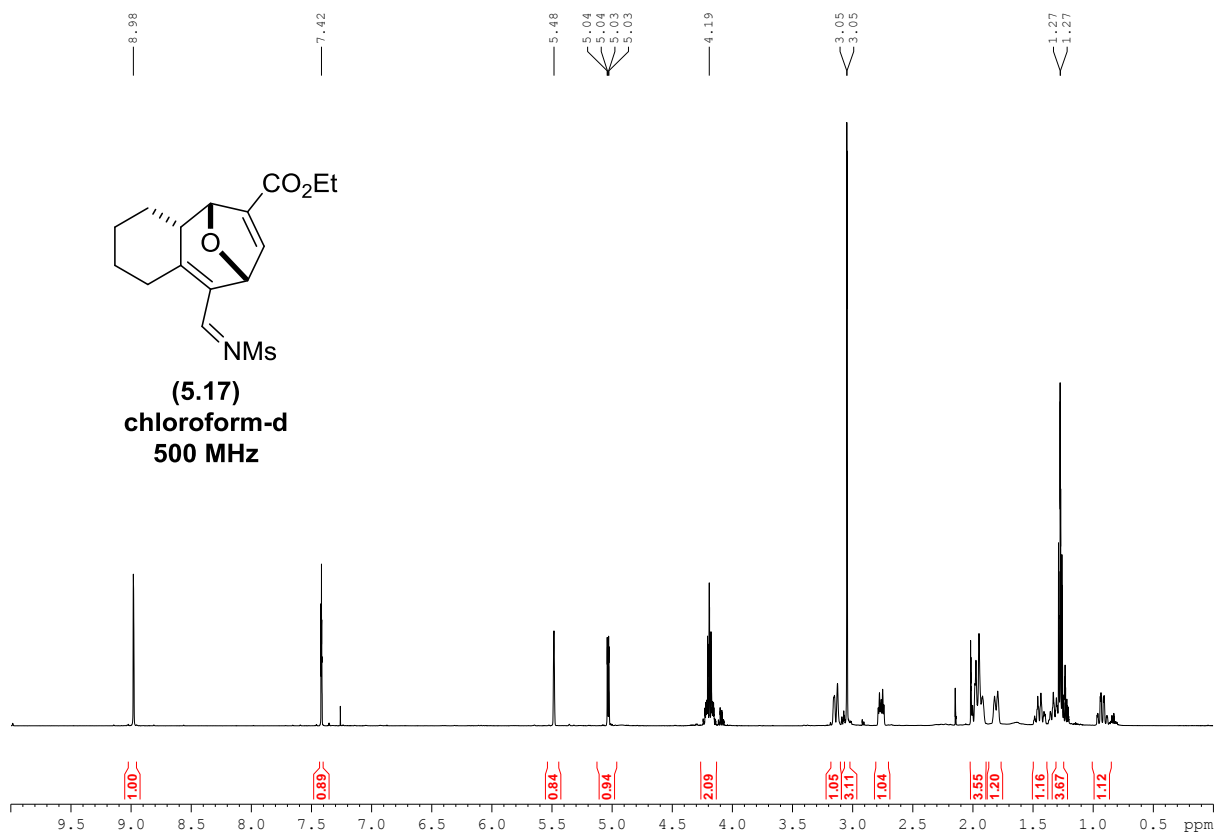
(5.14)
chloroform-d
500 MHz

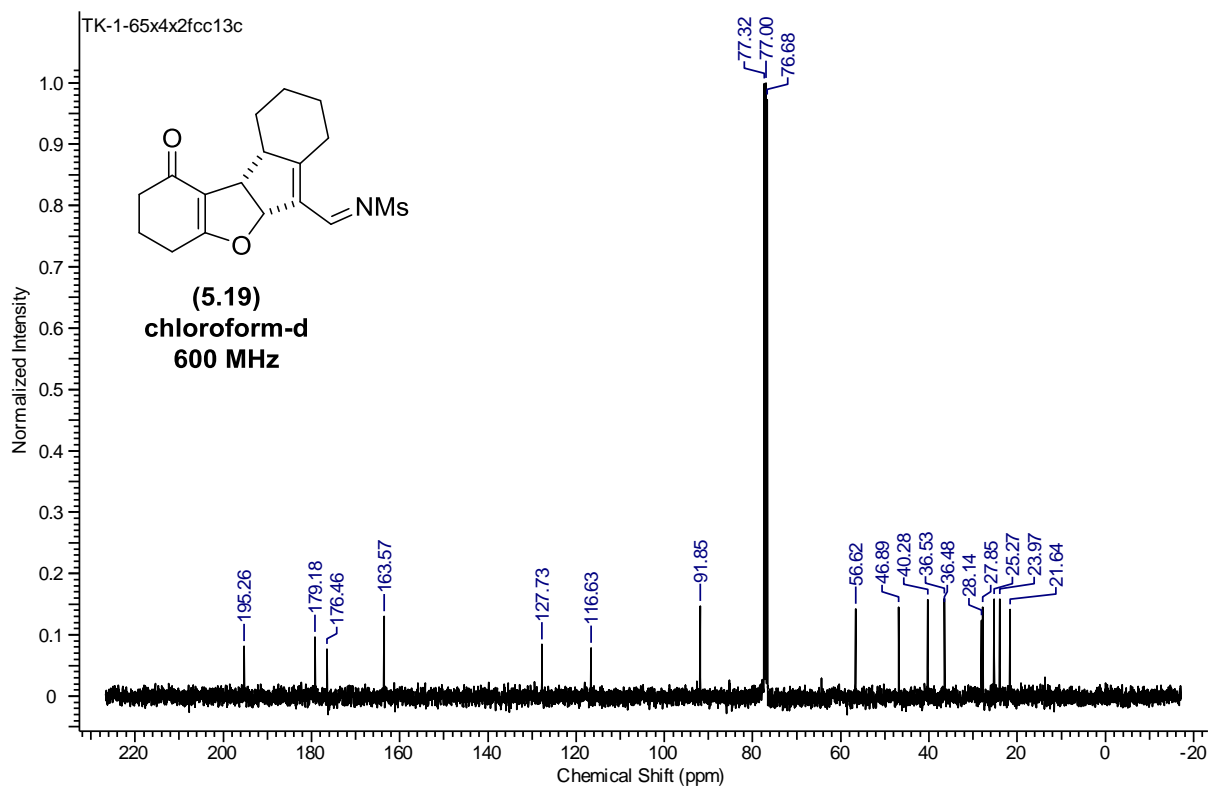
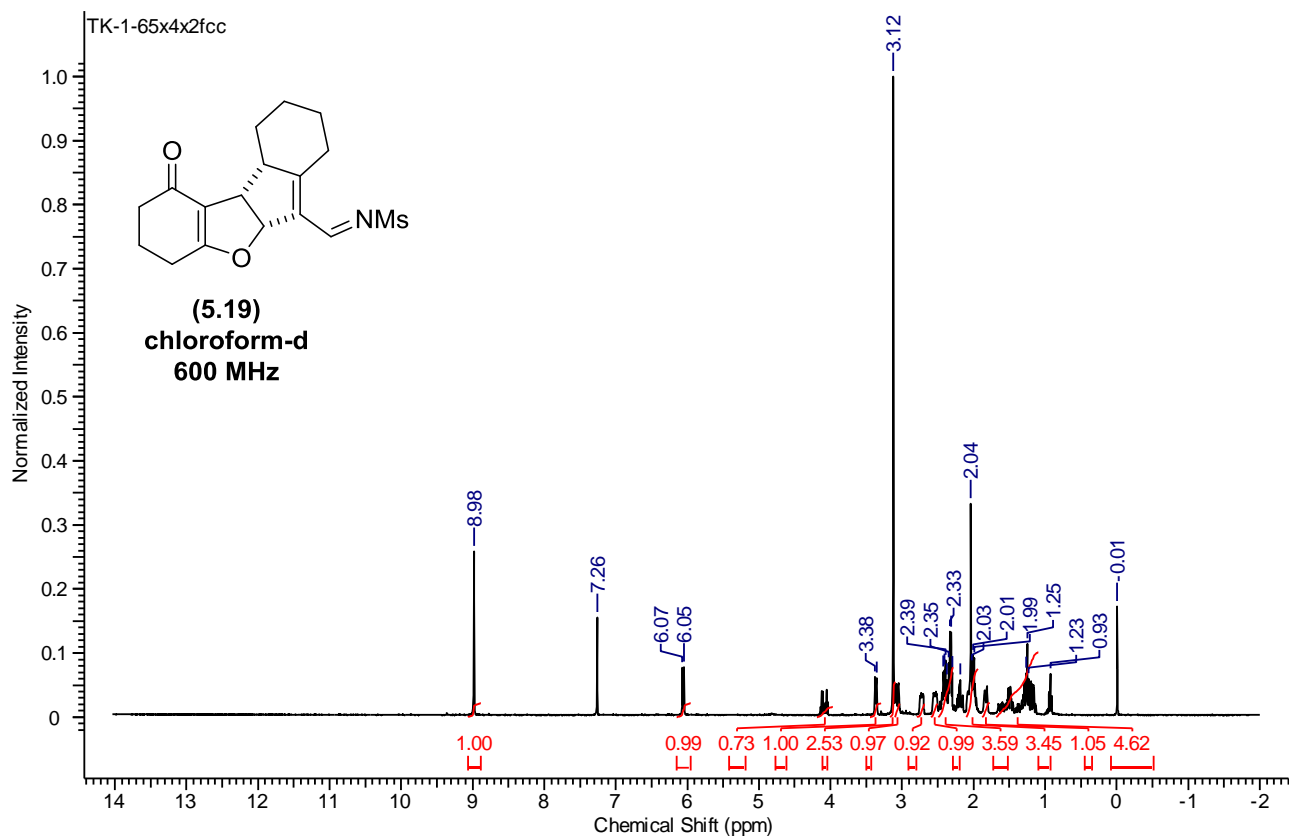


(5.14)
chloroform-d
500 MHz









8.4 Appendix D: X-Ray diffraction data

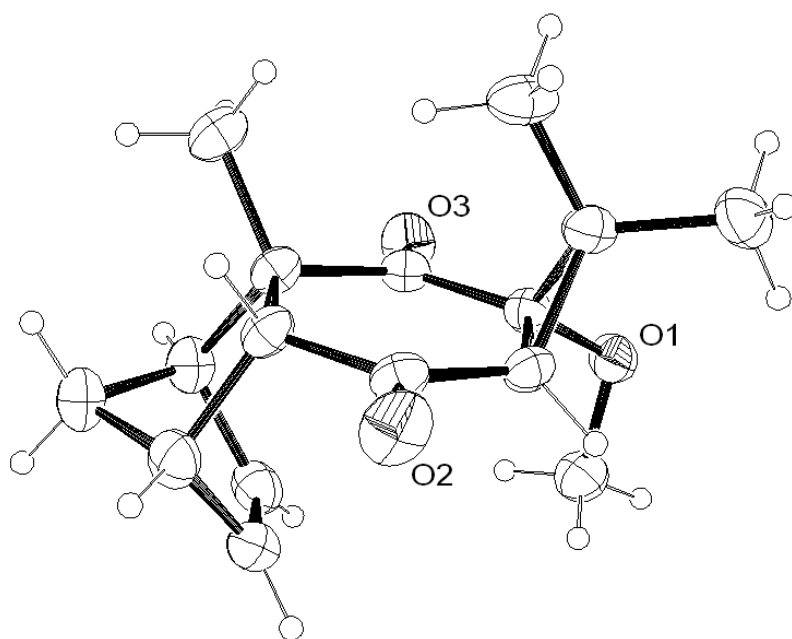


Table 1. Crystal data and structure refinement for **2.25**.

Empirical formula	C ₁₆ H ₂₀ O ₃	
Formula weight	260.33	
Temperature	293(2) K	
Wavelength	1.54184 Å	
Crystal system	Orthorhombic	
Space group	Pbca	
Unit cell dimensions	a = 7.9803(6) Å	α = 90°.
	b = 16.4730(10) Å	β = 90°.
	c = 20.843(2) Å	γ = 90°.
Volume	2740.0(4) Å ³	
Z	8	
Density (calculated)	1.262 Mg/m ³	
Absorption coefficient	0.690 mm ⁻¹	
F(000)	1120	
Theta range for data collection	4.24 to 62.51°.	
Index ranges	-9 ≤ h ≤ 6, -18 ≤ k ≤ 18, -20 ≤ l ≤ 23	
Reflections collected	6413	
Independent reflections	2175 [R(int) = 0.0315]	
Completeness to theta = 62.51°	99.6 %	
Refinement method	Full-matrix least-squares on F ²	
Data / restraints / parameters	2175 / 0 / 172	
Goodness-of-fit on F ²	0.799	
Final R indices [I > 2σ(I)]	R ₁ = 0.0420, wR ₂ = 0.1186	
R indices (all data)	R ₁ = 0.0574, wR ₂ = 0.1299	
Largest diff. peak and hole	0.150 and -0.175 e.Å ⁻³	

Table 2. Atomic coordinates ($\times 10^4$) and equivalent isotropic displacement parameters ($\text{\AA}^2 \times 10^3$) for 540tk1. $U(\text{eq})$ is defined as one third of the trace of the orthogonalized U^{ij} tensor.

	x	y	z	$U(\text{eq})$
O(3)	1414(2)	6213(1)	2644(1)	59(1)
O(2)	511(2)	6857(1)	5180(1)	69(1)
O(1)	1838(2)	7770(1)	3061(1)	51(1)
C(11)	1119(2)	6345(1)	3206(1)	41(1)
C(4)	691(2)	6713(1)	4610(1)	46(1)
C(1)	967(2)	7207(1)	3429(1)	40(1)
C(3)	806(2)	7379(1)	4144(1)	42(1)
C(5)	836(2)	5840(1)	4395(1)	44(1)
C(8)	4049(2)	5740(1)	3795(1)	57(1)
C(2)	-686(2)	7517(1)	3698(1)	45(1)
C(10)	968(2)	5626(1)	3667(1)	43(1)
C(13)	-446(3)	5062(1)	3428(1)	61(1)
C(14)	-2210(2)	6979(1)	3753(1)	59(1)
C(16)	3617(2)	7739(1)	3144(1)	58(1)
C(6)	2483(2)	5468(1)	4684(1)	54(1)
C(9)	2689(2)	5142(1)	3648(1)	52(1)
C(15)	-1146(3)	8390(1)	3551(1)	63(1)
C(12)	2615(3)	4691(1)	4293(1)	60(1)
C(7)	3921(2)	5945(1)	4403(1)	57(1)

Table 3. Bond lengths [Å] and angles [°] for 540tk1.

O(3)-C(11)	1.214(2)
O(2)-C(4)	1.220(2)
O(1)-C(1)	1.3900(19)
O(1)-C(16)	1.430(2)
C(11)-C(1)	1.499(2)
C(11)-C(10)	1.529(2)
C(4)-C(3)	1.469(3)
C(4)-C(5)	1.510(2)
C(1)-C(3)	1.523(2)
C(1)-C(2)	1.522(2)
C(3)-C(2)	1.527(3)
C(5)-C(10)	1.561(2)
C(5)-C(6)	1.570(3)
C(8)-C(7)	1.314(3)
C(8)-C(9)	1.498(3)
C(2)-C(14)	1.509(3)
C(2)-C(15)	1.515(3)
C(10)-C(13)	1.544(2)
C(10)-C(9)	1.589(3)
C(6)-C(7)	1.510(3)
C(6)-C(12)	1.520(3)
C(9)-C(12)	1.537(3)
C(1)-O(1)-C(16)	114.00(13)
O(3)-C(11)-C(1)	118.95(16)
O(3)-C(11)-C(10)	118.90(16)
C(1)-C(11)-C(10)	122.12(15)
O(2)-C(4)-C(3)	120.32(17)
O(2)-C(4)-C(5)	118.96(17)
C(3)-C(4)-C(5)	120.71(15)
O(1)-C(1)-C(11)	114.88(14)
O(1)-C(1)-C(3)	117.19(14)
C(11)-C(1)-C(3)	119.18(14)
O(1)-C(1)-C(2)	114.39(14)
C(11)-C(1)-C(2)	120.19(14)
C(3)-C(1)-C(2)	60.21(11)

C(4)-C(3)-C(1)	120.82(15)
C(4)-C(3)-C(2)	117.67(15)
C(1)-C(3)-C(2)	59.86(11)
C(4)-C(5)-C(10)	120.56(15)
C(4)-C(5)-C(6)	108.78(14)
C(10)-C(5)-C(6)	103.20(14)
C(7)-C(8)-C(9)	108.12(18)
C(14)-C(2)-C(15)	112.17(17)
C(14)-C(2)-C(1)	121.93(15)
C(15)-C(2)-C(1)	117.00(17)
C(14)-C(2)-C(3)	119.71(17)
C(15)-C(2)-C(3)	116.89(16)
C(1)-C(2)-C(3)	59.93(12)
C(11)-C(10)-C(13)	108.72(15)
C(11)-C(10)-C(5)	116.21(14)
C(13)-C(10)-C(5)	113.55(14)
C(11)-C(10)-C(9)	107.74(14)
C(13)-C(10)-C(9)	108.72(14)
C(5)-C(10)-C(9)	101.32(14)
C(7)-C(6)-C(12)	100.21(16)
C(7)-C(6)-C(5)	106.51(14)
C(12)-C(6)-C(5)	100.43(15)
C(8)-C(9)-C(12)	99.53(16)
C(8)-C(9)-C(10)	106.91(15)
C(12)-C(9)-C(10)	100.79(15)
C(9)-C(12)-C(6)	93.75(14)
C(8)-C(7)-C(6)	107.38(18)

Symmetry transformations used to generate equivalent atoms:

Table 4. Anisotropic displacement parameters ($\text{\AA}^2 \times 10^3$) for 540tk1. The anisotropic displacement factor exponent takes the form: $-2\pi^2 [h^2 a^{*2} U^{11} + \dots + 2 h k a^* b^* U^{12}]$

	U^{11}	U^{22}	U^{33}	U^{23}	U^{13}	U^{12}
O(3)	81(1)	63(1)	35(1)	-4(1)	6(1)	7(1)
O(2)	100(1)	70(1)	36(1)	-12(1)	4(1)	-9(1)
O(1)	46(1)	51(1)	55(1)	13(1)	0(1)	-4(1)
C(11)	36(1)	50(1)	36(1)	-3(1)	1(1)	-2(1)
C(4)	46(1)	53(1)	39(1)	-8(1)	1(1)	-8(1)
C(1)	38(1)	43(1)	39(1)	2(1)	1(1)	-2(1)
C(3)	43(1)	41(1)	42(1)	-9(1)	-3(1)	-5(1)
C(5)	50(1)	44(1)	36(1)	-1(1)	7(1)	-12(1)
C(8)	44(1)	62(1)	63(1)	14(1)	3(1)	6(1)
C(2)	41(1)	51(1)	44(1)	-11(1)	-2(1)	3(1)
C(10)	46(1)	44(1)	39(1)	-7(1)	5(1)	-7(1)
C(13)	65(1)	54(1)	63(1)	-16(1)	1(1)	-15(1)
C(14)	38(1)	78(1)	61(1)	-23(1)	4(1)	-1(1)
C(16)	48(1)	62(1)	64(1)	11(1)	4(1)	-10(1)
C(6)	69(1)	54(1)	40(1)	7(1)	-3(1)	-2(1)
C(9)	60(1)	48(1)	48(1)	-1(1)	8(1)	5(1)
C(15)	64(1)	61(1)	64(1)	-11(1)	-8(1)	18(1)
C(12)	73(1)	49(1)	59(1)	10(1)	5(1)	2(1)
C(7)	53(1)	58(1)	60(1)	8(1)	-13(1)	-4(1)

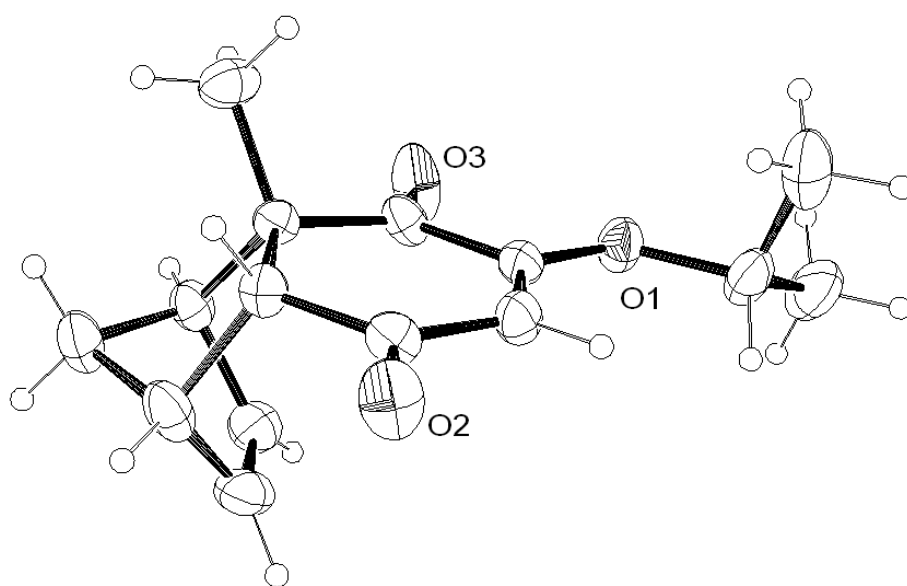


Table 1. Crystal data and structure refinement for **2.53**.

Empirical formula	C ₁₅ H ₁₈ O ₃	
Formula weight	246.31	
Temperature	293(2) K	
Wavelength	0.71073 Å	
Crystal system	Monoclinic	
Space group	P2 ₁ /c	
Unit cell dimensions	a = 6.365(2) Å	α = 90°.
	b = 21.464(5) Å	β = 100.69(3)°.
	c = 9.837(3) Å	γ = 90°.
Volume	1320.6(7) Å ³	
Z	4	
Density (calculated)	1.239 Mg/m ³	
Absorption coefficient	0.085 mm ⁻¹	
F(000)	528	
Theta range for data collection	3.26 to 29.00°.	
Index ranges	-6 ≤ h ≤ 8, -28 ≤ k ≤ 26, -13 ≤ l ≤ 13	
Reflections collected	11398	
Independent reflections	3132 [R(int) = 0.0280]	
Completeness to theta = 29.00°	89.1 %	
Refinement method	Full-matrix least-squares on F ²	
Data / restraints / parameters	3132 / 0 / 163	
Goodness-of-fit on F ²	1.175	
Final R indices [I > 2σ(I)]	R ₁ = 0.0581, wR ₂ = 0.1701	
R indices (all data)	R ₁ = 0.0857, wR ₂ = 0.1890	
Largest diff. peak and hole	0.200 and -0.169 e.Å ⁻³	

Table 2. Atomic coordinates ($\times 10^4$) and equivalent isotropic displacement parameters ($\text{\AA}^2 \times 10^3$) for 860tk3. $U(\text{eq})$ is defined as one third of the trace of the orthogonalized U^{ij} tensor.

	x	y	z	$U(\text{eq})$
O(1)	3033(2)	4256(1)	4591(1)	55(1)
O(3)	948(3)	4703(1)	2319(2)	83(1)
C(10)	1318(3)	4150(1)	2300(2)	45(1)
C(9)	673(3)	3781(1)	993(2)	39(1)
C(2)	2831(3)	3223(1)	3642(2)	48(1)
O(2)	2485(3)	2254(1)	2626(2)	70(1)
C(4)	1011(3)	3067(1)	1140(2)	43(1)
C(1)	2467(3)	3845(1)	3581(2)	42(1)
C(3)	2149(3)	2813(1)	2498(2)	45(1)
C(8)	-1810(3)	3828(1)	518(2)	46(1)
C(5)	-1317(3)	2805(1)	752(2)	60(1)
C(11)	-2248(3)	3254(1)	-411(2)	61(1)
C(12)	1847(3)	4064(1)	-76(2)	60(1)
C(7)	-2778(3)	3623(1)	1711(2)	60(1)
C(13)	4245(4)	4056(1)	5926(2)	66(1)
C(14)	6554(4)	3994(1)	5834(2)	80(1)
C(6)	-2481(3)	3016(1)	1846(2)	67(1)
C(15)	3864(5)	4557(1)	6913(2)	85(1)

Table 3. Bond lengths [Å] and angles [°] for 860tk3.

O(1)-C(1)	1.328(2)
O(1)-C(13)	1.458(2)
O(3)-C(10)	1.211(2)
C(10)-C(9)	1.502(2)
C(10)-C(1)	1.488(2)
C(9)-C(4)	1.550(2)
C(9)-C(12)	1.525(2)
C(9)-C(8)	1.566(2)
C(2)-C(1)	1.353(2)
C(2)-C(3)	1.431(2)
O(2)-C(3)	1.223(2)
C(4)-C(3)	1.499(2)
C(4)-C(5)	1.565(3)
C(8)-C(7)	1.489(3)
C(8)-C(11)	1.529(3)
C(5)-C(6)	1.486(3)
C(5)-C(11)	1.529(3)
C(7)-C(6)	1.320(3)
C(13)-C(15)	1.499(3)
C(13)-C(14)	1.495(4)
C(1)-O(1)-C(13)	120.13(14)
O(3)-C(10)-C(9)	120.53(16)
O(3)-C(10)-C(1)	119.09(16)
C(9)-C(10)-C(1)	120.37(14)
C(10)-C(9)-C(4)	115.56(13)
C(10)-C(9)-C(12)	106.77(15)
C(4)-C(9)-C(12)	112.38(14)
C(10)-C(9)-C(8)	108.78(14)
C(4)-C(9)-C(8)	101.94(13)
C(12)-C(9)-C(8)	111.40(14)
C(1)-C(2)-C(3)	123.15(16)
C(3)-C(4)-C(9)	118.54(14)
C(3)-C(4)-C(5)	111.43(15)
C(9)-C(4)-C(5)	102.96(14)
C(2)-C(1)-O(1)	127.01(16)

C(2)-C(1)-C(10)	121.71(15)
O(1)-C(1)-C(10)	111.27(14)
O(2)-C(3)-C(2)	120.07(16)
O(2)-C(3)-C(4)	119.70(16)
C(2)-C(3)-C(4)	120.23(15)
C(7)-C(8)-C(11)	100.17(16)
C(7)-C(8)-C(9)	106.73(14)
C(11)-C(8)-C(9)	100.86(14)
C(6)-C(5)-C(11)	100.02(17)
C(6)-C(5)-C(4)	106.87(16)
C(11)-C(5)-C(4)	99.98(15)
C(8)-C(11)-C(5)	93.34(15)
C(6)-C(7)-C(8)	107.39(19)
C(15)-C(13)-O(1)	104.47(18)
C(15)-C(13)-C(14)	112.4(2)
O(1)-C(13)-C(14)	109.49(17)
C(7)-C(6)-C(5)	108.00(18)

Symmetry transformations used to generate equivalent atoms:

Table 4. Anisotropic displacement parameters ($\text{\AA}^2 \times 10^3$) for 860tk3. The anisotropic displacement factor exponent takes the form: $-2\pi^2 [h^2 a^{*2} U^{11} + \dots + 2 h k a^* b^* U^{12}]$

	U^{11}	U^{22}	U^{33}	U^{23}	U^{13}	U^{12}
O(1)	74(1)	44(1)	42(1)	0(1)	-1(1)	-7(1)
O(3)	110(1)	40(1)	80(1)	-8(1)	-35(1)	15(1)
C(10)	41(1)	34(1)	56(1)	1(1)	-4(1)	-1(1)
C(9)	38(1)	36(1)	43(1)	5(1)	5(1)	1(1)
C(2)	52(1)	44(1)	44(1)	9(1)	-5(1)	-2(1)
O(2)	88(1)	37(1)	76(1)	4(1)	-10(1)	13(1)
C(4)	48(1)	37(1)	43(1)	-3(1)	5(1)	4(1)
C(1)	44(1)	39(1)	42(1)	1(1)	4(1)	-8(1)
C(3)	42(1)	34(1)	57(1)	5(1)	5(1)	3(1)
C(8)	40(1)	45(1)	47(1)	3(1)	-4(1)	4(1)
C(5)	65(1)	40(1)	66(1)	2(1)	-13(1)	-12(1)
C(11)	62(1)	55(1)	55(1)	-2(1)	-15(1)	-5(1)
C(12)	56(1)	64(1)	64(1)	20(1)	17(1)	5(1)
C(7)	37(1)	78(2)	63(1)	8(1)	7(1)	3(1)
C(13)	103(2)	53(1)	38(1)	9(1)	1(1)	-21(1)
C(14)	95(2)	71(2)	62(1)	4(1)	-21(1)	8(1)
C(6)	43(1)	81(2)	73(1)	24(1)	3(1)	-15(1)
C(15)	123(2)	88(2)	45(1)	-8(1)	20(1)	-24(2)

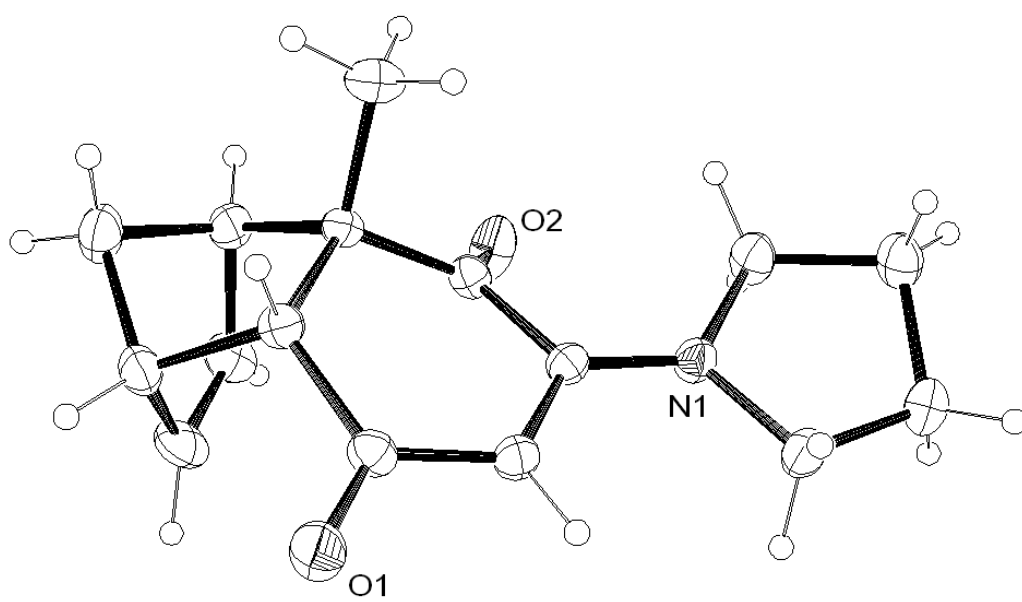


Table 1. Crystal data and structure refinement for **2.37**.

Empirical formula	C ₁₆ H ₁₉ N O ₂	
Formula weight	257.33	
Temperature	293(2) K	
Wavelength	0.71073 Å	
Crystal system	Monoclinic	
Space group	P2 ₁ /c	
Unit cell dimensions	a = 7.5182(18) Å	α = 90°.
	b = 18.417(8) Å	β = 93.68(2)°.
	c = 9.558(2) Å	γ = 90°.
Volume	1320.7(7) Å ³	
Z	4	
Density (calculated)	1.294 Mg/m ³	
Absorption coefficient	0.085 mm ⁻¹	
F(000)	552	
Theta range for data collection	2.93 to 28.97°.	
Index ranges	-9 ≤ h ≤ 10, -23 ≤ k ≤ 24, -12 ≤ l ≤ 11	
Reflections collected	5845	
Independent reflections	2958 [R(int) = 0.0546]	
Completeness to theta = 28.97°	84.7 %	
Refinement method	Full-matrix least-squares on F ²	
Data / restraints / parameters	2958 / 0 / 172	
Goodness-of-fit on F ²	0.952	
Final R indices [I > 2σ(I)]	R ₁ = 0.0686, wR ₂ = 0.1619	
R indices (all data)	R ₁ = 0.1343, wR ₂ = 0.2098	
Largest diff. peak and hole	0.198 and -0.201 e.Å ⁻³	

Table 2. Atomic coordinates ($\times 10^4$) and equivalent isotropic displacement parameters ($\text{\AA}^2 \times 10^3$) for 895tk5. $U(\text{eq})$ is defined as one third of the trace of the orthogonalized U^{ij} tensor.

	x	y	z	$U(\text{eq})$
O(1)	3856(3)	5296(1)	2966(2)	54(1)
O(2)	9101(3)	7127(1)	2437(2)	53(1)
N(1)	9317(3)	6260(1)	4833(2)	36(1)
C(1)	8062(4)	6166(2)	3797(3)	30(1)
C(2)	6512(4)	5786(2)	3939(3)	36(1)
C(10)	8262(4)	6568(2)	2451(3)	32(1)
C(4)	5729(4)	5783(2)	1320(3)	32(1)
C(3)	5268(4)	5616(2)	2800(3)	34(1)
C(9)	7414(3)	6243(2)	1112(3)	30(1)
C(5)	4238(4)	6204(2)	461(3)	42(1)
C(8)	6677(4)	6855(2)	99(3)	39(1)
C(13)	11122(4)	6553(2)	4703(3)	44(1)
C(15)	10890(4)	6125(2)	7012(3)	45(1)
C(16)	9164(4)	5930(2)	6221(3)	45(1)
C(7)	5489(4)	7310(2)	938(3)	46(1)
C(14)	12199(4)	6183(2)	5886(3)	45(1)
C(6)	4052(4)	6926(2)	1168(3)	51(1)
C(12)	8892(4)	5803(2)	482(3)	48(1)
C(11)	5264(4)	6431(2)	-795(3)	51(1)

Table 3. Bond lengths [Å] and angles [°] for 895tk5.

O(1)-C(3)	1.233(3)
O(2)-C(10)	1.208(3)
N(1)-C(1)	1.334(3)
N(1)-C(16)	1.469(3)
N(1)-C(13)	1.474(4)
C(1)-C(2)	1.373(4)
C(1)-C(10)	1.500(4)
C(2)-C(3)	1.424(4)
C(10)-C(9)	1.516(4)
C(4)-C(9)	1.547(4)
C(4)-C(3)	1.510(4)
C(4)-C(5)	1.553(4)
C(9)-C(12)	1.530(4)
C(9)-C(8)	1.564(4)
C(5)-C(6)	1.502(5)
C(5)-C(11)	1.527(4)
C(8)-C(11)	1.533(4)
C(8)-C(7)	1.496(4)
C(13)-C(14)	1.510(4)
C(15)-C(16)	1.503(4)
C(15)-C(14)	1.508(4)
C(7)-C(6)	1.321(5)
C(1)-N(1)-C(16)	121.6(2)
C(1)-N(1)-C(13)	126.6(2)
C(16)-N(1)-C(13)	110.7(2)
N(1)-C(1)-C(2)	123.8(2)
N(1)-C(1)-C(10)	117.9(2)
C(2)-C(1)-C(10)	117.9(2)
C(1)-C(2)-C(3)	123.9(3)
O(2)-C(10)-C(9)	121.2(3)
O(2)-C(10)-C(1)	120.7(2)
C(9)-C(10)-C(1)	118.1(2)
C(9)-C(4)-C(3)	118.1(2)
C(9)-C(4)-C(5)	103.2(2)
C(3)-C(4)-C(5)	113.3(2)

O(1)-C(3)-C(2)	122.4(3)
O(1)-C(3)-C(4)	118.0(2)
C(2)-C(3)-C(4)	119.5(2)
C(10)-C(9)-C(12)	105.4(2)
C(10)-C(9)-C(4)	114.2(2)
C(12)-C(9)-C(4)	112.4(3)
C(10)-C(9)-C(8)	110.6(2)
C(12)-C(9)-C(8)	112.1(2)
C(4)-C(9)-C(8)	102.3(2)
C(6)-C(5)-C(11)	100.2(3)
C(6)-C(5)-C(4)	106.8(2)
C(11)-C(5)-C(4)	99.7(2)
C(11)-C(8)-C(7)	99.7(3)
C(11)-C(8)-C(9)	100.6(2)
C(7)-C(8)-C(9)	105.8(2)
N(1)-C(13)-C(14)	102.9(2)
C(16)-C(15)-C(14)	103.9(2)
N(1)-C(16)-C(15)	103.9(2)
C(6)-C(7)-C(8)	108.2(3)
C(13)-C(14)-C(15)	102.9(3)
C(7)-C(6)-C(5)	107.4(3)
C(8)-C(11)-C(5)	93.9(2)

Symmetry transformations used to generate equivalent atoms:

Table 4. Anisotropic displacement parameters ($\text{\AA}^2 \times 10^3$) for 895tk5. The anisotropic displacement factor exponent takes the form: $-2\pi^2 [h^2 a^{*2} U^{11} + \dots + 2 h k a^* b^* U^{12}]$

	U^{11}	U^{22}	U^{33}	U^{23}	U^{13}	U^{12}
O(1)	40(1)	73(2)	49(1)	12(1)	1(1)	-27(1)
O(2)	68(2)	44(1)	45(1)	12(1)	-11(1)	-29(1)
N(1)	33(1)	44(2)	30(1)	5(1)	1(1)	-8(1)
C(1)	33(2)	29(2)	29(1)	-1(1)	3(1)	0(1)
C(2)	33(2)	43(2)	31(2)	7(1)	5(1)	-5(1)
C(10)	30(1)	31(2)	36(2)	3(1)	1(1)	-2(1)
C(4)	32(2)	30(2)	34(1)	-3(1)	3(1)	-5(1)
C(3)	31(2)	33(2)	39(2)	3(1)	4(1)	-3(1)
C(9)	27(1)	31(2)	31(1)	1(1)	5(1)	0(1)
C(5)	30(2)	55(2)	40(2)	8(2)	-3(1)	-4(2)
C(8)	38(2)	47(2)	33(2)	12(1)	3(1)	-4(2)
C(13)	39(2)	50(2)	41(2)	4(2)	-3(1)	-15(2)
C(15)	53(2)	47(2)	35(2)	3(1)	-8(2)	-1(2)
C(16)	41(2)	63(2)	31(2)	10(2)	1(1)	-5(2)
C(7)	46(2)	35(2)	57(2)	14(2)	6(2)	9(2)
C(14)	39(2)	49(2)	47(2)	3(2)	-7(2)	-10(2)
C(6)	36(2)	55(2)	61(2)	14(2)	7(2)	17(2)
C(12)	44(2)	49(2)	52(2)	-3(2)	16(2)	6(2)
C(11)	49(2)	66(3)	37(2)	11(2)	-7(2)	-11(2)

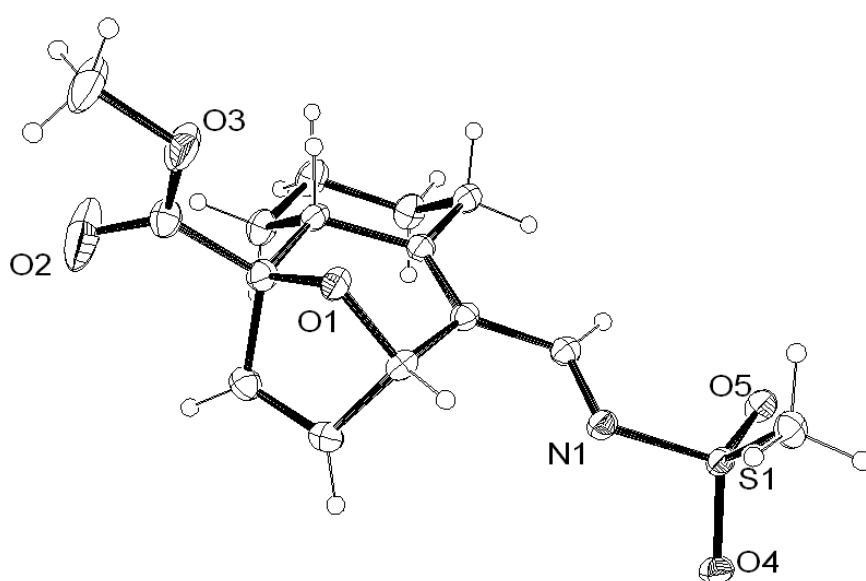


Table 1. Crystal data and structure refinement for **5.16**.

Empirical formula	C ₁₅ H ₁₉ N O ₅ S	
Formula weight	325.39	
Temperature	293(2) K	
Wavelength	1.54180 Å	
Crystal system	Triclinic	
Space group	P-1	
Unit cell dimensions	a = 5.5067(2) Å	α = 79.253(4)°.
	b = 8.1430(4) Å	β = 83.454(4)°.
	c = 18.1212(8) Å	γ = 76.625(4)°.
Volume	774.53(6) Å ³	
Z	2	
Density (calculated)	1.395 Mg/m ³	
Absorption coefficient	2.072 mm ⁻¹	
F(000)	344	
Theta range for data collection	4.98 to 62.41°.	
Index ranges	-6 ≤ h ≤ 4, -9 ≤ k ≤ 7, -20 ≤ l ≤ 20	
Reflections collected	4843	
Independent reflections	2444 [R(int) = 0.0311]	
Completeness to theta = 62.41°	99.1 %	
Refinement method	Full-matrix least-squares on F ²	
Data / restraints / parameters	2444 / 0 / 199	
Goodness-of-fit on F ²	1.242	
Final R indices [I > 2σ(I)]	R1 = 0.0594, wR2 = 0.1621	
R indices (all data)	R1 = 0.0676, wR2 = 0.1690	
Largest diff. peak and hole	0.890 and -0.483 e.Å ⁻³	

Table 2. Atomic coordinates ($\times 10^4$) and equivalent isotropic displacement parameters ($\text{\AA}^2 \times 10^3$) for 1054tk6. $U(\text{eq})$ is defined as one third of the trace of the orthogonalized U^{ij} tensor.

	x	y	z	$U(\text{eq})$
S(1)	1533(1)	7440(1)	9669(1)	27(1)
O(5)	2378(4)	5703(3)	9538(1)	34(1)
O(1)	404(4)	7981(3)	12781(1)	29(1)
O(4)	2739(4)	8709(3)	9212(1)	34(1)
N(1)	1695(5)	7652(3)	10556(1)	29(1)
C(5)	2515(5)	6453(4)	11813(2)	27(1)
C(1)	2502(6)	7336(4)	13231(2)	30(1)
C(2)	4370(6)	8378(4)	12855(2)	34(1)
C(11)	3468(6)	5415(4)	13160(2)	29(1)
C(6)	3384(5)	5122(4)	12357(2)	27(1)
C(9)	7013(7)	2795(5)	13343(2)	42(1)
C(10)	6101(6)	4653(4)	13440(2)	39(1)
C(14)	2421(5)	6292(4)	11036(2)	27(1)
C(7)	4343(6)	3299(4)	12251(2)	33(1)
C(15)	-1702(6)	8053(4)	9591(2)	34(1)
O(3)	-631(5)	7433(5)	14226(1)	63(1)
C(3)	3841(6)	8906(4)	12148(2)	34(1)
C(4)	1607(6)	8216(4)	12034(2)	30(1)
C(8)	6972(7)	2599(5)	12526(2)	40(1)
O(2)	2981(6)	7772(7)	14470(2)	111(2)
C(12)	1662(6)	7542(4)	14043(2)	36(1)
C(13)	-1582(9)	7637(8)	14988(2)	76(2)

Table 3. Bond lengths [Å] and angles [°] for 1054tk6.

S(1)-O(4)	1.438(2)
S(1)-O(5)	1.438(2)
S(1)-N(1)	1.662(2)
S(1)-C(15)	1.750(3)
O(1)-C(4)	1.438(3)
O(1)-C(1)	1.431(4)
N(1)-C(14)	1.288(4)
C(5)-C(6)	1.359(4)
C(5)-C(4)	1.518(4)
C(5)-C(14)	1.446(4)
C(1)-C(12)	1.519(4)
C(1)-C(2)	1.507(4)
C(1)-C(11)	1.556(4)
C(2)-C(3)	1.316(5)
C(11)-C(6)	1.525(4)
C(11)-C(10)	1.543(4)
C(6)-C(7)	1.497(4)
C(9)-C(10)	1.516(5)
C(9)-C(8)	1.523(5)
C(7)-C(8)	1.531(5)
O(3)-C(12)	1.288(4)
O(3)-C(13)	1.447(4)
C(3)-C(4)	1.515(4)
O(2)-C(12)	1.186(4)
O(4)-S(1)-O(5)	117.37(13)
O(4)-S(1)-N(1)	105.73(13)
O(5)-S(1)-N(1)	113.26(13)
O(4)-S(1)-C(15)	109.66(14)
O(5)-S(1)-C(15)	108.75(15)
N(1)-S(1)-C(15)	100.78(14)
C(4)-O(1)-C(1)	101.9(2)
C(14)-N(1)-S(1)	118.3(2)
C(6)-C(5)-C(4)	118.0(2)
C(6)-C(5)-C(14)	123.9(3)
C(4)-C(5)-C(14)	118.1(3)

O(1)-C(1)-C(12)	109.1(3)
O(1)-C(1)-C(2)	103.2(2)
C(12)-C(1)-C(2)	115.0(3)
O(1)-C(1)-C(11)	107.1(2)
C(12)-C(1)-C(11)	111.0(2)
C(2)-C(1)-C(11)	111.0(2)
C(3)-C(2)-C(1)	107.5(3)
C(6)-C(11)-C(10)	110.6(3)
C(6)-C(11)-C(1)	111.4(2)
C(10)-C(11)-C(1)	113.4(2)
C(5)-C(6)-C(11)	120.4(3)
C(5)-C(6)-C(7)	125.8(3)
C(11)-C(6)-C(7)	113.8(2)
C(10)-C(9)-C(8)	110.7(3)
C(9)-C(10)-C(11)	112.0(3)
N(1)-C(14)-C(5)	118.9(3)
C(8)-C(7)-C(6)	111.2(3)
C(12)-O(3)-C(13)	116.6(3)
C(2)-C(3)-C(4)	107.6(3)
O(1)-C(4)-C(5)	107.1(2)
O(1)-C(4)-C(3)	102.5(2)
C(5)-C(4)-C(3)	109.3(3)
C(7)-C(8)-C(9)	110.9(3)
O(2)-C(12)-O(3)	123.0(3)
O(2)-C(12)-C(1)	123.7(3)
O(3)-C(12)-C(1)	113.3(3)

Symmetry transformations used to generate equivalent atoms:

Table 4. Anisotropic displacement parameters ($\text{\AA}^2 \times 10^3$) for 1054tk6. The anisotropic displacement factor exponent takes the form: $-2\pi^2 [h^2 a^{*2} U^{11} + \dots + 2 h k a^* b^* U^{12}]$

	U^{11}	U^{22}	U^{33}	U^{23}	U^{13}	U^{12}
S(1)	26(1)	31(1)	22(1)	0(1)	-3(1)	-7(1)
O(5)	40(1)	32(1)	28(1)	-4(1)	-3(1)	-4(1)
O(1)	25(1)	38(1)	23(1)	-4(1)	-2(1)	-6(1)
O(4)	34(1)	38(1)	30(1)	3(1)	0(1)	-15(1)
N(1)	30(1)	32(1)	25(1)	0(1)	-5(1)	-8(1)
C(5)	24(1)	31(2)	24(1)	-2(1)	-1(1)	-7(1)
C(1)	26(2)	36(2)	29(2)	-3(1)	-6(1)	-7(1)
C(2)	30(2)	37(2)	37(2)	-8(1)	-4(1)	-10(1)
C(11)	28(2)	35(2)	22(1)	1(1)	-2(1)	-9(1)
C(6)	22(1)	33(2)	26(1)	-3(1)	-1(1)	-9(1)
C(9)	44(2)	43(2)	34(2)	-1(2)	-13(2)	3(2)
C(10)	38(2)	43(2)	32(2)	-3(1)	-12(1)	-3(2)
C(14)	21(1)	30(2)	28(2)	-3(1)	0(1)	-5(1)
C(7)	40(2)	32(2)	26(1)	0(1)	-4(1)	-8(1)
C(15)	26(2)	42(2)	36(2)	-5(1)	-6(1)	-7(1)
O(3)	47(2)	125(3)	30(1)	-26(1)	10(1)	-39(2)
C(3)	35(2)	31(2)	37(2)	-4(1)	0(1)	-12(1)
C(4)	32(2)	32(2)	23(1)	-1(1)	-2(1)	-6(1)
C(8)	42(2)	34(2)	37(2)	-4(1)	-9(1)	2(2)
O(2)	54(2)	253(5)	53(2)	-73(2)	7(2)	-54(3)
C(12)	33(2)	44(2)	32(2)	-9(1)	-6(1)	-5(1)
C(13)	56(3)	153(5)	30(2)	-31(2)	11(2)	-38(3)

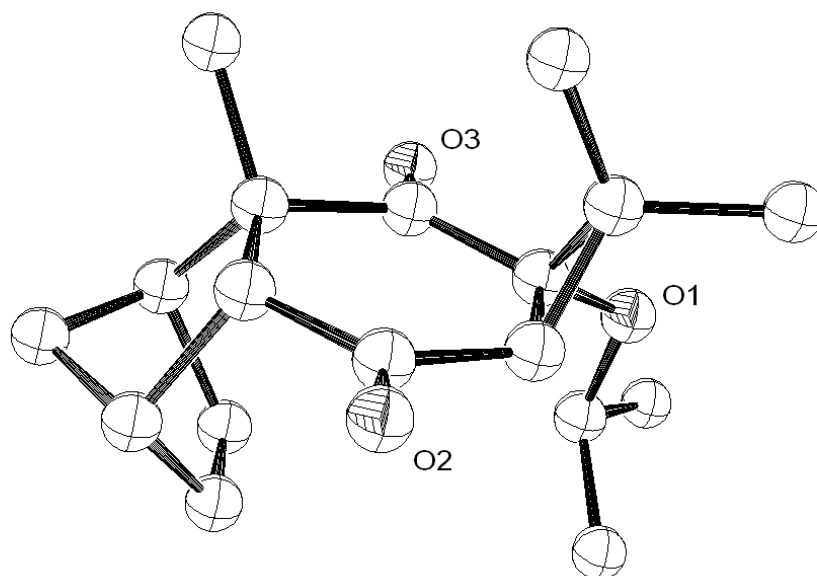


Table 1. Crystal data and structure refinement for **2.54**.

Empirical formula	C ₁₈ H ₂₄ O ₃	
Formula weight	288.39	
Temperature	293(2) K	
Wavelength	1.54180 Å	
Crystal system	Monoclinic	
Space group		
Unit cell dimensions	a = 8.3706(8) Å b = 17.019(2) Å c = 11.1609(9) Å	α = 90°. β = 99.617(8)°. γ = 90°.
Volume	1567.6(3) Å ³	
Z	4	
Density (calculated)	1.222 Mg/m ³	
Absorption coefficient	0.650 mm ⁻¹	
F(000)	624	
Crystal size	0.4 x 0.2 x 0.1 mm ³	
Theta range for data collection	4.79 to 62.48°.	
Index ranges	-9 ≤ h ≤ 9, -19 ≤ k ≤ 11, -10 ≤ l ≤ 12	
Reflections collected	6198	
Independent reflections	2484 [R(int) = 0.0393]	
Completeness to theta = 62.48°	99.1 %	
Refinement method	Full-matrix least-squares on F ²	
Data / restraints / parameters	2484 / 0 / 190	
Goodness-of-fit on F ²	1.343	
Final R indices [I > 2σ(I)]	R1 = 0.0736, wR2 = 0.1842	
R indices (all data)	R1 = 0.0868, wR2 = 0.1963	
Largest diff. peak and hole	0.471 and -0.341 e.Å ⁻³	

Table 2. Atomic coordinates ($\times 10^4$) and equivalent isotropic displacement parameters ($\text{\AA}^2 \times 10^3$) for 1112tk-111-75. $U(\text{eq})$ is defined as one third of the trace of the orthogonalized U^{ij} tensor.

	x	y	z	$U(\text{eq})$
O(3)	2000(2)	7615(1)	3820(2)	55(1)
O(1)	1160(2)	6337(1)	2391(2)	47(1)
O(2)	766(3)	8092(1)	-1068(2)	59(1)
C(4)	991(3)	7985(2)	21(2)	43(1)
C(3)	1149(3)	7178(2)	523(2)	43(1)
C(2)	1625(3)	7034(1)	1884(2)	41(1)
C(1)	1803(3)	7720(2)	2737(2)	41(1)
C(8)	-1290(3)	8435(2)	2399(3)	48(1)
C(11)	-268(4)	9629(2)	1868(3)	56(1)
C(15)	-443(3)	6324(2)	2727(3)	50(1)
C(10)	1645(3)	8571(2)	2270(2)	43(1)
C(5)	1116(3)	8685(2)	869(2)	44(1)
C(7)	-1718(3)	8495(2)	1212(3)	49(1)
C(13)	3211(4)	9019(2)	2784(3)	56(1)
C(17)	4289(3)	7434(2)	1032(3)	50(1)
C(18)	3230(4)	6050(2)	793(3)	61(1)
C(14)	-357(4)	5740(2)	3739(3)	56(1)
C(9)	171(3)	8963(2)	2770(2)	47(1)
C(12)	2854(3)	6898(2)	1042(2)	46(1)
C(6)	-593(3)	9086(2)	770(3)	51(1)
C(16)	-1722(4)	6132(3)	1673(3)	79(1)

Table 3. Bond lengths [Å] and angles [°] for 1112tk-111-75.

O(3)-C(1)	1.206(3)
O(1)-C(2)	1.398(3)
O(1)-C(15)	1.453(3)
O(2)-C(4)	1.212(3)
C(4)-C(5)	1.514(4)
C(4)-C(3)	1.482(4)
C(3)-C(12)	1.524(4)
C(3)-C(2)	1.525(4)
C(2)-C(12)	1.522(3)
C(2)-C(1)	1.498(4)
C(1)-C(10)	1.537(4)
C(8)-C(7)	1.318(4)
C(8)-C(9)	1.518(4)
C(11)-C(6)	1.522(4)
C(11)-C(9)	1.519(4)
C(15)-C(16)	1.489(5)
C(15)-C(14)	1.498(4)
C(10)-C(9)	1.583(4)
C(10)-C(5)	1.564(4)
C(10)-C(13)	1.541(4)
C(5)-C(6)	1.572(4)
C(7)-C(6)	1.515(4)
C(17)-C(12)	1.509(4)
C(18)-C(12)	1.514(4)
C(2)-O(1)-C(15)	116.62(18)
O(2)-C(4)-C(5)	119.4(2)
O(2)-C(4)-C(3)	120.5(2)
C(5)-C(4)-C(3)	120.1(2)
C(12)-C(3)-C(2)	59.92(16)
C(12)-C(3)-C(4)	116.8(2)
C(2)-C(3)-C(4)	121.1(2)
O(1)-C(2)-C(3)	119.7(2)
O(1)-C(2)-C(12)	112.6(2)
C(3)-C(2)-C(12)	60.02(16)
O(1)-C(2)-C(1)	114.2(2)

C(3)-C(2)-C(1)	119.3(2)
C(12)-C(2)-C(1)	120.3(2)
O(3)-C(1)-C(2)	120.2(2)
O(3)-C(1)-C(10)	118.0(2)
C(2)-C(1)-C(10)	121.7(2)
C(7)-C(8)-C(9)	107.4(2)
C(6)-C(11)-C(9)	94.1(2)
O(1)-C(15)-C(16)	111.9(3)
O(1)-C(15)-C(14)	105.9(2)
C(16)-C(15)-C(14)	112.8(2)
C(9)-C(10)-C(5)	101.1(2)
C(9)-C(10)-C(13)	109.0(2)
C(5)-C(10)-C(13)	113.1(2)
C(9)-C(10)-C(1)	107.8(2)
C(5)-C(10)-C(1)	116.7(2)
C(13)-C(10)-C(1)	108.7(2)
C(4)-C(5)-C(10)	120.4(2)
C(4)-C(5)-C(6)	109.3(2)
C(10)-C(5)-C(6)	103.1(2)
C(8)-C(7)-C(6)	107.4(2)
C(11)-C(9)-C(10)	101.4(2)
C(11)-C(9)-C(8)	99.5(2)
C(10)-C(9)-C(8)	107.2(2)
C(3)-C(12)-C(2)	60.06(17)
C(3)-C(12)-C(17)	120.4(2)
C(2)-C(12)-C(17)	122.3(2)
C(3)-C(12)-C(18)	116.0(2)
C(2)-C(12)-C(18)	116.1(2)
C(17)-C(12)-C(18)	112.6(2)
C(11)-C(6)-C(7)	100.2(2)
C(11)-C(6)-C(5)	99.7(2)
C(7)-C(6)-C(5)	107.2(2)

Symmetry transformations used to generate equivalent atoms:

Table 4. Anisotropic displacement parameters ($\text{\AA}^2 \times 10^3$) for 1112tk-111-75. The anisotropic displacement factor exponent takes the form: $-2\pi^2 [h^2 a^{*2} U^{11} + \dots + 2 h k a^* b^* U^{12}]$

	U^{11}	U^{22}	U^{33}	U^{23}	U^{13}	U^{12}
O(3)	57(1)	66(1)	42(1)	8(1)	10(1)	1(1)
O(1)	39(1)	47(1)	60(1)	11(1)	22(1)	3(1)
O(2)	72(1)	65(1)	41(1)	6(1)	13(1)	5(1)
C(4)	41(1)	53(2)	37(2)	3(1)	11(1)	1(1)
C(3)	41(1)	48(1)	42(1)	-4(1)	13(1)	-3(1)
C(2)	37(1)	43(1)	45(1)	8(1)	14(1)	1(1)
C(1)	34(1)	53(2)	38(2)	4(1)	12(1)	-2(1)
C(8)	43(1)	51(2)	53(2)	0(1)	17(1)	5(1)
C(11)	63(2)	51(2)	56(2)	2(1)	21(1)	4(1)
C(15)	41(1)	46(1)	68(2)	6(1)	26(1)	0(1)
C(10)	41(1)	49(1)	40(1)	1(1)	11(1)	-3(1)
C(5)	47(1)	44(1)	43(1)	5(1)	14(1)	-3(1)
C(7)	40(1)	53(2)	56(2)	-3(1)	11(1)	6(1)
C(13)	52(2)	62(2)	55(2)	-4(1)	13(1)	-14(1)
C(17)	42(1)	63(2)	50(2)	8(1)	18(1)	1(1)
C(18)	60(2)	59(2)	73(2)	11(2)	34(2)	13(1)
C(14)	54(2)	62(2)	56(2)	3(1)	24(1)	-9(1)
C(9)	52(2)	49(2)	41(1)	-4(1)	15(1)	1(1)
C(12)	45(2)	54(2)	43(1)	8(1)	18(1)	4(1)
C(6)	56(2)	51(2)	48(2)	8(1)	12(1)	11(1)
C(16)	47(2)	111(3)	77(2)	32(2)	10(2)	-11(2)

